Distinct regulatory pathways controlling NLRP3 inflammasome in infectious and non-infectious diseases

Dissertation

in partial fulfilment of the requirements for the degree of
doctor rerum naturalium (Dr. rer. nat.)

Submitted to the Faculty of Medicine,
Friedrich Schiller University, Jena

by

M.Sc., Mohamed Abdulmajid Ghait

born on 15.10.1986 in Misurata, Libya

GUTACHTER

Prof. Dr. Michael Bauer

Center for Sepsis Control and Care, Jena University Hospital, Jena, Germany

Prof. Dr. Olaf Groß

Institute of Neuropathology, Medical Center, University of Freiburg, Freiburg, Germany

Prof. Dr. Hortense Slevogt

Centre for Innovation Competence Septomics, Jena University Hospital, Jena, Germany

Tag der öffentlichen Verteidigung: 01.02.2022

Table of content

List of Abbreviations

ACLF	Acute-on-chronic liver failure
AIM2	Absent in melanoma 2
ASC	Apoptosis-associated speck-like protein containing a CARD
ATP	Adenosine triphosphate
AUC	Area under the curve
BCA	Bicinchoninic acid
BMDM	Bone marrow derived macrophages
bp	Base pair
BRG1	Brahma-related gene 1
BSA	Bovine serum albumin
bsDNA	Bi-sulfate-DNA
Ca^{++}	Calcium
CAPS	Cryopyrin-associated periodic syndromes
CARD	Caspase activation and recruitment domain
Cas9	CRISPR-associated systems 9
CASP	Caspase
CD	Cell differentiation antigen
cDNA	Complementary DNA
cGAS	Cyclic GMP-AMP synthase
CGIs	CpG Islands
CNPY3	Canopy FGF signaling regulator 3
CpG	Cytosine-phosphate-guanine
CRISPR	Clustered regularly interspaced short palindromic repeats
CRP	C reactive protein
crRNA	CRISPR RNA
DAMP	Damage-associated molecular patterns
DD	Death Domain
DED	Death effector domain
DNA	Deoxyribonucleic acid
dsDNA	Double strand DNA
dsRNA	Double strand RNA
DSS	Disuccinimidyl suberate
E. coli	*Escherichia coli*
EDTA	Ethylenediaminetetraacetic acid
EIEEs	Early infantile epileptic encephalopathy
ELISA	Enzyme-linked immunosorbent assay
ER	Endoplasmic reticulum
FACS	Fluorescence-activated cell sorting
FGF	Fibroblast growth factor
FLICA	Fluorescent labeled inhibitor of caspases
FMF	Familial Mediterranean Fever
FSL-I	Pam2CGDPKHPKSF
g	X gravity

Gal-1	Galectin-1
GAPDH	Glyceraldehyde-3-phosphate dehydrogenase
GBP	Guanylate-binding proteins
GBS	Group B streptococcus (*Streptococcus agalactiae*)
Gp96	Glycoprotein 96
GSDMD	Gadermin-D
h	hour
HLA-DR	Major Histocompatibility Complex, Class II, DR
HLA-DRA	Major Histocompatibility Complex, Class II, DR Alpha
IFN	Interferon
IgG	Immunoglobulin G
IL-	Interleukin-
iLPS	Intracellular lipopolysaccharide (LPS)
INF	Infection
IPAF-1	Apoptotic protease activating factor-1 ice protease-activating factor
IRAK	interleukin-1 receptor associated kinases
IRF	Interferon regulatory factors
ISGs	interferon-stimulated genes
K^+	Potassium
kDa	Kilo Dalton
LDH	Lactate Dehydrogenase
Log	Logarithm
LPS	Lipopolysaccharide
Lys	Lysate
MAVS	Mitochondrial antiviral signaling protein
MDM	Monocyte-derived macrophage
MELD	End-stage liver disease scores
min	minutes
miR	Micro-RNA
MOF	Multiple organ dysfunction
MOI	Multiplicity of infection
MyD88	Myeloid differentiation primary response 88
NF-κB	nuclear factor-kappa B
NLRP	NLR Family Pyrin Domain Containing 1
NLRP3	NLR Family Pyrin Domain Containing 3
OD	Optical density
$P2X_7$	Purinergic $P2X_7$ receptor
PAK1	Protein A kinase 1
Pam_3CSK_4	$Pam_3CysSerLys_4$
PAMP	Pathogen-associated molecular patterns
PBMCs	Peripheral blood mononuclear cells
PGRN	Progranulin
PMA	Phorbol myristate acetate
pmol	picomol

PMSF	Phenylmethylsulfonyl fluoride
PMTs	Post-translational modifications
Poly(I:C)	Polyinosinic-polycytidylic acid
PRAT4A	Protein associated with Toll-like receptor 4A
PRR	Pattern-recognition receptors
PYD	Pyrin domain
qPCR	Quantitative Polymerase chain reaction
RFU	Relative fluorescence units
RIGI	Retinoic acid inducible gene I
RNA	Ribonucleic acid
rpm	Round per minute
S. aureus	*Staphylococcus aureus*
SD	standard deviation
SEM	Standard error of the mean
ssDNA	Single strand DNA
ssRNA	Single strand RNA
STAT	Signal transducer and activator of transcription
STING	stimulator of interferon response cGAMP interactor 1
Sup	Supernatant
SWI/SNF	Switch/Sucrose non-fermentable
T3SS	Type III secretion system
TFBS	Transcription Factor Binding Site
TIR	Toll/interleukin 1
TIRAP	TIR-containing adaptor protein
TLR	Toll like receptor
TNF	tumor necrosis factor
Tom20	Translocase of outer mitochondrial membrane 20
tracrRNA	Trans-activating crRNA
TRAF	TNF receptor-associated factor
TRIF	TIR domain-containing adaptor-inducing interferon-β
TSS	Transcription start site
TYK2	Tyrosine Kinase 2
UNC93B	Unc-93 Homolog B1
UTR	Untranslated region

Summary

The adequate responsiveness of mammalian immune cells to pathogenic cues is tightly regulated by elaborate mechanisms to control their onset and termination and to avoid malfunctions, ranging from auto-aggressive and over-active immunity to immune-deficiency. Different responses are regulated by various pathways and initiate distinct immunologic outcomes. Inflammasomes are equipped with checkpoints that prevent inappropriate activation and maintain homeostasis. They are large multimolecular complexes well known for their ability to control activation of the inflammatory enzymes: caspase-1, -4, and -5 in human and Caspase-1, and -11 in mouse, which in turn regulate the production and secretion of cytokines, as well as a rapid, noxious, inflammatory form of cell death termed pyroptosis following the detection of pathogenic microorganisms and danger signals in the host cells. Mouse caspase-11 is activated by intracellular lipopolysaccharide (LPS) and is the major contributor to LPS induced lethality rather than caspase-1. Similarly, human caspase-4 and caspase-5 sense and are activated by direct binding to cytosolic LPS to trigger Gasdermin-D (GSDMD)-mediated pyroptosis and mediate caspase-1 autoproteolysis cleavage via NLRP3 inflammasome activation, which instigates further proinflammatory forces. During proinflammatory responses numerous inflammasome components are known to undergo upregulation in their expression level. However, regulation of inflammasome pathways during immunosuppression in sepsis and acutely decompensated liver cirrhosis has not been closely examined. To this end, we include PBMCs, $CD14^{+}$ monocytes and plasma derived from patients with acute decompensated liver cirrhosis and septic patients according to the Sepsis-3 criteria. First, we uncovered and established miRNA-222 as a surrogate to define patients with immuno-suppression and organ damage. This finding was further employed to study genes encoding inflammatory caspases *CASP4*, *CASP5*, and *CASP1;* and the pyroptosis effector *GSDMD* during sepsis-related immunosuppression. Unlike *CASP1* and *CASP5*, *CASP4* expression was substantially suppressed and inversely correlated with markers of organ damage including MELD and SOFA scores and intriguingly correlated with impaired interferon-signaling witnessed by downregulation of interferon regulatory factors 1 and 2. In addition, a highly active state of inflammasome was witnessed in critically ill patients by the detection of active GSDMD and the release of inflammasome-dependent alarmins, which in turn associate with the baseline of organ dysfunction and active pyroptosis. Thus, our data suggest that downregulation of *CASP4* but not *CASP5*, might contribute to the immunosuppressive phenotype in acute decompensated liver cirrhosis and sepsis.

Another part of the thesis provides a mechanistic insight into how the NLRP3 inflammasome is tightly regulated via CNPY3 chaperoning activity in homeostasis and host response. CNPY3 is known to chaperone and regulate the proper trafficking and subcellular distribution of multiple Toll-like receptors (TLRs) with exception of TLR3. We proposed that an upstream activation of canonical and non-canonical NLRP3 inflammasomes may require the chaperone activity of CNPY3 along with its known role in regulating multiple TLRs. Using THP-1 *CNPY3*$^{-/-}$ macrophages and macrophages derived from a patient with previously unknown loss-of-function variant (c.548delA) in *CNPY3* gene, we revealed that CNPY3 is required for sufficient activation of caspase-1 and secretion of the mature and exported forms of IL-1β and IL-18 as well as to induce rapid pyroptosis in response to well-known NLRP3 triggers including nigericin, cytosolic LPS, *Escherichia coli*, *Staphylococcus aureus,* and Group B streptococcus infection. Importantly, this function of CNPY3 is distinct and distinguishable from its role as TLR chaperone. Mechanistically, CNPY3 regulates the inflammasome independently of the oligomerization of the adaptor molecule apoptosis-associated speck-like protein (ASC specks) and NLRP3 stabilization. Intriguingly, CNPY3 is required to recruit caspase-1 into ASC-inflammasome complex upon NLRP3 activation.

Collectively, this work demonstrates that regulation of different caspases can differ during systemic inflammatory states and provides a mechanistic insight into how the NLRP3 inflammasome pathways intersect for maintaining a balance between inflammation in disease. In addition, this thesis reveals an unexpected, PRR-independent role of CNPY3 in canonical inflammasome activation, underlining a more complex, dedicated role of CNPY3 to the inflammatory response than anticipated.

Zusammenfassung

Die Immunantwort von Eukaryonten auf Pathogene und Pathogenbestandteile ist durch Immunzellen streng reguliert, wobei deren Beginn, Verlauf, und Beendigung durch komplexe Mechanismen gesteuert wird, um Fehlfunktionen, deren Spektrum von Hyperaktivität bis hin zu Autoimmunität sowie Immundefizienz reicht, zu vermeiden. Immunantworten auf unterschiedliche Erregerspezies sind durch distinkte Signalwege reguliert, die wiederum unterschiedliche immunologische Konsequenzen einleiten. In einem dabei gebildeten Proteinkomplex, dem Inflammasom, finden sich Kontrollpunkte, die zur Aufrechterhaltung der Homöostase und Verhinderung einer unangemessenen Immunantwort beitragen. Inflammasome sind hoch-molekulare Signaltransduktions-plattformen, die zur Aktivierung von sog. inflammatorischen Caspasen-1, -4, und -5 im Menschen und Caspase-1 und -11 im Maus, führen. Inflammatorische Caspasen vermitteln die in Folge der Erkennung von in die Wirtszelle eingedrungene mikrobielle Pathogene oder endogener Alarmine ausgelöste Produktion und Sekretion von Zytokine, sowie die Induktion eines speziellen Zelltods (Pyroptose). Dabei involvierte Schlüsselenzyme wie die murine Caspase-11 werden durch intrazellulär aufgenommenes Lipopolysaccharid (LPS) aktiviert, wobei diese unabhängig von Caspase-1 zur LPS-induzierten Letalität im Mausmodell beiträgt. Demgegenüber erkennen im Menschen Caspase-4 und Caspase-5 intrazelluläres LPS in ähnlicher Weise. Beide Proteinasen werden durch Bindung von LPS aktiviert, was in Folge zum Gasdermin-D- (GSDMD) vermittelten pyroptotischen Zelltod sowie zur autokatalytischen Spaltung und Aktivierung von Caspase-1 durch ein Sensorprotein des Inflammasoms (NLRP3) führt. Während die Überregulation der Inflammasom-Komponenten in der pro-inflammatorischen Immunreaktion gut aufgeklärt ist, ist im Gegensatz dazu über die Regulation der Inflammasom-Signalwege während der Phase einer Immunsuppression, welche in den Krankheitsbildern Sepsis- und akute dekompensierte Zirrhose auftreten, wenig bekannt. In dieser Arbeit wurden zirkulierenden Immunzellen (PBMCs und $CD14^+$ Monozyten) sowie Plasma von Patienten mit akut- dekompensierter Leberzirrhose und Sepsis, die die Sepsis-3-Kriterien erfüllen, eingesetzt und auf Gen- und Protein-regulatorischer Ebene untersucht. Als ein wesentliches Resultat, konnte miR-222 als Surrogatparameter aus zirkulierenden Immunzellen etabliert werden, um Patienten mit Symptomen einer Immunsuppression und Organdysfunktion zu identifizieren. Dieser Befund wurde im Hinblick auf die Regulation der inflammatorischen Caspasen (*CASP4*, *CASP5* und *CASP1*) sowie *GSDMD* als Effektor der Pyroptose während der Sepsis-assoziierten Immunsuppression näher analysiert. Im Gegensatz zu *CASP1* und *CASP5* ist die Expression von *CASP4* signifikant vermindert und korreliert invers mit Markern einer Organdysfunktion,

insbesondere MELD- und SOFA-Score. Außerdem korreliert *CASP4* mit einer verminderten Aktivität des Interferon-Signalwegs, was sich wiederum bei der Verminderung von Regulation von *Interferon regulatory factors* 1 und 2 widerspiegelt. Darüber hinaus lässt sich ein aktiver Inflammasom-Status in schwererkrankte Patienten durch die Erfassung von aktiven GSDMD und Freisetzung von Inflammasom-abhängigen Alarminen nachweisen, die mit dem Grad der Organdysfunktion und einer aktiven Pyroptose assoziieren. Somit demonstriert diese Arbeit, dass die Runterregulation von *CASP4*, aber nicht *CASP5* möglicherweise an der Immun-suppression von Patienten mit Sepsis und akut-dekompensierter Leberzirrhose beteiligt ist.

Darüber hinaus liefert die vorliegende Arbeit zusätzlich mechanistische Einblicke dazu, wie das NLRP3-Inflammasom durch die Aktivität des Chaperons CNPY3 zur Aufrechterhaltung der Homöostase und Wirtsreaktion reguliert ist. Mit Ausnahme des Subtyps 3 der Toll-like Rezeptoren (TLR) ist CNPY3 für die korrekte Faltung und subzelluläre Verteilung dieser *pathogen recognition receptors* (PRR) beteiligt. Eine weitere Hypothese in dieser Arbeit verfolgt die Frage, ob die Funktion der CNPY3-Chaperonaktivität und dessen funktionelle Rolle bei der Regulation der TLRs von einer PRR-abhängigen Aktivierung der *canonical* und *non-canonical NLRP3 Inflammasome* gesteuert wird. Hierzu wurden Versuche an THP-1 *CNPY3*$^{-/-}$ Makrophagen sowie an primären humanen Makrophagen, die aus Trägern einer bisher unbekannten *Loss-of-function*-Variante des *CNPY3* Gens (c.548delA) isoliert wurden, durchgeführt. Nach der Stimulation der Zellen mit NLRP3-Aktivatoren wie Nigericin, intrazellulärem LPS und pathogenen Mikroorganismen wie *Escherichia coli*, *Staphylokokkus aureus* und Streptokokken der Gruppe B konnte gezeigt werden, dass CNPY3 für die Aktivierung der Caspase-1 und somit für die Spaltung und Freisetzung von IL-1ß und IL-18 sowie für die Induktion der raschen Pyroptose essentiell ist. Mechanistisch reguliert CNPY3 das Inflammasom unabhängig von der Oligomerisierung des *Apoptose-Speck-like-Proteins* (ASC *speck*) und der NLRP3-Stabilisierung. Stattdessen ist CNPY3 erforderlich, um Caspase-1 in den ASC-Inflammasomkomplex während der NLRP3-Aktivierung zu rekrutieren.

Zusammenfassend demonstriert diese Arbeit eine differntielle Steuerung und komplexe Regulation einzelner Inflammasom-Signalwege. Der Unterschied in der Regulation der Expression der inflammatorischen Caspasen ist ein Beleg dafür, wie einzelne Inflammasom-Signalwege eigene Aufgaben in der Aufrechterhaltung des Inflammations-geschehens übernehmen. Darüber hinaus demonstriert diese Studie eine neue Ebene der Regulation des NLRP3-Inflammasoms durch CNPY3 und enthüllt somit eine unerwartete, PRR-unabhängige Rolle von CNPY3 bei der Inflammasom-Aktivierung, was eine komplexere, einschlägige Rolle von CNPY3 in der Entzündungsreaktion hervorhebt.

1. Introduction

1.1 Innate immunity

The innate and adaptive immune systems are the two major complementary systems of host defense, which have evolved in vertebrates to detect and fight against microbial pathogens (Kawai and Akira, 2011; Wu and Chen, 2014). Innate immunity reacts in a rapid but non-specific manner to pathogens, whereas the adaptive immune system reacts slowly and specifically with the generation of long-lived immunological memory (Iwasaki and Medzhitov, 2010; Netea et al., 2019). These two immune systems work tightly together and take on distinct tasks. Thus, components of the innate system contribute to the activation of the antigen-specific cells (Chaplin, 2010). Innate immunity is an evolutionary conserved immunological subsystem that constitutes the first critical line of defense against invading pathogens and sterile insults through distinct processes (Iwasaki and Medzhitov, 2010). The host cell, in particular cells of myeloid lineage such as a monocyte, macrophage, dendritic cell, and neutrophil employs multiple, distinct germ-line-encoded pattern-recognition receptors (PRRs) to detect the molecular structures named pathogen-associated molecular patterns (PAMPs) that are uniquely present in microorganisms and are essential for the pathogen life cycle (Medzhitov, 2008; Wu and Chen, 2014; Brubaker et al., 2015). Activation of these PRRs can be initiated also in response to the host derived endogenous 'damage'-associated molecular patterns (DAMPs) that are released in response to cell death, tissue injury or stress with functionally important immune consequences (Medzhitov, 2008; Zhang et al., 2010). PRRs are important for sensing their respective ligands and initiating downstream signaling cascades which drive gene expression, protein production and release, upregulation of costimulatory molecules and cell death while also shaping the adaptive immune response to dictate the fitness of the immune system (Pasare and Medzhitov, 2004; Kanneganti, 2019). Regardless of their origin, a wide range of microbial targets of recognition by PRRs are molecularly varied and include complex polysaccharides, lipoproteins, carbohydrates, flagellin, nucleotides, and microbial-derived nucleic acids (Iwasaki and Medzhitov, 2015; Brubaker et al., 2015). Except for nucleic acids, PAMPs are found in microbes but not the host, allowing the host to distinguish non-self from self through PRRs (Wu and Chen, 2014). Presumably, the mode of recognition of PRRs have evolved general classes: membrane-bound receptors (Cell-extrinsic recognition) and intracellular receptors (Cell-intrinsic recognition). Based on protein domain homology, PRRs can be broadly categorized into membrane bound receptors and cytosolic receptors. The former include Toll-like receptors (TLRs) and C-type lectin receptors (CLRs) and the latter include nucleotide-binding domain

and leucine-rich repeat (LRR) containing receptors (NLRs), and DNA sensors including AIM2-like receptors (ALRs) family members, as well as a family of enzymes that function as intracellular sensors of nucleic acids, including oligo adenylate synthase 1 protein, cyclic GMP-AMP synthase (cGAS), and RNA-sensing retinoic acid inducible gene I (RIG-I)–like receptors (RLRs) (Schroder and Tschopp, 2010; Hornung et al., 2014; Brubaker et al., 2015; Iwasaki and Medzhitov, 2015). In such a cellular network, comprehensive, and multi-level mechanisms have evolved to tightly regulate the strength and duration of the PRR downstream signaling cascade (Liu and Cao, 2016).

1.2 Mode of action of PRRs

To mediate specificity, the innate immune system is equipped with different modes of recognition and actions that render the different but suitable types of effector responses for a specific pathogen and promotes immunological memory (Iwasaki and Medzhitov, 2015).

1.2.1 Spatio-temporal regulation of PRRs responses

To modulate spatially (where) and temporally (when) signaling events, compartmentalization of multiple host receptors within a complex cellular infrastructure provides activation of distinct signaling events in a context-specific manner and this can define and orchestrate a unique signaling outcome (Brubaker et al., 2015; Antonescu and Liu, 2019). This aspect of innate immunity aids cells to protect from inappropriate immune response to self-encoded molecules that are not associated with infection such as nucleic acids sensing. For example, TLRs are compartmentalized within the intracellular space thereby limiting these receptors accessibility to host nucleic acids that are in the cytosol (Kagan et al., 2008; Barton and Kagan, 2009; Brubaker et al., 2015). Receptors of the innate immune system such as membrane bound TLRs or CLRs are typically specialized in the recognition of extracellular cues derived from different pathogens and allow cells to respond to changing environmental conditions (Iwasaki and Medzhitov, 2015; Brubaker et al., 2015). This class of recognition is a key factor in the spatiotemporal regulation, as it constitutes a priming signaling hub that integrates signals within and across the cell. The engagement of membrane bound PRRs is transcriptionally regulated and leads to the production of chemical and anti-microbial mediators. The released mediators (messengers) have context-dependent roles that initiate in turn the non-transcriptional responses such as innate and adaptive immunity as well as the induction of phagocytosis, inflammatory cell death, autophagy, and cytokine processing (Brubaker et al., 2015; Barrat et al., 2019). Unlike membrane bound receptors, intracellular receptors activate responses that differ from cell surface receptors such as cell death, a common feature of cytosolic receptor detection but

not generally a feature of cell surface signaling (Brubaker et al., 2015). The spatiotemporal regulation of membrane bound and intracellular PRRs can be mediated via different cellular processes such as chaperone-mediated trafficking of TLRs (Takahashi et al., 2007; Yang et al., 2007; Barton and Kagan, 2009; Liu et al., 2010; Saito et al., 2015) or nuclear modulation of signaling mediated by binding with nucleosomes such as the case for cGAS (Kujirai et al., 2020; Michalski et al., 2020; Pathare et al., 2020; Piperno et al., 2020).

1.2.2 Recognition molecules share effector mechanisms

Ligand binding induces the conformational changes in the respective receptors and promotes thereby the oligomerization of adaptor proteins or effector enzymes such as kinases and caspases through putative protein-protein interactions (Kagan et al., 2014). For a proper functioning of various signaling platforms, the innate immune signaling involves multivariant interactions, which are often assembled by adaptor proteins. The latter are vital cellular compartments that provide mechanisms controlling the crosstalk between or among signaling cascades in time and space to elucidate the precise specificity of cell signaling. Because adaptor proteins can be required by more than one receptor, they present a more functional complexity than the receptors (Brubaker et al., 2015; Kieser and Kagan, 2017). In this way, the adaptors perform a function that is more critical than the function of each receptor alone. Typically, each adaptor or adaptor set contains domains that allow for protein-protein interactions with an upstream receptor as well as a downstream signaling protein (Kieser and Kagan, 2017). The TLRs simultaneously utilize a set of sorting and signaling adaptors to engage the downstream enzymatic cascade. The TIR-containing adaptor protein (TIRAP) and the protein myeloid differentiation primary response 88 (MyD88) comprise one functional adaptor set for TLR signaling (Kieser and Kagan, 2017). MyD88 the downstream adaptor of most TLRs, activates the transcription protein NF-κB (nuclear factor-kappa B), which drives the expression of pro-inflammatory genes as part of the immune response, thus making MyD88 a central node of inflammatory pathways and adaptive immunity (Iwasaki and Medzhitov, 2010; Deguine and Barton, 2014). The common adaptor protein for the RLR pathway was initially shown to localize to the outer membrane of mitochondria and is referred to as the mitochondrial antiviral signaling protein (MAVS). In addition, the ASC, [apoptosis-associated speck-like protein containing a CARD (caspase recruitment domain)] is an important adaptor molecule for downstream singling of receptors that activate inflammasomes (Schroder and Tschopp, 2010; Zheng et al., 2020; Seoane et al., 2020). In short, signal transductions require serious modifications including, conformational changes to receptors, activation of enzymes and generation of second messengers resulting ultimately in the generation of transcriptional and

non-transcriptional effects to complete signal transmission and amplification as a mode of signal transduction and amplification (Wu, 2013; Kagan et al., 2014).

1.2.3 Macromolecular complex formation

The cell biology and dynamics of PRR signaling pathways is an elaborate process carried out in nature and assign high-order oligomeric structures containing a combination of protein, nucleic acid, cofactors and regulatory molecules, addressing thus the aspect of supramolecular organizing canters (SMOCs) (Wu, 2013; Kagan et al., 2014). Using different scaffolds and cellular compartments, molecules can drive the formation of new complexes and can even alter the location and function of cellular factors. These macromolecular complexes are spatially distributed on various membrane-bound organelles or other intracellular sites and aid signal amplification to define an ad hoc response threshold and specificity of cellular responses (Peterson-Kaufman et al., 2010; Kagan et al., 2014). Some well-studied examples illustrate these key concepts such as the formation of myddosome and inflammasome that form high-order assemblies of intracellular signalosomes to coordinate the cell´s internal machinery (Wu, 2013; Kieser and Kagan, 2017). The death domain-fold superfamily presents an almost ubiquitous feature of innate immune pathways. It consists of four subfamilies: the death domains (DDs), the death effector domains (DEDs), the caspase recruitment domains (CARDs), and the pyrin domains (PYDs). These domains are putative homotypic interaction modules that enable the formation of higher order multimeric complexes, which contribute predominantly to cell death and inflammation by activating caspases or protein kinases. Unlike G-protein coupled receptors, stimulation of TLR and interleukin (IL-)-1 superfamilies including IL-1R, IL-18, and IL-33 mediate the formation of myddosome via homotypic TIR/TIR (Toll/interleukin-1 (IL-1) receptor) and DD/DD interactions. Mechanistically, binding of a ligand (LPS, IL-1β, etc.) to TLR or IL-1R sequentially induces conformational changes to the respective receptors for stimulating downstream signaling pathway through homotypic death domains, DDs interaction of helical symmetry MyD88 adaptors. The latter seeds the formation of this multimeric structure through interactions with several interleukin-1 receptor associated kinases (IRAK) IRAK4 and IRAK2 or IRAK1 molecules (6:4:4), which in turn trigger the activation of multiple signaling cascades such as activation of the NF-κB (Burns et al., 2003; Gay et al., 2011; Netea et al., 2012; Wu, 2013). However, signaling of myddosome can be negatively regulated via the short form of MyD88s, which lacks the intermediate domain (INT) to block the recruitment of IRAK4 to IL-1R signaling (Burns et al., 2003) or via IRAK-M by trapping IRAK1 (in the activating receptor complex) and IRAK-4 from MyD88, preventing as a result the formation of IRAK- TRAF6 (TNF receptor-associated factor 6) complexes

(Kobayashi et al., 2002; Shalova et al., 2015). This trend of assembly can be formed either at the plasma membrane or on endosomes and culminate the other assemblies on organelles such as inflammasomes. Inflammasome assembly will be introduced hereafter in chapter 1.5.

1.3 Gene-specific regulation of innate immune system

To maintain genomic stability and ensure the specific subset of genes are activated or silenced at the right time and space, diverse epigenetic mechanisms such as DNA methylation, histone modifications, and non-coding RNA including micro-RNA (miRNA) are employed by the innate immune system (Jaenisch and Bird, 2003; Liu and Cao, 2016; Zhang and Cao, 2019). These regulatory mechanisms of gene expression have emerged to play crucial roles in gene-specific transcriptional regulation and activation of immune cells such as macrophages via controlling chromatin accessibility and selective pattern of gene expression (Liu and Cao, 2016; Seeley and Ghosh, 2016).

1.3.1 Histone modifications and chromatin remodeling

Establishing gene regulatory networks and functional re-programming during primary response mediated by TLRs or other stimuli requires chromatin modifiers/remodelers, that disrupt the closed nucleosome conformation and enable other factors to bind. Chromatin modifiers enable structural adaption of chromatin regions to signal the extracellular stimuli into the complex gene expression programs during inflammatory responses and chronic infection. Thus, chromatin modifications provide invaluable information for the crosstalk between inflammatory responses against different pathogens and induction of innate immune memory (Carson et al., 2011; Liu and Cao, 2016; Netea et al., 2019; Seeley and Ghosh, 2017). For instance, in naïve innate immune cells, certain genomic domains in which nucleosomes are occluded by histones and can be further occluded by higher order of chromatin structure and repression complexes such as the inactive enhancers that are usually occupied by lineage-determining transcription factors known as pioneers, such as PU.1 and marked with a combination of methylation of histone H3 at lysine 4 (H3K4me1) and repressive trimethylation of histone H3 at lysine 27 (H3K27me3) (Zaret and Carroll, 2011; Liu and Cao, 2016). Upon an immune response e. g. TLR activation, the pioneer transcription factor PU.1 opens up the local chromatin and directly makes it competent for the binding of other factors such as signal-dependent transcription factors such as NF-κB, IFN regulatory factor (IRFs), Activator protein 1 (AP-1), and signal transducer and activator of transcription (STAT) and relaxes chromatin structure with acquisition of acetylation of histone H3 at lysine 27 (H3K27ac) (marker of active transcription) and removal of H3K27me3 marks (marker of repressive transcription) (Liu and

Cao, 2016; Netea et al., 2019). However, various chromatin remodeling enzymes interact with chromatin and are implicated in adding, reading, or removing post-translational modifications (PTMs) to regulate expression of inflammatory genes via controlling chromatin status (Liu and Cao, 2016). In contrast, epigenetic silencing is engaged by acquisition of nonpermissive histone modifications (silent chromatin) and a block in TLR-induced nucleosome remodeling, resulting in a platform for insulating transcription factors (Foster et al., 2007; Chen and Ivashkiv, 2010; Seeley et al., 2018). In macrophages and monocytes, stimulation with LPS increases H3K4me3 on genes encoding factors involved in innate immunity that allows differential expression of subset of TLR-inducible genes classified into anti-inflammatory and anti-microbial genes (Foster et al., 2007; Chen and Ivashkiv, 2010; Seeley et al., 2018). Based on the dynamic progression of transcription initiations and the requirement of de novo protein synthesis for their expression in innate immune cells, primary response genes, which do not require de novo protein synthesis for pro-inflammatory response owing to permissive chromatin states at their promoters in a naïve state. For most of the secondary response genes, the induction of which require de novo protein synthesis during the initial response largely coincides with a strong dependency on SWI/SNF (switch/sucrose non-fermentable) complex-mediated chromatin remodeling. However, primary response genes are further divided into SWI/SNF- dependent, which result in increased chromatin accessibility to transcription factors, and SWI/SNF-independent which depends on the methylation pattern of CpG (cytidine-phosphate-guanosine) dinucleotides at the promotors of genes (Ramirez-Carrozzi et al., 2006; Ramirez-Carrozzi et al., 2009; Deaton and Bird, 2011). Moreover, non-CpG-promotors of IRF3-dependent primary response genes and type I interferon-induced factors exhibit strong dependence on SWI/SNF mediated nucleosome remodeling (Ramirez-Carrozzi et al., 2009). Furthermore, many studies have highlighted the importance of gene-specific regulation in immune-tolerant state of macrophages, which promote selective nucleosome remodeling to silence a subset of TLR-inducible genes (Foster et al., 2007; Chen and Ivashkiv, 2010; Carson et al., 2011; Seeley et al., 2018). The requirement of specific chromatin modifications illustrates an adaptive response in innate immune cells and exhibit a component specific regulation of acute and chronic inflammation.

1.3.2 DNA-Methylation (CpG islands)

Vertebrate CpG-dinucleotides islands (CGIs) are short genomic stretches that deviate considerably from the average genomic pattern with approximately 70% high and 30% low CGIs contents. The overall depletion of CpGs throughout the genome is assumed to be a consequence of the methylation of some germline CpGs and their susceptibility to mutation

(Saxonov et al., 2006). CGI promoters turn out to have characteristic patterns of transcription initiation and chromatin configuration. CGIs can locate on transcription start site (TSS), within gene bodies or between annotated genes remote from currently annotated TSSs (Deaton and Bird, 2011). Shared DNA sequence contains adapt CGIs for promoter function by destabilizing chromosome structure and regulating accessibility of the transcription machinery to regions of DNA to influence local chromatin structure and simplify the regulation of gene activity (Saxonov et al., 2006; Deaton and Bird, 2011). Thus, using their distinctive DNA sequence composition, silencing of CGI promoters is generally achieved through dense CpG methylation. While methylated CpGs within or in the vicinity of a gene restricts transcription, unmethylated CpGs allow that gene to be expressed, emphasizing strong correlation between CGIs and transcriptional regulation (Ramirez-Carrozzi et al., 2009). However, most of the promoters of constitutively expressed genes and primary response genes activated in response to an acute stimulus, such as a subset of TLR-induced genes were found in an open chromatin structure. This suggests that their transcriptional regulation is intrinsically induced in chromatin-state-independent manner such as SWI/SNF complexes and are rather attributed to the assembly of CGIs at proximal gene promoters into unstable nucleosomes. In contrast to primary response genes most secondary response gene lack CGIs (Ramirez-Carrozzi et al., 2006; Ramirez-Carrozzi et al., 2009; Deaton and Bird, 2011; Smale, 2014).

1.3.3 miRNAs as regulatory elements in immune system sense

Several factors contribute to the modulation of immune function and development including miRNA (Mehta and Baltimore, 2016). miRNAs are a class of endogenous small (~18–23 bp) non-coding RNAs that negatively regulate gene expression by directly binding in most cases within the 3´untraslated region (3´UTR) of specific target messenger RNA (mRNA) for cleavage or translational repression (Bartel, 2009; Mehta and Baltimore, 2016). miRNA genes are transcribed from DNA sequences as pri-miRNA (~60bp) by RNA polymerase II resulting in ssRNA molecule with a stem loop secondary structure (Taganov et al., 2006). Through sequential cleavage within the nucleus by ribonuclease III (RNASEN, also known as DROSHA) and *DGCR8* (DiGeorge critical syndrome region gene 8, also known as *PASHA*), pri-miRNAs are processed into a smaller mature form. The resulting RNA termed preliminary miRNAs (pre-miRNA) are then transported into the cytoplasm by exportin 5. Pre-miRNA is loaded onto Argonaute (AGO) family and subsequently processed by an endonuclease cytoplasmic RNase III enzyme Dicer to create a 18-23 bp mature miRNA. The resulting mature miRNA is then incorporated into the RNA-induced silencing complexes (RISCs), where they direct the recognition and translational repression or degradation of bound target mRNA

(Taganov et al., 2006; Mehta and Baltimore, 2016). Silencing occurs as a consequence of a combination of translational repression, de-adenylation, and de-capping 5′-3′ mRNA leading to mRNA degradation (Jonas and Izaurralde, 2015). miRNAs are abundant in multicellular species and can vary following the onset of cellular stress (O'Connell et al., 2007; Bartel, 2009). Numerous miRNAs have been found to take part in network architectures that influence both innate and adaptive immune cell development and function and serve therefore as a key developmental checkpoint for maintaining an optimal protein expression threshold during responses to inflammatory signal (Mehta and Baltimore, 2016). Inflammatory responses modify the biogenesis of miRNAs, which provide quantitative control of gene output in a context-dependent manner. Several miRNAs are enriched in immune cells and are regulated in a similar manner to other inflammatory genes to govern the immune response (O'Connell et al., 2007). Enforced expression of those miRNAs including the miR-146, miR-155, miR-132, miR-223 and miR-221/222 can modulate the immune system by targeting important regulators of the upstream signaling response to infection (Taganov et al., 2006; O'Connell et al., 2007; Neudecker et al., 2017; Seeley et al., 2018). miR-146a and miR-155 play an important role in macrophages′ development and immunity. They are strongly inducible by TLR signaling pathways via NF-κB. However, they exhibit a combined positive and negative feedback network controlling NF-κB activity (Taganov et al., 2006; Zhao et al., 2011a), thus serving as a brake to prevent aberrant immune activation (Taganov et al., 2006; O'Connell et al., 2007; Lu et al., 2010; Mehta and Baltimore, 2016). Targeting transcription factors or their regulator (repression or induction) via miRNA leads to altered feedback to the external signal. Recently, we recently reported that the miR-221/222 cluster gene regulates immunosuppression via the transcriptional silencing of *BRG1*, a transcription factor that leads to chromatin remodeling mediated by SWI/SNF and STAT, which in turn promotes immunosuppression (Seeley et al., 2018).

1.4 Pattern recognition receptors

1.4.1 Toll like receptors

1.4.1.1 TLRs signaling

Many families of PRRs have been identified. The most extensively studied PRRs are Toll-like receptors (TLR) and interleukin-1 receptors (IL-1R). TLRs were originally identified based on their homology with Drosophila *Toll* as essential receptors to govern the activation of a transcription factor called *dorsal* (Takeda and Akira, 2004; Beutler, 2009). Cell-surface TLRs recognize conserved, common microbial components that are accessible on the cell surface,

such as (LPS) of Gram-negative bacteria (TLR4), bacterial lipoproteins (TLR1/2 and TLR2/6), and flagellin (TLR5). Endosomal TLRs mainly detect microbial nucleic acids or their degradation products, such as double-stranded RNA (dsRNA) (TLR3), single stranded RNA (ssRNA) (TLR7), ssRNA and free uridine (TLR8), and CpG-rich DNA (TLR9) (**Fig. 1**) (Lee and Barton, 2014; Roers et al., 2016; Greulich et al., 2019). Nucleic acid sensing is typically linked with viral infections but are also a sign of living pathogens such as Gram-positive bacteria (Deshmukh et al., 2011; Roers et al., 2016; Greulich et al., 2019). Although the members of TLRs family have emerged as the primary evolutionarily highly conserved sensors of PRRs, TLR signaling appears as divergent and they play vital roles in many aspects of immune responses to given pathogens (Pasare and Medzhitov, 2004; Iwasaki and Medzhitov, 2015). TLRs have a horseshoe-like ectodomain structure built from LRR motifs and forming dimers that are strikingly similar in shape. TLRs interact with their ligands by sandwiching their respective ligands bringing the transmembrane and cytoplasmic domains in close proximity and triggering downstream signaling by recruiting intracellular adaptor proteins (**Fig. 1**) (Jin and Lee, 2008; Lee and Barton, 2014). Thus, the nature of the interactions of the TLR extracellular domains with their respective ligands varies widely across all TLRs. However, all TLRs induce downstream signals in a similar fashion because of the presence of conserved intracytoplasmic TIR domains that coordinates and specifies the regulation of several functionally distinct assembly of signaling cascades (Takeda and Akira, 2004). Except for TLR3, the TIRAP (known also as Mal) and MyD88 signaling adaptors comprise one functional adaptor set for activated TLRs (Fitzgerald et al., 2001; Takeda and Akira, 2004; Kieser and Kagan, 2017). Thus, TIR domain-containing adaptor MyD88 is essential for the inflammatory responses mediated by almost all the TLR family members to promote pro-inflammatory response through activation of NF-κB as part of immune response (Fitzgerald et al., 2001; Horng et al., 2002; Takeda and Akira, 2004; Deguine and Barton, 2014). A subgroup of TLRs including TLR3 and TLR4, can engage the adaptor protein TRIF which acts as a scaffold recruiting a kinase enzyme to add phosphate group to the transcription factor IRF3. However, TLR4 selectively uses the adaptor protein TRAM to bridge TLR4 with TRIF and the hallmark of this pathway is the production of type I interferon molecules (Kawai et al., 2001; Yamamoto et al., 2003a; Yamamoto et al., 2003b).

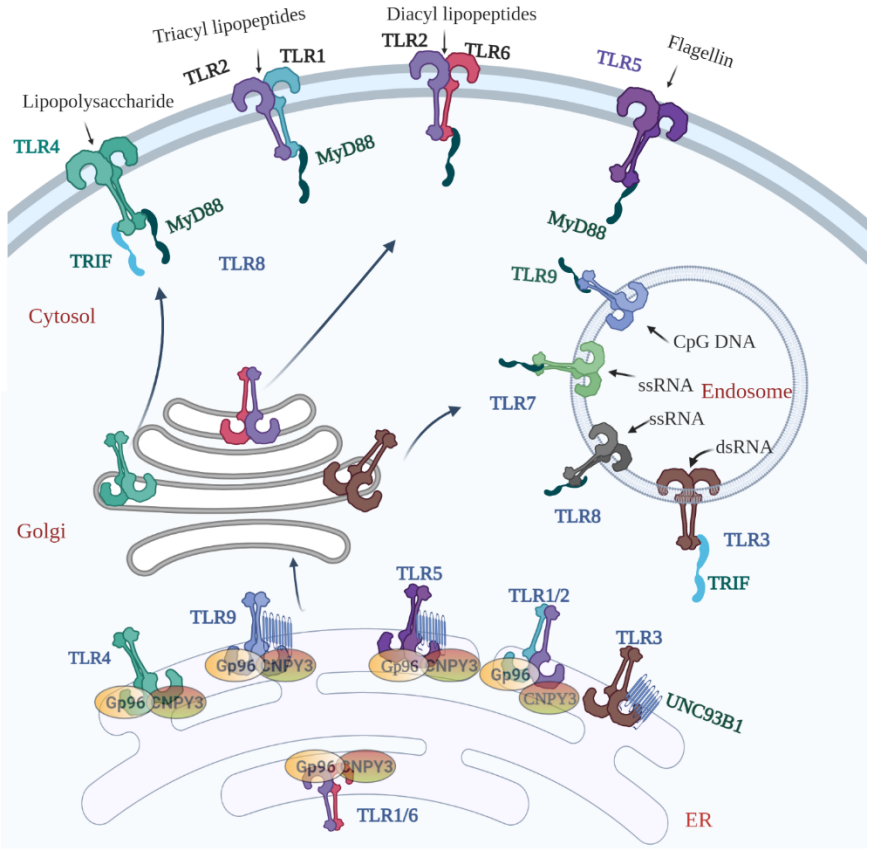

Fig. 1: Membrane bound and endosomal TLRs require specific chaperone binding partners for their correct assembly subcellular trafficking.
The TLRs are synthesized in the ER, traffic to the Golgi and ultimately localize to the cell surface or into endosomes. All TLRs have a horseshoe-like ectodomain structure and interact with their ligands as homodimers (TLRs, 3, 4, 5,7, and 9) or heterodimer (TLR2/1 and 2/6). Whereas surface resident TLRs 1, 2, 4, 5 and 6 recognize extracellular microbial ligands such as LPS, lipoproteins, and flagellin. The endosomal TLRs (3, 7, 8, and 9) recognize microbial nucleic acids. With exception of TLR3, most of the TLRs require folding chaperones Gp96 and its co-chaperon CNPY3. Surface TLRs and endosomal TLR9 require Gp96 and its co-chaperon CNPY3. Endosomal TLR3, 7, 8 and 9 and surface TLR5 require UNC93B1 to exit the ER. To mediates inflammatory signaling cascades, all TLRs with exception of TLR3 utilize MyD88, whereas TLR3 and TLR4 use the TRIF adaptor protein. (Created with BioRender.com).

1.4.1.2 Trafficking of TLRs via molecular chaperones

Molecular chaperones aid immunologically important proteins in the following ways: help folding during and after synthesis on the ribosome; translocation to the cellular site and across the membranes in which they normally reside and exert their functions; and refolding after incomplete denaturation by stressors (Nardai et al., 2006; Kim et al., 2013). To attain functionality, alongside the adaptors of TLRs within the cells, several chaperone protein mediated localization and trafficking of TLRs (clients) appear to play an important role not only in ligand recognition but also in the downregulation of signaling following ligand stimulation (Zanoni et al., 2011; Lee and Barton, 2014; Rajaiah et al., 2015; Majer et al., 2019a; Majer et

al., 2019b). All TLRs are synthesized in the endoplasmic reticulum (ER) and belong to type I transmembrane receptors that form dimers in the ER for subsequent subcellular trafficking and function (**Fig. 1**) (Wu et al., 2012). Hence TLRs require proper trafficking and localization to their compartments to exert their functions, TLRs traffic from the ER to the Golgi, and are translocated into the cell surface or to intracellular compartments such as endosomes via molecular chaperones (**Fig. 1**) (Kawasaki and Kawai, 2014). Regardless of TLRs destinations, with exception of TLR3, most TLRs including cell surface (TLR1, TLR2, TLR4, and TLR5) and intracellular (TLR7 and TLR9) seem to be folded by Glycoprotein 96 (Gp96), a paralogue of heat-shock protein 90 (HSP90) and acts as a master chaperone (Yang et al., 2007) and protein associated with TLR4 A (PRAT4A), (also known as Canopy FGF Signaling Regulator 3; hereafter referred to as CNPY3), which is a folding co-chaperone of Gp96 (**Fig. 1**) (Liu et al., 2010). With exception of cell-surface TLR5, the multi-spanning membrane protein Unc-93 homolog B1 (UNC93B1) controls the trafficking of intracellular TLRs including TLR3, 7 and 9 from the ER to endosomes to facilitate TLR cleavage and ligand recognition (Tabeta et al., 2006; Brinkmann et al., 2007; Kim et al., 2008; Kawasaki and Kawai, 2014; Huh et al., 2014; Pelka et al., 2018). In fact, UNC93B1 utilizes different trafficking mechanisms to regulate the activation of nucleic acid-sensing TLRs in endosomes (Fukui et al., 2009; Pelka et al., 2018; Majer et al., 2019a; Majer et al., 2019b). Interestingly, UNC93B1 governs the balance between TLR7 and TLR9 by favoring the trafficking of TLR9 instead of TLR7 and this is likely a potential mechanism to restrict the excessive activation of TLR7 to prevent autoimmunity (Fukui et al., 2009; Majer et al., 2019a). In addition, this path may functionally require endogenous chaperone Hsp90 (Saito et al., 2015). Moreover, TLR3 activation via poly(I:C) (Polyinosinic-polycytidylic acid) up-regulates UNC93B1, which in turn modulates the trafficking of differentially glycosylated forms of TLR3 to the plasma membrane and maintains the responsiveness of TLR3 and TLR9 signaling (Pohar et al., 2013). In addition to its function in trafficking of TLRs, Gp96 is an essential chaperone for folding integrins (Randow and Seed, 2001; Yang et al., 2007), however, this mechanism appears to be different than trafficking of TLRs (Wu et al., 2012). Thus, chaperones may offer distinct functional roles that do not rely on TLR-signaling.

1.4.2 NLRs and ALRs

Nucleotide-binding and oligomerization domain (NOD)-like receptors (NLRs) and Absent in melanoma 2 (AIM2)-like receptors (ALRs) are cytosolic PRRs that play a crucial role in the regulation of innate immune response and cell death pathways by recognizing PAMPs and DAMPs as well as environmental irritants (Schroder and Tschopp, 2010; Takeuchi and Akira,

2010; Nakaya et al., 2017). The NLR family consists of 23 human and 34 murine members that play various roles in the mammalian immune system to perform cytosolic surveillance for PAMPs and DAMPs (Dubois et al., 2016). NLR proteins have a common domain organization with a central NOD domain (NACHT: NAIP, CIITA, HET-E, and TP-2), which is generally flanked by N-terminal effector domain CARD or pyrin (PYD), and C-terminal LRR domain. The NACHT domain is involved in dNTPase activity and oligomerization. The C-terminal LRR domains are involved in ligand binding or activator sensing. The N-terminal domains perform effector functions by interacting with other proteins for downstream signaling (**Fig. 2**). ALRs including AIM2 and IFI6I (Interferon Alpha Inducible Protein 6) are characterized by the N-terminal PYD domain and one or two C-terminal hematopoietic interferon-inducible nuclear (HIN) domains, respectively (**Fig. 2**) (Schroder and Tschopp, 2010; Malik and Kanneganti, 2017). In the absence of a pathogenic ligand, NLRs and ALRs are maintained in an inactive monomeric state by autoinhibitory molecular interactions that stabilize their closed conformations and hinders their oligomerization and activation which is a common regulatory mechanism to protect against spurious activation of inflammasome (Feerick and McKernan, 2017; Malik and Kanneganti, 2017). Upon recognition and sensing of insults, a conformational change occurs in the monomeric receptors, allowing the NLRs and ALRs to homo-oligomerize through PYD-PYD associations and become activated via their NACHT and HIN domains, respectively. Activated NLRs show various functions by forming homo-oligomerize and act as a signaling platform for the assembly of adaptor and effector molecules. The variable N-terminal content dictates whether the receptor will respond to the insults by instigating signalosome (priming) or inflammasome assembly (activation) (Schroder and Tschopp, 2010; Jin et al., 2013; Dubois et al., 2016; Feerick and McKernan, 2017). In this study, I focus on the signalosome and the high molecular weight activating platforms (inflammasome).

1.5 The Inflammasomes

Inflammasomes are multiprotein complexes that assemble in response to the presence of a diverse range of microbial or endogenous danger signals to mediate an inflammatory form of cell death (pyroptosis) as well as the maturation and secretion of IL-1β and IL-18, key cytokines for innate and adaptive immune responses (Martinon et al., 2002; Schroder and Tschopp, 2010). Typically, inflammasomes are activated by different members of NLRs named after their sensors (NLRP1, NLRP3, NLRC4, and NAIP), AIM2, and Pyrin inflammasomes. In addition, a number of other NLR-family proteins, including NLRP2, NLRP6, NLRP7, NLRP9, and NLRP12, among others, have been proposed to serve as sensors in inflammasome complexes (Christgen et al., 2020). In response to PAMPs and DAMPs, a subset of sensors including

NLRs, ALRs, and Pyrin causes a series of downstream events and ultimately induce a unique innate immune response. This subset of sensors recruits zymogene protease, caspase-1 indirectly via ASC adaptor or directly via CARD and/or PYD domains into the complex, which then is converted into bioactive caspase-1 by proximity-induced self-cleavage (**Fig. 2**) (Dubois et al., 2016; Malik and Kanneganti, 2017; Yi, 2017; Boucher et al., 2018). Caspase-1 is recruited in these inflammasome scaffolds through direct homotypic associations involving its CARD motif and that of the nucleating PRR (NLRC4 (NOD-, LRR- and CARD-containing protein 4), Nlrp1b), or indirectly through homotypic interactions with the bipartite PYD/CARD inflammasome adaptor protein ASC in the case of PYD-containing NLRP3, AIM2, and Pyrin receptors (**Fig. 2**) (Broz et al., 2010; Dubois et al., 2016). The active caspase-1 protease controls the maturation of pro-IL-1β and pro-IL-18 to their active and exported forms, as a part of the canonical inflammasome pathway (Martinon et al., 2002; Malik and Kanneganti, 2017). Mechanistically, inflammasome activation is initially licensed by downstream signaling of PRRs which transcriptionally upregulate the expression of inflammasome components and gives rise to immature pro-inflammatory cytokine production "referred to as priming or signal 1", allowing cells to respond to its activation signal. In a second step "referred to as activation or signal 2", inflammasome assembly is induced by invading microbial or danger signals to process the immature cytokines generated by signal-1 (**Fig. 2**) (Bauernfeind et al., 2009; Franchi et al., 2009; Feerick and McKernan, 2017; Groslambert and Py, 2018). In addition, inflammasome activation coincides with cleavage of the Gasdermin-D (GSDMD), a substrate of caspases including murine caspase-1 and 11 and human caspase-1, 4 and 5 in order to trigger a regulated lytic cell death mode named pyroptosis (from Greek roots pyro, relating to fire fever, and ptosis, relating to falling) (**Fig. 2**) (Shi et al., 2015; He et al., 2015; Kayagaki et al., 2015; Liu et al., 2016). All inflammatory caspases cleave the cytoplasmic GSDMD between its N- and C-terminal domains, which leads to the release of the autoinhibitory interactions between the C-terminal inhibitory domain and N-terminal domain. The N-terminal domain oligomerizes as pores in the plasma membrane and mediates the release of the mature forms of (IL)-1α/β, IL-18 and many other alarmins as well as ASC specks. Thus, the absence of GSDMD does not influence the maturation of pro-IL-1β and pro-IL-18 mediated by caspase-1, but instead inhibits it release, suggesting that GSDMD acts as a conduit for the release of IL-1β, IL-18, and other mediators of pyroptosis (**Fig. 2**) (Moltke et al., 2012; Franklin et al., 2014; He et al., 2015; Shi et al., 2015; Kayagaki et al., 2015; Ding et al., 2016; Aglietti et al., 2016). In this perspective and in line with the detrimental consequences of inflammasome activation, I discuss emerging evidence on how this process is tightly regulated.

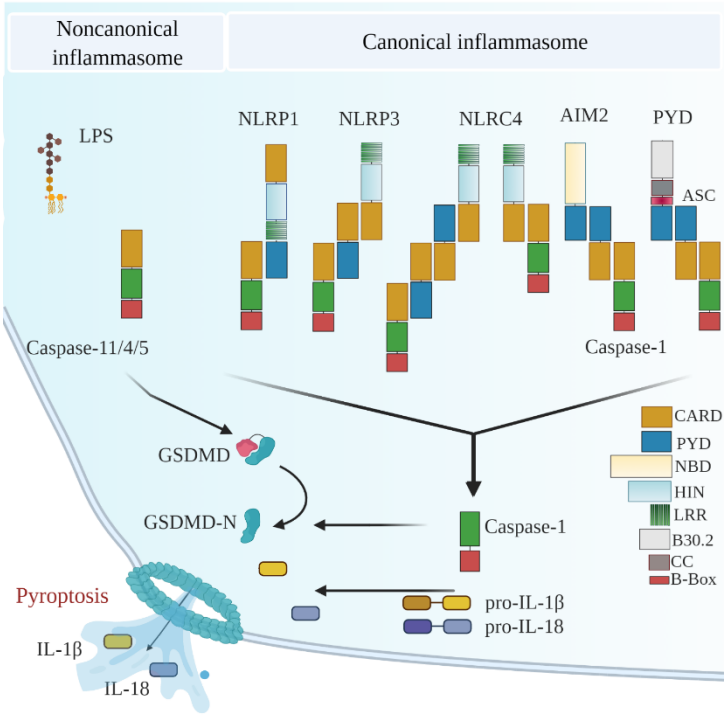

Fig. 2: Activation of inflammatory caspases in the canonical and noncanonical inflammasome pathways.
Canonical inflammasome assemble downstream of cytosolic PRRs to control the activation of caspase-1 and ultimately the maturation of pro-IL-1β and pro-IL-18 as well as induction of pyroptosis by mediating the cleavage of GSDMD. The domain structure of NLRP3, NLRP1, AIM2 and PYRIN contains a PYD domain, which directly interact with ASC adaptor. NLRC4 lacks a PYD domain but harbors a CARD domain. NLRC4 can directly interact with caspase-1 or indirectly with ASC via CARD-CARD interactions. The noncanonical inflammasome is mainly activated by cytosolic LPS and results in oligomerization of caspase-11/4/5. Activation of both paths independently results in activation of GSDMD-N, which then forms cytosolic pores leading to pyroptosis and release of active forms of IL-1β and IL-18. Domain: CC, coiled-coiled; B-Box, B-box region; B30.2 Pyrin C-terminal B30.2 domain. (Created with BioRender.com).

1.5.1 Inflammasome activation mechanisms

1.5.1.1 NLRP3 inflammasome

Of all inflammasomes, the best and most well-characterized and studied inflammasomes to date is the sensor NLRP3, as well as the adaptor protein ASC and the effector enzyme caspase 1, which is known as the canonical NLRP3 inflammasome (**Fig. 2**) (Schroder and Tschopp, 2010). The canonical NLRP3 inflammasome is engaged by a plethora of stimuli including PAMPs (peptidoglycan, flagellin, viral RNA, fungal hyphae, etc.), DAMPs (ATPs, cholesterol crystals, uric acid, etc.) (Mariathasan et al., 2006; Hornung et al., 2008; Muñoz-Planillo et al., 2013), as well as environmental irritants (alum, asbestos, silica, alloy particles, UV radiation, skin irritants, etc.) and medical relevant crystals and particles (Martinon et al., 2006; Hornung et al., 2008; Dubois et al., 2016). Due to the chemical and structural diversity of the vast array of NLRP3 inflammasome activators and their ability to trigger multiple cellular signals, a direct

ligand sensing model for the NLRP3 inflammasome is highly, unlikely, and not fully understood, but instead senses commonly induced intracellular signals (Mariathasan et al., 2004; Mariathasan et al., 2006; Shenoy et al., 2012; Latz et al., 2013; Muñoz-Planillo et al., 2013; Iwasaki and Medzhitov, 2015; Dubois et al., 2016; Liston and Masters, 2017; Groslambert and Py, 2018; Fisch et al., 2020). Indeed, the presence of pathogens can be detected based on structural and functional features. In this respect, NLRP3 activation presumably involves defined cellular events or secondary messengers that are commonly and selectively triggered by sensing functional characteristics that are indicative of a pathogenic presence (Mariathasan et al., 2006; Schroder and Tschopp, 2010; Iwasaki and Medzhitov, 2015; Liston and Masters, 2017). Cytoplasmic ion changes are responsible for sufficient recruitment and activation of NLRP3 inflammasome (Walev et al., 2000; Franchi et al., 2007; Franceschini et al., 2015). Among the most frequently reported ions in the modulation of NLRP3 activation is potassium (K^+) which utilizes the purinergic $P2X_7$ receptor and is a powerful activator of NLRP3 inflammasome (**Fig. 3**) (Mariathasan et al., 2006; Franchi et al., 2007; Muñoz-Planillo et al., 2013; Dubois et al., 2016). However, independent of $P2X_7$ receptors, various known NLRP3 activators and specific pathogenic microbes promote the activation of inflammasome, suggesting that intracellular depleted K^+ is sufficient but not a prerequisite for inflammasome activation (Mariathasan et al., 2006; Franchi et al., 2007; Allam et al., 2011; Franchi et al., 2012; Muñoz-Planillo et al., 2013; Kanneganti and Lamkanfi, 2013; Groß et al., 2016). Importantly, in human monocytes but not murine, Fas associated with death domain (FADD) and caspase-8 independently of K^+ efflux and pyroptosis were identified as activators of NLRP3 inflammasome, downstream of TLR4-TRIF-RIPK1 signaling axis, a pathway named alternative NLRP3 inflammasome (Gaidt et al., 2016). Notably, activation of the NLRP3 inflammasome requires several post-transcriptional and translational modifications, highlighting the importance of the tight regulation of this pathway; this will be introduced below (see chapter 1.5.2).

1.5.1.2 NAIP/NLRC4 inflammasome

NLRC4 (known also as ice protease-activating factor, IPAF) possesses a CARD domain, that can either directly recruit pro-caspase-1 or trigger the formation of ASC filaments, serving as an amplification mechanism required for cytokine maturation but dispensable for pyroptosis in response to the cytosolic presence of specific bacterial proteins (**Fig. 2**) (Broz et al., 2010; Man et al., 2014). NLRC4 inflammasome is activated in response to bacterial flagellin (Miao et al., 2006; Franchi et al., 2006) and inner rod and needle proteins of bacterial type III secretion systems (T3SSs) (Miao et al., 2010; Zhao et al., 2011b; Kofoed and Vance, 2011). However,

NLRC4 is activated indirectly by employing their sensor proteins, known as NAIPs (NLR family Apoptosis Inhibitory Proteins), that integrate cytosolic pathogen sensing and NAIP/NLRC4 inflammasome activation (Rauch et al., 2016). In mice, bacterial needle or inner rod proteins bind the Naip1 and Naip2 respectively, whereas Naip5 and Naip6 bind flagellin (Kofoed and Vance, 2011; Hu et al., 2015; Rauch et al., 2016). Humans possess a single NAIP (hNAIP) that functions analogously to Naip2/5 in mice and responds specifically to T3SS needle proteins (Zhao et al., 2011b; Yang et al., 2013). Upon interaction with their cognate ligands, NAIPs associate with NLRC4 to form a 10 to 12-spoks wheel-shaped oligomeric complex composed of 1 NAIP and 9-11 NLRC4 proteins (Halff et al., 2012; Zhang et al., 2015; Hu et al., 2015). The assembled NAIP/NLRC4 inflammasome then recruits and activates caspase-1 via the CARD in NLRC4 (Miao et al., 2006; Franchi et al., 2006; Rauch et al., 2016).

1.5.1.3 AIM2 and IFI16 inflammasomes

The human ALR family members AIM2 and IFI16 reside in the cytosol or nucleus respectively and bind to and sense bacterial and viral dsDNA and host DNA derived from damaged cellular organelles via their HIN-200 domains. (Fernandes-Alnemri et al., 2009; Hornung et al., 2009; Unterholzner et al., 2010; Dutta et al., 2015). AIM2 and IFI16 feature an N-terminal PYD and C-terminal HIN domain with tightly packed oligonucleotide or oligosaccharide binding folds. AIM2 does not contain a CARD domain and hence requires recruitment of ASC through their PYD domain for inflammasome activation in a NLRP3 signaling independent fashion (**Fig. 2**) (Vanaja et al., 2015; Broz and Dixit, 2016). In contrast, IFI16 and its mouse orthologue IFI204 is predominantly located in the nucleus and emerged as crucial regulators of STING (stimulator of interferon genes)-dependent IFN production and antiviral immunity and ASC-caspase-1 dependent inflammasome activation (Unterholzner et al., 2010; Kerur et al., 2011; Broz and Dixit, 2016; Li et al., 2019).

1.5.1.4 NLRP1, NLRP6 and pyrin inflammasomes

Similar to NLRC4, NLRP1 inflammasome binds directly to its ligand including muramyl dipeptide and long dsRNA to be sufficient to activate the assembly of the inflammasome (Martinon and Tschopp, 2004; Bauernfried et al., 2021). However, activation of NLRP1 inflammasome requires NOD2 as a coreceptor to activate inflammasome (Latz et al., 2013). Similarly, NLRP6 directly binds to lipoteichoic acid to regulate Gram-positive pathogen infection by induction of caspase-11 processing, which in turn promotes caspase-1 activation and maturation of IL-1β and IL-18 in macrophages (Hara et al., 2018). In addition, Pyrin inflammasome recruits caspase-1 via ASC and ultimately mediates caspase-1 activation (**Fig. 2**) in a specific response to Rho-glucosylation activity of *clostridium difficile* toxin B (TcdB)

and toxins of *Vibrio parahaemolyticus*, *Histophilus somni*, *Clostridium botulinum*, and *Burkholderia cenocepacia* (Xu et al., 2014).

1.5.1.5 Non-canonical inflammasome

Resistance to LPS, a major constituent of the envelope of Gram-negative bacteria, is conferred by genetic disruption of LPS-signaling elements including *Tlr4*, *Cd14*, *Md-2*, *Myd88*, *Tirap*, and *Irak-4* (Karaghiosoff et al., 2003; Tan and Kagan, 2014). LPS induced endotoxemia was assumed to be triggered via its cell surface response to TLR4 ligation and its subsequent downstream signaling. However, blocking of TLR4 via inhibitors such as TAK-242 or eritoran did not clinically meet the expectations in clinical trials as anti-sepsis drugs (Rice et al., 2010; Opal et al., 2013). For almost a decade, two independent studies have underlined the TLR4-independent mechanism, when priming of *Tlr4* $^{-/-}$ mice with poly(I:C), which activates TLR3, remodeled the cellular prerequisites for LPS induced lethality, indicating thereby an alternative pathway for LPS-sensing termed non-canonical inflammasome (Kayagaki et al., 2011; Hagar et al., 2013; Kayagaki et al., 2013). Unlike the NLRP3 canonical pathway, the non-canonical inflammasome pathway employs caspase-11 in mice and its human orthologs caspase-4 and -5 and are required for cytosolic-LPS induced lethality (**Fig. 2**). Caspase-11, 4 and 5 engage pyroptosis independently of the NLRP3 inflammasome while maturation of pro-IL-1β and pro-IL-18 is relayed through the NLRP3-ASC-caspase-1 inflammasome complex after Gram-negative bacterial infection or cytosolically delivered LPS (**Fig. 3**) (Kayagaki et al., 2013; Hagar et al., 2013; Kajiwara et al., 2014; Shi et al., 2014; Baker et al., 2015; Schmid-Burgk et al., 2016). Interestingly, intact LPS or its acetylated lipid A moiety LPS binds the N-terminal CARD domain of caspase-11, 4 and 5 but not -1 (Shi et al., 2014; An et al., 2019). In contrast to penta- and hexa-acylated lipid A, tetra acylated lipid A failed to bind to caspase-11. Like caspase-11, the lipid tail of LPS binds directly to caspase-4 and 5 (Shi et al., 2014). However, in contrast to caspase-11, caspase-4 can recognize under-acylated LPS to engage non-canonical inflammasome (Lagrange et al., 2018). Activation of caspase-11, 4, 5 activate GSDMD and its pyroptosis inducing activity in turn promotes both pyroptosis and NLRP3-dependent activation of caspase-1 in a cell-intrinsic manner (**Fig. 2**) (Shi et al., 2014; Baker et al., 2015; Kayagaki et al., 2015; Ding et al., 2016; Aglietti et al., 2016). Since *Nlrp3*$^{-/-}$ and *Casp1*$^{-/-}$ mice are not resistant as *Casp11*$^{-/-}$ mice, IL-1β and IL-18 cytokines were not found to be the key effector of caspase-11 mediated sepsis shock, suggesting that caspase-11-elicited pyroptotic cell death is the primary driver in LPS-lethality (Kayagaki et al., 2011; Gurung et al., 2012; Broz et al., 2012; Aachoui et al., 2013; Pfalzgraff and Weindl, 2019).

Upon Gram-negative infection, caspase-11 innate immunity is transcriptionally licensed by IFN signaling (Schauvliege et al., 2002; Kayagaki et al., 2011; Broz et al., 2012; Gurung et al., 2012; Rathinam et al., 2012; Aachoui et al., 2013) and post-transcriptionally by host IFN-induced GBPs together with immunity-related GTPase family member b10 (IRGB10) which destabilize Gram-negative bacteria-containing vacuoles and LPS-containing vesicles such as outer membrane vesicles (OMVs) in order to liberate LPS into the cytosol and subsequently enhance the accessibility to caspase-11 (Meunier et al., 2014; Pilla et al., 2014; Finethy et al., 2015; Vanaja et al., 2016; Wacker et al., 2017; Wandel et al., 2020; Santos et al., 2020). Interferon treatment induces the expression of GTPases signaling including GBPs and IRGs (immunity related GTPases) as well as non-canonical inflammasome constituents *CASP4*, *CASP5* and *GSDMD* during Gram-negative infections (Rathinam et al., 2012; Pilla et al., 2014; Man et al., 2015; Santos et al., 2018; Benaoudia et al., 2019; Kayagaki et al., 2019; Kutsch et al., 2020; Brubaker et al., 2020). GBPs are the most highly expressed interferon-stimulated gene (ISGs) family of antimicrobial proteins (human GBP1-7, and mice GBP1-13) by host cells to target intracellular pathogens and pathogen containing vacuoles (Kim et al., 2016). In this context, emerging recent studies have demonstrated that GBPs are required for non-canonical inflammasome activation by Gram-negative bacterial infection or cytosolically-delivered LPS. To facilitate cytosolic detection, GBP-1 binds to cytosolic LPS and initiates the assembly of signaling platform cooperatively with other GBPs (GBP2-4) on the surface of bacterial cells to drive the recruitment and activation of caspase-4 and thus disrupt Gram-negative bacterial cell envelope functions (Fisch et al., 2019; Santos et al., 2020; Wandel et al., 2020; Fisch et al., 2020; Kutsch et al., 2020). However, this process can be dampened in a feedback loop manner by caspase-1-mediated GBP1 cleavage to suppress caspase-4 triggered pyroptosis (Fisch et al., 2020). Consequently, the targeted genetic deletion of non-canonical inflammasome components including *Casp11*, *Gsdmd*, and *Gpbs* (Wang et al., 1998; Kayagaki et al., 2013; Hagar et al., 2013; Aachoui et al., 2013; Finethy et al., 2015; Tang et al., 2018) or its upstream regulatory molecules such as *IFNB*, *C3aR*, *TIRF* transcription factors including *Irf2,* and *Stat1* (at low doses of LPS), and enzyme kinase *Tyk2* are highly resistant to LPS-induced lethality independently of caspase-1 (Cuesta et al., 2003; Karaghiosoff et al., 2003; Napier et al., 2016; Tang et al., 2018). Thus, these regulators play a key role in non-canonical inflammasome function and emphasize the physiological importance of pyroptosis during sepsis progression. In addition, independently of caspase-1, activation of non-canonical inflammasome is not only associated with pyroptosis, but also accompanied with release of several alarmins or DAMPs such as IL-1α, HMGB1, prothymosin-α, Galectin-1 and S100A8. These danger-signaling

molecules might contribute to tissue damage, subsequently organ failure, and poor outcomes during sepsis (Lorey et al., 2017; Russo et al., 2018; Russo et al., 2021; Phulphagar et al., 2021). However, little is known about the overlapping or divergent functions of caspase-11 human orthologue caspase-4 and -5, which may in turn consequently initiate a major hub for translational machinery or activation of caspase-1 in infectious and chronic diseases.

1.5.2 Signaling pathways controlling NLRP3 inflammasome assembly and activation

Recent studies have shed a light on the eminent importance of transcriptional and post-transcriptional regulations/modifications to orchestrate inflammasome mediated signaling.

1.5.2.1 Transcriptional Regulation of NLRP3 Inflammasomes

Inflammasome activation requires a proper magnitude of response during acute and chronic inflammation and is often dependent on the regulation of specific sensors and/or their downstream adaptors/effectors (Gurung et al., 2015; Kanneganti, 2019; Christgen et al., 2020; Cornut et al., 2020). Upstream regulatory molecules such as transcription factors are crucial for the downstream activation of inflammasome machinery. Multiple studies have shown that NF-κB and IRF family transcription factors play a key role in the upstream regulation of inflammasome (Bauernfeind et al., 2009; Benaoudia et al., 2019; Kayagaki et al., 2019; Christgen et al., 2020). NF-κB is a well-known mediator during inflammatory responses. Upon activation, NF-κB modulates the expression of numerous genes involved in the immune response including inflammasome genes such as pro-IL-1β and NLRP3 which are critical checkpoints for NLRP3 inflammasome activation (Bauernfeind et al., 2009; Viganò et al., 2015). During infections such as *F. novicida*, IRF1 enhances the expression of ISGs and inflammasome associated genes including *CASP4*, *CASP5*, *CASP1*, *Casp11, AIM2* and *GSDMD* encoding genes as well as *GBPs* and *IRGB10* to carry out their roles in liberating bacterial ligands e. g. LPS and DNA to govern a host defense against invading pathogens (Rathinam et al., 2012; Meunier et al., 2014; Zhu et al., 2018; Kayagaki et al., 2019; Benaoudia et al., 2019). The basal expression of *CASP4* and *GSDMD* is operated by IRF2, however, in some cases, IRF1 cooperates with IRF2 to induce their expression in presence of infection /inflammation or IFN-treatment (Kayagaki et al., 2019; Benaoudia et al., 2019). IRF8 is required for the expression of the key components of NLRC4 inflammasome, which includes *Naip1*, *Naip2*, *Naip5*, and *Naip6* (Karki et al., 2018). In contrast, the adaptor protein ASC is constitutively expressed and remains unchanged during inflammatory responses, *CASP1* is constitutively expressed, however the promotor of *CASP1* contains putative binding sites of NF-κB and IRF and was reported to be upregulated by NF-κB and IRF1 under pathological

conditions (Lee et al., 2015; Benaoudia et al., 2019; Christgen et al., 2020). In contrast, *CASP5* regulation is poorly understood. The human THP-1 and U937 macrophages fail to express *CASP5* in steady state (Shi et al., 2014; Schmid-Burgk et al., 2015; Benaoudia et al., 2019), however, unlike *CASP4* but like murine *Casp11*, *CASP5* requires a *de novo* expression via e. g. LPS and IFN signaling (Lin et al., 2000; Bauernfeind et al., 2009; Viganò et al., 2015; Schmid-Burgk et al., 2015; Brubaker et al., 2020). However, this regulation mechanism of inflammasome via IRF family can vary in a cell specific manner. In this context, expression of IRF4 and IRF8 in conventional dendritic cells (cDCs) inhibits inflammasome- associated genes to circumvent pyroptosis and preserve their ability for T cell priming to initiate an adaptive immune response (McDaniel et al., 2020). Moreover, recent studies have documented that epigenetic mechanisms play an important role in the modulation of inflammasome as reviewed by Poli and colleagues (Poli et al., 2020).

1.5.2.2 Post-transcriptional regulation and trafficking toward the NLRP3 inflammasome

A complex array of post-transcriptional modifications (PTMs) of inflammasomes provide it´s tight regulation in homeostasis and in disease (Strowig et al., 2012; Groslambert and Py, 2018; Seoane et al., 2020). NLRP3 is thought to be constitutively (non-degradative) ubiquitinated and non-translational priming induced by e. g. TLR ligation leads to NLRP3 deubiquitination in a mitochondrial reactive oxygen species (mtROS) dependent fashion (Juliana et al., 2012). IRAK-1 kinase activity bypasses the priming step to establish a rapid NLRP3 inflammasome activation by modulating its deubiquitination of NLRP3 independent of new protein synthesis (Juliana et al., 2012; Fernandes-Alnemri et al., 2013; Lin et al., 2014). In a phosphorylation independent manner, NEK7, a member of the family of mammalian NIMA-related kinases (NEK proteins), physically interacts with NLRP3 protein in interphase and acts downstream of K^+ efflux to regulate NLRP3 inflammasome but not NLRC4 or AIM2 inflammasomes (**Fig. 3**) (He et al., 2016; Shi et al., 2016). Under resting conditions, ASC is found in the mitochondria, cytosol, and nucleus, caspase-1 localized in the cytosol, whereas NLRP3 associates mainly with the ER (**Fig. 3**) (Zhou et al., 2011; Sharma and Kanneganti, 2016). Notably, nucleation of the inflammasome requires a subcellular re-arrangement of these molecules to facilitate their associations (Misawa et al., 2013; Chen and Chen, 2018; Magupalli et al., 2020). Under NLRP3 priming or activation NLRP3 migrates from ER to MAM by assistance of microtubule-affinity regulating kinase 4 MARK4, which directly binds to NLRP3 to proceed the interaction with its adaptor protein ASC in close proximity (Misawa et al., 2013; Sharma and Kanneganti, 2016; Li et al., 2017; Elliott et al., 2018).

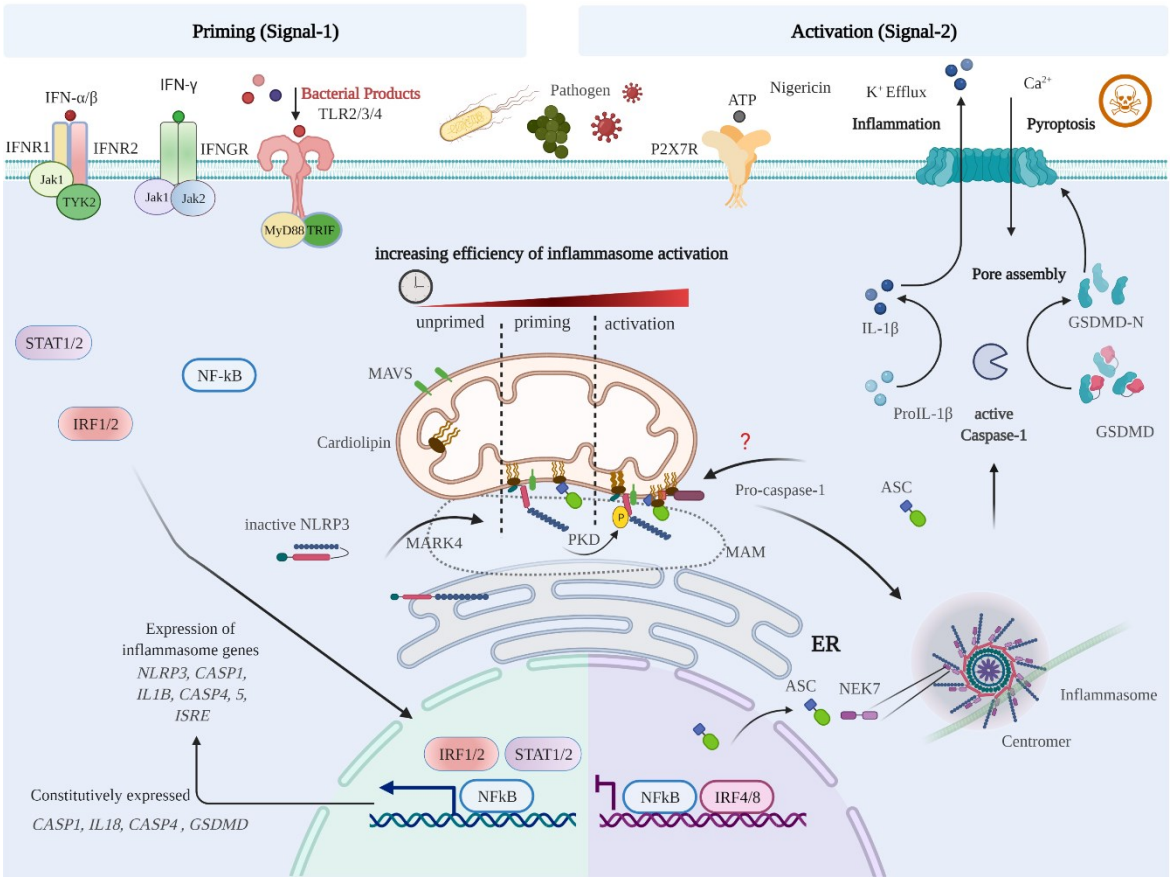

Fig. 3: Control of NLRP3 inflammasome activation.
The assembly of NLRP3 inflammasome requires tightly regulated priming and activating signals in response to infections and cellular damage. Different pathways can successively control priming of NLRP3 following TLR and IFN activation (Signal-1). Signal-1 primes the expression of inflammasome core components which relies on different adaptor molecules such as MyD88, TRIF, TYK2 proteins and transcription factors such as NF-κB and STAT and IRF families following e. g. TLR2/3/4 activation. Downregulation of IRF4 and IRF8 can permit macrophages to maintain expression of inflammasome-associated genes. Post -transcriptionally, priming licenses the migration of NLRP3 from ER into MAM via MARK4. NLRP3 can anchor to MAMs via adaptor proteins such as MAVS and cardiolipin. Following an activation event (Signal-2), inactive NLRP3 can be activated by phosphorylation via PKD resulting in recruitment of ASC and zymogene caspase-1 to culminate autoactivation of pro-caspase-1 with assistance from NEK7, as an integral inflammasome component. Inflammasome assembly and its downstream function occur at the MTOC to form a single speck in the perinuclear region of the affected cell. Activation of caspase-1 results in maturation of pro-IL-1β and pro-IL-18 as well as activation of GSDMD-N to oligomerize in the cell membrane to form pores and ultimately induce pyroptosis and secretion of mature IL-1β. (Created with BioRender.com).

An array of interactors mediates NLRP3 translocation have been described to facilitate its activation including cardiolipin (Iyer et al., 2013) and cFLIPL (Wu et al., 2014) which interact with LRR domain as well as MAVS that interacts with PYD domain of NLRP3 (Subramanian et al., 2013). These changes in localization allows NLRP3 to undergo self-oligomerization and mediates the subsequent apposition of ASC on NLPR3 at MAMs before being released in the cytosol (Misawa et al., 2013; Sharma and Kanneganti, 2016; Elliott et al., 2018). However,

clustering of mitochondria around (at) the Golgi and phosphorylation of NLRP3 by Golgi-associated protein kinase D (PKD) at S295 controls this release. NLRP3 and ASC then colocalize into one cytosolic perinuclear speck that is located at the centrosome, also known as the microtubule-organizing center (MTOC) and leads to the recruitment and activation of caspase-1 (**Fig. 3**) (Zhang et al., 2017; Li et al., 2017; Groslambert and Py, 2018; Magupalli et al., 2020; Seoane et al., 2020). Phosphorylation of ASC and caspase-1 have also been reported to be critical for inflammasome activation (Basak et al., 2005; Hara et al., 2013). Moreover, other inflammasomes and their components including ASC, caspase-1, and its substrate pro-IL-1β, pro-IL-18, and GSDMD were reported to undergo post-transcriptional modification such phosphorylation and S-glutathionylation (Shim and Lee, 2018; Seoane et al., 2020).

1.5.2.3 Negative regulation of NLRP3 inflammasome

As a part of transcriptional and post-transcriptional programs, several molecules and pathways can directly or indirectly impede the assembly of inflammasomes by employing several negative feedback paths. This coordinated regulation of the inflammasomes is necessary to prevent tissue damage and other harmful consequences of excessive inflammasome activation(Gurung et al., 2015; Matusiak et al., 2015; Zheng et al., 2020). To this end, different mechanisms and factors that interact with priming and activation signals of inflammasome assembly have been reported. Exposure of myeloid cells to chronic activation involves upregulation and downregulation of hundreds of pro- and anti-inflammatory cytokines (Matusiak et al., 2015).Acute activation of TLRs leads to transient upregulation of inflammasome NLRP3 but during chronic inflammation dampened activation of NLRP3 inflammasome via IL-10 signaling aids to reduce the effect of acute priming step in an autocrine manner (Gurung et al., 2015). Induction of type-I interferon signaling through TLR-TRIF-STAT1 pathway induces IL-10, which in turn inhibits NLRP3 and NLRP1 pathways in an autocrine dependent manner via STAT3 dependent signaling (Guarda et al., 2011). Surprisingly, NF-κB can also negatively regulate the activation of inflammasome to prevent an excessive NLRP3-inflammasome activation in general (Greten et al., 2007; Zhong et al., 2016). Different studies suggested that NF-κB promotes autophagy, a quality control process that negatively regulates inflammasome pathways. Autophagy pathway keeps inflammasome activation in check by the elimination of mitochondrial signals including mtROS, mtDNA, and damaged mitochondria to restrict inflammasome activity (Zhong et al., 2016; Harris et al., 2017). Because the assembly of inflammasome requires homotypic CARD–CARD and PYD–PYD interactions, certain PYD-only proteins (POPs) and CARD-only proteins (COPs) can act as dominant-negative regulators by sequestering key components of the inflammasome

signaling pathway to impede downstream signaling (Greten et al., 2007; Matusiak et al., 2015). miRNAs have recently emerged as an alternative mechanism for regulating inflammasome such as miR-223, which restrains inflammasome activation by regulating NLRP3 for intestinal homeostasis (Neudecker et al., 2017). Together, these priming mechanisms provide effective checkpoints that impede accidental inflammasome activation (Dubois et al., 2016). Noteworthy, chaperones on the other hand such as suppressor of the G2 allele of skp1 (SGT1) and heat shock protein 90, which have E3 ligase activity, undergo interaction with specific NLRs including NLRP3, as well as NLRC4, NOD2, NOD1, and NLRP12 to retain an inactive but stabilized structure in resting conditions (Mayor et al., 2007). In contrast to phosphorylation mediated by PKD (Zhang et al., 2017), phosphorylation of NLRP3 via protein kinase A (PKA) at S295 mediates its inactivation process (Mortimer et al., 2016; Guo et al., 2016). For fine tuning of inflammasome signaling, different negative regulatory mechanisms such as nitrosylation, ubiquitination, succination, and de-ubiquitination also exist and underly the tight network of mechanical and kinetic regulation of inflammasome (Shim and Lee, 2018; Groslambert and Py, 2018; Humphries et al., 2020). Lastly, for the non-canonical inflammsome, endogenous molecules such as Stearoyl lysophosphatidylcholine (LPC) (Li et al., 2018) and oxidized phospholipid oxPAPC (Chu et al., 2018) were found to directly bind to caspase-4 and -11 and thus they *in vivo* compete with LPS for caspase binding to reduce LPS-induced lethality.

1.5.3 Inflammasome associated diseases

In terms of its importance to maintaining the balance between inhibition and activation of the inflammation and its function to eliminate any sources of danger without causing harm to the host, dysregulation of signaling pathways of inflammasomes are associated with prevalent diseases.

1.5.3.1 Inflammasome associated non-infectious inflammatory diseases

In patients where inflammation does not meet with infections, it is highly likely that diseases are related to genetic factors. Despite regularly providing protection against invading pathogens, inflammasome activation is often detrimental in a wide range of auto-inflammatory, autoimmune, metabolic, neurodegenerative, and tumorigenesis disorders. Dysregulated inflammasome activity has been implicated in the pathogenesis of human heritable and acquired inflammatory diseases. *NLRP3*, also known as cryopyrin, or *CIAS1*, was initially described for its genetic association with hereditary inflammatory diseases known as familial cold autoinflammation syndrome (FCAS), Muckle-Wells syndrome (MWS), and neonatal-onset multisystem inflammatory disease/chronic infantile neurologic cutaneous articular syndrome

(NOMID/CINCA), in the order of increasing severity (Strowig et al., 2012; Saxena and Yeretssian, 2014; van Gorp et al., 2016; Mangan et al., 2018; Heneka et al., 2018; Voet et al., 2019). Auto-inflammatory disorders related to defects in *NLRP3* gene are then collectively named cryopyrin-associated periodic syndromes (CAPS). The gain of function mutations in the Pyrin-encoding gene, *MEFV*, causes a human autoinflammatory disease known as familial Mediterranean fever (FMF). Moreover, dysregulation of inflammasome regulators and effectors has been additionally associated with other prevalent metabolic disorders including type 2 diabetes mellitus and Gout as well as several neurodegenerative diseases, including Alzheimer's and Parkinson's diseases, and other aging-related diseases (Kastner et al., 2010; Chae et al., 2011; Saxena and Yeretssian, 2014; Heneka et al., 2018).

1.5.3.2 NLRP3 Inflammasome-associated infectious diseases.

Growing evidence such as the deletion of a wide range of virulence factors and toxins that interact with and influence the pathway either within or on host cells through specific receptors and on or within cellular compartment supports the central role of the inflammasome during infectious disease (Ramachandran, 2014; Storek and Monack, 2015). During the process of systemic inflammation such as sepsis and cirrhosis, activation of inflammasomes plays a critical role in the defense and clearance of invading pathogens. Cell death pathways including apoptosis, necroptosis, and pyroptosis are derived by multiple caspases, that are undeniably linked to be important in sepsis through considerable substantial crosstalk (Aziz et al., 2014; Kesavardhana et al., 2020; Stengel et al., 2020).

1.5.3.2.1 Sepsis

Sepsis is life-threatening organ dysfunction that results from the body´s response to invasive infection (Sepsis-3 definition) (Singer et al., 2016). Undeniably, sepsis is still the largest cause of death in most intensive care units with an estimated 11 million deaths annually worldwide, which accounts for almost 20% of all global deaths (Rudd et al., 2020). A wide array of manifestations including an unbridled systemic inflammatory response termed SIRS, multiple organ damage and host factors (age, sex, comorbidities, etc.) and the causative pathogen (virulence, load) shape the biological and clinical heterogeneity of the disease and the varied severity degree in affected individuals (Hotchkiss et al., 2013; Boomer et al., 2014; Singer et al., 2016). An additional factor to consider is that responses in sepsis can alternate between hyperactivity and immunosuppression "immune paralysis", providing very limited capacity for therapeutic intervention in this condition (Osuchowski et al., 2012; Boomer et al., 2014; Rubio et al., 2019). Immunosuppression is associated with susceptibility to secondary infections (often with the opportunistic pathogen), organ dysfunction/failure, dysfunction of adaptive immune

response, and ultimately poor outcome. Therefore, patients who survive early sepsis but continue to be dependent on intensive care have numerous indications of immunosuppression; which shape a predominant driving force for morbidity and mortality in sepsis (Boomer et al., 2011; Carson et al., 2011; Hotchkiss et al., 2013). Distinct studies have highlighted the reduced responsiveness of cells in both the myeloid and lymphoid cell lineages to pathogens in patients with sepsis in part reflected by decreased expression of human leucocyte antigen DR (HLA-DR) on myeloid cells (van der Poll and Opal, 2008; Carson et al., 2011; Boomer et al., 2011; Winkler et al., 2017). Boomer et al., have indicated strong impairments of cell functionalities in cells collected from spleen and lung of patients who had died from sepsis in the intensive care unit (ICU) and that sepsis induces several overlying mechanisms of immunosuppression. It has been suggested that these chronic manifestations are induced to counteract the effect of the initial hyperinflammatory phase (Boomer et al., 2011). According to the criteria of Sepsis-3, organ dysfunction is currently considered by an increase in the Sequential Organ Failure Assessment (SOFA) score of 2 points or more (Singer et al., 2016). During the process of sepsis, activation of inflammasomes plays a critical role in the defense and clearance of invading pathogens. Cell death pathways are engaged by active caspases, that are undeniably linked to be important in sepsis through considerable overlapping functions (Aziz et al., 2014; Kesavardhana et al., 2020). In contrast to accidental and non-lytic cell deaths, programmed lytic cell death pathways like pyroptosis is highly inflammatory (Jorgensen et al., 2017). During sepsis, the activation of both canonical and non-canonical NLRP3 inflammasome signaling pathways is associated with induction of pyroptosis and generation of the functional forms of IL-1β, IL-18, IL-33, IL-1α cytokines and release alarmins like HMGB1, Progranulin (PGRN), and Galectin-1 (Gal-1) as well as extracellular active ASC-oligomers. Release of such mediators in turn exerts different inflammatory responses, but it can also damage non-infected tissues and lead to the dysfunction of different organs and systems (Franklin et al., 2014; Song et al., 2016; Kumar, 2018; Deng et al., 2018; Martínez-García et al., 2019; Russo et al., 2021). In addition to pyroptotic cell death and inflammation, functionally activate inflammasomes are linked also with pathogen detection, mitochondrial failure, DNA damage, and activation of coagulation in sepsis (Martínez-García et al., 2019; Yang et al., 2019; Zhang et al., 2020).

1.5.3.2.2 Cirrhosis

Cirrhosis, in which the hepatic architecture is distorted, can arise from various etiologies like infectious (sepsis) and exogenous toxic and allergic processes and account for the most common cause of liver-related death globally (Wiegand and Berg, 2013; Angeli et al., 2018). Cirrhosis is classified into two key prognostic stages: compensated (almost asymptomatic), and

decompensated (symptomatic; ascites, variceal hemorrhage, and hepatic encephalopathy) (Garcia-Tsao, 2018). These stages can directly or indirectly lead to acute-on-chronic liver failure (ACLF). ACLF is a clinical syndrome of acute hepatic decompensation defined by an acute deterioration of liver function in patients with pre-existent chronic liver disease alongside organ failure (Ampuero et al., 2015). Thus, almost all of the cirrhosis-associated mortality and morbidity is caused by the decompensated stages of liver cirrhosis (Angeli et al., 2018). Irrespective of the etiology of ACLF, cirrhotic patients are at increased risk of sepsis and sepsis-associated mortality (Mateos and Albillos, 2019; Mateos et al., 2019). Piano et al. have recently validated Sepsis-3 and quick SOFA (qSOFA) criteria in cirrhotic patients (Piano et al., 2018). Accordingly, Sepsis-3 and qSOFA are suggested in clinical practice guidelines for the decompensated cirrhosis management (Angeli et al., 2018; Mateos and Albillos, 2019). Monocytes of patients with sepsis and cirrhotic patients with a high grade of organ failure showed low surface expression of HLA-DR and low levels of cytokines secretion in response to LPS. Thus, cirrhosis patients with ACLF syndrome are widely considered to be immunocompromised (Wasmuth et al., 2005; Berres et al., 2009). The bacterial infection is very common as precipitating events of ACLF in patients with cirrhosis, occurring in 30% of hospitalized patients and are associated with the development of ACLF and increased mortality. Since the development of ACLF associates with systemic inflammation, systemic inflammatory response via leukocyte counts and C reactive protein (CRP) gets set in motion. Leukocyte count and CRP levels are elevated in patients with ACLF compared to those of patients with cirrhosis without ACLF and correlates with prognosis (Moreau et al., 2013; Solé et al., 2016). Inflammasomes are considered as intracellular sensor of tissue damage such as NLRP3. In this way, activation of different inflammasomes may occur during development of ACLF (Stengel et al., 2020; Praktiknjo et al., 2020; Monteiro et al., 2021). A variety of cytokines such as IL-1α and IL-1β and alarmins such as HMGB1 are released in cirrhosis patients, and their release requires activation of inflammasomes. However, recent/limited studies investigated the regulation of inflammasome during sepsis and cirrhosis, it is not yet reported how inflammasomes are modulated during sepsis- and cirrhosis-associated immunosuppression. Although, several independent studies have uncovered a protective function of inflammasome during infections, others observed that inflammasome activation by certain cytokines is crucial for innate immune and healing processes. Mechanisms underlying organ failure are associated not only with the hemodynamic imbalance, but also with cell dysfunction and cell death mechanisms including pyroptosis (Hotchkiss et al., 2013; Angeli et al., 2018; Mateos et al., 2019).

2. Aims of this thesis

The inflammasome pathways (priming, licensing, activating, limiting) are critical for host defense and contribute to infectious and non-infectious diseases. The characterization of molecular and cellular mechanisms regulating inflammasome function are of paramount medical importance. Prior to this thesis, inflammasome regulation during sepsis and sepsis associated ACLF research were performed without considering the heterogeneity of immune status of patients with sepsis and patients with acute decompensated liver cirrhosis, which involves switching from a robust inflammatory response to profound immunosuppression. To better characterize the immune changes associated to immune suppression in critically ill patients, the following objectives were addressed:

1. establishing a reliable miRNA surrogate that can identify sepsis/sepsis-like patients with or without immunosuppression signs and whether and how it relates to organ damage or presence of infection in human material derived from acute decompensated liver cirrhosis and septic patients
2. examining the regulation pattern of core components of canonical and non-canonical inflammasome including *CASP4*, *CASP5*, *CASP1*, and the pyroptotic effector molecule *GSDMD* in patients with signs of immunosuppression and organ failure.
3. verifying the activation status of the inflammasome by the hallmark of inflammasome activation, GSDMD activation and release of inflammasome-dependent alarmins and their association with the extent of organ failure during sepsis and sepsis-associated ACLF.
4. investigating the association of interferon signaling with the regulation of non-canonical inflammasome during immunosuppressive state of patients and *in vitro* induced LPS-induced tolerance in primary human macrophages.

Inflammasome-mediated processes are important during microbial infections but have also been linked to neurodevelopmental processes. Another aim of this study, therefore, was to identify a particular dedicated role of CNPY3 in regulating inflammasome priming, assembly, and activation, which might rationalize the clinical manifestations observed in CNPY3 deficiency. For this aim the following objectives were addressed:

1. verifying the role of CNPY3 chaperone in regulating the trafficking and subcellular distribution of multiple TLRs in cell line and primary macrophages with *CNPY3* deficiency.
2. examining the priming and activation paths that affect activation of the inflammasome in a CNPY3-dependent but TLR-independent manner and its contribution to production of inflammasome mediated cytokines and induction of pyroptotic cell death.
3. identifying the role of CNPY3 in regulating inflammasome assembly.

3. Materials and Methods

3.1 Materials

Table 1: List of chemicals

Chemical	Source
Agarose	Genaxxon bioscience
Bicin	Roth
BisTris	Roth
CHAPS	Roth
DMSO	Merck
DSS	Thermo fisher
EGTA	Roth
Ethanol (≥ 99.5%)	Roth
Ethidium bromide	Roth
Ethidiumbromid	Roth
Ethylenediaminetetraacetic acid (EDTA)	Roth
Glycerol	Roth
Glycin	Roth
Glycine	Roth
Hefeextract	Roth
Hefeextrakt	Roth
Hydrochloric Acid (HCl)	Roth
LB Medium	Roth
Magnesium Chloride (MgCl2)	Roth
MES	Roth
Methanol	VWR
NaCl	Roth
PMSF	Sigma
Potassium chloride (KCl)	Roth
Sodium Chloride (NaCl)	Roth
Sodium dodecyl sulfate (SDS)	Roth
Sodium hydroxide (NaOH)	Roth
Todd-Hewitt-Bouillon	Roth
Tris base	Roth
Tris HCl	Roth
Tryptone	Roth
Tween 20	Sigma Aldrich
Yeast extract	Roth
β-mercaptoethanol	Roth

Table 2: List of medium and buffers used for cell culture

Medium	Catalogue no, Source
Biocoll Seperating solution	L6715, Merck
Dulbecco's modified eagle medium - high glucose (DMEM)	61965059, Thermo Fisher
Fetal bovine serum (FBS), Charge no. BCBW7154/0742C	F7524, Merck
Gibco™ RPMI 1640 Medium, GlutaMAX™ Supplement	61870044, Thermo Fisher
Gibco™ Opti-MEM™ I Serum reduced Medium,	51985034, Thermo Fisher
PBS-buffer without Ca^{2+}, Mg^{2+}	14190169, Thermo Fisher
TRYPSIN 0.25% EDTA	25200072, Thermo Fisher

Table 3: List of antibiotics

Antibiotic	Catalogue no, Source
Ciprofloxacin	15LF506R1, Fresenius Kabi
Gentamycin	A2712 Biochrom
Normocin	ant-nr-1, invivogen
Penicillin/streptomycin	11548876, Fisher Scientific
Zeocin	ant-zn-1, invivogen

Table 4: List of agonists and reagents used for cell culture

Agonist/Inhibitors	Catalogue no, Source	Preparation	Final conc.
Flagellin (*Salmonella typhimurium)*	tlrl-epstfla, Invivogen	in 40 µl H_2O	250 µg/ml
FSL-1 (*Mycoplasma salivarium)*	tlrl-fsl, Invivogene	in 50 µl H_2O	200 µg/ml
Lipofectamine 2000	11668-027, Invitrogen	Ready to use	1 mg/ml
LPS-EB (*E. coli* 0111:B4 strain)	tlrl-peklps, Invivogene	in 1 ml H_2O	5 mg/ml
LPS-EK (E. coli K12 strain)	tlrl-3pelps, Invivogene	in 1 ml H_2O	1 mg/ml
Nigericin (*Streptomyces hygroscopicus*)	tlrl-nig, Invivogen	in 1 ml 100% EtOH	6.5 mM
Pam_3CSK_4 (synthetic)	tlrl-pms, Invivogene	in 1 ml H_2O	1 mg/ml
Phorbol myristate acetate (PMA)	tlrl-pma, Invivogen	in 1 ml DMSO	5 mg/ml
Poly(I:C) (High molecular weight)	tlrl-pic, Invivogene	in 10 ml H_2O	100 µg/ml
Recombinant Human IFN-γ	570202, Biolegend	in 100 µl H_2O	100 µg/ml
Recombinant Human M-CSF	574804, Biolegend	in 250 µl H_2O	100 µg/ml

Table 5: List of reagents used for CRISPR/Cas9 editing technology

Materials	Catalogue no, Source
Edit-R Cas9 Nuclease protein NLS 20 µM	CAS11200, Dharmacon
Edit-R CRISPR-Cas9 Synthetic tracrRNA, 5 nmol	U-002005-05; Dharmacon
Edit-R Human CNPY3 (10695) crRNA, 2 nmol	CM-019437-01-0002, Dharmacon

Table 6: List of cell lines

Cell line
THP-1 wild-type, ATCC
THP-1 *CNPY3*$^{-/-}$ clones, Current study
THP-1 *CASP1*$^{-/-}$ (Clone A5) (Schmid-Burgk et al., 2015)
THP-1 *ASC*$^{-/-}$ (Clone C12) (Schmid-Burgk et al., 2015)
THP-1 ASC-GFP reporter cells, Kind Gift from Prof. Tony Bruns
THP-1 ASC-GFP-*CNPY3*$^{-/-}$ reporter cells, Current study

Table 7: List of primers used for real time PCR (mRNA)

Gene ID		Sequence	Amplicon (bp)	Tm °C
BRG1	FW	5′-AACTGGGCGTACGAGTTTGA-3′	117	60
	REV	5′-GACGTTGAACTTCCCACTCC-3′		
CASP1	FW	5′-GCCTGTTCCTGTGATGTGGA-3′	97	60
	REV	5′-TCACTCTTTCAGTGGTGGGC-3′		
CASP4	FW	5′-AAGAGAAGCAACGTATGGCAGGAC-3′	145	60
	REV	5′-GGACAAAGCTTGAGGGCATCTGTA-3′		
CASP5	FW	5′-AGCATCCTTGGCACTCATCT-3′	124	61
	REV	5′-CCAGGACACGTTATGTGGTG-3′		
GAPDH	FW	5′-AGGGCTGCTTTTAACTCTGGT-3′	152	60
	REV	5′-CCCCACTTGATTTTGGAGGGA-3′		
GSDMD	FW	5′-*GTAGACTGGCCACATGGCTA*-3′	249	59
	REV	5′-*CTGGGTCTTGCTGGACGAGT*-3′		
HLA-DRA	FW	5′-TTTCCGCAAGTTCCACTATCTCCC-3′	193	63
	REV	5′-AATAATGATGCCCACCAGACCCAC-3′		
IL1B	FW	5′-AAACAGATGAAGTGCTCCTTCCAGG-3′	132	61
	REV	5′-CTTGTCCATGGCCACAACAACTGAC-3′		
IL6	FW	5′-CCAGAGCTGTGCAGATGAGT-3′	86	60
	REV	5′-GTCAGGGGTGGTTATTGCAT-3′		
IRF1	FW	5′-CTCCACCTCTGAAGCTACAA-3′	133	60
	REV	5′-TCCAGGTTCATTGAGTAGGT-3′		
IRF2	FW	5′-GGCTCAAGTGGCTTAACAA-3′	135	60
	REV	5′-CTGGTTGATGCTTTCCTGTAT-3′		
NLRP3	FW	5′-CACTGCTGCTGGGATCTTTC-3′	259	60
	REV	5′-CCCGTTTCCACTCCTACCAA-3′		
TNFA	FW	5′-AGCCCATGTTGTAGCAAACC-3′	226	60
	REV	5′-CTGGTAGGAGACGGCGATG-3′		

Table 8: List of primers used for qPCR (miRNA)

miRNA name	Target Sequence	Catalogue no, Source
hsa-miR-222-3p	AGCUACAUCUGGCUACUGGGU	YP00204551, Qiagen
hsa-miR-221-3p	AGCUACAUUGUCUGCUGGGUUUC	YP00203907, Qiagen
U6 small nuclear RNA		YP00203907, Qiagen

Table 9: List of kits

Kits	Catalogue no, Source
Biozym Blue S´Green qPCR Kit	331416, Biozym
Biozym cDNA Synthesis Kit	331470L, Biozym
Cell Fractionation Kit	9038, Cell Signaling
Cytotoxicity Detection Kit (LDH-Assay)	MK401, Takara Clontech
EZ DNA Methylation-Gold	D5005, Zymo research
FAM-YVAD-FMK	ABD-13473, Biomol
Fluoroshield with DAPI histology mounting medium	F6057, Sigma
GenUP™ gDNA Kit	350700602, Biozym
Human Galectin Dou Set ELISA	DY1152-05, R&D systems
Human IL-1β ELISA MAX™ Deluxe	437004, BioLegend
Human Progranulin DuoSet ELISA	DY2420, R&D systems
Human TNF alpha DuoSet ELISA	DY210-05, R&D Systems
Human Total IL-18 DuoSet ELISA	DY318-05, (R&D systems
innuPREP DOUBLEpure kit	845-KS-5050050, Analytik Jena
miRCURY LNA RT Kit	339340, Qiagen
miRCURY LNA SYBR Green PCR Kit	339345, Qiagen
miRNeasy Micro Kit (50)	217084, Qiagen
Neon Transfektionskit 10µl	MPK1025, Thermo Fisher
NucleoSpin® Gel and PCR Clean-up	740609.50 M&N
Pierce™ BCA Protein Assay Kit	23225, Thermo Fisher
RNeasy Mini Kit	74104, Qiagen
TMB substrate Reagenz A und B	421101, BioLegend
Q5® High-Fidelity DNA Polymerase	M0491S, NEB
WesternBright ECL ,	541004, Biozym

Table 10: List of antibodies used for FACS

Antigen /Isotype	Clone	Catalogue no, Source
APC human IgG1 isotype Ctrl	REA293	130-113-446, Miltenyi
APC-anti CD282 (TLR2) Antibody, human IgG1	REA109	130-120-138, Miltenyi
FITC anti- HLA-DR Antibody, Mouse IgG2a, κ	L243	307604, Biolegend
FITC Mouse IgG2a, κ Isotype Ctrl	MOPC-173	400209, Biolegend
PE human IgG1 isotype Ctrl	REA293	130-113-438, Miltenyi
PE-anti-CD14, human IgG1	REA599	130-110-577, Miltenyi

Table 11: List of materials used for Immunoblotting

Name	Catalogue no, Source
Albumin Fraktion V, (BSA)	8076.4, Roth
Blotting paper	TE26, VWR
Cell Lysis Buffer (10x)	9803S, Cell signaling
MagicMark™ XP Western Protein Standard	LC5603, Thermo Fisher
NuPAGE™ Novex™ 4-12% Bis-Tris Protein Gels	NP0323, Thermo Fisher
PageRuler™ Prestained Protein Ladder, 10 to 180 kDa	26616, Thermo Fisher
Powdered milk	T145, Roth
PVDF Membran	IPVH00010, Merck
Restore Western Blot Stripping Buffer	21059, Thermo Fisher
SDS buffer	S3401-10VL, Sigma
SuperSignal™ West Pico PLUS Chemiluminescent Substrate	34580, Thermo Scientific
Protease Inhibitor Cocktail	4693116001, Sigma

Table 12: List of primary antibodies

Antigen	Antibody type	Working concentration/ dilution	Catalogue no, Source
ASC	Mouse monoclonal	0.4 µg/ml (1:500)	sc-514414, Santa-Cruz
Biotinylated-anti-IL-1β	Mouse monoclonal	1 µg/ml (1:500)	508301, Biolegend
Caspase-1	Rabbit polyclonal	2 µg/ml (1:500)	GTX133447, GeneTex
Caspase-4	Rabbit polyclonal	0.2µg/ml (1:1000	#4450, Cell signaling
Caspase-5	Rabbit polyclonal	2 µg/ml (1:500)	b69641, abcam
CNPY3	Rabbit polyclonal	0.2µg/ml (1:1000)	GTX55574, GeneTex
GAPDH	Mouse Monoclonal	0.2µg/ml (1:5000)	60004-1-Ig, proteintech
GSDMD	Rabbit Polyclonal AB	0.22 µg/ml (1:1000)	20770-1-AP, Proteintech
MyD88	Mouse monoclonal	0.4µg/ml (1:500)	Sc-74532, Santa-Cruz
NLRP3	Rabbit monoclocal	1 µg/ml (1:1000)	D4D8T/Cell signaling
STING	Mouse monoclonal	0.2 µg/ml (1:500)	MAB7169/ R&D systems
Tom20	Rabbit polyclonal	0.2 µg/ml (1:1000)	11802-1-AP, proteintech
α-Tubulin	Rabbit polyclonal	0.4 µg/ml (1:500)	11224-1-AP, proetintech

Table 13: List of secondary antibodies

Antibody	Specificity	Conjugated to	Dilution	Catalogue no, Source
Goat anti-Mouse	Mouse-IgG (H+L)	HRP	1:5000	074-1806, KPL
Goat anti-Mouse	Mouse IgG (H+L)	Alexa-Fluor 647	1:300	115-605-003, Jackson ImmunoResearch
Goat anti-Rabbit	Rabbit -IgG (H+L)	HRP	1:5000	074-1506, KPL
Goat anti-Rabbit	Rabbit IgG (H+L)	DyLight 488	1:300	35552, Thermo Fisher
Strepatiavidin	Biotinylated antibodies	HRP	1:40	893975, R&D systems

Table 14: List of software and databases used in this study

Software	Provider
Citavi-6.8 (reference management)	Swiss Academic Software
CytExpert Acquisition and Analysis Software Version 2.4	BECHMAN COULTER
FlowJo Version 10.6.2 (flow cytometry analysis)	BD Life Sciences
GATCViewer 1.00	GATC Biotech
GeneSys Softwar version 1.5.6	SYNGENE
GraphPad Software, Version 6	GraphPad
iControl Version 1.10 (Infinite® 200 PRO)	Tecan
ImageJ software 1.49b	FIJI
LAS-3000 software 2.0	FujiFilm
Rotor-Gene 6000 software 1.7 (Rotorgene)	Qiagen
Spark® Control	Tecan
ZEN Black 16.0.1.306 (LSM-780)	Carl Zeiss microscopy GmbH
ZEN Blue 3.0	Carl Zeiss microscopy GmbH

Table 15: List of consumable materials

Material	Source
0.5/1.5/ 2 ml centrifuge tubes	Eppendorf
15/ 50 ml conical tubes	Greiner bio-one
25 cm^2/75 cm^2 culture flasks	Greiner bio-one
96 Well ELISA Microplates	Greiner bio-one
Cell culture multiwell plates (96, 24, 6 well)	Greiner bio-one
Columbia Agar with 5% sheep Blood	BD
Cryovials	National lab
Multipurpose Bechers 100 ml	Greiner bio-one
PCR 0.2ml/0.1ml Stripes	Biozym
Petri Dish	Greiner bio-one
Round Cover Slips, Ø12 mm ,	Marienfeld
Serological pipettes (1-50 ml)	Greiner bio-one
EDTA tubes 9 ml	101228, Sarstedt

3.2 Methods

3.2.1 Human blood samples

3.2.1.1 Patients with decompensated liver cirrhosis

Peripheral blood mononuclear cells (PBMCs), $CD14^+$ monocytes, and plasma of patient cohorts with decompensated liver cirrhosis and suspected bacterial infection were obtained from hospitalized patients. Written informed consent was obtained from patients or their legal surrogates prior to inclusion. Baseline clinical characteristics and outcome of the patients with decompensated liver disease in the absence or presence of multiple organ failure syndrome (according to the EASL CLIF-C criteria for acute-on-chronic liver failure) are given in **Table 16**. Baseline characteristics of immunomagnetically sorted $CD14^+$ monocytes cohort are described in **Table 17.** Clinical scores including model for end-stage liver disease scores, bacterial culture count, protein analysis, blood count and plasma levels of CRP and creatinine were obtained from routine laboratory analysis. The results of these experiments are shown in **Fig. 4-10**. The isolation and characterization of human immune cells and plasma and the use of clinical data was approved by the Internal Review Board of the Jena University Hospital (no. 3683-02/3). The procedure was performed according to the ethical guideline of the 1975 Declaration of Helsinki (World Medical Association, 2013).

3.2.1.2 Patients with sepsis

Septic patients infected with Gram-negative and Gram-positive bacteria were recruited through a clinical cohort study performed on the surgical multidisciplinary intensive care unit (ICU) of Jena University Hospital (Sponholz et al., 2016). All patients admitted to the ICU were screened within 2h of admission for evidence of a systemic inflammatory response syndrome (SIRS) resulting from presumed or proven infection. Patients were diagnosed with severe sepsis septic shock according to Sepsis-1 criteria (Bone et al., 1992). Thus, samples included in this study are in line with Sepsis-3 definition (Singer et al., 2016) and were eligible for study conclusion. Blood samples and plasma were drawn within the first 24 h after clinical diagnosis. After the approval by the local ethics committee (no., 2160-11/07, 2712-12/09 and 3824-11/12), all patients or their legal surrogates gave written informed consent for blood collection and data evaluation. The study was conducted in accordance with the declaration of Helsinki (World Medical Association, 2013). The results of these experiments are shown in **Fig. 11** and basic characteristics of the septic patient cohort is given in **Table 18**.

3.2.1.3 Septic patients for ex vivo study

The study "HemoSpec", a single-center and prospective phase-II study was approved by the local ethics committee of Jena University Hospital (German clinical trial registration number DRKS00006265). Septic patients were included if they were above or equal 18 years old and had sepsis according to Sepsis-3 definition. The immune tolerance state was determined following response to *ex vivo* stimulation of monocytes with LPS. Informed and written consent was obtained from all the patients and blood was collected within the first 24 h**.** The results of these experiments are shown in **Fig. 12** and characteristics of patients are shown in **Table 19**.

3.2.1.4 Patients with EIEEs

For CNPY3 study, parents of patient (newborn) consented to sample donation consistent with Jena Hospital University Institutional Review Board (no. 20191602). The procedures were conducted in accordance with the Declaration of Helsinki on ethical principles of medical research in human subjects (World Medical Association, 2013).

3.2.1.5 Healthy donors

Healthy blood donors without history of disease were included in this study as controls. Donors gave their written informed consent prior to inclusion.

3.2.2 Sample collection and processing

3.2.2.1 Primary macrophages

PBMCs were obtained from blood leukocytes preparation by gradient centrifugation with Bicoll gradients according to the manufacturer's instructions. Briefly, venous whole blood was collected in EDTA tubes. To obtain plasma, whole blood was centrifuged at 350×g for 10 min. Plasma was aseptically collected, aliquoted, and stored at -80°C. To isolate PBMCs, blood was diluted and mixed with equal amount of PBS (without Ca^{+2} and Mg^{+2}). The Bicoll was slowly overlayed with the diluted blood in the ration of 3:8 without breaking the surface plane. The tubes were centrifuged at 800×g for 20 mins at RT with the brakes off. The resulting monolayer (containing PBMCs) was collected with a disposable transfer pipet into a new sterile 50 ml conical tube. The mononuclear cells were mixed and washed twice with PBS by centrifugation at 350×g for 8 min at RT with centrifuge brakes on. After the last wash, supernatant was removed and the resulting pellet was resuspended in DMEM growth medium containing 10% FCS and 10 µg/ml ciprofloxacin. Cell concentration was determined using a haemocytometer. Monocytes (typically ~30%) were seeded at 1×10^5 or 5×10^5 cells per well in 96- or 24-well plates respectively and differentiated into monocytes-derived macrophages (MDM) by

cultivation with 10 ng/mL recombinant human macrophage colony-stimulating factor (M-CSF) for 5 days in DMEM supplemented with ciprofloxacin (10 µg/ml) and 10% FCS (vol/vol).

3.2.2.2 Monocytes-derived from septic patients

PBMCs isolated from septic patients (chapter 3.2.1.3) were isolated by gradient centrifugation as described above (chapter 3.2.2.1). PBMCs were seeded at density of 1×10^6 cells per well in DMEM supplemented with 10% human serum albumin (Merck). Next day, monolayer of monocytes (~3.5×10^5) was washed with warm PBS and stimulated with LPS as described in chapter 3.2.3.2).

3.2.3 Cell culture

3.2.3.1 Maintenance of THP1 wild type and knockout cell lines

All cell culture experiments were performed at 37°C in a humidified incubator with 5% CO2 and aseptically under a sterile laminar flow hood. THP-1 cells: wild type, *CNPY3*$^{-/-}$, *CASP1*$^{-/-}$ and *ASC*$^{-/-}$ cells were cultured in RMPI-1640 medium supplemented with 10% (vol/vol) FCS and penicillin (100 I.U./ml) and streptomycin (100 µg/ml). THP-1 stably expressing ASC-GFP inflammasome reporter cells, wild type cells and *CNPY3*$^{-/-}$ cells were cultured in RMPI-1640 medium supplemented with 10% (vol/vol) FCS and penicillin (100 I.U./ml), streptomycin (100 µg/ml). 100 µg/ml Normocin and Zeocin were added after at least two passages for maintaining culture ASC-GFP reporter cells according to supplier's protocol. All experiments of THP-1 cell lines were conducted in test medium (RMPI-medium supplemented with 10% FCS and penicillin-streptomycin. THP-1 cells were seeded at 80×10^3 cells per well in 96-wellplate and differentiated into macrophages by overnight incubation with 100 ng/ml phorbol 12-myristate 13-acetate (PMA).

3.2.3.2 Stimulations

Activation of TLRs: THP-1 macrophages were stimulated with 100 ng/ml Pam_3CSK_4 or 50 µg/ml HMW poly(I:C) for 16 h in OptiMEM®. Monocytes derived macrophages (MDM) were stimulated for 16 h with a panel of TLR Ligands: 1000 ng/ml ultrapure LPS-EK, 100 ng/ml Pam_3CSK_4, 50 ng/ml FSL-1, 100 µg/ml HMW poly(I:C), or 100 ng/ml ultrapure flagellin from *S. typhimurium* for 16 h followed by performing TNFα ELISA in supernatants. Expression of inflammasome components were assessed by immunoblotting after TLR3 activation via poly(I:C) for 4 h in THP-1 macrophages or by RT-qPCR after 16 h in primary macrophages for CNPY3 study.

Induction of LPS endotoxin tolerance: To induce immune tolerance in primary monocytes derived from septic patients (chapter 3.2.1.3), cells were stimulated with LPS (LPS-EB)

(1 µg/ml) for 72 h and supernatant were harvested at different time points as indicated (**Fig. 12**). Cells were then washed with ice-cold PBS and harvested at 72 h in QIAzol buffer (Qiagen) for isolation of total RNA. For healthy primary macrophages, on sixth day after differentiation, cells were washed and stimulated with LPS (50 ng/ml) or LPS (50 ng/ml) + IFN-γ (100 ng/ml) from 8 to 48 hours before RNA extraction for real time PCR or detached using Trypsin-EDTA 0.25 % for FACS analysis. Supernatants were stored at -80 C° upon harvest for TNF-α analysis.

Activation of NLRP3 inflammasome. THP-1 macrophages were primed with 100 µg/ml poly(I:C) for 4 h. Cells were then washed twice with Opti-MEM to remove residual poly(I:C), followed by stimulation with 6.5 µM nigericin in OptiMEM medium. For THP-1 macrophages, supernatants were harvested for detection of IL-1β and IL-18 by ELISA and pyroptosis by LDH release. Protein expression in cell lysate and release in supernatant were monitored by immunoblotting 3 h later after nigericin treatment. Primary macrophages were treated exactly in the same way except priming with poly(I:C) was for 6 h, followed by treatment with 6.5 µM nigericin for 3 h or 16 h.

Activation of non-canonical inflammasome (LPS transfection): THP-1 and primary macrophages were transfected with LPS in order to activate caspase-4 and capase-5. THP-1 and primary macrophages were primed with 100 µg/ml poly(I:C) for 4 h and 6 h, respectively. Cells were then washed twice with Opti-MEM and the culture media was replaced to remove residual poly(I:C). 10 µg ultra-pure LPS (LPS-EB) was transfected into cytosol by application of 0.5% lipofectamine (LF) in a final volume of 100 µL Opti-MEM. Cells were incubated a further 12-15 h before harvest. Stimulation with only LPS or lipofectamine was carried out as negative controls.

Bacterial infection: Group B streptococcus (GBS) or *Streptococcus agalactiae* (NEM316 strain) and *S. aureus (SA LS-1* strain) wild type strains were grown at 37°C in sterile THY (Todd-Hewitt-Yeast) medium (30 g TH (Todd-Hewitt) broth, 50 g yeast extract in 1 L distilled water) at 160 rpm. *E. coli* (K12 strain) was grown at 37°C in sterile Luria-Bertani broth medium (10 g peptone, 10 g NaCl, 5 g yeast extract in 1 L distilled water) with shaking at 160 rpm. Overnight (15 h) bacteria were harvested by centrifugation (3500×g for 5min) and washed twice with sterile PBS, all steps were performed aseptically under a sterile laminar flow hood. Optical density was measured by Infinite® 200 PRO microplate reader (Tecan). For all infections, bacterial numbers were calculated by assuming that an OD_{600} of 1 corresponds to 8×10^8 bacterial cells/ml. Wild type and *CNPY3*$^{-/-}$ THP-1 macrophages and MDM were infected or left untreated in antibiotic-free medium with *E. coli*, GBS or *S. aureus* at multiplicity of infection (MOI) 20, 20, and 10, respectively. After 1.5 h of infection, cells were washed with growth

medium and cultured in new media containing the following antibiotics: ciprofloxacin (10 µg/ml), penicillin (100 I.U./ml), streptomycin (100 µg/ml) and gentamycin (100 µg/ml) and 10% FCS for 16 h. Infection of THP-1 wild type and *CNPY3*$^{-/-}$ macrophages with *S. aureus* and GBS (**Fig. 20**) were carried out in exactly the same way except with 4 h poly(I:C) priming.

3.2.4 CRISPR/Cas9 mediated gene editing

Clustered regularly interspaced short palindromic repeats (CRISPR)/CRISPR-associated systems 9 (Cas9) CRISPR/Cas9-mediated deletion (Jinek et al., 2012) of CNPY3 gene was performed by electroporation of Cas9 ribonucleoprotein (RNP) guided by dual- RNA structure into THP-1 cells. The synthetic locus specific CNPY3 crRNA (CRISPER RNA) comprised of 20 nucleotides identical to the genomic DNA target site located in CNPY3 gene. The crRNA is base-paired to tracrRNA (trans-activating crRNA) by fusing the 3′end of targeting RNA with the 5′ end of tracrRNA to form a 100 nucleotide chimeric structure with a four tetraloop sequence (Jinek et al., 2012) termed single guide RNA (sgRNA). tracrRNA was mixed with CNPY3 gene locus-specific crRNA at a 1:1 stoichiometric ratio to form tracrRNA:crRNA (sgRNA). The chosen protospacer sequence in the target genomic DNA (TCCTCACCTTCGCATTTGCT) is immediately upstream of a short motif referred to as the protospacer adjacent motif (PAM) in the genomic DNA (NGG). sgRNA was mixed with recombinant Cas9 Nuclease protein with Nuclear Localization Signal (NLS) at a 3µL:1µL (sgRNA:Cas9) ratio per guide RNA incubated at RT for 10 min to generate the RNP complex. To produce gene knockouts, RNP complex directs the CRISPR/Cas9 to introduce double-stranded breaks in target DNA resulting in small insertions and deletions (indels) that can cause nonsense mutations resulting in gene disruptions (Jinek et al., 2012). 1×10^5 THP-1 cells were washed twice with PBS and resuspended in 10 µl nucleofector solution. RNP complex was added to the cells and gently mixed. This mixture was electroporated using the Neon electroporation device (Thermo Fisher). Electroporated cells were grown at 37% in 5% CO2 in a 24-wellplate and next day single cell dilutions were seeded into 96-wellplate. Positive clones were replated as required for functional assays including surface TLR2 protein expression and activation in response to TLR2/1 ligand (Pam_3CSK_4), verified by flow cytometry and TNFα ELISA, respectively. CNPY3 gene deletion was ultimately confirmed by Sanger sequencing (chapter 3.2.5.4) and immunoblotting (chapter 3.2.6).

3.2.5 Gene expression profiling

3.2.5.1 RNA extraction

Total cellular RNA including miRNA ~18 nt and total RNA (>200 nt) were extracted from PBMCs and $CD14^+$ monocytes or freshly *in vitro* treated cells using miRNeasy Micro Kit according to manufacturer's protocol. Briefly, cells were resuspended in 1 mL QIAzol buffer (Phenol/guanidine-based lysis reagent, Qiagen) by being passed through a pipette several times. After the required time of incubation 5 min at RT to dissociate the nucleoprotein complexes, 0.25 chloroform volume was added, thoroughly mixed, and incubated for 3 min at RT followed by centrifugation at 12000×g at 4°C for 15 min. After centrifugation, the upper aqueous phase containing RNA was transferred (~ 350 µl) into fresh microcentrifuge tube and 1.5 volumes of 100% ethanol was added and mixed thoroughly by pipetting up and down several times. 700 µl of the samples was transferred into a RNeasy mini spin column in a 2 ml-collection tube and centrifuged at 10000×g for 15 sec at RT. Samples were further washed several times with buffer washes as mentioned in the manufacturer´s protocol by centrifugation at 10000×g for 15 sec at RT each time. After drying the spin columns by centrifugation at maximal speed at RT to remove residual ethanol from last washing step, the spin column was replaced in RNase-free 1.5 ml microcentrifuge tube. 15-30 µl of RNase-free water was added and centrifuge at full speed to elute the RNA. RNA concentration was determined by NanoDrop and the purity was estimated at the ration of 260 nm and 280 nm.

3.2.5.2 Reverse transcription and RT-qPCR

3.2.5.2.1 micro-RNA analysis

Polyadenylation and reverse transcription of miRNA was performed in single reaction step using miRCURY LNA miRNA PCR kit (Qiagen). The procedure was performed according to the manufacturer´s protocol. Briefly, template RNA samples were diluted to concentration of 5 ng/µl using RNase-free water. 10 ng of template RNA was used to obtain miRNA-specific strand synthesis into complementary DNA (cDNA) in 10 µl reaction as follows:

Components	Volume
RNA-template (5 ng/µl)	2 µl
Reaction buffer (5x)	2 µl
Nuclease free water	5 µl
Enzyme mix (10x)	1 µl

Samples were then incubated at 42°C for 65 min followed by heat inactivation at 95°C for 5 min. cDNA samples were diluted in RNase free water (1:40) and locked nucleic acid primers for miR-221 and miR-222 were used for real time PCR using miRCURY LNA SYBR® Green PCR Kit according to manufacturer´s protocol as follows:

Components	Volume
ExiLENT SYBR-Green PCR-Master mix (2x)	5 µl
PCR Primer Mix	1 µl
cDNA	4 µl
Total	10

The reaction was mixed and cycling condition of real time qPCR was as following:

Step			Temperature	Time
Initial heat activation			95°C	2 min
Amplification	Denaturation	40 Cycles	95°C	10 sec
	Annealing		60°C	60 sec
Melting analysis			50-95°C	rinsing 0.5°C/step

Data acquisition was performed during the annealing step. The baseline expression of the specific genes was performed by determining Ct values at 0.01 threshold and normalized to small nuclear RNA U6 snU6 (hereafter referred to as U6) and exponential transformed $2^{-\Delta Ct}$. The fold change was calculated to respective control using exponential transformed $2^{-\Delta\Delta Ct}$ (Schmittgen and Livak, 2008).

3.2.5.2.2 mRNA analysis

For mRNA-expression, approximately 100-500 ng of RNA was reverse transcribed into cDNA using cDNA Synthesis Kit (Biozym). A total of 20 µl cDNA reaction was mixed as following:

Components	Volume	Final concentration
RNA Template	X µl (100-500ng)	5-25 ng/µl (variable)
Oligo(dT) (10µM)	0.5 µL	0.25 µM
RNase inhibitor 40 U/µl	0.25 µl	1 U/µl
Reverse transcriptase 200 U/µl	0.5 µl	10 U/µl
dNTP Mix 10mM (each)	2 µl	1 mM (each dNTP)
cDNA synthesis buffer 5x	4 µl	1 x
RNase-free water	X µl (to 20µl)	
Total	20 µl	

Cycling conditions of cDNA synthesis was as following: 10 minutes at 30°C (initial heat activation), 55°C for 40 mins (cDNA synthesis), and 99°C for 5 min (enzyme deactivation). Samples then were briefly spun down and diluted (1:10) using RNase-free water.

Human mRNA expression profiling by real time quantitative PCR (qPCR) was performed using specific primer pairs (**Table 7**) and normalized to *GAPDH* as a reference gene. Primer pairs were preferably designed to flank exon-exon junction to avoid amplification of contaminating genomic DNA and to have a calculated melting temperature of around 60°C, using default Primer 3 settings (http://frodo.wi.mit.edu/primer3/). Genes of interest were amplified with specific primers using SYBR-Green kit (Biozym) according to manufacturer's instructions. In

this method, SYBR-Green was used as emitting fluorescent which used to detect the specific DNA amount in the samples. A total of 15 µl reaction was mixed as following:

Components	Volume	Final concentration
Template cDNA	2µl	(variable)
FW primer 2µM	4µl	0.4 µM
REV primer 2µM	4µl	0.4 µM
SYBR Green 2x	10 µl	1x
Total	20µl	

The PCR was performed with one-step cycling program as follows:

Step			Temperature	Time
Initial activation			95°C	2 min
Amplification	Denaturation	30-40 Cycles	95°C	5 sec
	Annealing		60-63°C	30 sec
Melting analysis			50-95°C	rinsing 0.5°C/step

Amplification of HLA-DRA was combined with a final extension step for 5 sec at 72°C. No template controls (NTC) were routinely performed to check for DNA contamination of primer and reagent stocks. The baseline expression of the specific genes was performed by determining Ct values at 0.01 threshold and normalized to reference gene *GAPDH* and exponential transformed $2^{-\Delta Ct}$. The fold change was calculated to respective control using exponential transformed $2^{-\Delta\Delta Ct}$ (Schmittgen and Livak, 2008).

3.2.5.3 Isolation of genomic DNA

Genomic DNA (gDNA) was extracted from PBMCs of 10 patients with acute decompensated liver cirrhosis (5 patients with ACLF and 5 patients without ACLF) and 5 healthy donors as well as from 1×10^7 THP-1 cells and THP-1-*CNPY3*$^{-/-}$ cells were isolated using GenUP™ gDNA Kit (Biozym) according to manufacturer´s protocol. DNA was eluted in 50 µl of RNase-free water. DNA concentration was determined using UV/Vis spectrophotometer**.**

3.2.5.4 Sanger Sequencing

gDNA (500 ng) from 1×10^7 THP-1 cells and THP-1-*CNPY3*$^{-/-}$ cells was amplified using CNPY3 primer flanked the target sequence of CRISPR-CAS9-sgRNA (Chr6:42,929,709-42,929,728) using following primers FW, 5´-AGCTGTTGTCGTGGTTGCT-3´ and REV, 5´-GTTCAAGGAAGGAAGACACCCT-3´. DNA amplification was performed using Q5® High-Fidelity DNA Polymerase kit (NEB) to obtain high-fidelity PCR in 50 µl reaction as follows:

Components	Volume	Final concentration
gDNA Template	X µl	100 ng
Q5 Reaction Buffer (5X)	10 µl	1X
Forward primer 10 µM	2.5	0.5 mM
Reverse primer 10 µM	2.5	0.5 µM
dNTP Mix 10 mM	1 µl	200 µM
Q5 High-Fidelity DNA Polymerase	0.5 µl	0.02 U/µl
5X Q5 High GC Enhancer	10 µl	1X
Nuclease-free water	to 50µl	
Total	50 µl	

The reaction was mixed and thermocycling condition for PCR was as following:

Step			Temperature	Time
Initial denaturation			98°C	30 sec
Amplification	Denaturation	30 Cycles	98°C	5 sec
	Annealing		60°C	30 sec
	Extension		72°C	15 sec
Final extension			72°C	2 min

PCR amplicons were subjected to agarose gel electrophoresis to separate CNPY3 fragment using 1% agarose gel electrophoresis with ethidium bromide in TAE (Tris-Acetat-EDTA) running buffer buffer (1 mM EDTA, 40 mM Tris, 20 mM acetic acid, pH 8.3). A single band at the expected size (~397 bp) on the agarose gel verified the specifity and efficiency of the primers. The PCR product was excised from the agarose gel then purified using NucleoSpin® Gel and PCR Clean-up (M&N) according to manufacturer´s protocol. About 100 ng of purified DNA and 100 µM of sequencing primers were sent to GATC Biotech for sequencing. The resulting DNA sequences were analyzed by BLAST alignments against the wild type reference sequence (NCBI) and by visual inspection of sequence profiles.

3.2.5.5 Methylation and sequencing

400 ng of gDNA derived from PBMCs from patients with acute decompensated liver disease was converted into bisulfite-treated DNA (bsDNA) using the EZ DNA Methylation-Gold™ according to the manufacturer's protocol (Zymo Research). Identically treated unmethylated DNA (Qiagen) served as negative control. Positive control sample was created by *in-vitro* methylation using the CpG-Methyltransferase (*M.SssI*), according the supplier's protocol (New England BioLabs). A serial dilution using *in vitro* methylated and unmethylated control bsDNA was created to generate standard samples of 0 %, 3 %, 6%, 12 %, 24 % and 100 % methylation level. Samples and standards were amplified with bisulfite-specific primers (FW: 5´-TTTTTTGATAATGAGTTTGGAAT-3´; REV: 5´-ACCTACCATAAAAAACAACCTC-3´) targeting a region of the *CASP4* gene (Chr11:104968517-104968678). The PCR was performed

using the SybrGreen MasterMix (Roche) with 0.5 µM of each forward and reverse primer and approximatly 25 ng bsDNA in a Mastercycler Gradient (Eppendorf). After clean-up with the innuPREP DOUBLEpure kit (Analytik Jena), PCR products were sequenced by Sanger sequencing (Microsynth). Resulted Sequences were analyzed by BLAST alignments against the unmethylated reference sequence (NCBI) and by visual inspection of sequence profiles.

3.2.6 Immunoblotting and densitometric quantification

3.2.6.1 Cell lysate preparation

Cell monolayers were washed with cold PBS and ice-cold lysis buffer freshly supplemented with protease inhibitor cocktail (Sigma) was added, cells were then scraped and transferred into 1.5 ml microcentrifuge tube and left on ice for 30 min to ensure complete lysis of the cells. Cells in suspension was centrifuged by 500×g for 5 min and washed with ice cold PBS. The resulted pellet was resuspended in lysis buffer and processed as mentioned above. Lysate was then clarified by centrifugation (15000×g at 4°C for 15 mins) and supernatants were obtained and transferred into fresh 1.5 ml microcentrifuge tubes. The concentration of protein in cell lysate was measured using BCA (Bicinchoninic Acid) kit following the manufacturer´s instructions.

3.2.6.2 Protein precipitation

For protein precipitation in cell culture supernatants, stimulations were always performed in OptiMEM® reduced serum medium. To analyze excreted proteins, cell-free supernatants were obtained by centrifugation at 15000×g for 5 min at 4°C to pellet dead cells and bulk nuclei. Supernatants were transformed into new 2 ml microcentrifuge tube. Protein from supernatants was isolated when indicated by methanol/chloroform precipitation: Briefly, 0.25 volume of chloroform and 1 volume of methanol were mixed with cell free supernatant, vigorously vortexed, and centrifuged at 10000×g for 5 min at RT. Result is three layers: protein exists between large aqueous methanol layer on top and smaller chloroform layer on bottom and visible as a circular flake of protein in the interphase. The lower and upper phase were carefully removed. The interface (protein) was once washed with 1 volume methanol and centrifuged by 10000×g for 5 min at RT. Supernatant was removed without disturbing the pellet and protein pellet was briefly dried at 50°C for ~2 min and resuspended in 1X laemmli buffer.

3.2.6.3 Subcellular fractionation

Cellular fractionation has been important for defining the localization of many proteins, observing the translocation of proteins, and determining protein-protein complexes, such as ASC-oligomers. Cellular fractionation can be achieved using detergents that take advantage of

the inherent qualities and composition of different cellular membranes. Thus, detergent-based cellular fractionation was employed in this study to separate cellular components of THP-1 macrophages to assess the ability of NLRP3 to translocate from the cytosol to the ER as well as to monitor the ASC-oligomerization upon response NLRP3 activation via nigericin (Fernandes-Alnemri et al., 2007; Zhang et al., 2017; Elliott et al., 2018).

3.2.6.3.1 Assay of NLRP3 translocation

For NLRP3 translocation, subcellular fractionation was performed using cell fractionation kit (Cell signaling) according to manufacturer's protocol with minor modifications. Briefly, THP-1 wild type and *CNPY3*$^{-/-}$ cells were seeded in 6-wellplate at density of 1.5×10^6 per well. Cells were differentiated into macrophages using 100 ng/ml PMA overnight in complete RPMI growth medium. Next day, cells were washed with growth media and stimulated for 4 h with 100 µg/ml poly(I:C). Cell fractionation buffers allow for the determination of the subcellular localization of protein through separation into cytosolic, membrane, and nuclear fraction. All steps were performed on ice (4°C). Immediately before use, purification buffers were supplemented with protease inhibitor cocktail (Sigma) and 1 mM PMSF. After treatment, cells were washed twice with ice cold PBS and trypsinized using 0.25 % Trypsin/EDTA buffer (Thermo fisher). Trypsinization was stopped using cold growth media to deactivate trypsin. Cells were then scraped and collected into fresh 1.5 ml centrifuge tubes and spun down at 500×g for 5 mins at 4°C. Medium was aspirated and the resulting pellets were washed with ice cold PBS. Pellets were then resuspended in cytosolic isolation buffer, vortexed, and incubated for 5 min on ice followed by centrifugation at 500×g for 5 min. The supernatant was harvested (cytosolic fraction). Remaining pellets were resuspended in membrane and organelle fraction buffer, vortexed, and incubated for 5 mins and centrifuged by 8000×g for 5 min. Supernatants were aspirated (Membrane fraction). The resulting pellet was resuspended in nuclear fraction buffer (nuclear fraction). Protein concentration was determined using BCA assay. These fractions were then analyzed by SDS-PAGE and western blotting (chapter. 3.2.6).

3.2.6.3.2 Assay of ASC oligomerization in macrophages

In order to monitor ASC polymerization, a common downstream step in the activation of NLRP3 inflammasome. The whole cell extract was fractionated into soluble and insoluble fractions. This experiment was chemically performed using crosslinker DSS (disuccinimidyl suberate) with minor modifications as previously described (Fernandes-Alnemri et al., 2007; Hoss et al., 2017). DSS stabilizes the formed monomers and oligomers structure of ASC to physically approximate it assembly upon inflammasome activation (Hoss et al., 2017). THP-1 wild type and *CNPY3*$^{-/-}$ macrophages were seeded in 6-well plates at a density of 2×10^6 per well

and differentiated with 100 ng/ml PMA overnight in complete RPMI growth medium. The following day, THP-1-derived macrophages were primed with poly(I:C) for 4 h and stimulated with 10 µM nigericin in OPTI-MEM® medium for 45 min. Following stimulation, the cells were washed twice with cold PBS and pelleted by centrifugation. Resulting pellet was lysed in 0.5 ml buffer containing 20 mM Hepes-KOH [pH 7.5], 10 mM KCl, 1 mM EGTA, 1 mM EDTA, 1.5 mM $MgCl_2$, 320 mM sucrose, 0.1 mM PMSF, and protease inhibitors cocktail on ice by syringing 30 times using 25-gauge needle. The cell lysates were centrifuged at 4°C, 1500×g for 5 min to remove the bulk nuclei. The resulting supernatant (soluble fraction) was diluted with one volume of CHAPS buffer (20 mM Hepes-KOH [pH 7.5], 5 mM $MgCl_2$, 0.5 mM EGTA, 0.1 mM PMSF and 0.1% CHAPS) and then centrifuged at 5000×g to pellet ASC oligomers. The resulting supernatant (soluble fraction) was used to confirm the equivalent levels of ASC in treated and untreated cells. The resulting crude pellets (insoluble fraction) were resuspended in 400 µl CHAPS buffer. The resuspended pellets were then covalently cross-linked with freshly prepared DSS (4 mM) for 30 min at RT protected from light. The pellets were then isolated by centrifugation at 5000×g for 10 min. The cross-linked pellets enriched with ASC polymers were resuspended and boiled at 95°C for 3 min in 30 µL of 1X SDS-sample buffer and run on 4-12%-SDS-PAGE followed by immunoblotting with anti-ASC antibody as described in chapter 3.2.6.4. In order to confirm that ASC expression levels are equivalent in treated and untreated whole cell extract of wild type and *CNPY3*$^{-/-}$ macrophages, expression levels of ASC and GAPDH were assessed in the soluble fraction, whereas the oligomerization state of ASC were assessed in the DSS-cross-linked insoluble fraction.

3.2.6.4 SDS-PAGE and Immunoblotting

For immunoblotting, equal amount of cell extracts protein was diluted with 5X SDS-sample buffer and boiled at 95°C for 10 mins. Samples were centrifuged by 500×g for 3 min and 20 µl was loaded and separated on precast 4-12 % SDS-polyacrylamide gradient gel (Thermo Fisher). SDS-PAGE was carried out in SDS-running-buffer (50 mM MES, 50 mM Tris Base, 0.1% SDS, 1 mM EDTA, pH 7.3) at 70 volts constantly for approximately 3 h using Nupage Mini Gel Tank (Thermo Fisher). Proteins were then transferred onto 0.45 µM PVDF membrane in transfer buffer (25 mM Bicine, 25 mM Bis-Tris (free base), 1 mM EDTA, pH 7.2) using a wet blotting system at 20 volts constantly for 1 h. The membranes were blocked with 5% BSA or 5% skimmed dry milk prepared in TBS-Tween (0.1%) (TBST) with a gentle agitation for 1 h at RT. The membrane was probed overnight at 4°C under agitation with primary antibody (**Table 12**). After three rounds of washing with TBST buffer, the membrane was probed with secondary antibody (**Table 13**) with a gentle agitation for 1-2 h at RT. The membrane was

washed three times for 10 min each with TBST and soaked in freshly prepared ECL-substrate. The chemiluminescence reaction was detected using GBOX-Chemi-XX6 gel documentation system (Syngene).

3.2.6.5 Removal of bound antibodies from membranes

Membrane previously immunoprobed were incubated in stripping buffer (Thermo fisher) for 15 min at 37°C, then washed twice with TBST for 10 min and blocked for 30 min with blocking buffer prior to reprobing.

3.2.6.6 Densitometry

Acquisition and densitometric analysis of approximate relative differences in capase-4 and GSDMD protein expression in plasma of septic patients were performed using ImageJ software (FIJI). All band intensity was determined at the correct molecular weight (~45 kDa for caspase-4, and at ~22 kDa for cleaved GSDMD (p20)) as signal for that target protein. The densitometric analysis was performed to obtain the absolute intensity for each patient. Briefly, representative images shown **Fig. 11** were captured with chemiluminescence (black bands) using the LAS-3000 system, taken in LAS-3000 software (FujiFilm), and saved as TIFF files. The region of interest (ROI) encircling each band was defined manually using the same frame for all the protein bands across the other lanes. When bands in adjacent lanes or in the same lane were touching, the boundaries of ROI were placed at the point of minimum thickness between the bands. The density of a given band was measured as a total volume under the peak. The background subtraction was set by drawing a line across the base of the peak to enclose the peak and was not artificially affected by the detected signal.

3.2.7 Flow cytometric analysis

Flow cytometric analysis of mononuclear and THP-1 cells: freshly isolated mononuclear cells were washed twice with ice-cold PBS. Cells were resuspended in FACS buffer (2% FCS, 2 mM EDTA in PBS) and incubated with the following fluorochrome-conjugated antibodies for surface staining of TLR2, CD14 or isotype controls (**Table 10**) with 1:100 dilutions for 30 min on ice. THP-1 cells (wild type and *CNPY3*$^{-/-}$) or THP-1 ASC-GFP reporter cells (ASC-GFP-wild type and ASC-GFP-*CNPY3*$^{-/-}$) were washed once in ice cold FACS buffer, resuspended in FACS buffer and followed by incubation with APC-conjugated TLR2 or isotype IgG1 control antibodies for 30 min on ice. Cells were then washed with FACS buffer and analyzed on CytoFLEX flow cytometer (Beckman-Coulter) using CytExpert software.

For flow cytometric analysis of macrophages: following stimulation with LPS or LPS+IFN-γ for 72 h, monolayer of MDM was washed with PBS and trypsinized at 37°C for 10 min using

trypsin/EDTA buffer. Trypsinization was stopped using growth medium containing FCS. Cells were then scraped and collected into fresh 1.5 ml centrifuge tubes and washed twice with ice cold FACS buffer. Cells were then blocked with blocking buffer (2% FCS, 2 mM EDTA in PBS) supplemented with FcR blocking reagent for 20 min to avoid FcR-mediated non-specific labeling of the cells. Cells were then incubated with FITC anti-human HLA-DR antibody or FITC mouse IgG2a isotype control in FACS buffer with 1:100 dilution for 1 h. Samples were washed twice with FCS buffer and then analyzed on CytoFLEX flow cytometer using CytExpert software. Cells were gated on singlets. Dead cells were excluded by forward and side scattering gating. Data were analyzed using FlowJo software (BD).

3.2.8 Caspase-1 activity assay

To stain for active caspase-1, 8×10^4 of THP-1 wild-type, *CNPY3*$^{-/-}$ and *CASP1*$^{-/-}$ (as a negative control) cells were seeded in black-walled, clear bottom 96-wellplate and differentiated using 100 ng/ml PMA for overnight. Next day, THP-1-derived macrophages were primed with 100 µg/ml poly(I:C) for 4 h, followed by stimulation with 10 µM nigericin for 90 min in OptiMEM®. During the last 45 min 5-FAM-YVAD-FMK (5-carboxyfluorescein-Tyr-Val-Ala-Asp-fluoromethylketone) was prepared and added to the cells according to manufacturer's instructions. To detect active caspase-1 in whole, living cells, FAM-YVAD-FMK binds irreversibly to the active caspase-1 in nigericin-treated macrophages and generates a green fluorescence. Next, cells were washed three times with PBS and fluorescence intensity was recorded at Ex/Em 490/520 nm, with 5 reads per well option, using a Spark fluorescent microplate reader (Tecan). The signal is proportional to the amount of active caspase-1.

3.2.9 ASC specks quantitation in live cells

THP-1-ASC-GFP wild type and THP-1-ASC-GFP-*CNPY3*$^{-/-}$ reporter cell lines were seeded in 6-wellplate at density of 1×10^6 cell per well and differentiated into macrophages with 100 ng/ml PMA overnight. Macrophages were primed with poly(I:C) 100 µg/ml, the medium was replaced with 10 µM nigericin in optiMEM® fresh medium and the cells were observed by fluorescent microscopy after 60-90 min.

3.2.10 Immunofluorescence staining

THP-1 wild type and *CNPY3*$^{-/-}$ cells were seeded at density of 5×10^5 cells on sterile cover slides in 24-wellplates and differentiated with 100 ng/ml PMA overnight. Next day, THP-1-derived macrophages were washed with growth medium and primed with poly(I:C) for 4 h followed by stimulation with nigericin (10 µM) for 1.5 and 3 h. Macrophages were then fixed at indicated

time points with 100% methanol (prechilled to -20°C) for 10 min. Prior to performing intracellular staining, cells were permeabilized for 15 min with saponin-based permeabilization buffer (Invitrogen) diluted to 1X in PBS and blocked using 10% BSA in PBS for 1 h at RT. Primary mouse anti-ASC (1:300) and rabbit anti-caspase-1 (1:300) antibodies were prepared in blocking buffer and applied overnight in a humidity chamber for 16 h hours at 4°C with gentle agitation. Next day, the cells were extensively washed with PBS and then stained with secondary antibodies; anti-rabbit-conjugated with DyLight-488 and anti-mouse-conjugated with Alexa-Fluor-647 for 1 h at RT in dark under gentle agitation. After several washing steps, cell nuclei were counterstained in DAPI mounting medium. Slides were kept at 4 °C till examination.

3.2.11 Imaging and Imaging analysis

For both, when detected by antibodies (**Fig. 22A**) and when tagged by GFP (**Fig. 21H**), endogenous ASC and ASC specks are present in the cytoplasm of macrophage after treatment with nigericin. Living images of ASC tagged by GFP were performed using fluorescence microscope (Axio Observer 7) at RT using 10x objective with filter of GFP and brightfield. The number of cells containing ASC–GFP specks were counted in several fields at the end of the time period 60-90 min. The percentage of cells with ASC positive specks was calculated by dividing the number of the cells with ASC specks over the total cells in the brightfield as previously described (Fernandes-Alnemri et al., 2007; Stutz et al., 2013). Images of immunofluorescence were performed with a LSM 780 confocal microscopy (Carl-Zeiss microscopy) using 40x objective. Images were processed using ZEN blue software (Carl Zeiss microscopy). Intensity plot was profiled before and after cytoplasmic speck formation for green (caspase-1) and red (ASC) channels. To assess the approximate size of ASC and caspase-1 specks, a line was sat over the specks and relative fluorescence intensity (AFU, arbitrary fluorescence unit) was taken on the green and red channel and AUC was calculated for each speck. Number of detected ASC specks was divided by the number of nuclei detected by DAPI. The quantification of colocalized ASC and capase-1 (yellow spot) was calculated by dividing the number of yellow spots over the total number of ASC-specks in each field.

3.2.12 Enzyme-linked immunosorbent assay (ELISA)

Cell-free supernatants were analyzed for cytokine level by sandwich enzyme-linked immunosorbent assay (ELISA) kits, TNFα, IL-1β and IL-18. PGRN and Galectin-1 level were measured in plasma of acute decompensated liver cirrhosis and healthy donors. Microlon™ 96-well microtiter ELISA plate (Greiner bio-one) was coated with the capture antibody diluted in

PBS (50 µl/well) and incubated overnight at 4 °C under shaking. Coating solution was removed, and plates were three times washed by filling the wells with 400 µL wash buffer PBST (PBS/0.05% Tween-20 (v/v)) to remove unbound antibody. The solutions or washes are removed by flicking the plate over a sink. The remaining protein-binding sites in the coated wells were blocked for 1 h at RT by adding 150 µL blocking buffer per well (10% BSA blocking buffer was diluted to 1% in sterile water) under shaking. Plates were then washed with PBST as described above. 50 µL/well of cytokine standards (duplicate) or diluted sample (at least in triplicate) were added and incubated at RT for 2 hours und shaking. Unbound samples and standards were removed from the plate by four washes in PBST. Detection antibody (labeled with biotin) was added (50 µL/well) and incubated for 2 h at RT. Unbound detection antibody was removed by washing the plate four times in PBST. HRP-conjugated Streptavidin was diluted 1:40 and 50 µl was added to each well and incubated at RT for 30 mins. Plates were extensively washed with PBST before addition of 50 µl/well of TMB substrate. The reaction was stopped when lower standards had developed using 25 µl of 2 N H_2SO_4. Absorbance at 450 nm was read on Infinite M200 Pro microplate reader (Tecan) and cytokines in samples was calculated using data points generated from standard curve.

3.2.13 Lactate dehydrogenase (LDH)

Cell death is classically assessed by quantifying plasma membrane rupture. Lactate dehydrogenase (LDH) is a soluble cytosolic protein which is rapidly released amongst the myriad of released proteins by dead cells during pyroptosis after strong stimulation of inflammasome or cell lysis with detergents. Determination of LDH activity in culture supernatants is used as a proxy of cell death because of the ease of measuring its enzymatic activity (Rayamajhi et al., 2013). Prior to the determination of LDH activity, cells were removed from the culture medium (by centrifugation at 500×g at 4°C for 5 min). LDH was measured on fresh cell-free supernatants samples of treated cell culture according to manufacturer's protocol. Briefly, 50 µL of sample was transferred into a new 96- well plate. 50 µL of reaction mixture of the catalyst and tetrazolium salt (1:50) was immediately prepared before use. The LDH activity is determined in an enzymatic reaction, where LDH oxidizes lactate to pyruvate, transferring electrons to the cofactor nicotinamide adenine dinucleotide (NAD^+) to form NADH. The catalyst (Diaphorase contains FAD^+) transfers H/H^+ from $NADH/H^+$ to the tetrazolium salt which is reduced to formazan (Rayamajhi et al., 2013). While tetrazolium salt is yellow, formazan is red. The increased absorption is readily detected at 492 nm with a Infinite M200 Pro microplate reader (Tecan). The amount of light absorbed is directly proportional to

the number of lysed cells or cells with compromised membrane permeability. The relative LDH levels was calculated in percentage (%) as follows: 100 × ((LDH treated – LDH untreated) / (LDH total lysis – LDH untreated)). Total lysis was achieved by the addition of lysis solution at final concentration of 1% Triton X-100 in culture medium.

3.2.14 Statistical analysis

Statistical analyses and data representation were performed using GraphPad Prism 6.0 software (GraphPad Software, Inc.). Statistical comparison was performed using two tailed student *t*-test, two-tailed Mann-Whitney *U* test, Kruskall Wallis, as appropriate and as indicated in the figure legends. Real time PCR data obtained from patients were analyzed by unpaired two-tailed *t*-test for parametric after Log2 transformation to reach normal distribution. Correlations were using Pearson´s test representing r^2 or linear regression. *P* values are from two-tailed Pearson´s correlation of parametric regression analysis. Each data marker represents an individual patient and horizontal lines represent mean values. Comparisons were made between treatment groups using two-tailed Mann-Withney *U* test for nonparametric data. *P* values < 0.05 are regarded as statistically significant. For all tests, $*P < 0.05$, $**P < 0.01$, $***P < 0.001$, $****P < 0.0001$ was considered significant or ns as not significant. Data generated from *in vitro* experiments are presented as mean ± SEM. In vitro experiments of MDM derived from CNPY3 patient and her parents were performed once or twice as indicated, depending on available consent and ethical considerations.

4. Results

4.1 Distinct regulation of inflammatory caspases during sepsis- and sepsis-like cirrhosis-associated immunosuppression

The extent of pro-inflammatory response and immunosuppression can concomitantly occur and varies between individuals resulting in complexes clinical phenotypes that present in sepsis and sepsis-like immune paralysis in cirrhotic patients (Albillos et al., 2014; Rubio et al., 2019; Mateos et al., 2019). The regulation of inflammatory caspases and inflammasome-dependent cell death (pyroptosis) in patients with signs of immuno-suppression remains not well studied. Therefore, following the establishment of a surrogate marker that can discriminate patients with signs of immunosuppression, the expression profile of inflammatory caspases and its mechanistic expression were analyzed in these patients. To this end, I have investigated two inflammatory conditions associated with organ failure and impaired innate immune responses, sepsis (Singer et al., 2016) and acute-on-chronic liver failure (Moreau et al., 2013).

4.1.1 Highly regulated miR-222 correlates with sepsis-induced immunosuppression

Discovering a surrogate marker to discriminate patients based on inflammatory state can help clinicians in the early phase to timely stratify patients with sepsis into sub-cohorts on the basis of whether they would benefit from pro-inflammatory immunotherapies or classical anti-inflammatory treatments (Hotchkiss et al., 2013). Seeley et al have recently shown, that increased miR-222 and miR-221 expression correlates with *in vitro* LPS-induced tolerance. miR-221 and -222 are highly expressed at late stage of long exposure of LPS and induce immune tolerance via targeting of chromatin remolding factors (Seeley et al., 2018). In clinical settings and in line with septic patients, immunosuppression is maximally detectable at late stage of cirrhosis (Albillos et al., 2014). To gain a mechanistic insight into immunosuppression state during the course of sepsis and ACLF syndrome in human diseases, PBMCs from a patient cohort with acute decompensation of liver cirrhosis and suspected bacterial infection were obtained from hospitalized patients with and without ACLF. Clinical features of the patients with decompensated liver disease in the absence or presence of multiple organ failure syndromes (according to the EASL CLIF-C criteria for acute-on-chronic liver failure) are shown in **Table 16**. Of note, sample size was increased from 30 to 40 patients compared to data shown by Seeley et al., 2018. To distinguish the regulation pattern of miR-222 and -221 according to suspected infections and organ failure (ACLF), a stratified analysis was accordingly performed. Interestingly, stratification of patients according to absence (n=26) or presence of infections (INF) (n=14) did not reach statistical significance in regulation of miR-

222 or miR-221 (**Fig. 4A**, **B**). However, stratifying patients according to grade of organ damage based on ACLF revealed that miR-222 and miR-221 expression were significantly upregulated in patients with high grades of organ damage (ACLF) compared with mild patients (no ACLF) (**Fig. 4C**, **D**). Nevertheless, compared to miR-221 ($P = 0.012$), the miR-222 expression profile with $P = 0{,}0008$ markedly exhibits the highest level and lesser overlapping cluster of both patient groups.

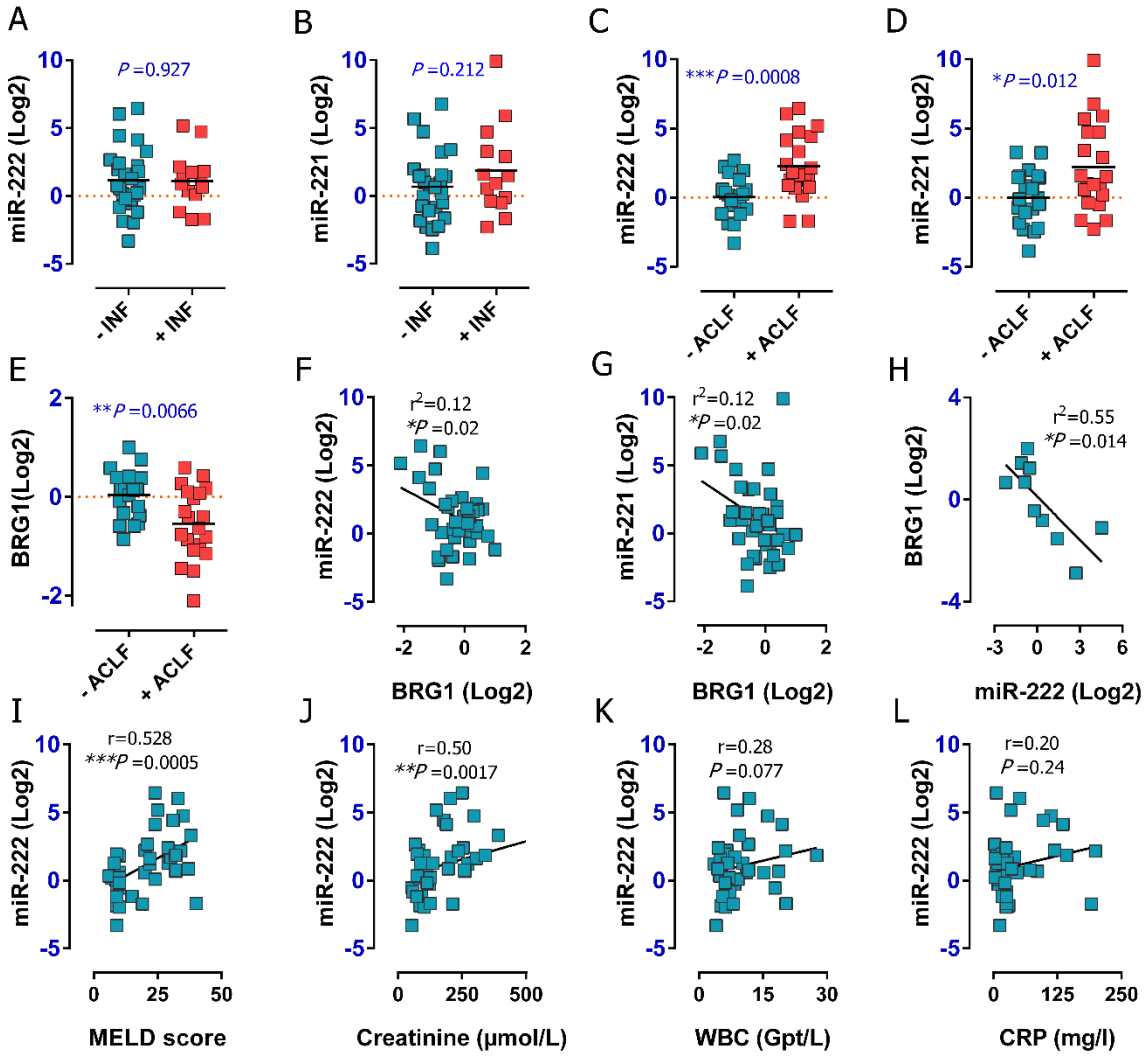

Fig. 4: miR-222 and miR-221 correlate with immunosuppression in patients with acute decompensated liver cirrhosis.

(**A-D**) Gene expression of the miR-222 and miR-221 in PBMCs from patients with acute decompensated liver cirrhosis stratified according to absence or presence of infection (INF) (**A, B**) or organ failure (ACLF) (**C, D**). mRNA expression of *BRG1* stratified according to presence or absence of ACLF (**E**). Correlation of mRNA expression of *BRG1* with miR-222 (**F**) or miR-221 (**G**). **(H)** correlation of *BRG1* with miR-222 in $CD14^+$ monocytes from patient with acute decompensated liver cirrhosis. (**I-L**) correlation of miR-222 expression in PBMCs with clinical scores of patients with acute decompensated liver cirrhosis including MELD score (**I**), Creatinine (**J**), WBC counts (**K**) and CRP (**L**). *P* values from two-tailed *t*-test. Horizontal lines represent mean values (**A-E**). *P* and r^2 values from two-tailed Pearson´s correlation of parametric regression analysis. Each data marker represents an individual patient. * $P < 0.05$, ** $P < 0.01$, *** $P < 0.001$, ns, not significant $p > 0.05$.

Mechanistically, the higher level of miR-222 and miR-221 expression enforces the immunosuppression epigenetically by transcriptional silencing of chromatin remodeling factor *BRG1*, leading to the potential suppression of *BRG1* dependent inflammatory genes (Seeley et al., 2018). Analysis of *BRG1* mRNA expression showed substantial suppression of *BRG1* expression in patients with ACLF compared to patients without ACLF (**Fig. 4F**). Correspondingly, suppression of *BRG1* expression was as expected inversely correlated with miR-222 and miR-221 (**Fig. 4F**, **G**). Based on the results of the miR-221 and 222 analysis shown in (**Fig. 4C**, **D**), miR-222 expression profile was selected for further correlation analysis. Moreover, the inverse correlation between miR-222 and *BRG1* was also observed in immune-magnetically sorted $CD14^+$ monocytes from the PBMCs of a second clinical cohort of cirrhosis patients (**Fig. 4H**), confirming changes in the miR-222 and BRG1 expression profiles in myeloid cells. Baseline features of $CD14^+$ monocytes sorted from patients with decompensated liver disease in the absence or presence of ACLF are shown in **Table 17.** In addition, clinical scores such as model for end-stage liver disease scores (MELD), white blood count (WBC) and plasma levels of C-reactive protein (CRP) and creatinine were subjected to linear regression analysis to identify parameters which may associate with miR-222 expression. Interestingly, routine clinical scores related to organ damage including MELD score and creatinine correlate positively with expression profile of miR-222 (**Fig. 4I**, **J**). In contrast to organ damage markers, the plasma level of generalized inflammatory markers including white blood counts (WBCs) and CRP did not correlate with the expression profile of miR-222 (**Fig. 4K**, **L**). Collectively, stratification of patients into two groups according to the grade of organ damage (ACLF) and miR-222 expression revealed that both immunosuppression and organ damage can concurrently occur.

4.1.2 Caspase-4 and caspase-5 genes are differentially regulated during immunosuppression-associated organ failure.

During abnormal host immune responses such as sepsis and cirrhosis, caspases have a major role in inflammation and cell death (Aziz et al., 2014; Napier et al., 2016; Stengel et al., 2020). Human caspase-4 (*CASP4*) and caspase-5 (*CASP5*) genes are closely related genes and known to be upregulated during inflammatory responses in monocytes and macrophages to drive inflammasome activation under certain conditions (Viganò et al., 2015; Casson et al., 2015). However, their regulation during immunosuppression remains unstudied. Taking our finding of miR-222 shown in **Fig. 4** further, I found that *CASP4* gene was significantly suppressed in patients with signs of immunosuppression and organ failure based on their miR-222 expression profile and the presence of ACLF, respectively (**Fig. 5A**). In contrast, the up-regulation of

CASP5 in patients with immunosuppression was not affected when compared to patients without ACLF (**Fig. 5B**). This agrees with known literature demonstrating that *CASP5* is highly expressed in patients with severe sepsis, although a stratification of patients in these reported studies was not taken in account (Napier et al., 2016; Esquerdo et al., 2017).

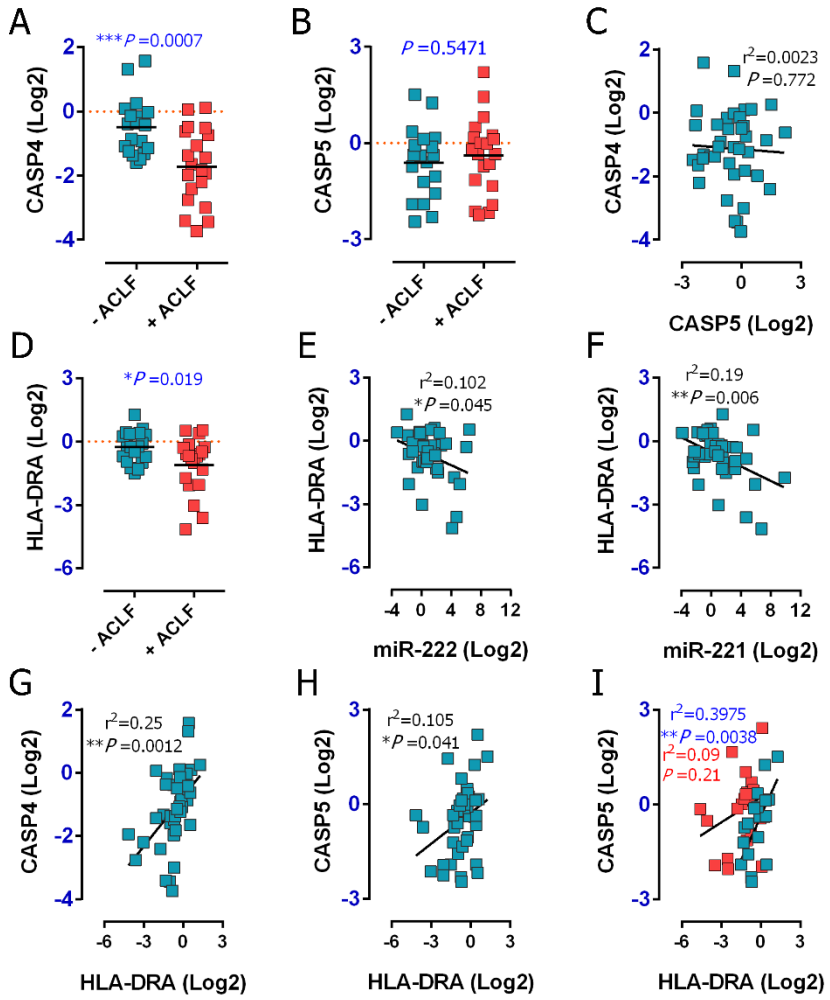

Fig. 5: *CASP4* and *CASP5* are differentially regulated during immunosuppression in patients with acute decompensated liver cirrhosis.
(**A, B, D**) mRNA expression of *CASP4* (**A**) *CASP5* (**B**) and *HLA-DRA* (**D**) in PBMCs of patients with acute decompensated liver cirrhosis stratified for acute-on-chronic liver failure (ACLF). (**C**) Correlation of mRNA expression of *CASP4* and *CASP5*. (**E-H**) correlation of *HLA-DRA* with miR-222 (**E**), miR-221 (**F**), *CASP4* (**G**) or *CASP5* (**H**). (**I**) Correlation of *HLA-DRA* expression with *CASP5* stratified for without ACLF (blue) and with ACLF (red). (**A**, **B**, **D**) *P* values from two-tailed *t*-test. Horizontal lines represent mean values. (**C**, **E-I**) *P* and r^2 values from two-tailed Pearson´s correlation of parametric regression analysis. Each data marker represents an individual patient. $*P < 0.05$, $**P < 0.01$, $***P < 0.001$, ns, not significant $P > 0.05$.

Interestingly, *CASP4* and *CASP5* expression were differentially regulated, hence no linear correlation was observed (**Fig. 5C**). Reduced expression of HLA-DR in circulating blood monocyte has been consistently associated with the common sepsis-associated immunosuppression and poor outcome (Monneret et al., 2006; Lukaszewicz et al., 2009;

Boomer et al., 2011; Winkler et al., 2017; Shankar-Hari et al., 2018) and sepsis-like immune dysfunction associated with cirrhosis (Wasmuth et al., 2005; Berres et al., 2009). In addition to the expression profile of miR-222, I assessed the expression of *HLA-DRA*, which encodes the major histocompatibility complex, class II, DR alpha, as a prognostic marker for critically ill cirrhotic patients with decompensated liver disease (Wasmuth et al., 2005; Berres et al., 2009). In line with the known literature, I found that patients with signs of immunosuppression and high grades of organ damage showed a significant decrease in the expression of *HLA-DRA* (**Fig. 5D**). Noteworthy, the expression of *HLA-DRA* as a surrogate for immunosuppression correlates inversely as expected with miRNA-222 (**Fig. 5E**) and miR-221 expression (**Fig. 5F**). Furthermore, I explored the correlation of *HLA-DRA* with *CASP4* and *CASP5* expression and found that *CASP4* and *HLA-DRA* expression are positively correlated (**Fig. 5G**). Although, the expression of *CASP5* also trended to correlate with *HLA-DRA* over both patient groups (with and without ACLF) (**Fig. 5H**), this correlation was not found in the group of patients with ACLF (**Fig. 5I**).

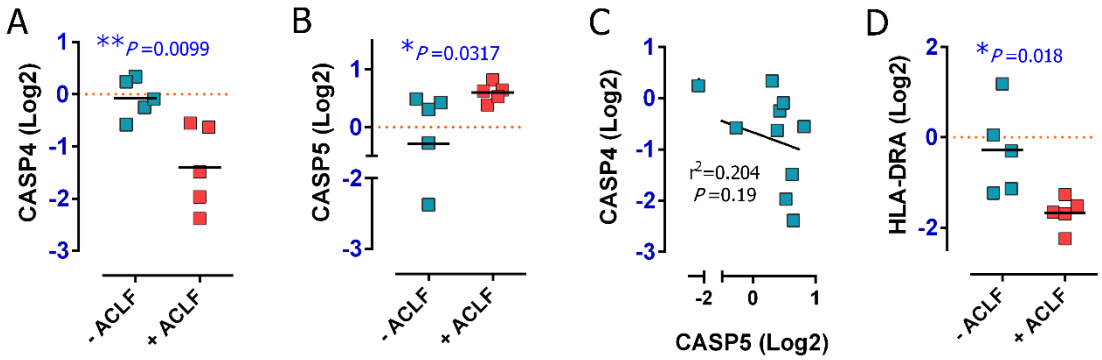

Fig. 6: *CASP4* and *CASP5* are differentially regulated during inflammatory organ failure in CD14$^+$ monocytes from patients with acute decompensated liver cirrhosis.
Gene expression of the indicated genes (**A-D**) in CD14$^+$ monocytes from patients with acute decompensated liver cirrhosis. (**A**, **B**, **D**) mRNA expression of *CASP4* (**A**) *CASP5* (**B**) and *HLA-DRA* (**D**) in patients PBMCs with acute decompensated liver cirrhosis stratified for acute-on-chronic liver failure (ACLF). (**C**) Correlation of mRNA expression of *CASP4* and *CASP5*. (**A**, **B**, **D**) *P* values from two-tailed *t*-test. Horizontal lines represent mean values. (**C**) *P* and r^2 values from two-tailed Pearson´s correlation of parametric regression analysis. Each data marker represents an individual patient. (*$P < 0.05$, **$P < 0.01$, ns, not significant $P > 0.05$). Each data marker represents an individual patient.

Consistent with PBMCs, CD14$^+$ monocytes from cirrhotic patients confirmed the downregulation of *CASP4* and upregulation of *CASP5* in patients with ACLF. In addition, the differential expression of *CASP4* and *CASP5* as well as downregulation of *HLA-DRA* was also observed in CD14$^+$ monocytes (**Fig. 6 A-D**). Altogether, these data indicate the conformity of *CASP4* and *CASP5* differential regulation during states of immunosuppression in myeloid cells. In addition, consistent with known literatures (Wasmuth et al., 2005; Berres et al., 2009) this

data also demonstrates an immunosuppressive state in ACLF patients based on *HLA-DRA* and miR-222 expression profiles (**Fig. 5D-F** and **Fig. 6D**).

4.1.3 Non-canonical inflammasome transcriptional regulators *IRF2*, and *IRF1* are suppressed during immunosuppression-associated organ damage

IRFs were initially identified as regulators of *IFNA* and *IFNB* genes (Sato et al., 2001). Recently, emerging evidence has shown that IRF2 and IRF1 are the key transcriptional regulators of *CASP4* in the steady state and infection, respectively (Benaoudia et al., 2019). To elucidate a cause for the downregulation of *CASP4* as shown in **Fig. 5A** during innate immunosuppression in patients, DNA methylation-specific sequencing PCR was first employed to examine methylation levels at the *CASP4* promoter in patients with signs of immunosuppression. As the presence of IRF1 and IRF2 transcription binding site (TFBS) within the promotor region of *CASP4* gene was confirmed using the Pscan algorithm (Zambelli et al., 2009). CpG sites within transcription factor palindromic consensus sequence of IRF2 and IRF1 or in its close proximity which might affect *CASP4* regulation were predicted and analyzed. The binding motif of IRF1/2 on promotor region of *CASP4* includes predictably three CpG probes cg05618647, cg16669455 and cg16315582 located approximately -30 to -98 base pairs around the TFBS of IRF1/2 as predicted by emsembl.org (**Fig. 29A**, **B**). Accordingly, DNA methylation was analyzed in PBMCs of healthy donors (n=5), patients with cirrhosis and ACLF (n=5), and patients with cirrhosis without ACLF (n=5). Although *CASP4* expression was significantly suppressed, all analyzed clinical PBMCs samples did not show methylation above the detection limit of 10% (**Fig. 29C**). Thus, the data exclude a major contribution of aberrant DNA methylation to the reduced *CASP4* expression in patients with ACLF. (Analysis of *CASP4* methylation was performed by Dr. Norman Häfner). Since no methylation in TFBS of IRF1 and IRF2 or its close proximity on *CASP4* promotor were identified, I directly investigated the transcriptional regulation of *IRF2* and *IRF1*. Interestingly, I found that expression levels of *IRF2* and *IRF1* were downregulated in patients with ACLF as compared to patients without ACLF (**Fig. 7A**, **B**). Interestingly, *IRF2* and *IRF1* are positively correlated (**Fig. 7D**) and since both positively correlate with *HLA-DRA* expression (**Fig. 7E**, **F**), our data revealed that *IRF2* and *IRF1* undergo immunosuppression. Correspondingly, *IRF2* and *IRF1* correlate positively with *CASP4* expression, demonstrating that damped expression of *IRF2* and *IRF1* lead ultimately to the impaired expression of *CASP4* (**Fig. 7F**, **G**). Notably, no correlations of *IRF1* and *IRF2* with *CASP5* were observed (**Fig. 7H**, **I)**, suggesting that IRF2 and IRF1 may not directly contribute to the regulation of *CASP5* expression.

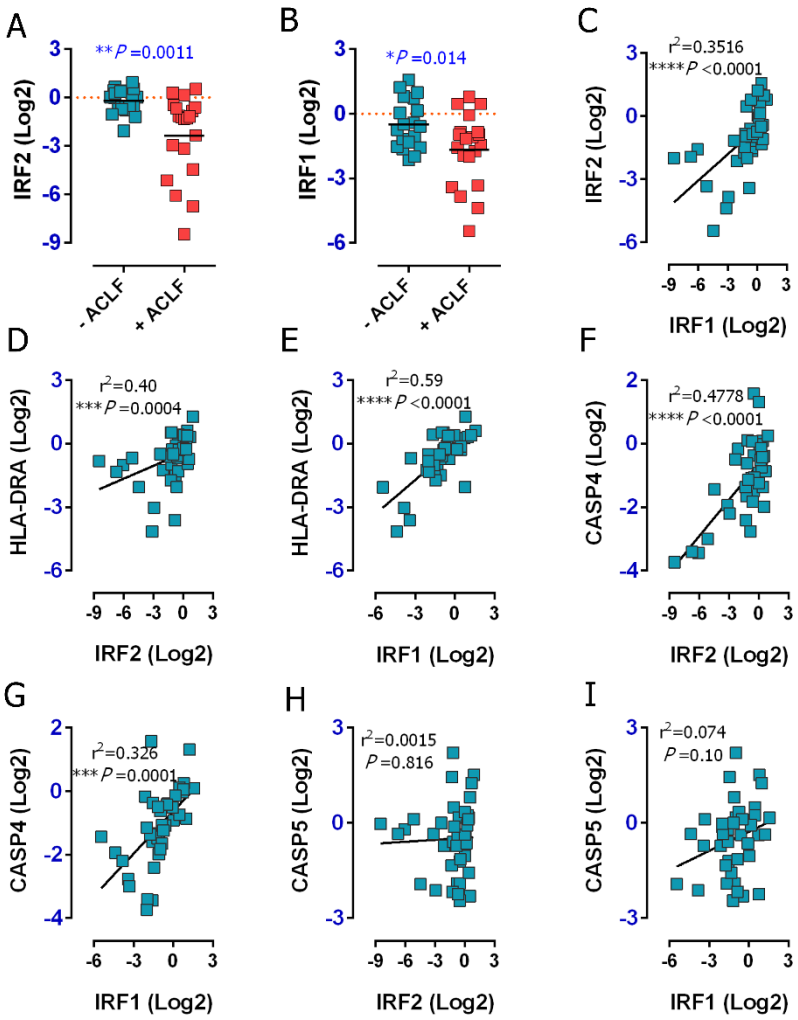

Fig. 7: *IRF1* and *IRF2* transcriptional regulators are suppressed during immunosuppression-associated organ damage in cirrhotic patients with ACLF.
Data were obtained as described in **Fig. 4**. (**A**, **B**) mRNA expression of *IRF2* (**A**), and *IRF1* (**B**) in PBMCs of cirrhotic patients with or without ACLF. (**C**) Correlation of mRNA expression of *IRF1* and *IRF2*. (**D**, **E**) Correlation of mRNA expression of *HLA-DRA* in PBMCs of patients with *IRF2* (**D**), and *IRF1* (**E**). (**F**, **G**) Correlation of mRNA expression of *CASP4* with *IRF2* (**F**) and *IRF1* (**G**). (**H**, **I**) Correlation of mRNA expression of *CASP5* with *IRF2* (**H**) and *IRF1* (**I**). *P* values determined by unpaired two-tailed *t*-test, horizontal lines represent mean values. *P* and r^2 values from two-tailed Pearson´s correlation of parametric regression analysis., $*P < 0.05$, $**P < 0.01$, $***P < 0.001$, $****P < 0.0001$, ns, not significant $P > 0.05$. Each data marker represents an individual patient.

In addition to *CASP4*, IRF2 and IRF1 regulate the expression of *GSDMD* and *CASP1* (Kayagaki et al., 2019; Benaoudia et al., 2019). Consistent with *CASP4*, *IRF2*, and *IRF1*, the expression of *GSDMD* was significantly downregulated (**Fig. 8A**). Noteworthy, gene expression of *GSDMD* correlates with their regulators *IRF2*, *IRF1* as well as *CASP4* and *HLA-DRA*, but not *CASP5* **(Fig. 8B-F)**. Interestingly, *CASP1* expression profile was not changed in patients with ACLF compared to patients without ACLF **(Fig. 8G)**. This is consistent with a recently reported study in patient with cirrhosis (Stengel et al., 2020). However, Caspase-1 expression correlates with *IRF1* and *IRF2* **(Fig. 8H-I)**. Collectively, non-canonical inflammasome sensor *CASP4* and

executor *GSDMD* are downregulated during innate immunosuppression and their expression profile associates with dampened expression of *IRF2* and *IRF1*.

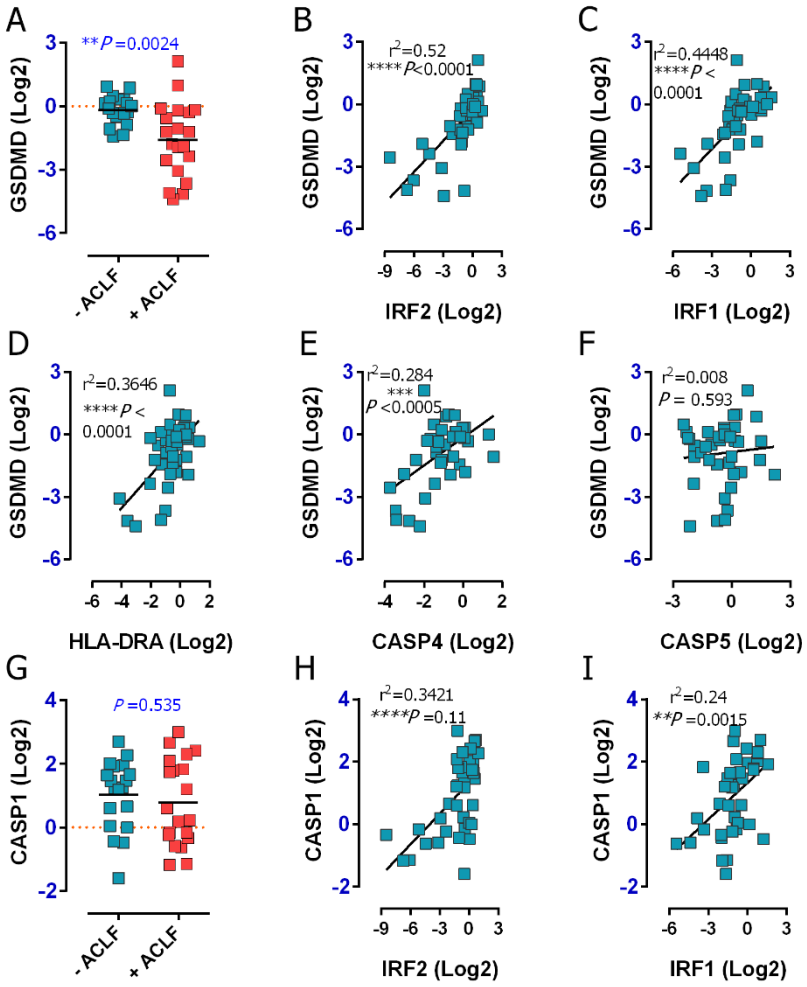

Fig. 8: *GSDMD* and *CASP1* regulation and their association with *IRF2* and *IRF1* expression in cirrhotic patients with or without ACLF.
Data were obtained as described in **Fig. 4**. (**A**) mRNA expression of *GSDMD* (**A**) in PBMCs of patients without ACLF (n=19) and with ACLF (n=20). (**B-F**) Correlation of mRNA expression of GSDMD with *IRF2* (**B**), *IRF1* (**C**), *HLA-DRA* (**D**), *CASP4* (**E**), or *CASP5* (**F**) in PBMCs of cirrhosis patients with and without ACLF. (**G**) *CASP1* mRNA expression in PBMCs of cirrhosis patients with or without ACLF. (**H**, **I**) Correlation of *CASP1* with *IRF2* (**H**) or *IRF1* (**I**). *P* values determined by unpaired two-tailed *t*-test, horizontal lines represent mean values (**A**, **G**). *P* and r^2 values from two-tailed Pearson´s correlation of parametric regression analysis (**B-F**, **H**, **I**). $*P < 0.05$, $**P < 0.01$, $***P < 0.001$, $****P < 0.0001$, ns, not significant $p > 0.05$. Each data marker represents an individual patient.

The MELD scoring system as an organ damage assessment is associated with complications caused by infection-triggered organ failure (Bruns et al., 2014) and immunosuppression (Seeley et al., 2018). In this context, I assessed the correlation between expression profile of *HLA-DRA* as an immunosuppression marker and *IRF2* and *IRF1* as *CASP4* regulators with MELD score. As seen in (**Fig. 9A-C**) a significant correlation of *HLA-DRA*, *IRF2* and *IRF1* with MELD score was observed. Furthermore, I determine a prospective correlation of *CASP4* and *CASP5*

expression with MELD score, I interestingly found that the MELD score inversely correlate with expression profile of *CASP4* but not with *CASP5* (**Fig. 9D**, **E**). In addition, MELD score correlates negatively with GSDMD expression (**Fig. 9F**). Altogether, these data indicate that the immunosuppression-associated organ damage is accompanied with down-regulation of *CASP4* but not *CASP5*.

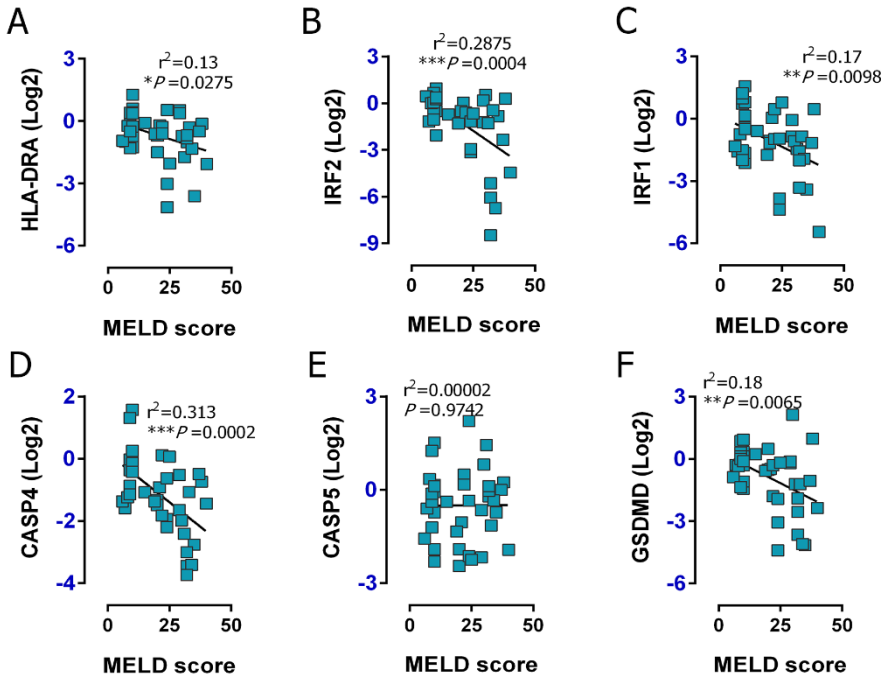

Fig. 9: *CASP4*, but not *CASP5* expression correlates with MELD score in cirrhotic patients with and without ACLF.
(A-F) Correlation of MELD score with mRNA expression of *HLA-DRA* (**A**), *IRF2* (**B**), *IRF1* (**C**), *CASP4* (**D**), *CASP5* (**E**), or *GSDMD* (**F**) in PBMCs of cirrhosis patients with or without ACLF. *P* and r^2 values from two-tailed Pearson´s correlation of parametric regression analysis. **P* < 0.05, ***P* < 0.01, ****P* < 0.001, ns, not significant *P* > 0.05. Each data marker represents an individual patient.

4.1.4 Outcomes of the differential regulation of *CASP4* and *CASP5* during immunosuppression

Inflammasome activation coincides with release of certain cytokines, alarmins and DAMPs. Recent studies have suggested that caspase-4 and 5 play an interchangeable role during infection (Baker et al., 2015). The outcome of these mechanical signals is the specific release of certain alarmins and cytokines. Triggering the non-canonical inflammasome results in caspase-4-dependent release of Gal-1 (Russo et al., 2021) and caspase-5-dependent release of progranulin (Duduskar et al., 2019). To functionally examine the differential regulation of caspase-4 and 5 during immunosuppression, Gal-1 and PGRN were assessed in the plasma of the patient cohort with cirrhosis (**Table 16)**. Interestingly, both Gal-1 and PGRN were highly released in cirrhotic patients with and without ACLF when compared to healthy donors. However, consistent with mRNA expression of *CASP4* (**Fig. 5A**), the release of GAL-1 in

patient with ACLF tends to be marginally down-regulated in compare to patients without ACLF (**Fig. 10A**). In contrast, PGRN was significantly released in patient with ACLF compared to patients without ACLF (**Fig. 10B**), this is consistent with sustained regulation of caspase-5 expression (**Fig. 5B**).

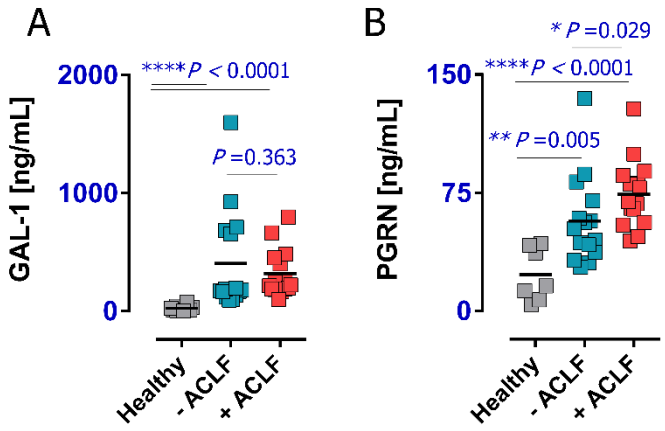

Fig. 10: Gal-1 and PGRN release from cirrhosis patient with or without ACLF and their association with regulation of *CASP4* and *CASP5*. Levels of Gal-1 (**A**) and PGRN (**B**) were measured in the plasma of cirrhosis patients with or without ACLF compared with healthy donors. *P* values determined by unpaired Mann-Whitney *t*-test, $*P < 0.05$, $**p < 0.01$, $***P < 0.001$, $****P < 0.0001$, not significant $P > 0.05$. Horizontal lines represent mean values.

To further investigate the suppression of caspase-4 during immunosuppression state and organ damage, I analyzed the amount of caspase-4 protein along with the inflammasome activation in plasma derived from patients with sepsis caused by bacterial infections. Interestingly, protein expression of caspase-4 was reversely correlated with SOFA scores in septic patients (**Fig. 11A**, **B**). Activation of inflammatory caspases results in cleavage of GSDMD into two subunits p20 and p30 to induce the pyroptotic cell death (Shi et al., 2014; Kayagaki et al., 2015; Aglietti et al., 2016). To determine an active inflammasome state during sepsis and its association to baseline of organ damage, I investigated the proteolytic active subunit p20 of GSDMD in plasma patients with sepsis as a pyroptotic executor of inflammasome activity (He et al., 2015). First, we investigate the release of GSDMD subunit p20 in plasma of patients diagnosed with sepsis compared with ICU critically ill patients and healthy donors. Intriguingly, whereas plasma of healthy donors and ICU patients did not show an active GSDMD (p20), sepsis patients showed a dominant active p20 of processed GSDMD (**Fig. 11C**). In order to distinguish patients with high grad of organ damage, a cut-off value of $\geq 8 <$ SOFA score was selected. Interestingly, I found that the active GSDMD was processed and detectable in sepsis patients (**Fig. 11D**), implicating thereby an inflammatory caspase catalytic activity in patients with high SOFA score and organ damage.

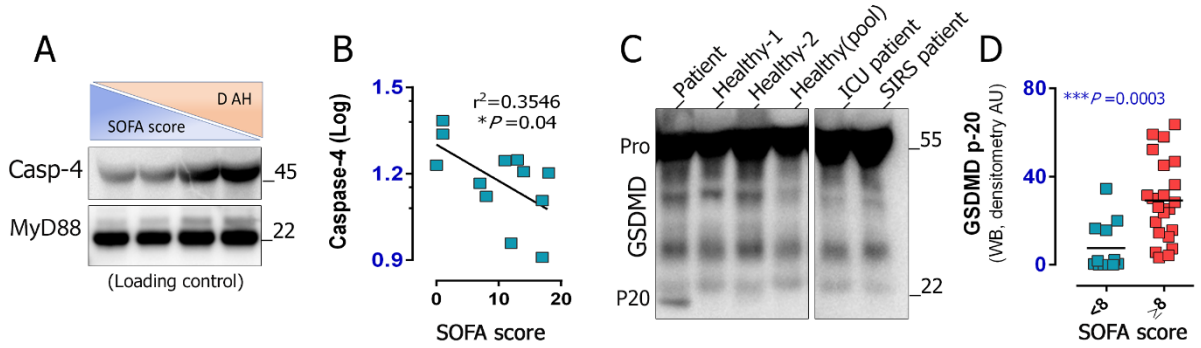

Fig. 11: Inflammasome activation is associated with organ failure during course of sepsis. (**A**) A representative immunoblotting of the protein amount of caspase-4 and MyD88 (loading control) in plasma of septic patient along with SOFA score and days after hospitalization (D AH). (**B**) Linear correlation of caspase-4 protein expression and SOFA score. A representative immunoblotting of the protein amount of GSDMD (pro) and (p20) in plasma of septic patients, healthy donors (HS), ICU patient, and SIRS patient. Densitometric values of GSDMD (p20) quantified in plasma of septic patients as indicated in (**C**) stratified according to a cut-off value of ≥ 8 < SOFA score (**D**). *P* value from two-tailed Pearson´s correlation (**B**) and Mann-Whitney test (**D**). **P*< 0.05, ****P* < 0.001, r^2 value from the Pearson correlation coefficient.

4.1.5 Regulation of *CASP4* and *CASP5* during tolerance state in monocytes derived from sepsis-patients

Monocytes of sepsis patients often show desensitized phenotype and do not respond to an *ex vivo* LPS challenge in terms of TNF-α release, a key feature of LPS tolerization (Randow et al., 1995; Döcke et al., 1997; Wolk et al., 2000; Widdrington et al., 2018). To examine the influence of this phenomenon on the regulation of *CASP4* and *CASP5*, expression of *CASP4* and *CASP5* was analyzed in primary cultured monocytes derived from patients with sepsis **(Table 19)** after LPS *ex vivo* challenge. Consistent with previous reports (Randow et al., 1995; Döcke et al., 1997; Winkler et al., 2017; Widdrington et al., 2018), tolerized monocytes with features of endotoxin tolerance showed impaired TNFα production (**Fig. 12A**). Accordingly, and as recently demonstrated (Seeley et al., 2018), miR-222 expression in monocytes can distinguish between tolerized and non-tolerized patients (**Fig. 12B**). However, *CASP4* expression was markedly diminished in monocytes of tolerized patients but remain upregulated in non-tolerized patients as compared with untreated control (**Fig. 12C**). Irrespective of the inflammatory state of patients, expression of *CASP5* remained upregulated in tolerized and non-tolerized patients (**Fig. 12D**). Collectively, these data indicate that *CASP4* and *CASP5* are differentially regulated and may exert thereby different functions during the immunosuppression state in monocytes.

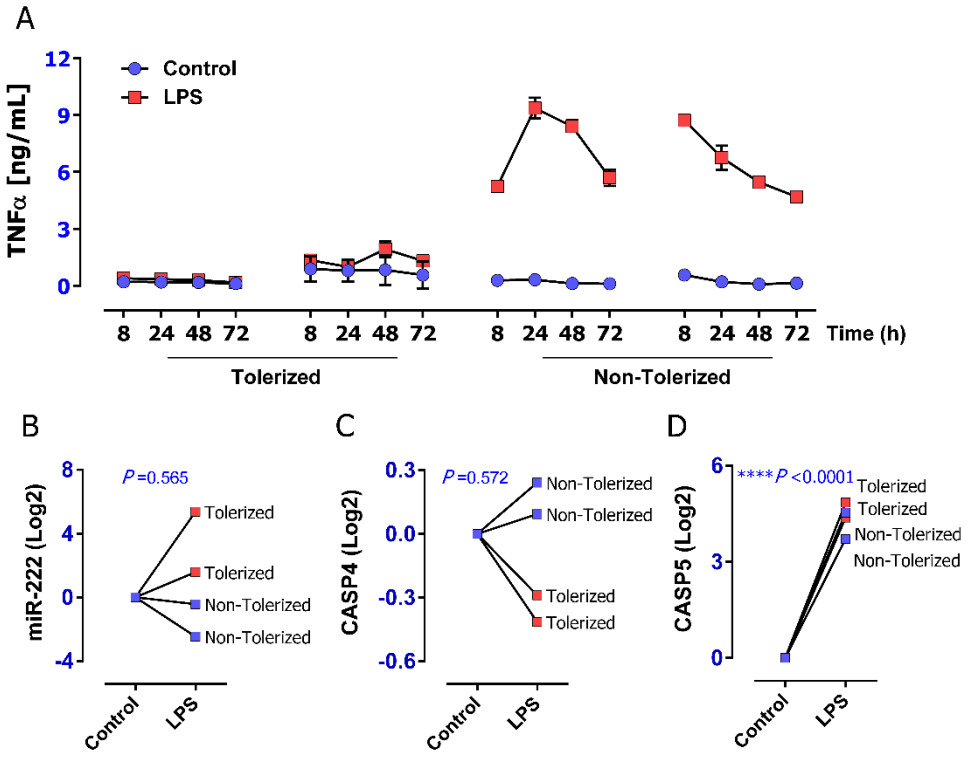

Fig. 12: *CASP4* but not *CASP5* is suppressed in *ex vivo* tolerized monocytes derived from patients with sepsis.
(**A**) Monocytes derived from septic patients were stimulated or not with LPS for 72 h and TNF-α was measured by ELISA in supernatants over the indicated time. (**B-D**) Gene expression of miR-222 (**B**), *CASP4* (**C**), and *CASP5* (**D**) after 72 h LPS stimulation. *P* values from unpaired two-tailed *t*-test. ****$P < 0.0001$, $P > 0.05$, ns, not significant.

4.1.6 IFN-γ abrogates CASP4 suppression via upregulation of IRF2 and IRF1 expression during endotoxin tolerance.

Synergistic activation of cytokines production by TLR- and IFN-γ -signaling is important for innate immune defense. Different studies have shown that diminished LPS response can be restored through treatment with IFN-γ. The latter enhances sustained occupancy of transcription factors STAT1, IRF-1, and primed chromatin environments to enforce TLR-induced gene transcription e. g. *TNFA* and *IL6* (Chen and Ivashkiv, 2010; Qiao et al., 2013; Seeley et al., 2018; Kang et al., 2019). To investigate the association of *CASP4* expression and IFN response during *in vitro* course of LPS-induced tolerance, human monocytes-derived macrophages (MDM) of seven separate healthy donors were treated with LPS alone or with IFN-γ. The capacity of IFN-γ to restore gene expression of *HLA-DRA*, *CASP4*, *IRF1* and *IRF2* as well as the production of TNFα and surface HLA-DR expression in MDM were analyzed across a dense time course. Initially, consistent with known literature, (Döcke et al., 1997; Chen and Ivashkiv, 2010; Seeley et al., 2018) prolonged exposure of macrophages to LPS results in diminished TNFα production, whereas co-stimulation with IFN-γ prevents LPS-induced tolerance in macrophages (**Fig. 13A**). Furthermore, MDM were subjected to fluorescence-

activated cell sorting (FACS) analysis for surface expression of HLA-DR after 72 h treatment with LPS or LPS+IFN-γ. As expected, IFN-γ enhances the surface expression of HLA-DR in macrophages (**Fig. 13B**, **C**). In particular, surface expression of HLA-DR was augmented by IFN-γ compared to the slightly induced expression upon stimulation with LPS alone (**Fig. 13D**). The gating strategy of macrophages was carried out as following: Initially, cells were selected according to morphology (forward vs. side scatter). Afterwards, cellular aggregates were excluded based on FSC-A vs. FSC-H. Finally, cells were gated based on HLA-DR expression (**Fig. 13D**).

Gene expression of HLA-DR subunit A was additionally analyzed by quantitative PCR. mRNA expression of HLA-DRA was modestly induced upon stimulation with LPS alone after 8h but clearly downregulated after 24h (**Fig. 13E**). In contrast, co-stimulation with IFN-γ prevented the diminished HLA-DRA expression, hence it remained at basal level of expression. In order to examine whether LPS and IFNy affects the expression of *CASP4* in cells undergoing tolerance, *CASP4* gene expression was assessed during LPS responses. As shown in (**Fig. 13F**) and in agreement with previous studies (Viganò et al., 2015) LPS transiently induces *CASP4* expression but declines thereafter and its expression profile was abolished to basal level after 24h. Interestingly, *CASP4* expression remained upregulated when macrophages were co-stimulated with IFN-γ (**Fig. 13F**). We further sought the association of *IRF2* and *IRF1* with *CASP4* expression upon LPS and IFN-γ stimulation. *IRF2* was upregulated upon stimulation with LPS alone, peaking at 24h with LPS alone and at 48h by co-stimulation with IFN-γ (**Fig. 13G**). IRF1 is the most-rapidly induced IRF among IRF members upon TLR4 activation, which peaks at 0.5-4h (Ohmori and Hamilton, 2001; Baillie et al., 2017). However, unlike *IRF2*, LPS alone did not induce IRF1 expression later in time point (8h) in this study. IRF1 remained constantly upregulated throughout the experimental period by IFN-γ (**Fig. 13H**). Since *IRF2* and *IRF1* were also constantly upregulated upon IFN-γ treatment course and consistent with Benaoudia et al (2018) our data suggests that the abrogated *CASP4* tolerization is mediated cooperatively via IRF2 and IRF1 in human macrophages. Collectively, our data showed that IFN-γ can induce the sustained expression of *CASP4*, which might enhance the recognition of cytosolic derived LPS in course of Gram-negative infections.

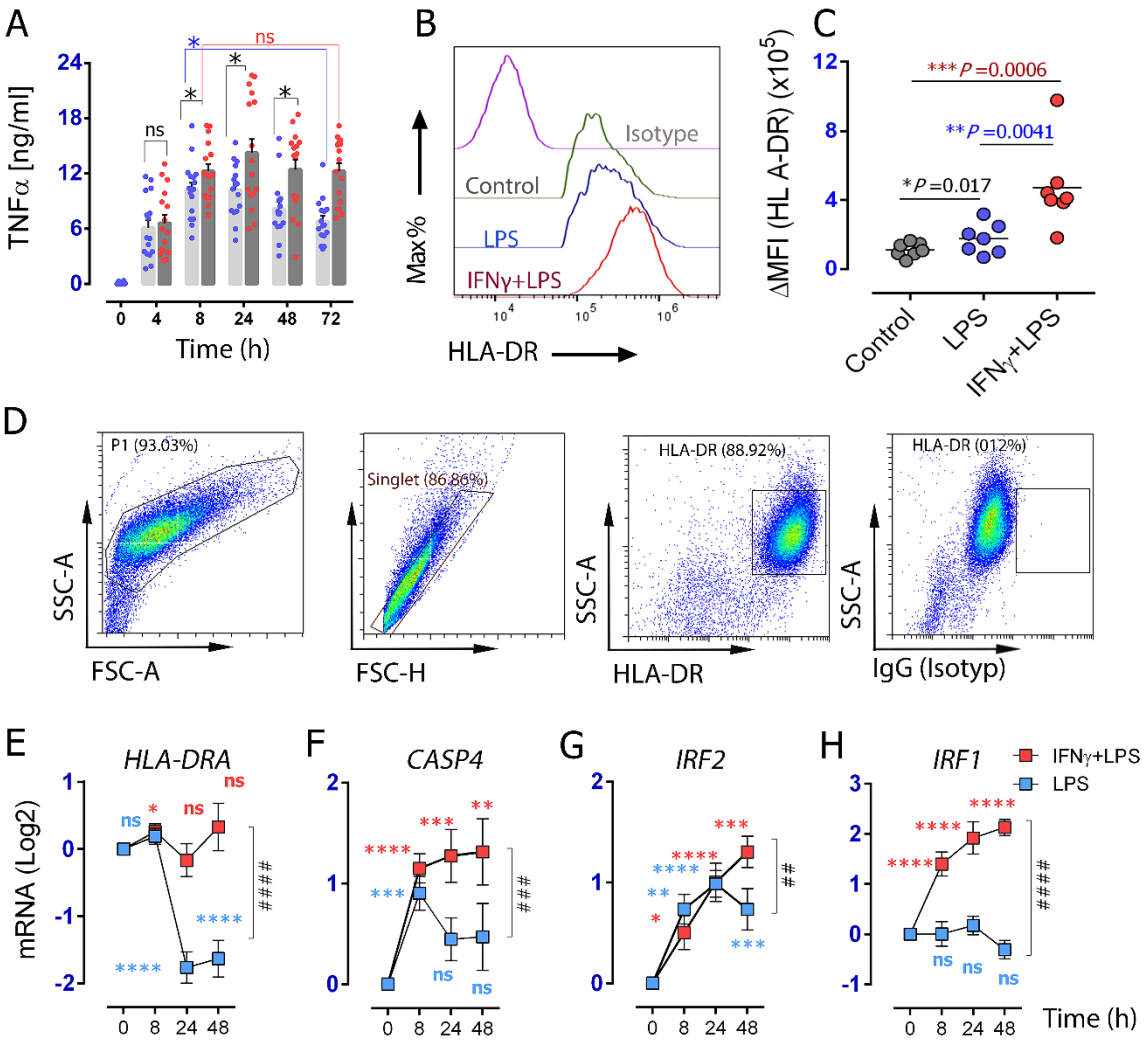

Fig. 13: IFN-γ abrogates endotoxin tolerance *in vitro*.
Monocytes-derived macrophages (MDM) isolated from healthy donors (n=7) were stimulated with LPS alone or with IFN-γ and analyzed over indicated time (hours) for TNF-α production by ELISA (**A**) or for HLA-DR expression by flow cytometry (**B**, **C**). (**C**) Median fluorescent intensity was measured by flow cytometry on macrophages of healthy donors. Each data marker represents an individual donor (n=7). (**D**) A representative flow cytometry analysis of HLA-DR expression on MDM stained with HLA-DR antibody or IgG-Isotype control as indicated (**D**) expression of indicated genes in MDM of healthy donors (n=7) in response to LPS alone or LPS with IFN-γ. (**A**) statistical difference between indicated groups determined by Wilcoxon test for paired and nonparametric data. (**C**) statistical difference between indicated groups determined by Mann-Whitney two tailed *t*-test for unpaired nonparametric values. (**D-H**) significant to time-point zero determined by Student's *t-test* for unpaired parametric values. $*P < 0.05$, $**P < 0.01$, $***P < 0.001$, $****P < 0.0001$. (**D-G**) $^{\#}$ significant to time point 48 h (LPS versus LPS+IFN-γ) determined by two-tailed *t*-test for paired parametric values. $^{\#\#}P < 0.01$, $^{\#\#\#}P < 0.001$, $^{\#\#\#\#}P < 0.0001$, ns, not significant $P > 0.05$. For all bar and line graphs, mean ±SEM is plotted

4.1.7 Expression of CASP5 and CASP4 can be differentially induced in human macrophages.

Multiple studies have shown, that *CASP4* and *CASP5* are upregulated in response to LPS (Lin et al., 2000; Viganò et al., 2015). However, whether different PAMPs can differ in regulating *CASP4* and *CASP5* has not yet been reported. Taking the knowledge, that *Casp11* is not

inducible by TLR2 signaling in mice (Rathinam et al., 2012), we raised the intriguing question whether TLR2 signaling in human differs in induction of caspase-4 or/and capsase-5. THP1 macrophages were employed as they are known for lacking expression of *CASP5* at steady state (Shi et al., 2014; Schmid-Burgk et al., 2015; Benaoudia et al., 2019). PMA-differentiated THP1 macrophages were challenged with Pam_3CSK_4, a TLR2 bona fide ligand. *IL1B* as an inducible pro-inflammatory gene was markedly induced in response to TLR2 activation (**Fig. 14A**). Interestingly, expression of *CASP4* was not changed upon Pam_3CSK_4 stimulation (**Fig. 14B**), while *CASP5* expression was significantly induced. Analysis of *CASP4* and *CASP5* expression revealed that regulation of *CASP4* and *CASP5* genes can also be differentially induced and suggest that distinct pathways induce the expression of *CASP5* and *CASP4* and confirmed the *de novo* expression of *CASP5* in macrophages (**Fig. 14C**). As shown in **Fig. 14D** and consistent with previous observations (Shi et al., 2014; Schmid-Burgk et al., 2015), *CASP4* is a constitutively expressed gene **Fig. 14D**, whereas *CASP5* gene expression was not detected in at steady state (naïve) THP1 macrophages (**Fig. 14D**) but requires de novo expression after TLR2 activation. This confirms a further complexity in the upstream regulation and function of human caspase-4 and -5.

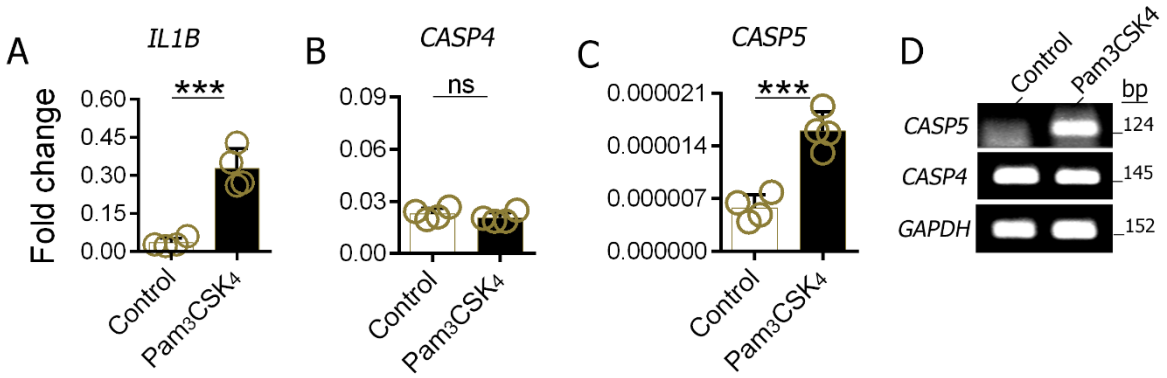

Fig. 14: TLR2/1 activation via Pam_3CSK_4 selectively upregulates the expression of *CASP5* but not *CASP4*.
(**A-C**) THP-1 macrophages were stimulated with Pam_3CSK_4 for 3 h and mRNA expression of *IL1B* (**A**), *CASP4* (**B**), and *CASP5* (**C**) were analyzed by qPCR. (**D**) Confirmation of results obtained in **B** and **C**, amplicons of *CASP5*, *CASP4* and *GAPDH* were subjected for Agarose-gel-electrophoresis. *P* values from unpaired two-tailed *t-test*. ***$P < 0.001$, ns, not significant $P > 0.05$.

4.2 Loss-of-Function Variant in CNPY3 Gene impairs Caspase-1 Activation and IL-1β Processing in Human Macrophages

A number of studies have shown that ER-resident chaperone CNPY3 leads to the loss of function of many TLRs (Takahashi et al., 2007; Liu et al., 2010), which in turn, due to deficiencies in signaling and gene induction in response to TLR ligands, may lead to PRR-dependent reduction of canonical and non-canonical inflammasome activity. To further clarify the role of CNPY3 during infection and specific inflammasome activators we were interested in whether it has a direct role in the activation of the inflammasome. Using different CRISPR-Cas9 mediated gene deletions of CNPY3 in THP1 macrophages lines and primary macrophages carrying a loss-of-function mutation of *CNPY3* c.485delA, we further investigated the role of the chaperone CNPY3 in regulating NLRP3 inflammasome activation. Thus, CNPY3 may function as key regulator of surface responses such as TLRs as well as intracellular signaling in terms of inflammasome activation.

4.2.1 CNPY3 is required for the plasma membrane translocation of TLRs in human macrophages.

The prominent role of CNPY3 in innate immunity as a chaperone is the folding and trafficking of various TLRs including TLR1, 2, 4, 5 and 9 but not TLR3. Therefore, CNPY3 deficiency results in an impairment for the translocation of its client TLRs to the plasma membrane (Takahashi et al., 2007; Shibata et al., 2012). How this affects other downstream signaling pathways including inflammasome activation has not yet been studied. In order to study a potential role of CNPY3 in regulating inflammasome activation, stable CNPY3 deficient human THP-1 cell lines were generated using CRISPR/Cas9 genome-editing (Jinek et al., 2012). The targeted genomic region corresponds to the crRNA sequence of the sgRNA located in the exon-intron border of exon-1 and intron-1 of CNPY3 gene on chromosome 6 to create double-stranded breaks, inducing a frameshift mutation within the open reading frame of CNPY3 gene (**Fig. 15A**). Resulting clones were characterized by Sanger sequencing using specific primers flanking the CRISPR targeted regions. Sequencing of the target region revealed multiple mutations, which ultimately resulted in internal deletion of the CNPY3 gene as shown in **(Fig. 15B).** Taking this further, protein expression of CNPY3 were analyzed in THP-1 wild type and *CNPY3*$^{-/-}$ cells. As shown in **Fig. 15C**, CNPY3 is expressed predominantly in the THP-1 cells, however, *CNPY3*$^{-/-}$ THP1 cells failed to express CNPY3 protein. Results obtained from Sanger sequencing and immunoblotting genetically confirmed that indeed the cells are appropriately targeted in both alleles. Since CNPY3 chaperone is required for trafficking of TLRs, I performed a functional characterization of the *CNPY3*$^{-/-}$ clone. I first determined the

surface expression of TLR2, one of the TLRs known to require CNPY3 (Takahashi et al., 2007; Kiyokawa et al., 2008; Liu et al., 2010). As shown in **Fig. 15D** CNPY3 deficiency in THP-1 cells results in a total loss of TLR2 surface translocation, whereas wild type cells exhibited a pronounced expression of TLR2 on the plasma membrane (**Fig. 15D**). *CNPY3*$^{-/-}$ macrophages were further functionally characterized by challenging them with TLR2 agonists. Consistent with the defective trafficking of TLR2 to plasma membrane, TLR2 signaling in terms of TNFα production in *CNPY3*$^{-/-}$ macrophages was fully impaired, when challenged with the TLR2/1-ligand (Pam_3CSK_4) (**Fig. 15B**). Unlike TLR2, chaperoning of endomembrane-resident TLR3 is UNC93B1 dependent but CNPY3 independent (Tabeta et al., 2006; Takahashi et al., 2007; Pelka et al., 2018). By contrast, challenging the wild type and *CNPY3*$^{-/-}$ macrophages with the TLR3 ligand poly(I:C) led to an equal production of TNFα in a CNPY3-independent manner (**Fig. 15F**). In sum, the loss of CNPY3 function in macrophages exerted the predicted member-selective effects on TLR subcellular translocation and immune response.

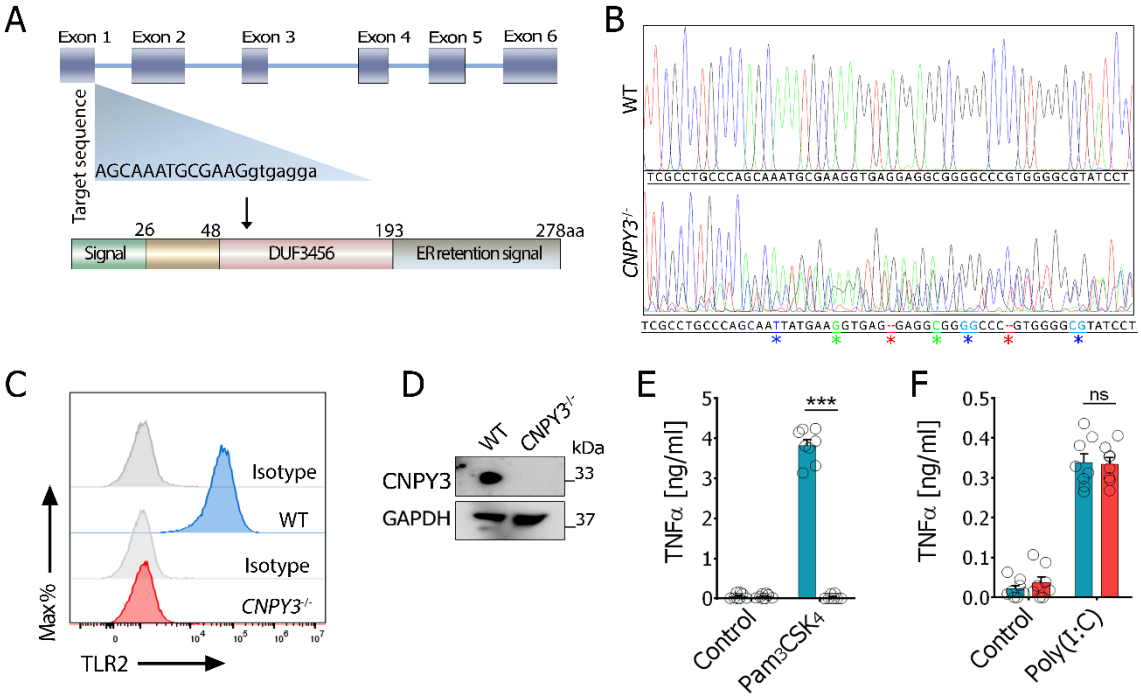

Fig. 15: Characterization of *CNPY3*$^{-/-}$ THP-1 cells generated by CRISPR/Cas9 genome-editing system.

(**A**) Sequence analysis of *CNPY3* gene with targeting sequence sgRNA and gene edited clonal sequencing analysis of *CNPY3*$^{-/-}$ THP-1 cells. (**B**) *CNPY3* gene analyzed by Sanger sequencing with corresponding mutations compared to wild type sequence. (**C**) CNPY3 protein expression in wild type and *CNPY3*$^{-/-}$ THP-1 cells. (**D**) Surface expression of TLR2 in wild type and *CNPY3*$^{-/-}$ THP-1 cells as indicated. (**E**, **F**) CNPY3 wild type and *CNPY3*$^{-/-}$ THP-1 macrophages were stimulated with Poly(I:C) (**E**) or Pam_3CSK_4 (**F**) and TNFα was measured in supernatants by ELISA (Mann-Whitney U test, ***$P < 0.001$, ns; not significant, $P > 0.05$) (data are mean ±SEM).

4.2.2 Expression of core inflammasome components and NLRP3 translocation to mitochondria-associated membrane are unaffected by CNPY3 deficiency upon TLR3 activation

Inflammasome activation requires licensing triggers (surface signaling) to produce key components of the inflammasome (intracellular signaling) before activation by second stimuli (Schroder and Tschopp, 2010; Groslambert and Py, 2018). As numerous studies have shown that TLR stimulation plays an important role in priming cells for inflammasome activity, priming of CNPY3 cells may therefore be impaired. To gain a mechanistic insight into, whether macrophages can mediate a chaperone-mediated inflammasome activation, protein expression of key inflammasome components were confirmed in wild type and *CNPY3*$^{-/-}$ macrophages. THP-1 wild type and *CNPY3*$^{-/-}$ macrophages were stimulated with TLR3 agonist (poly(I:C)) for 4 h to confirm an equal priming event occurred in both cell lines. Importantly, release of certain inflammatory cytokines is differentially regulated. Cytokines such as IL-6 and TNFα, all of which are activated downstream of membrane-bound receptors, are regulated at the transcriptional level, whereas other cytokines such as IL-1β and IL-18 are expressed as precursor forms (pro) that are subsequently processed in response to intracellular inflammatory cues. The inflammasome activation-dependent cytokine IL-1β is an inducible gene and requires therefore a *de novo* expression triggered e. g. by TLR2/3/4 activation in macrophages (Groslambert and Py, 2018; Fitzgerald and Kagan, 2020). To examine the impact of CNPY3 on the induction/expression of pro-IL-1β in *CNPY3*$^{-/-}$ macrophages, wild type and *CNPY3*$^{-/-}$ macrophages were stimulated with poly(I:C) and protein expression of pro-IL-1β was analyzed. Importantly, CNPY3 was dispensable for pro-IL-1β synthesis in response to TLR3 stimulation (**Fig. 16A**). Next, further key components of inflammasome assembly were assessed. Accordingly, compared to wild type macrophages, the expression of critical canonical inflammasome components including caspase-1, NLRP3, and ASC were unaffected in *CNPY3*$^{-/-}$ macrophages upon stimulation with poly(I:C) (**Fig. 16A**). Noteworthy, activation of TLR3 licenses TRIF-mediated signaling, which engage coincidently non-canonical inflammasome components including caspases-4/11 and GSDMD (Schauvliege et al., 2002; Rathinam et al., 2012; Gurung et al., 2012; Benaoudia et al., 2019; Kayagaki et al., 2019). Expression of GSDMD is required, as an executor of pyroptosis, for the secretion of the exported form of IL-1β and IL-18 (He et al., 2015). Interestingly, protein expression of GSDMD was not affected in *CNPY3*$^{-/-}$ macrophages (**Fig. 16A**). Taken together, these findings agree with the notion that CNPY3 is required for signaling elicited by its client TLR receptors, but not TLR3. In support of this finding, we showed that CNPY3 is dispensable for the precursor expression of pro-IL-1β, pro-caspase-1 and other key NLRP3 inflammasome components in macrophages.

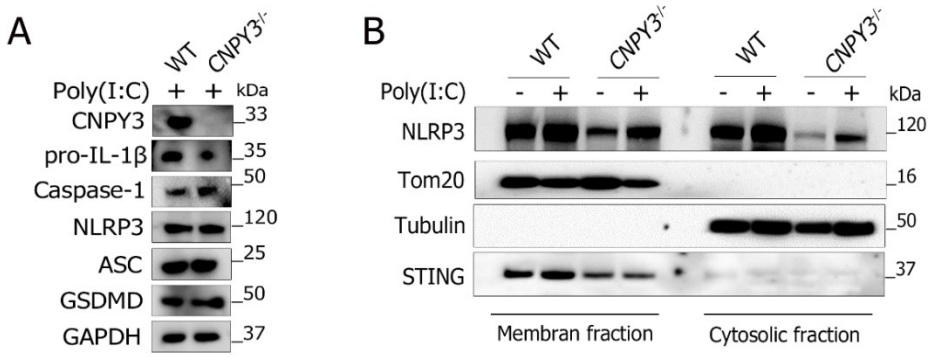

Fig. 16: CNPY3 is dispensable for expression of inflammasome proteins and NLRP3 migration in human macrophages following TLR3 activation.
(**A**) Western blot analysis of inflammasome components in THP-1 wild type and *CNPY3*$^{-/-}$ macrophages were stimulated with poly(I:C) for 4 h. (**B**) THP-1 wild type and *CNPY3*$^{-/-}$ macrophages were stimulated or not with poly(I:C) and then membrane and cytosolic fractions were immunoblotted as indicated.

In addition to transcriptional regulation, post-transcriptional controls of different inflammasome components are thought to be an important consideration in TLR activation. At steady state, NLRP3 is a cytosolic and ER-associated protein. However, under priming conditions such as TLR-activation, NLRP3 migrates from the ER to mitochondria and mitochondria-associated membranes (MAMs) in perinuclear region of cells (Iyer et al., 2013; Elliott et al., 2018; Chen and Chen, 2018; Groslambert and Py, 2018). Migration of NLRP3 from ER to MAMs is a vital process for ensuing a more intense and coordinated inflammasome activation in macrophages (Zhou et al., 2011; Subramanian et al., 2013; Zhang et al., 2017; Elliott et al., 2018). To address if CNPY3 plays a role in this process, we examined the capacity of NLRP3 translocation into mitochondria and MAMs upon TLR3 activation via poly(I:C) prior to an activation signal. Accordingly, subcellular fractionations of poly(I:C) treated and non-treated macrophages were subjected to immunoblotting analysis. Initially, we used Tom20 and α-Tubulin as separate protein markers for mitochondria/membrane and cytosolic fractions, respectively and ensured the efficacy of subcellular fractionation. In addition, STING as an ER-associated membrane protein and important regulator for NLRP3 inflammasome activation was additionally examined (Gaidt et al., 2017; Wang et al., 2020) (**Fig. 16B**). This analysis revealed a sufficient redistribution of NLRP3 from cytosolic to membrane fractions upon TLR3-activation in a CNPY3-independent manner. Despite a reduced amount of distributed NLRP3, NLRP3 expression was efficiently promoted in the cytosolic and membrane fractions of poly(I:C) treated CNPY3 sufficient and deficient macrophages (**Fig. 16B**), which is in line with known literature (Elliott et al., 2018). Altogether, NLRP3expression and translocation were not fully compromised or affected in *CNPY3*$^{-/-}$ macrophages (**Fig. 16**).

4.2.3 CNPY3 is required for the efficient activation of caspase-1 and processing of pro-IL-1β

Pro-caspase-1, is an important converging point for initiating inflammation and defense, and requires prior recruitment to the inflammasome assembly site after being triggered by PAMPS and danger signals. Subsequent pro-caspase-1 auto-activation then results in the generation of the large (p20) and small (p10) subunits of the catalytically active enzyme (Broz et al., 2010; Schroder and Tschopp, 2010). After confirmation, that priming events of inflammasome (Signal-1) similarly occur in *CNPY3*$^{-/-}$ and wild type macrophages in a TLR-independent fashion, I further examined the requirement of CNPY3 in NLRP3 inflammasome activation (Signal-2). To ultimately prove this hypothesis, pro-caspase-1 conversion/activation to active caspase-1 was dissected. Caspase-1-dependent cleavage of newly expressed pro-IL-1β and constitutively expressed IL-18 represents the final step of the inflammasome reaction cascade. We tested the response of *CNPY3*$^{-/-}$ macrophages to nigericin, a specific NLRP3 inflammasome activator (Mariathasan et al., 2006; Coll et al., 2015). To our surprise, *CNPY3*$^{-/-}$ macrophages were highly impaired in terms of secretion of mature forms of IL-1β and IL-18 (**Fig. 17A**, **B**). Interestingly, although wild type and CNPY3$^{-/-}$ macrophages showed comparable expression levels of pro-IL-1β, *CNPY3*$^{-/-}$ macrophages were not able to efficiently process pro-IL-1β into mature IL-1β (**Fig. 17C**). In contrast to pro-IL-1β, pro-IL-18 is expressed more constitutively and entirely independent of priming events (Schroder and Tschopp, 2010; Groslambert and Py, 2018). Like pro-IL-1β, processing of pro-IL-18 to its mature form was also impaired in *CNPY3*$^{-/-}$ macrophages compared to wild type (**Fig. 17B**). The deficit in pro-IL-1β processing observed for *CNPY3*$^{-/-}$ macrophages was striking as it was comparable in magnitude to the phenotypes of cells lacking the sufficient expression inflammasome components caspase-1 and ASC (**Fig. 17E**). The inability to process pro-IL-1β and pro-IL-18 was probably caused by the inadequate activation of pro-caspase-1 to its active form, as *CNPY3*$^{-/-}$ impaired caspase-1 activation in response to nigericin, despite the presence of high levels of pro-caspase-1 (**Fig. 17C**). In addition to the proteolytic activation of pro-IL-1β and IL-18 precursors, active caspase-1 is required for the rapid induction of pyroptosis by mediating cleavage and assembly of GSDMD in the membrane which forms pores and serves as conduit for active forms of IL-1β and IL-18 (Shi et al., 2015; He et al., 2015). Thus, the inflammasome mediated pyroptosis is associated with the leakage of cytosolic constituents such as LDH (Fernandes-Alnemri et al., 2007; Broz et al., 2010). Consistent with the observed deficit in caspase-1 activation that precluded IL-1β and IL-18 processing, *CNPY3*$^{-/-}$ macrophages showed a marked impairment in nigericin-mediated pyroptosis compared to wild type (**Fig. 17D**).

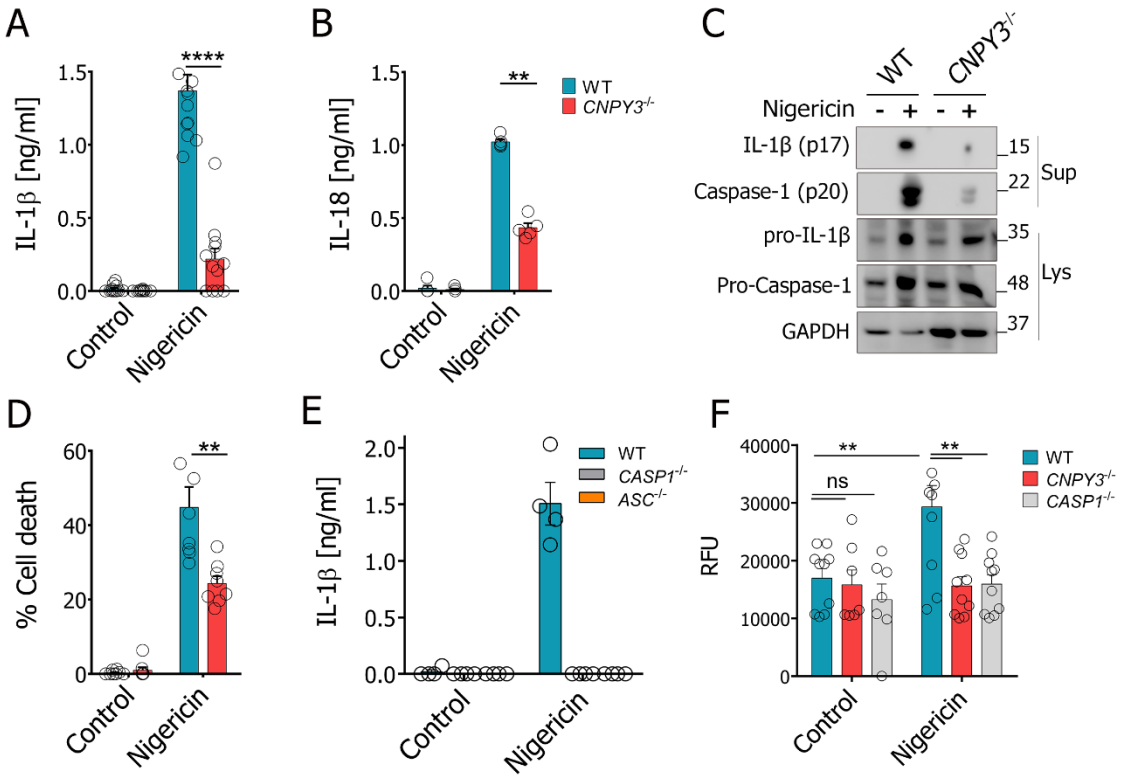

Fig. 17: CNPY3 is essential for efficient activation of caspase-1, processing of pro-IL-1β and pro-IL-18, and induction of pyroptosis.
(**A**, **B**) Poly(I:C)-primed CNPY3 wild type (WT) and *CNPY3*$^{-/-}$ THP-1 macrophages were stimulated with nigericin and IL-1β (**A**) and IL-18 (**B**) was measured in supernatants by ELISA. (**C**) Poly(I:C)-primed CNPY3 wild type and *CNPY3*$^{-/-}$ THP-1 macrophages were stimulated with nigericin. Cleaved products of IL-1β (p17) and caspase-1 (p20) were detected in cell supernatants (Sup) and pro-IL-β and pro-caspase-1 and GAPDH in lysates (Lys) by immunoblotting. (**D**) Poly(I:C)-primed CNPY3 wild type and deficient *CNPY3*$^{-/-}$ THP-1 macrophages were stimulated with nigericin and cell death was measured by LDH release (Mann-Whitney U test, $^{**}P<0{,}01$). (**E**) Poly(I:C)-primed CNPY3 wild type, *CASP1*$^{-/-}$ and *ASC*$^{-/-}$ THP-1 macrophages were stimulated with nigericin and IL-1β was measured in supernatants by ELISA (**B**). (**F**) Poly(I:C)-primed *CNPY3* wild type, *CNPY3*$^{-/-}$, and *CASP1*$^{-/-}$ (as a negative control) THP-1 macrophages were stimulated with nigericin for 30 min followed by intracellular staining with fluorescent probe for active caspase-1 (FLICA, green), Fluorescence intensity is measured in relative fluorescence units (RFU). All data represent the means ±SEM of two independent experiments. Mann-Whitney U test, $^{**}P < 0.001$, $^{***}P < 0.001$; ns, not significant $P > 0.05$.

To better understand, whether CNPY3 chaperone is required for secretion or processing, intracellular detection of caspase-1 activation was performed at an earlier time point (30 min). FAM-YVAD-FMK an inhibitor that irreversibly binds only to intracellular active caspase-1 (Man et al., 2014; Nagar et al., 2019) was employed. Despite detecting pro-caspase-1 in nigericin-stimulated *CNPY3*$^{-/-}$ macrophages as shown in **Fig. 17F**, an active caspase-1 using FAM-YVAD-FMK staining was not observed and was similar to *CASP1*$^{-/-}$ macrophages. Taken together, we concluded that CNPY3 is essential for an efficient and rapid caspase-1 activation to engage the caspase-1 dependent processing including the maturation of pro-IL-1β and pro-IL-18 and induction of pyroptosis in macrophages.

4.2.4 CNPY3 chaperone is dispensable for non-canonical NLRP3 inflammasome activation

In contrast to the canonical inflammasome, the non-canonical inflammasome is activated by direct binding of LPS to Caspase-4 and -5 in humans (caspase-11 in mice) in the cytosol, which in turn can also converge towards the activation of NLRP3 inflammasome (Kayagaki et al., 2011; Hagar et al., 2013; Kayagaki et al., 2013; Shi et al., 2014; Baker et al., 2015; Schmid-Burgk et al., 2015). To test whether CNPY3 was also critical for activation of the non-canonical inflammasome, TLR3-primed macrophages were exposed to intracellular LPS (iLPS) by transfecting LPS using Lipofectamine (LF). In line with known literatures (Hagar et al., 2013; Kayagaki et al., 2013; Shi et al., 2014; Schmid-Burgk et al., 2015), cytosolic LPS resulted in IL-1β release (**Fig. 18A**) as consequence of caspase-1 activation (**Fig. 18B**), while extracellular LPS did not induce caspase-1 processing or IL-1β secretion in poly(I:C) primed wild type macrophages (**Fig. 18A**, **B**). In contrast to wild type macrophages, caspase-1 activation (**Fig. 18B**) and IL-1β secretion (**Fig. 18A**, **B**) were strongly impaired in *CNPY3*$^{-/-}$ macrophages. Importantly, both wild type and *CNPY3*$^{-/-}$ macrophages showed an efficient priming by poly(I:C), as macrophages showed appropriate transcription of pro-caspase-1 and pro-IL-1ß independent of CNPY3 (**Fig. 18B**). Indeed, the release of active IL-1β relies on the proteolytic activation and assembly of the N-terminal subunit (p30) of GSDMD, which forms large pores in the plasma membrane upon inflammasome activation (Aglietti et al., 2016; Liu et al., 2016). Cytosolic LPS is known to promote GSDMD cleavage by activating caspase-4 and -5 resulting in caspase-1-dependent release of IL-1β and caspase-1-independent cell death (Shi et al., 2015; Kayagaki et al., 2015; Schmid-Burgk et al., 2015; Baker et al., 2015). To complete our analysis of inflammasome activation, we studied the engagement of GSDMD upon non-canonical inflammasome activation by analyzing the release of LDH as well as the cleaved subunits of caspase-5 (p20) and GSDMD (p30) in the supernatants, as readout for pyroptotic cell death (Viganò et al., 2015; Aglietti et al., 2016). Accordingly, we interestingly found that cell death was equally well engaged in CNPY3 wild type and *CNPY3*$^{-/-}$ macrophages when exposed to cytosolic LPS (LDH release, **Fig. 18C**). In keeping with this GSDMD-p30, which mediates the release of LDH (Shi et al., 2014; Ding et al., 2016) was equally induced in wild type and *CNPY3*$^{-/-}$ macrophages in response to cytosolic LPS (**Fig. 18B**). However, although GSDMD cleavage and the resulting cell death was not affected, we noticed that activation of caspase-5 was impaired in CNPY3 macrophages compared to wild type macrophages, suggesting that cell death in response to cytosolic LPS is mainly induced by caspase-4, as a main inflammatory

caspase following cytosolic LPS in THP-1 macrophages (Baker et al., 2015). Collectively, these data suggest that CNPY3 chaperone is dispensable for non-canonical inflammasome activation.

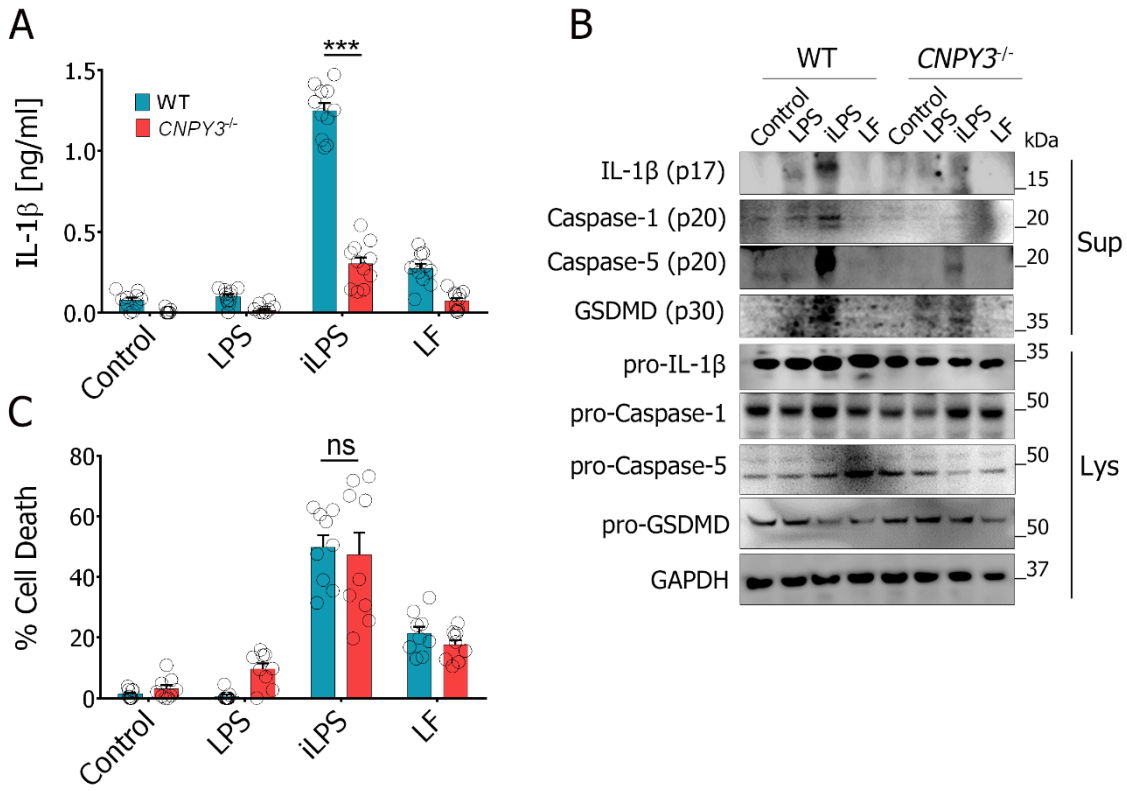

Fig. 18: CNPY3 chaperone is essential for IL-1β responses upon non-canonical inflammasome activation.
(**A**, **C**) Poly(I:C)-primed CNPY3 wild type (WT) and *CNPY3*$^{-/-}$ THP-1 macrophages were stimulated with LPS, LPS+lipofectamine (intracellular LPS, iLPS) or lipofectamine (LF) alone followed by released IL-1β (**A**) and LDH measurement (**C**) in supernatants by ELISA or LDH assay, respectively. (Mann Whitney U test, ***P < 0,001, P > 0.05 ns; not significant). (**B**) Poly(I:C)-primed CNPY3 wild type and *CNPY3*$^{-/-}$ THP-1 macrophages were stimulated with LPS, iLPS, or LF and cell supernatants (Sup) and cell lysates (Lys) as indicated were subjected to immunoblotting for the indicated proteins. Mann-Whitney U test, ns, not significant P > 0,05). All data represent the means ±SEM of two independent experiments.

4.2.5 CNPY3 is required for inflammasome activation in response to *Escherichia coli*, *Staphylococcus aureus* and Group B streptococcus

At least, different signaling pathways can drive the transcription-independent priming of NLRP3, namely the immediate MyD88-dependent pathway and the intermediate TRIF-dependent pathway (Song et al., 2017). Since TLR3 activation via poly(I:C) does not signal via Myd88 but rather TRIF signaling (Yamamoto et al., 2003a), we examined the importance of CNPY3 for inflammasome activation in context of bacterial infections. In contrast to purified surface-bound receptor triggers such as LPS or poly(I:C), which elicit a one-way activation path, microbes address multiple pathways targeting both priming and activation steps to engage the inflammasomes (Miao et al., 2006; Franchi et al., 2007; Muruve et al., 2008; Franchi et al., 2012; Kayagaki et al., 2013; Sha et al., 2014; Storek and Monack, 2015). To determine whether

the inflammasome activation in *CNPY3*$^{-/-}$ macrophages was defective due to the requirement of certain PRR ligands or certain adaptor proteins upstream of caspase-1 that were not stimulated by TLR3, THP-1 wild type and *CNPY3*$^{-/-}$ macrophages were infected with live Gram-negative bacteria and Gram-positive bacteria that are known to promote IL-1β release via non-canonical and canonical inflammasome pathways, respectively (Storek and Monack, 2015). As illustrated in **Fig. 19A**, **B** wild type macrophages showed an abundant release of IL-1β upon infection with *E. coli*, whereas *CNPY3*$^{-/-}$ macrophages failed to secrete and process pro-IL-1β. Moreover, CNPY3 was essential for caspase-1 activation in response to *E. coli*, as the p20 subunit of active caspase-1 was not detectable in CNPY3 deficient macrophages (**Fig. 19C**). Similar results were obtained using Gram-positive bacterial infection including *Staphylococcus aureus* and Group B streptococcus (GBS; *Streptococcus agalactiae*), that have been previously documented to activate the canonical NLRP3 inflammasome (Mariathasan et al., 2006; Franchi et al., 2007; Sha et al., 2014). In contrast to wild type, infection of *CNPY3*$^{-/-}$ macrophages with *S. aureus* and GBS results in negligible release of IL-1β (**Fig. 19D**, **G**). In addition, *CNPY3*$^{-/-}$ macrophages exhibited similar defect in activation of caspase-1 and subsequent processing of pro-IL-1β. Noteworthy, CNPY3 sufficient and deficient macrophages produced comparable levels of pro-IL-1β and pro-caspase-1 when infected with Gram-negative *E. coli* or Gram-positive *S. aureus* and GBS (compare blots in **Fig. 19**), indicating that the defect in pro-IL-1β processing observed in *CNPY3*$^{-/-}$ macrophages was not due to impaired protein expression of pro-IL-1β and pro-caspase-1.

To exclude unspecific results obtained from a single CRISPR clone, which might display a wide variety of phenotype that are not associated with the CRISPR knockout, different CNPY3 clones were independently generated and analyzed at protein and functional level as described above (chapter 4.2.1). As seen in **Fig. 20A** all independently generated clones CNPY3KO#2-5 (CNPY3KO1 is mentioned above as THP-1-*CNPY3*$^{-/-}$) invariably failed to express CNPY3 protein. In addition, all CNPY3 clones functionally failed to translocate TLR2 on the surface (**Fig. 20B**). This observation was further confirmed, when all the clones failed as well to respond to TLR2 activation in compare to wild type macrophages (**Fig. 20C**). Regarding inflammasome activation, clones of *CNPY3* deficient macrophages were challenged with nigericin, in agreement with observation in **Fig. 17** *CNPY3*$^{-/-}$ clones showed an impaired activation of caspase-1 (**Fig. 20D**) and ultimately pro-IL-1β release (**Fig. 20D**, **E**).

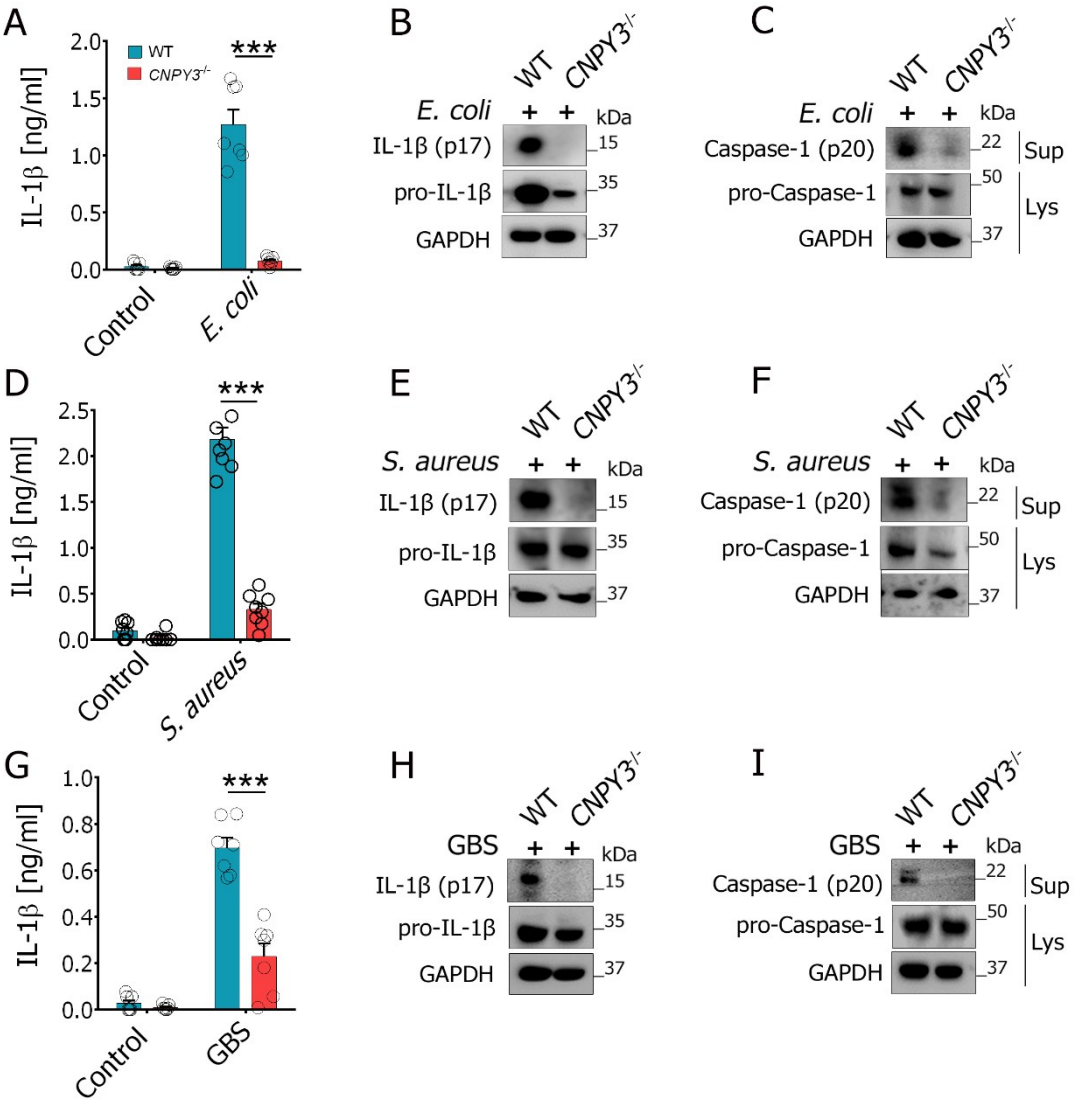

Fig. 19: *E. coli, S. aureus* and GBS induce CNPY3-dependent caspase-1 activation and IL-1β secretion.
(**A**, **B**, **C**) CNPY3 wild type and *CNPY3*$^{-/-}$ THP-1 macrophages were infected or not with *E. coli* (**A**), *S. aureus* (**B**), or GBS (**C**) (MOI, 20, 10, 20 respectively) and IL-1β was measured in supernatants by ELISA (Mann-Whitney U test, ***$P < 0{,}001$). All data represent the means ±SEM of two independent experiments. (**D-F**) CNPY3 wild type and *CNPY3*$^{-/-}$ THP-1 macrophages were infected with *E. coli* (**D**), *S. aureus* (**E**), or GBS (**F**). IL-1β (p17) and pro-IL-1β were detected by immunoblotting in cell supernatants (Sup) and lysates (Lys) respectively. (**G-I**) CNPY3 wild type *CNPY3*$^{-/-}$ THP-1 macrophages were infected with *E. coli* (**G**), *S. aureus* (**H**) or GBS (**I**) and cleaved (p20) and pro-caspase-1 were detected by immunoblotting in cell supernatants and lysates, respectively. (**D-I**) Blots were decorated with GAPDH in lysate as a loading control.

Furthermore, all CNPY3 clones were infected with *S. aureus* and GBS. However, in contrast to results obtained above as shown in **Fig. 19D-I**, prior to bacterial infection, THP1 wild type and all CNPY3KO clones were primed with poly(I:C), that might on one hand increase the susceptibility to infection and response of inflammasome pathways and on the other hand ensure that results seen in **Fig. 19** are not due to unequally primed cells.

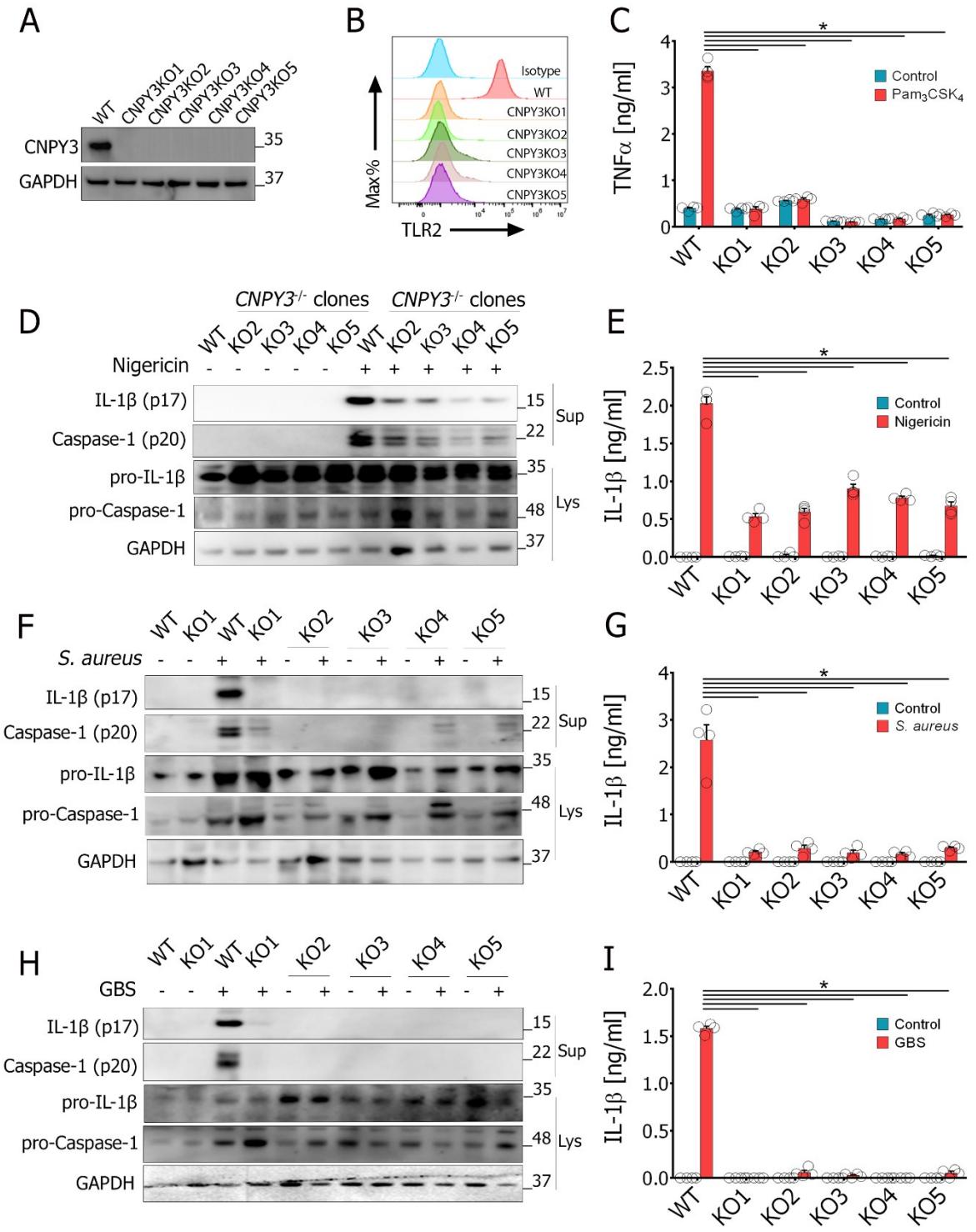

Fig. 20: Phenotypic and functional validation of the *CNPY3*$^{-/-}$ THP-1 clones.
(**A**) Protein expression of CNPY3 protein in wild type and *CNPY3*$^{-/-}$ clones of THP1 cells. (**B**) Evaluation of TLR2 surface expression in wild type and *CNPY3*$^{-/-}$ clones of THP-1 cells. (**C**) wild type and *CNPY3*$^{-/-}$ macrophages stimulated with Pam_3CSK_4 followed by TNFα measurements by ELISA. (**D**, **F**, **H**) Immunoblotting of poly(I:C)-primed macrophage were stimulated with nigericin (**D**) or infected with *S. aureus* (**F**), or GBS (**H**), as indicated cleaved IL-1β (p17) and cleaved caspase-1 (p20) were detected by immunoblotting in cell supernatants (Sup). pro-IL-1β, pro-caspase-1, and GAPDH were detected in lysates (Lys). (**E**, **G**, and **I**) measurement of IL-1β by ELISA in supernatants of poly(I:C)-primed macrophages after nigericin treatment (**E**) or infected with *S aureus* (**G**) or GBS (**I**). (Mann-Whitney U test, $*P < 0.05$, $**P < 0.01$, $***P < 0.001$, ns; not significant, $P > 0.05$) (data are mean ±SD).

Despite priming with poly(I:C) all CNYP3 clones invariably failed to activate caspase-1 and to release IL-1β compared to wild type when infected with *S. aureus* and GBS bacteria (**Fig. 20F-I**). Collectively, all CRISPR-knock out of CNPY3 clones showed the perquisite of CNPY3 to activate inflammasome and the results obtained from a single clone are not due to unknown genetic errors resulting from the generation of the knockout.

4.2.6 ASC-oligomerization is unaffected by CNPY3 deficiency

As shown in **Fig. 16B**, NLRP3 can efficiently migrate to mitochondria- and MAM- upon priming of macrophages in *CNPY3*$^{-/-}$ macrophages. Worthy of note, upon an activation signal, NLRP3 undergoes self-oligomerization and recruits ASC molecules before moving to the cytosol and forming a single bright point termed ASC-speck. NLRP3 inflammasome assembly is closely linked to the formation of ASC specks, a crucial event in NLRP3 inflammasome activation and indicative for cell death. (Fernandes-Alnemri et al., 2007; Stutz et al., 2013; Zhang et al., 2017). To be able to examine whether CNPY3 plays a role in ASC-speck formation, the THP-1 cell line expressing ASC-fused to GFP was used (THP1-ASC-GFP cells). Accordingly, I utilized CRISPR/Cas9 genome-editing strategy as described above (chapter 4.2.1) to generate CNPY3 deficient THP1 cells stably expressing ASC-GFP (THP1-ASC-GFP-*CNPY3*$^{-/-}$) (**Fig. 17**). Consistent with **Fig. 15**, I ascertained that THP-1-ASC-GFP-*CNPY3*$^{-/-}$ cells were unable to express CNPY3 protein (**Fig. 21A**) and failed to express and respond to TLR2 as shown by FACS analysis and TNFα production, respectively (**Fig. 21B**, **C**). To engage the signaling pathway that leads to the formation of ASC specks, THP-1-ASC-GFP-WT and *CNPY3*$^{-/-}$ macrophages were challenged with nigericin. Compared to THP1-ASC-GFP wild type, ASC-GFP-*CNPY3*$^{-/-}$ macrophages showed a highly reduced processing of pro-IL-1β, pro-IL-18 and cell death in a background of elevated heterologous ASC-GFP levels in response to nigericin (**Fig. 21D-F**). This was further confirmed by immunoblotting of caspase-1 and IL-1β processing and secretion. Whereas THP1-ASC-GFP wild type substantially induce the active form of IL-1β and caspase-1 in supernatants, THP1-ASC-GFP-*CNPY3*$^{-/-}$ exhibited a highly reduced processing of IL-1β and caspase-1 (p20). The level of pro-IL-1β and pro-caspase-1 in the ASC-GFP wild type and *CNPY3*$^{-/-}$ expressing cells were considerably expressed (**Fig. 21G**), confirming that their reduced processing and release was not attributable to reduced pro-caspase-1 and pro-IL-1β expression in the ASC-GFP expressing cells. Finally, to test the formation of ASC-specks, we visualized the switch of ASC-GFP molecules from a diffuse signal through the cell to specks by live-cell fluorescence microscopy in response nigericin.

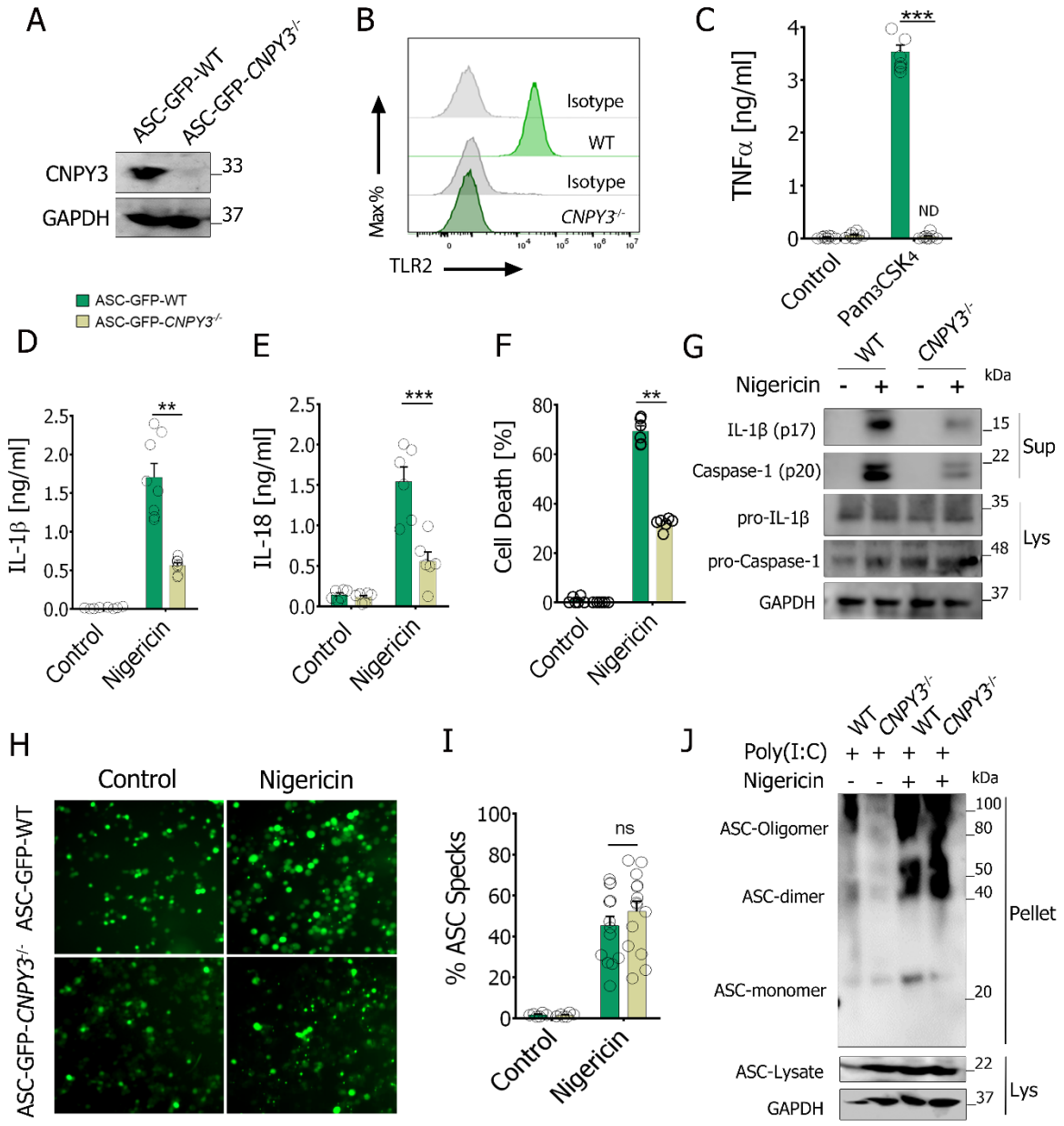

Fig. 21: ASC-oligomerization is unaffected by CNPY3 deficiency.
(**A**) CNPY3 protein expression in wild type and *CNPY3*$^{-/-}$ ASC-GFP reporter cells. (**B**) Surface expression of TLR2 in CNPY3 wild type and *CNPY3*$^{-/-}$ ASC-GFP reporter cells. (**C**) wild type and *CNPY3*$^{-/-}$ THP-1 ASC-GFP macrophages were stimulated with Pam_3CSK_4 and TNFα was measured in supernatants by ELISA. (**D-F**) Poly(I:C)-primed CNPY3-ASC-GFP wild type and *CNPY3*$^{-/-}$ THP-1 macrophages were stimulated with nigericin and IL-1β (**D**) and IL-18 (**E**) were measured by ELISA or cell death was measured by LDH assay (**F**). Cleaved IL1β (p17) and caspase-1 (p20) were detected in cell supernatants (Sup) and pro-IL-1β, pro-caspase-1, and GAPDH in cell lysates (Lys) by immunoblotting. (**H**) ASC-GFP expression in wild type and *CNPY3*$^{-/-}$ THP-1 macrophages unstimulated (**H**, **left**) or stimulated with nigericin (**H**, **right**) after poly(I:C) priming were observed by live fluorescence microscopy. ASC-GFP-specks represented by green dots. (**I**) The percentage of ASC-GFP specks was counted in different fields (n=14) in images depicted in **H**, ASC-specks number in percentage (%) of total unstimulated (control) or stimulated (nigericin) CNPY3-ASC-GFP wild type and *CNPY3*$^{-/-}$ macrophages. (**J**) Poly(I:C)-primed wild type and *CNPY3*$^{-/-}$ THP-1 macrophages were stimulated with nigericin. DSS-cross-linked pellet (Pellet) and cell lysates (Lys) were subjected to immunoblotting for ASC and GAPDH proteins. Mann-Whitney U test, $^{**}P < 0{,}01$, $^{***}P < 0{,}001$, ns, not significant $P > 0{,}05$.

As expected and consistent with known literatures (Fernandes-Alnemri et al., 2007; Zhang et al., 2017), in both TLR3-primed wild type and *CNPY3*$^{-/-}$ macrophages, ASC-GFP was diffused throughout the cytosol of unstimulated macrophages (**Fig. 21G**, **left**) but condensed into single cytosolic speck per macrophage after nigericin stimulation (**Fig. 21H**, **right**). Interestingly, the formation of ASC specks occurred in a CNPY3-independent manner (**Fig. 21I**), suggesting that CNPY3 did not interfere with inflammasome supramolecular assembly. The percentages of cells containing ASC specks were calculated as described under the methods. Since propensity of ASC to aggregate in cultured cell under overexpression conditions is well documented (Stutz et al., 2013; Sester et al., 2015), speck formation therefore was additionally tested by an independent assay. Accordingly, the ASC-oligomeric state was biochemically examined by purification of ASC assembly from nigericin-stimulated THP-1 macrophages (Fernandes-Alnemri et al., 2007).To this purpose, ASC-oligomers present in the insoluble fraction of macrophage extracts were pelleted and covalently cross-linked using non-cleavable protein agent DSS, as this would provide direct biochemical evidence that ASC accumulate equally in wild type and *CNPY3*$^{-/-}$ macrophages. As visualized by immunoblotting of the soluble fractions (lysate) of all points, cells exhibit comparable presence of only ASC-monomers (~22 kDa) (**Fig. 21J**). However, insoluble fractions (crosslinked ASC) of nigericin-treated wild type and *CNPY3*$^{-/-}$ cells revealed the presence of not only monomeric, but also dimers, trimers and higher order oligomers of ASC. This in line with the unperturbed capacity of *CNPY3*$^{-/-}$ macrophages to form ASC-specks, where ASC-GFP was overexpressed. Taken together, these data suggest that ASC-specks formed in a fully CNPY3-independent manner.

4.2.7 CNPY3 is required for the functional assembly of caspase-1 into the canonical inflammasome complex

Activation of caspase-1 is engaged when it is recruited to the assembly of ASC and NLRP3 upon canonical inflammasome activation induced by NLRP3 stimuli such as nigericin (**Man et al., 2014**). To overview the capacity of caspase-1 and ASC co-localization state in *CNPY3*$^{-/-}$ macrophages, cells were fixed and immunolabeled with caspase-1 and ASC specific antibodies after treatment with or without nigericin for 1 h and 3 h. Confocal imaging revealed that unstimulated macrophages exhibited basal expression of ASC and caspase-1 which equally distributed throughout the cytosol of THP-1 wild type and *CNPY3*$^{-/-}$ macrophages. However, following nigericin treatment, both THP1 wild type and *CNPY3*$^{-/-}$ macrophages exhibited undistinguishable capacity to form ASC-specks (**Fig. 22A**, **above** and **B**). This is in line with results obtained from THP-1-ASC-GFP (**Fig. 21H-I**) and THP-1 macrophages (**Fig. 21J**).

However, to our surprise ASC speck formed in *CNPY3*$^{-/-}$ macrophage appears larger in size when compared to ASC speck formed in wild type macrophages (**Fig. 22A**, **below**).

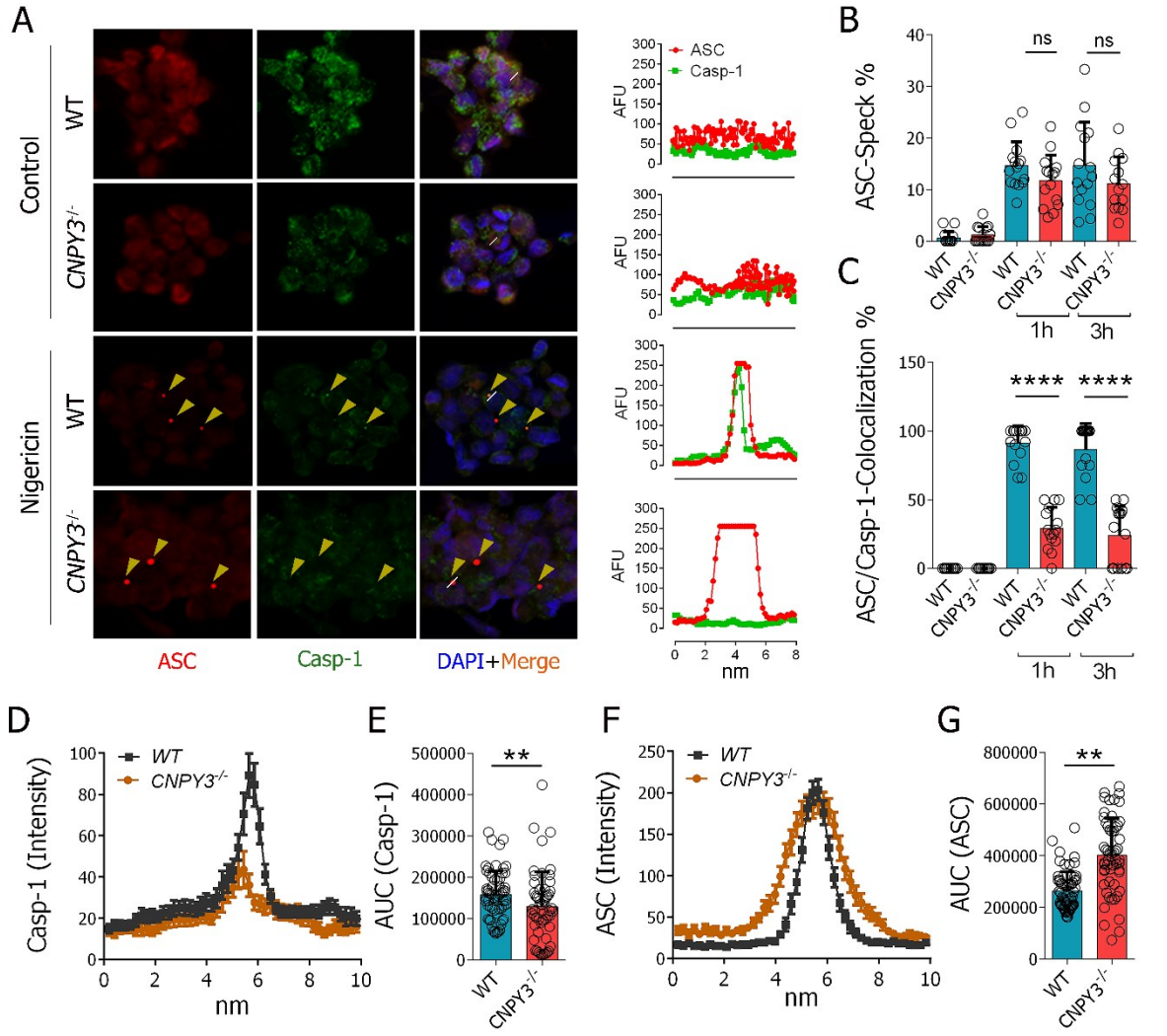

Fig. 22: CNPY3 is required for the proper recruitment of Caspase-1 to ASC-containing inflammasome.
(**A**, **left**) Poly(I:C)-primed wild type and *CNPY3*$^{-/-}$ THP-1 macrophages were unstimulated (**A**, **above**) or stimulated with nigericin (**A**, **below**) for 3h. Cells were then fixed and stained with caspase-1 (green), ASC (red) and DNA (blue) and subjected to confocal imaging. The fluorescence intensities of green (Casp-1) and red (ASC) channels were quantified along the white lines in (**A**, **left**). (**B**, **C**) Percentage (%) of ASC-specks (**B**) and colocalization of caspase-1 and ASC (**C**) in images as indicated in **A**, each dote indicate the % in each image (n=15). (**D**, **F**) Area under the curve (AUC) of green (Casp-1) (**D**) and red (ASC) (**F**) channels were quantified along lines, where sat on the center of individual speck formed by wild type (n=55) or *CNPY3*$^{-/-}$ (n=62) THP-1 macrophages. (**E**, **G**) AUC of Casp-1 (**E**) and ASC (**G**) intensities were numerically calculated and blotted (Mann-Whitney U test, $^{**}P < 0{,}01$, $^{***}P < 0{,}001$, $^{****}P < 0{,}0001$, ns, not significant $P > 0{,}05$) (data are mean ±SD).

Consistent with known literature (Man et al., 2014), wild type macrophages showed that caspase-1 formed a small and more centralized speck which in turn exhibit a predominant co-localization with the ASC-specks. In contrast, caspase-1 speck formed in *CNPY3*$^{-/-}$ macrophages was markedly impaired (**Fig. 22A**, **below** and **C**). Furthermore, the assembly of

ASC and caspase-1 upon response to nigericin was further quantitatively determined per speck utilizing baseline levels set for area under the curve (AUC) of fluorescence signal intensity (%) (**Fig. 22A**, **left**). Remarkably, AUC for caspase-1 signal intensity revealed a prominent impairment of caspase-1 colocalization with ASC in *CNPY3*$^{-/-}$ macrophages when compared to wild type macrophages (**Fig. 22D**, **E**), which in turn associate with the magnitude of caspase-1 enzymatic activity seen in **Fig. 17**. Notably, recent studies have shown, that the area of ASC specks appears larger when caspase-1 is enzymatically inactive (Stein et al., 2016; Nagar et al., 2019). Keeping with this notion, the size of ASC specks formed in CNPY3 was larger compared to wild type macrophages (**Fig. 22F**, **G**). Thus, aberration of ASC and caspase-1 colocalization in *CNPY3*$^{-/-}$ macrophages suggests dependency on CNPY3 chaperone to drive a proper assembly of caspase-1 to the ASC-oligomers in macrophage. Altogether, these data suggest, that CNPY3 exerts an important function in the recruitment of caspase-1 into the inflammasome assembly and implicate CNPY3 chaperone activation in dictating features of such organization.

4.2.8 Homozygous frameshift CNPY3 variant in an individual with early infantile epileptic encephalopathy

CNPY3 is expressed in various tissues and evolutionary conserved in eukaryotes. Human *CNPY3* encodes for a 278 amino acids protein with a molecular weight of 33kDa that is targeted to the ER via signal peptide and putative C-terminal ER retention sequence (Wakabayashi et al., 2006; Morales and Li, 2017; Mutoh et al., 2018). Loss-of-function variants in *CNPY3* is clinically associated with Early Infantile Epileptic Encephalopathy (EIEE) manifesting in the first months of life in three patients from two unrelated families (Mutoh et al., 2018). We have identified a family with five affected by unique biallelic *CNPY3* variants and four unaffected siblings (**Fig. 23A**). The index patient (II.10) presented after birth with seizures, laryngomalacia and impaired swallowing. Clinically, epileptic encephalopathy with no neurological development could be observed leading to severe neurodevelopmental impairment. In addition, an extreme growth retardation but no signs of immune system deficiency were present. Clinical analysis of *CNPY3* (ENST00000372836) demonstrated homozygous single base deletion c.548delA in exon 5 (p.Asn183Thrfs*7). *CNPY3* variant was annotated using transcript (NM_006586.5). This variant was the sole candidate due to its predictively truncating nature and the autosomal recessive inheritance in patient (II:10) which supports the clinical presentations described above and by Mutoh et al. 2018. Of note, biallelic variants in 19 genes including *PITPNM3*, *MAST1*, and *KMT2B* were predictively prioritized and excluded because of their reportedly dominant inheritance and different clinical presentations (Köhn et al., 2007; Meyer et al., 2017; Tripathy et al., 2018). The variant was subsequently validated by Sanger

sequencing in a homozygous state in the affected index patient II:9, while both parents and unaffected siblings being heterozygous carriers. No DNA from the deceased siblings (II:2, II:5, and II:7) was available (**Fig. 23A**). In patient II:10, prenatal genetic testing was performed on genomic DNA from a chorionic villi sample revealing homozygosity carrier for the *CNPY3* variant (c.548delA). This variant is absent from an GnomAD database (accessed 11/2020). Performing and analysis of whole genome sequencing was conducted by Dr. med. Ralf Husain and Prof. Dr. Tobias Haack. Index patient (II:10) is mentioned hereafter as the affected patient.

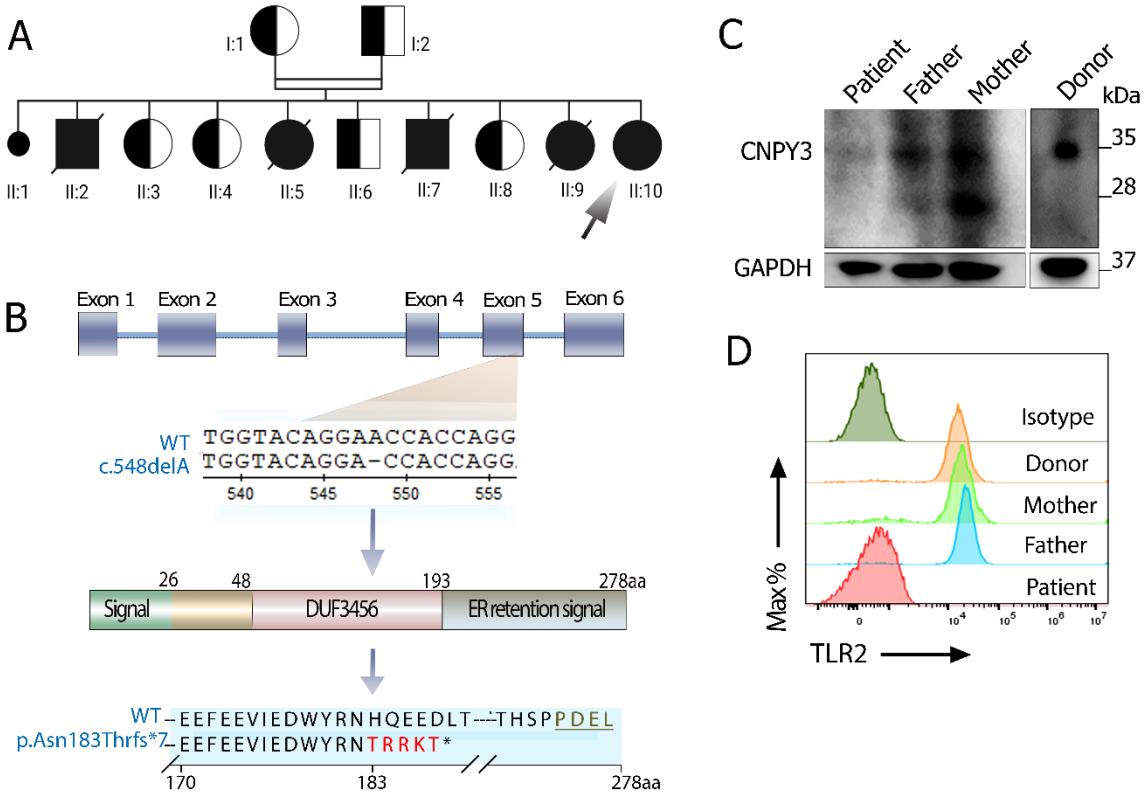

Fig. 23: A family segregating recessive CNYP3 germline mutation.
(**A**) Pedigree of the family harbouring *CNPY3* c.548delA mutation. Patients II:1, II:2, II:5, and II:7 were not available. Whereas probands family I:1, I:2, II:3, II:4, II.6, and II:8 are heterozygous, probands family II:9 and II:10 carry a homozygous recessive c.548delA mutation. Familial pedigree demonstrates the inheritance in a family with c.548delA(p.Asn183Thrfs*7) *CNPY3* variant. (**B**) Schematic view of Exon-intron genomic organization of CNPY3with position of identified c.548delA mutation. (blue boxes represent exons and blue fields represent introns) and its effect on protein structure depicting location of frameshift variant c.548delA on the DUF3456 domain CNPY3 protein expression (p.Asn183Thrfs*7). (**C**) Cell lysates of PBMCs isolated from peripheral blood of CNPY3-variant family, patient, and parent (I:1, I:2 and II:10) and unrelated healthy donor were subjected to immunoblotting. Immunoblot was decorated with CNPY3 and GAPDH antibodies. (**D**) Surface expression of TLR2 on $CD14^{+}$ monocytes isolated from peripheral blood of *CNPY3*-variant family, patient, parent, and unrelated donor.

The homozygous 1 bp deletion of c.548 in exon 5 causes a frameshift at amino acid 183 (of 278 total) and premature termination (p.Asn183Thrfs*7), resulting in a severely truncated protein causing the loss of the C-terminal ER retention signal (**Fig. 23B**). To ascertain the influence of

this variant on protein expression of CNPY3, protein derived from PBMCs from the *CNPY3*-variant family members were compared with an unrelated healthy donor. As assessed by immunoblotting, the patient with homozygous *CNPY3* variant showed a complete loss of protein expression, confirming that biallelic c.(548delA) are loss of function variants (**Fig. 23C**). In contrast, the parents´ PBMCs harbored the wild type (~33 kDa) and presumably predicted mutant variant form (~22 kDa) in varying ratios. The unrelated donor showed expression of the wild type variant (~33 kDa), only (**Fig. 23C**). The functionally critical role of CNPY3 in the TLR stabilization and trafficking in the patient was confirmed by surface TLR2 membrane staining. CD14 positive cells of the patient, the patient´s parent and an unrelated donor were subjected to flow cytometric analysis and analyzed for cell surface TLR2 (**Appendix Fig. 29**). In contrast to all healthy probands, $CD14^+$ monocytes from the patient showed a complete absence of TLR2 plasma membrane staining (**Fig. 23D**). This demonstrates that homozygous mutation c.548delA in *CNPY3* causes its loss-of-function and is accompanied by a lack of TLR2 translocation into the plasma membrane of the patient´s monocytes.

4.2.9 *CNPY3* Variant (c.548delA) macrophages failed to respond to surface TLRs and show deficiency in IL-1β secretion upon inflammasome activation.

For functional characterization of c.548delA mutation in *CNPY3* in vitro, monocytes of healthy donors and patient were differentiated into macrophages and exposed to a panel of TLRs ligands, including LPS (TLR4), Pam_3CSK_4 (TLR2/1), FSL-1 (TLR2/6), Flagellin (TLR5) and poly(I:C) (TLR3). The role of CNPY3 in chaperoning of TLR9 has been comprehensively studied (Tabeta et al., 2006; Takahashi et al., 2007; Brinkmann et al., 2007; Kim et al., 2008). Patients' macrophages were compared with macrophages obtained from healthy donors and the patient´s parents. Macrophages of healthy donors responded normally and invariably to all ligands in terms of TNFα release (**Fig. 24A**). Consistent with previous studies (Wakabayashi et al., 2006; Takahashi et al., 2007; Liu et al., 2010; Shibata et al., 2012) and in contrast to donor´s macrophages, patient macrophages with c.548delA mutation in *CNPY3* were severely defective in response to TLR4, TLR2/1, TLR2/6 and TLR5 ligands, whereas no reproducible differences were detected between donor and patient macrophages in response to TLR3 agonist poly(I:C) (**Fig. 24A**). This is in line with previous studies (Wakabayashi et al., 2006; Takahashi et al., 2007; Liu et al., 2010; Shibata et al., 2012). In addition, the gene expression of certain pro-inflammatory cytokines and inflammasome key components were assessed in response to TLR3-ligand. Gene expression of pro-inflammatory cytokines including *TNFA*, *IL-6*, and *IL1B* as well as inflammasome components including *NLRP3* and *CASP1* did not depend on CNPY3 upon TLR3 activation (**Fig. 24A**). Collectively, these data indicated that downstream signaling

pathways via TLR3 were intact and effective in macrophages carrying loss-of-function mutation (c.548delA).

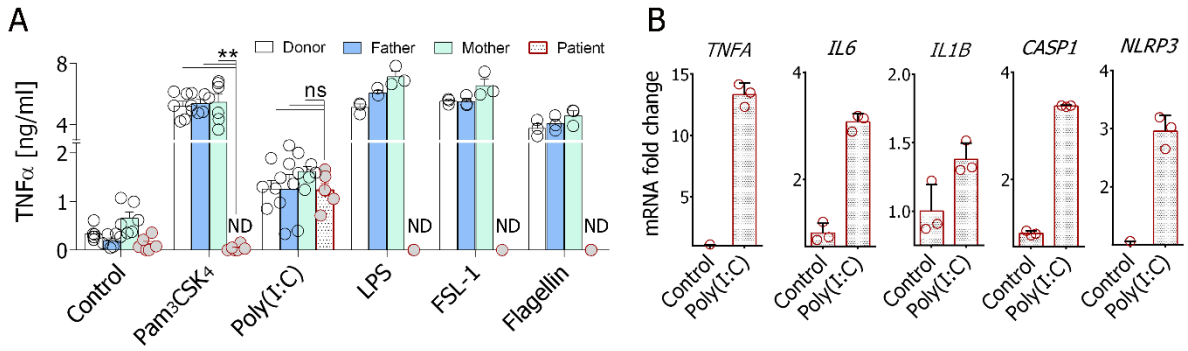

Fig. 24: CNPY3 deficient macrophages fail to respond to surface TLRs and show deficiency in IL-1β secretion upon inflammasome activation.
(**A**) MDM derived from peripheral blood of c.548delA *CNPY3*-variant family, parent, patient and unrelated donor were stimulated with the indicated ligands followed by measurement of TNFα in supernatant by ELISA (Mann-Whitney *U* test, $^{**}P < 0{,}01$; ns, not significant $P > 0{,}05$). Control, Pam_3CSK_4, poly(I:C) data represent two independent experiments (means ±SD), Data of LPS, FSL-1, and Flagellin represent the means ±SD of one experiment. (**B**) Patient´s MDM derived from peripheral blood were stimulated with poly(I:C) and mRNA expression of *TNFA, IL6, IL1B, CASP1, NLRP3* and *GAPDH* were analyzed (Data are means ±SD of one experiment).

To examine whether *CNPY3* deficiency alters the functional output of the inflammasome in poly(I:C)-primed human monocyte derived macrophages (MDM) of the affected patient, IL-1ß production and LDH as standard measures of pyroptosis upon nigericin treatment were monitored for inflammasome activation. Interestingly, in contrast to unrelated donor and the patient´s parents, the patient´s macrophages showed a considerably reduced release of IL-1ß (**Fig. 25A**, **B**) and impairment in nigericin-induced pyroptosis (**Fig. 25C**). Furthermore, intracellular LPS (iLPS) was used to identify the requirement of CNPY3 in activation of non-canonical inflammasome in the primary macrophages (Kayagaki et al., 2013; Hagar et al., 2013; Shi et al., 2014). Transfection of LPS into the cytosol (iLPS) resulted in pronounced release of IL-1β from macrophages of donor and patient´s parents, whereas the patient macrophages failed to release IL-1β (**Fig. 25D**). Finally, infection with Gram-negative (*E. coli*) or Gram-positive bacteria (*S. aureus* and GBS) failed to induce IL-1ß secretion in the patient's CNPY3 mutant macrophages (**Fig. 25E**). Pro-IL-1β synthesis was considerably induced, at least as indicated upon *E. coli* infection but the maturation to its exported form IL-1β was fully impaired. As shown above for THP-1 macrophages, the inability to secrete IL-1ß was a consequence of a strongly impaired processing of pro-caspase-1 as indicated additionally by LDH. All these findings strongly indicate that CNPY3 was required for sufficient activation of canonical and non-canonical NLRP3 inflammasome.

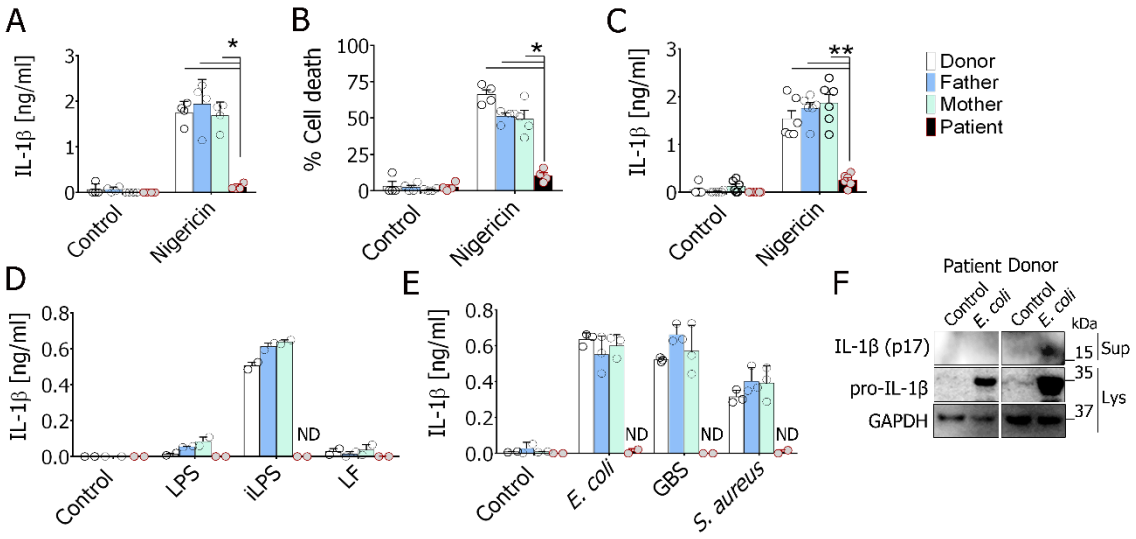

Fig. 25: Patient´s MDMs display defective IL-1β secretion and LDH release upon inflammasome activation.

(**A**, **B**) MDM derived from peripheral blood of c.548delA *CNPY3*-variant family, parent, patient and unrelated donor were primed with poly(I:C) followed by stimulation with nigericin and IL-1β release was measured in supernatants by ELISA after 24h (**A**) or 3h (**B**); or cell death was measured after 3h (**C**). (Mann-Whitney *U* test, $^{**}P < 0{,}01$; $^{*}P < 0{,}05$; ns, not significant $P > 0{,}05$). (**D**) MDM of *CNPY3*-variant family, parent, patient, and unrelated donor were primed with poly(I:C) and stimulated with LPS, iLPS and LF and IL-1β ELISA was measured in supernatants by ELISA (Data are means ±SD of one experiment). (**E**) MDM derived from peripheral blood of *CNPY3*-variant family, parent, patient, and unrelated donor were infected or not with *E. coli*, GBS or *S. aureus* (MOI 20, 20, 10, respectively) and IL-1β was measured in supernatants by ELISA (Data are means ±SD of one experiment). ND, not detected. (**F**) MDM derived from peripheral blood of *CNPY3*-variant patient and unrelated donor were infected or not with *E. coli* and supernatants and cell lysate were subjected to immunoblotting using specific antibodies as indicated.

5. Discussion

5.1 Regulation of non-canonical inflammasome during innate immunosuppression-associated organ damage

Various studies have highlighted the importance for tight regulation of NLRP3 inflammasome at transcriptional and post-transcriptional levels. In following chapter, I have focused on how key inflammasome components are regulated during sepsis-induced innate immuno-suppression and organ failure.

5.1.1 Indication of patients with sings of innate immunosuppression

Inflammasome-mediated pyroptotic cell death provides a major secretion pathway to facilitate proteins exiting the cells, among which DAMPs and alarmins are important, which may protect or even worse the inflammation process and can lead to organ damage (Deng et al., 2018; Russo et al., 2021; Phulphagar et al., 2021). Regulation of inflammasome encoding genes is known for their upregulation during proinflammatory response in myeloid cells (Lin et al., 2000; Viganò et al., 2015; Casson et al., 2015; Napier et al., 2016; Esquerdo et al., 2017; Benaoudia et al., 2019). However, the initial pro-inflammatory phase is followed by an immunosuppressive phase, leaving patients with decreased production of cytokines and reduced aptitude to clear existing or opportunistic pathogens (Hotchkiss et al., 2013). To study the regulation of inflammatory caspases and GSDMD as a pyroptotic executor, we first aim to characterize the state of immune response of patients by establishing a surrogate parameter that pave the way to distinguish between patients with and without the signs of immunosuppression. miRNAs are consistently reported to be associated to sepsis phenotype and may be driving the protracted immunosuppression phase. A better understanding of the miRNA role in regulating sepsis-associated immunosuppression can lead to the development of diagnostic tools and might provide an important source of novel molecular targets for new therapies (Liu and Cao, 2016; Seeley and Ghosh, 2016). Clinically, several studies have shown, that cirrhosis patients with ACLF are often under an innate immunosuppressive state, which in turn is pathologically related to the high incidence of severe infections (Wasmuth et al., 2005; Berres et al., 2009; Solé et al., 2016; Mateos et al., 2019). In this study, using PBMCs and $CD14^+$ monocytes from patients with acute decompensated liver cirrhosis, we revealed that upregulation of miR-221/222 can discriminate patients with sign of immunosuppression and organ damage but not with infection (**Fig. 4**). Although the expression of miR-221 and miR-222 act as a cluster gene (Zhang et al., 2018), they exhibit differences in their expression. In brief, miR-222 is more expressed in macrophages in response to LPS (Seeley et al., 2018) and thus potentially

associates with systemic and *in vitro* induced immunosuppression (Seeley et al., 2018; **Fig. 4**; **Fig. 12**). Furthermore, miR-222 markedly showed the highest level of significance as compared to miR-221 and was less overlapping cluster in both patient groups with presence and absence of organ damage, thereby demonstrating its potential association with immunosuppression and organ damage (**Fig. 4**). Notably, the inflammatory responses caused by bacterial infection, as a common precipitating event of ACLF, presents in 30% of patients and is the most frequent trigger of ACLF and links to a high risk of mortality (Piano et al., 2018; Mateos and Albillos, 2019). Thus, elevated levels of CRP and WBC-counts is a typical sign of infection and inflammatory response (Deutsch et al., 2018), but weakly associate with mortality (Piano et al., 2018). Indeed, we found that miR-222 does not associate with inflammatory markers including CRP and WBC counts. In contrast, organ damage markers such as creatinine and MELD score correlate with miR-222 expression (**Fig. 4I-L**). These markers are also known to be associated with the presence of immune dysfunction and mortality (Piano et al., 2018). Thus, miR-222 expression associates with those organ damage markers and can distinguish between patients with organ damage and high risk of mortality from those with only infection. Several miRNAs can mechanistically act either in a cooperative or antagonistic fashion and a single miRNA may regulate several targets in protein coding genes of the same signaling pathway (Bartel, 2009; Jonas and Izaurralde, 2015; Mehta and Baltimore, 2016). miR-221 and miR-222 potentially bind to BRG-1-mRNA, as one of many target genes, and drive its degradation, leading to silencing of a subset of SWI/SNF-dependent inflammatory genes (Seeley et al., 2018). Intriguingly, a significant and reverse correlation of *BRG1* with miR-221 and -222 expression profiles over the course of acutely decompensated cirrhosis in myeloid cells was observed (**Fig. 4E-H**). Compared to the mechanistic functions of several other miRNAs, which have a broader effect to influence the upstream signaling pathways like TLR-4 signaling, they are associated with anti-inflammatory roles by targeting MyD88 signaling in macrophages (Taganov et al., 2006; O'Connell et al., 2007; Neudecker et al., 2017). The role of mir-222 and -221 provide a critical and novel contribution to induce innate immune memory that is driven by changes in chromatin remodeling. These types of epigenetic changes may be required for cellular memory and physiologic changes that comprise the tolerance phenomenon. In summary, since miR-221 and miR-222 act as downstream effectors of innate immune memory, they modulate synergistically innate immunosuppressive state. This also supports the notion that immunosuppression is associated with organ dysfunction/failure in patients with systemic inflammation such as sepsis and cirrhosis. Taken together, these results show that miR-222 has clinical value in determining whether or not patients underwent immunosuppression in order to

establish target therapies. In addition to miR-222 and consistent with a body of literature, the expression profile of HLA-DR can also discriminate patients with immunosuppression signs (**Fig. 5**). Moreover, the expression of HLA-DRA significantly correlates with miR-221 and -222 expression profiles (**Fig. 5D-F**). Thus, these results support the notion that immunosuppression associates with organ damage (**Fig. 4** and **Fig. 5**). These findings were further employed to examine the regulation of inflammatory caspases, *CASP4*, *CASP5*, and *CASP1*, which reflect controlled inflammasome pathways during immunosuppression in infectious diseases such as cirrhosis and sepsis.

5.1.2 *CASP4* and *CASP5* are differentially regulated during sepsis-associated immunosuppression and organ damage

The onset of sepsis is compiled with over-exuberant inflammatory responses. This condition is further amplified and perpetuated by release of DAMPs by damaged cells due to apoptosis, necrosis and pyroptosis, leading to immune imbalance, unbridled inflammatory responses and/or immunoparalysis. A major cause of the immunoparalysis of sepsis is owing to extensive cell death of key immune effector cells using modulators of caspases (Hotchkiss et al., 2013; Aziz et al., 2014; Mateos et al., 2019; Rubio et al., 2019). However, little is known about regulation of pyroptosis in sepsis related immunoparalysis/ immunosuppression. The expression of LPS-responsive caspases including murine caspase-11 and its human orthologues caspase-4 and -5 along with interferon and complement pathways play an important role to restrict and eliminate the cytosolic invading Gram-negative bacterial pathogens throughout the course of sepsis ((Broz et al., 2012; Casson et al., 2015; Baker et al., 2015; Viganò et al., 2015; Vanaja et al., 2016; Napier et al., 2016). In this study, we noticed apparent differences in the transcriptional regulation of *CASP4* and *CASP5* genes in PBMCs and $CD14^{+}$ monocytes derived from patients with acute decompensated liver cirrhosis with and without signs of innate immunosuppression-associated organ damage (**Fig. 5**, **Fig. 6**). We also observed these differences in regulation during *ex vivo* LPS induced tolerance in monocytes derived from septic patients (**Fig. 12**). Unlike *CASP5*, *CASP4* expression was markedly decreased in patients with signs of immunosuppression, as defined by elevated levels of miR-222(**Fig. 4C** and **Fig. 12B**). Furthermore, *CASP4* suppression associates with hyporesponsiveness to LPS in a model of monocytes derived from septic patients with signs of immunosuppression. Thus, suppression of *CASP4* expression during immunosuppression suggests that efficient cytosolic recognition of LPS or Gram-negative bacterium is abrogated which might worsen the pathogenicity of sepsis to Gram-negative infection in patients. However, consistent with previous studies which included multiple sepsis cohorts (Napier et al., 2016; Esquerdo et al., 2017), *CASP5* expression

remained upregulated independent of inflammatory state of patients (**Fig. 5B** and **Fig. 12D**), implying that *CASP5* does not undergo immunosuppression and might remain upregulated in a cell autonomous manner due to continual stimulation by the released DAMPs and/or metabolic components in sepsis milieu. In addition, the regulation of *CASP4* and *CASP5* present differentially in term of clinical characteristics. Here I show that *CASP4* expression but not *CASP5*, negatively associates with organ damage markers including creatinine, MELD scores and SOFA scores. Multiple studies have shown that the substantial expression of *Casp11* can be mediated via MyD88 and TRIF-mediated TLR4 activation via e. g LPS (Kayagaki et al., 2011; Broz et al., 2012; Rathinam et al., 2012; Casson et al., 2015; Napier et al., 2016). In contrast, TLR2 ligation, which mediates TRIF-independent but MyD88-dependent signaling failed to upregulate *Casp11* expression (Rathinam et al., 2012). Accordingly, we stimulated THP-1 macrophages with TLR2/1 agonist (Pam_3CSK_4) to evaluate the transcriptional regulation of *CASP4* and *CASP5*. Interestingly, I observed that the TLR2 response induces *CASP5* transcripts in human macrophages (**Fig. 14**). Therefore, *CASP5* gene shares an inducible nature with *Casp11*, suggesting a potential overlapping mechanism governing transcriptional regulation, but not *CASP4.* Mechanistically, TLR2 activation triggers IFNβ production via TRAM-IRF7-IRF3 signaling (Stack et al., 2014), which might in turn act as an autocrine signal to induce the expression of *CASP5*. Recently, Poelzl et al., have reported that upstream signaling of non-canonical inflammatory caspases is governed by Tyrosine kinase TYK2. TYK2 regulates the expression of *Casp11* in mice and *CASP5* in human but appears dispensable for *CASP4* expression (Poelzl et al., 2021). Interestingly, the mechanism underlying this TYK2 pathway regulation during inflammatory responses is probably NF-κB independent but IRF3-dependent (Karaghiosoff et al., 2003), thereby supporting the importance of a selective interferon signaling for licensing non-canonical inflammasome (Rathinam et al., 2012; Poelzl et al., 2021). Thus, the different expression patterns of caspase-4 and -5 may occur because of their different inducibility of expression in a cell autonomous and non-cell autonomous fashion. Our data implies a distinctive prerequisite upstream mechanism that contributes to the expression of *CASP4* and *CASP5* depending on the activated receptor. In addition, this study indicates that *CASP5* is likely to play a vital role in invasive Gram-negative sepsis at immunosuppressive stages**.** However, these caspases require further investigations to determine their potential as therapeutic targets for the treatment of sepsis.

5.1.3 IRF1 and IRF2 provide potential mechanisms that govern the transcriptional regulation of non-canonical inflammasome during immune tolerance

Immunosuppression is associated with impaired expression of several interferon signaling genes, leading to defective autocrine and paracrine IFN-signaling and secondary activation of the STAT and IRF families of transcription factor (Baillie et al., 2017; Seeley et al., 2018; Kang et al., 2019). Different studies have demonstrated that tolerized components of LPS response can be selectively restored following stimulation with IFN-γ *in vitro* and *in vivo*. This is mechanistically mediated by IRF1 and stable STAT1 occupancy and increased histone acetylation, facilitating thereby the chromatin remodeling of genes involved in TLR-responses (Döcke et al., 1997; Chen and Ivashkiv, 2010; Leentjens et al., 2012; Qiao et al., 2013; Kang et al., 2019). Thus, interferon pathways require upstream signaling that in turn regulate priming and activation of inflammasome. INF-β mediates amplification of p38 MAPK signaling that results in induction of *Casp11* expression through C3aR-MAPK signaling (Napier et al., 2016). Unlike INF-β, IFN-γ induces expression of *Casp11* through STAT1 (Schauvliege et al., 2002) and is independent of C3aR signaling (Napier et al., 2016). Brubakar and colleagues have recently shown that pretreatment of macrophages with IFN-γ enhances selectively the magnitude of non-canonical but not canonical inflammasome activation (Brubaker et al., 2020). Using macrophages with *IRF2* deficiency, recent reports noticed that *IRF2* gene is required for the non-canonical inflammasome response upon Gram-negative bacterial infections by mediating robust *CASP4* and *GSDMD* expression in human cells. Mechanistically, *IRF2* is a constitutively expressed gene that regulates the expression of *CASP4 and GSDMD* at steady state in monocytes and macrophages (Benaoudia et al., 2019; Kayagaki et al., 2019). However, IFN-γ pretreatment compensates IRF2 deficiency by IRF1 activation, presenting their key roles in regulating downstream signaling of non-canonical inflammasome pathway (Benaoudia et al., 2019). Here, we found that *IRF1* and *IRF2* transcripts are markedly downregulated in patients with signs of immunosuppression and immunosuppression combined with-organ failure (**Fig. 7A**, **B**) as defined by their correlation with *HLA-DRA* expression and MELD score respectively (**Fig. 9B**, **C**). *IRF1* and *IRF2* correlate as well with *CASP4* and *GSDMD* but not with *CASP5* expression. Interestingly, gain-of-function mutation of C/EBPε transcription factor expressed in myeloid cells in humans possesses an induced pattern of *CASP5* expression along with interferon-regulated genes, which in turn results in promoting non-canonical inflammasome (Göös et al., 2019). Like *CASP5*, *Casp11* can be induced by CCAAT enhancer–binding protein epsilon C/EBP homologous protein in mice (Endo et al., 2006). Thus, IRF1 and IRF2 might not be involved in regulation of *CASP5* and *Casp11*. Interestingly, mice with *IRF2* deficiency

phenocopy the resistance of *Gsdmd*$^{-/-}$ and *Casp11*$^{-/-}$ to the LPS-induced septic shock (Cuesta et al., 2003; Kayagaki et al., 2015). Thus, downregulation of *IRF1* and *IRF2* indirectly provide negative regulation of non-canonical inflammasome activation through orchestrating the transcriptional regulation of both *CASP4* in human and *GSDMD* in human and mice. Consistent with Stengel et al., 2020 and similar to *CASP5*, *CASP1* expression remained unchanged in PBMCs from ACLF patients in comparison to patients without ACLF (**Fig. 8G**). Of note, the expression of *CASP1* can be regulated by distinct transcription factors (Christgen et al., 2020). Although *CASP1* was not downregulated during immunosuppression, its expression significantly correlates with *IRF1* and *IRF2* expression, suggesting, that other transcription factors such as IRF8 (Lv et al., 2018) or NF-κB (Lee et al., 2015) may contribute to maintaining the upregulation of *CASP1* during immunosuppression and chronic diseases. The canonical and non-canonical inflammasome pathways function differentially, but cooperatively to control infection. Activation of the canonical inflammasome drives IFN-γ to prime non-canonical inflammasome to defend against vacuole bacterium via IL-18 release which is a well-known inducer of IFN-γ secretion which is produced by NK and T cells (Aachoui et al., 2015). Importantly, it is unclear whether the downregulation of *CASP4* observed in patients with ACLF is due to epigenetic changes such as DNA-methylation in the promotor regions of *CASP4* gene. The binding sites of IRF1 and IRF2 are palindromic (Chang et al., 1992; Tanaka et al., 1993; Wang et al., 1996) and so they directly bind to the same promotor element of their target genes such as *CASP4* (**Appendix Fig. 28A**, **B**). This suggests, that in the presence of IFN-γ, IRF1 and 2 can co-occupy the IRF-binding sequence of *CASP4* promotor and may ensure and enhance a robust and redundant expression of *CASP4*. Interestingly, based on the analysis of DNA-methylation of the sequences of target ICGs, we did not detect relevant changes in ICGs onto the IRF1/2 binding element and its proximity within *CASP4* gene in all patients as compared to healthy donors (**Appendix Fig. 28C**). Thus, we ruled out contribution of DNA methylation in regulation of *CASP4* expression during immunosuppression and suggest that decreased expression of both nuclear factors IRF1 and IRF2 results in downregulation of *CASP4* along with the *HLA-DRA* expression, as *HLA-DRA* is also a target gene regulated by IRF1 and IRF2 (Chang et al., 1992; Hobart et al., 1996). It is widely known that TLR-4 activation by LPS rapidly induces the expression of IFN-β in a MyD88-independent fashion and induces expression of IRF1 and STAT1 target genes (Schauvliege et al., 2002; Karaghiosoff et al., 2003) and that long term exposure to LPS results in downregulation of IRF1 and STAT1-dependent genes (Baillie et al., 2017; Kang et al., 2019). Using primary human macrophages, we demonstrated that LPS induced suppression of *CASP4* along with *HLA-DRA*

expression and TNFα production were restored by IFN-γ treatment (**Fig. 13A-E**). IFN-γ enhances the activation of IRF1 and IRF2 signaling which in turn restores the requirements for *CASP4* expression. Noteworthy, activation of TLR4 via the TRIF-dependent axis leads to activation of IFN-signaling and upregulation of type I interferon and ISGs including a family of IFN-inducible GTPases termed guanylate-binding proteins (GBPs) (Liehl et al., 2015). Casp11/4/5 are produced as monomeric zymogens that dimerize after being activated upon recognition of cytosolic LPS (Shi et al., 2014; Vanaja et al., 2016). GBPs are involved in cytosolic detection and interruption of bacterial vacuoles and allow bacterial production to enter the host cell cytosol promoting inflammasome activation via non-canonical pathway (Pilla et al., 2014; Meunier et al., 2014; Liehl et al., 2015). The structure of inflammasome complex is assembled via domain interactions among the protein components. Unlike other inflammasomes such as NLRP3, NLRC4, AIM2, NLRP1 and Pyrin, the non-canonical inflammasome is thought to be dispensable for co-receptors and adaptor proteins to recognize its ligand LPS. Given the specificity of NLRC4 in recognizing its ligand via Naip proteins, it is possible that ligand specificity can be achieved via recruitment of different cofactors for the engagement of non-canonical inflammasome (Jorgensen et al., 2017). Recent studies have determined that the recruitment of different GBPs enhance caspase-4 activation in human macrophages, leading to sufficient elimination of pathogens and conferring the requirement of IFN-signaling as prerequisite for caspase-4 dependent pathway (Fisch et al., 2019; Santos et al., 2020; Wandel et al., 2020). Overall, downregulation of caspase-4 along with interferon singling is a critical event for host defense against virulent Gram-negative bacteria. However, this role may be taken over by overexpression of caspase-5 during immune dysfunction. Therefore, it would be of interest to determine if GBPs coordinate caspase-5 activation as well during critical inflammatory phases. Collectively, treatment of patients with immune modulator enhancers such as IFN-γ can impede and reverse the sepsis-immunosuppression stage and enhance pathogen clearance.

5.1.4 Functional association of caspase-4 and caspase-5-dependent responses define outcome of cell death during critically ill patients

In sepsis and sepsis-like cirrhosis, the mechanisms causing organ damage are associated not only with hemodynamic derangement, but also to cell dysfunction and cell death events induced by the exacerbated immune activation and concurrent release of DAMPs (Singer et al., 2016; Piano et al., 2018; Deng et al., 2018; Mateos and Albillos, 2019). During cytosolic LPS or Gram-negative bacterial infection, caspase-4 and -5 differentially regulate the release of certain alarmins with multiple physiological functions. In brief, while Caspase-4 and -11 elicit the

release of HMGB1 and Gal-1 (Shi et al., 2014; Schmid-Burgk et al., 2015; Deng et al., 2018; Russo et al., 2021), Caspase-5 and -11 elicit the cleavage and subsequent release of IL-1α (Deng et al., 2018; Wiggins et al., 2019) and PGRN (Duduskar et al., 2019). Thus, caspase-4/5 (in human) and caspase-11 (in mice) presumably exhibit certain overlapping and divergent functions during inflammation/infection. In line with the difference in transcriptional regulation of *CASP4* and *CASP5* our data additionally reflects this in terms of the systemic release of Gal-1 and PGRN in plasma of acute decompensated liver cirrhosis patients (**Fig. 10**). We found that cirrhosis patients exhibit higher release of PGRN compared to healthy volunteers. However, the PGRN release was markedly higher in patients with ACLF in comparison to patients without ACLF, which is likely due to increased expression and activation of caspase-5. Release of PGRN is increased in septic patients and enhances bacterial clearance and host defense during sepsis by promoting recruitment of macrophage and its involvement in a broad array of physiological and pathological conditions (Song et al., 2016; Yan et al., 2016), suggesting that caspase-5-mediated release of PGRN may enhance survival in patients. Similarly, Gal-1 is increased in plasma of patients with sepsis and plays a determinant role during sepsis by facilitating lethal inflammation via inhibition of CD45 (Russo et al., 2021). Conversely and consistent with *CASP4* expression, Gal-1 production was higher in both patient groups, however it tends to be tolerated and associates with transient upregulation of *CASP4* in patients with signs of immunosuppression (**Fig. 10B**). Thus, caspase-5 mediated release of PGRN is protective but caspase-4 mediated release of Gal-1 is lethal. This is in line with reported studies where *Pgrn*$^{-/-}$ mice are highly vulnerable in response to LPS-induced sepsis (Yan et al., 2016; Song et al., 2016), whereas *Lgals1*$^{-/-}$ (Gal-1 deficient) mice are more resistant (Russo et al., 2021). Although caspase-4 and -5 share more than 70% homology at the amino acid level but they carry out unique functions (Baker et al., 2015). Interestingly, *CASP4* overexpression in mice associates with mortality and a hyperinflammatory phenotype in response to LPS (Kajiwara et al., 2014; Baker et al., 2015). Thus, suppression of caspase-4 during immunosuppressive state may circumvent additional tissue damage by abrogating its unique inflammatory response. GBPs, which play a vital role in sensing LPS and lysis of pathogens containing vacuole, require IFN signaling during Gram-negative sepsis (Finethy et al., 2015; Santos et al., 2020; Wandel et al., 2020). Fisch et al., have recently reported that caspase-1 cleaves and inactivates GBP1, which is required for caspase-4 recruitment on bacterial vacuole to drive its lysis (Fisch et al., 2020). In this study, the regulation of *CASP1* gene remain upregulated (**Fig. 8**), suggesting, that caspase-1 may indirectly contributes to abrogate caspase-4 activity. However, all these mechanisms appear to be upstream of pore forming activity of

GSDMD via inflammatory caspases to initiate the lethal phase of pyroptosis (Shi et al., 2015; Kayagaki et al., 2015; He et al., 2015; Liu et al., 2016; Ding et al., 2016; Aglietti et al., 2016). Interestingly, GSDMD cleavage product (p20) was detectible in plasma of septic patients and could be associated with extent of organ damage as presented by a cut-off of SOFA score <8≥ (**Fig. 11**), indicating that activation of inflammasome is associated with sepsis progression. Collectively, our results suggest that pyroptosis plays a vital role in dysregulation of immune response during sepsis. GSDMD cleavage occurs not only because of the activation of inflammatory caspases (Caspase-1, 4, 5 and -11) in macrophages, but it can also be governed by other cell death types including NETosis and apoptosis (Chen et al., 2020). This suggests, that other cell death pathways may overlap with pyroptosis and play a critical role in dysregulation of immune response during sepsis. In addition, GSDMD activation also dampens the cGAS-dependent type I IFN response by triggering K^+ efflux across the plasma membrane and thus it contributes to affect both innate and adaptive immunity (Banerjee et al., 2018). Taken together, the results from the present study indicate an activation of immunologically active cell deaths that associate with infections and extent of organ damage in various inflammatory states including sepsis and cirrhosis. This reveals potential targets for therapeutic intervention for lethal infection.

5.2 Role of CNPY3 in regulating cytosolic immune responses toward NLRP3 inflammasome

Regulation of the inflammasome via chaperones is still not well studied. In this study, we sought further to examine the role of CNPY3 in regulating the canonical and non-canonical inflammasome activation. Stable CRISPR/Cas9 generated *CNPY3* deficient THP-1 macrophages and primary macrophages carrying c.548delA *CNPY3* mutation were used to unravel the importance of CNPY3 in regulating inflammasome activation beyond its role in TLRs trafficking.

5.2.1 A Crucial function of CNPY3 in activity of canonical NLPR3 inflammasome pathway.

As the most widely characterized CNPY family members, CNPY3 is a highly evolutionary conserved protein through vertebrates (Takahashi et al., 2007; Morales and Li, 2017; Mutoh et al., 2018). Unlike many chaperones including heat shock proteins, which are induced during stress (Nardai et al., 2006), expression of CNPY3 was detected under basal condition in macrophage lines and in PBMCs of healthy donors. This indicates the importance of CNPY3 network in these cells and suggests unanticipated roles other than its known function in trafficking of TLR and immune function as a chaperone. Using primary macrophages carrying

c.548delA *CNPY3* mutation and stable CRISPR/Cas9 generated *CNPY3* deficient THP1 macrophages clones, I demonstrated that loss of functional CNPY3 is associated with impairment of activation of the NLRP3 canonical inflammasome along with its known function in TLRs trafficking. Our study identified a novel mutation in a family carrying the autosomal recessive variant c.548delA in *CNPY3* gene. As illustrated in **Fig. 23**, the frameshift mutation c.548delA in *CNPY3* results in a truncated CNPY3 (p.Asn183Thrfs*7) which results in a loss-of-function mutation. Intriguingly, different well-studied inflammasome activators including nigericin,cytosolic LPS and pathogens, failed to activate NLRP3 inflammasome in terms of proteolytic activation of caspase-1. Ultimately this resulted in an impaired maturation and secretion of pro-IL-1β and pro-IL-18 as well as induction of cell death (**Fig. 17-Fig. 25**). In keeping with the observation of pyroptotic cell death, the response of *CNPY3*$^{-/-}$ macrophages to cytosolic LPS, which is mediated by GSDMD via caspase-4 and -5 activation, was unaffected, an event that is dispensable for caspase-1 activation (Shi et al., 2015; Kayagaki et al., 2015). Importantly, pyroptosis which engaged upon non-canonical inflammasome activation, is coincided with GSDMD-elicited pore formation that leads to rupture of active cells, and in turn synoptically activates the canonical NLRP3 inflammasome (Baker et al., 2015). However, *CNPY3*$^{-/-}$ macrophages lacked a hub to activate NLRP3 inflammasome as a secondary effect of non-canonical inflammasome activation upon response to LPS (**Fig. 18**) and alive *E. coli* bacteria (**Fig. 19A-C**), that efficiently reached the cytosol. This indicates that CNPY3 chaperone is dispensable for non-canonical inflammasome activation. In addition to unimpaired non-canonical inflammasome activation, failed intracellular staining of caspase-1 in *CNPY3*$^{-/-}$ macrophages (as measured by intracellular staining of caspase-1) (**Fig. 17**) revealed that alteration of the secretion pathway is unlikely to account for this effect. Inflammasome activation is a key event in response to bacterial infection (Mariathasan et al., 2006; Broz et al., 2010). In this regard, CNPY3 is a prerequisite to activate inflammasome by macrophages cultured with alive Gram-positive and -negative bacteria including *S. aureus*, GBS and *E. coli* which possess an excess of inflammasome activators (Mariathasan et al., 2006; Muruve et al., 2008; Strowig et al., 2012). CNPY3 deficient and mutant macrophages were also profoundly failed to activate caspase-1 and secrete IL-1β. Collectively, our findings identify CNPY3 as a unique regulator of canonical inflammasome to alive bacteria and their components.

5.2.2 TLR-3 activation licenses efficient upstream signaling to activate NLRP3 inflammasome in *CNPY3* deficient macrophages

TLR pathways are not only required for sensing extracellular pathogens but also for enhanced responsiveness that initiate the assembly and activity of inflammasomes (Schroder and Tschopp, 2010; Broz and Dixit, 2016; Fitzgerald and Kagan, 2020). Consistent with previous studies (Takahashi et al., 2007; Liu et al., 2010), primary macrophages carrying loss of function of c.548delA *CNPY3* variant and stable CRISPR/Cas9 engineered THP1 macrophages lines with CNPY3 deficiency results in impaired responses to multiple TLRs including TLR1, 2, 4, 5 but not TLR3 (**Fig. 15**, **Fig. 24**). This suggests the patient macrophages and CRISPR clones are a good model for studying the effect of defective CNPY3 function on other signaling pathways such as the inflammasome pathway. Activation of NLRP3 inflammasome is regarded to require a priming signal that results from TLR activation. Despite the multiple TLR deficiencies, CNPY3 deficient macrophages were able to respond to TLR3 in order to culminate the post-transcriptional activation of canonical and non-canonical NLRP3 inflammasome pathways toward distinct stimuli. Thus, CNPY3 was not involved in expression or folding of core inflammasome components; hence their protein expression was intact in CNPY3 deficient macrophages (**Fig. 16**), implying that macrophages with CNPY3 deficiency can invariably undergo inflammasome activation. In contrast to pro-IL-1β, pro-IL-18 and GSDMD are constitutively expressed and do not required TLR-activation to induce their expression (Bauernfeind et al., 2009; Groslambert and Py, 2018; Kayagaki et al., 2019). Pretreatment of *CNPY3*$^{-/-}$ macrophages with poly(I:C) can effectively compensates the priming signal and satisfies thereby the requirement for a subsequent activating signal. Despite this priming signal CNPY3 deficient macrophages showed impaired maturation of pro-IL-18 and GSDMD. These results further indicate that failed maturation and secretion of IL-1β and IL-18 are not a consequence of a compromised priming signaling.

The NLRP3 protein is an inactive cytosolic protein that is post-transcriptionally translocated into the ER upon priming to overcome its auto-repressed state (Groslambert and Py, 2018; Elliott et al., 2018). NLRP3-assembly is therefore organized by cell organoids such as mitochondria and MAMs (Zhou et al., 2011; Iyer et al., 2013; Subramanian et al., 2013; Misawa et al., 2013; Zhang et al., 2017; Elliott et al., 2018). Upon TLR3 activation, NLRP3 can efficiently migrate into ER in CNPY3-independent manner. Thus, the findings presented here illustrate that CNPY3 was not required for NLRP3 expression, stability or its association to MAMs (**Fig. 16**). Additionally, these results corroborate the notion that priming signaling in *CNPY3*$^{-/-}$ macrophages were intact when challenged with TLR3 activator (poly(I:C).

Noteworthy, dysregulated protein processing can lead to the accumulation of misfolded protein aggregates that exceed the ER loading capacity and results in ER stress (Li et al., 2020). Consequently, signaling that induce ER-stress such as unfolded and damages proteins can initiate inflammasome to induce inflammatory responses via oxidative stress, calcium homeostasis and NF-κB activation (Menu et al., 2012; Li et al., 2020). I found that CNPY3 deficiency probably does not affect the status of ER, hence ER proteins like STING and Tom20 were equally expressed and were comparable to wild type macrophages **(Fig. 16B).** Altogether, TLR3 can compensate inflammasome priming in *CNPY3* deficient macrophages in absence of multiple TLRs. Although we cannot fully rule out an unknown priming effect of macrophages in *in vitro*, our data on multiple THP-1 lines and human macrophages with CNPY3 deficiency, all showed the dispensability of priming for inflammasome activation. Moreover, through different regulation mechanisms, bacterial recognition pathways can lead to an aberrant upstream and downstream regulation of inflammasome assembly, composition, and activation (Miao et al., 2006; Franchi et al., 2007; Muruve et al., 2008; Kayagaki et al., 2013; Sha et al., 2014; Storek and Monack, 2015). However, priming of THP-1 macrophages that were cultured with bacteria behave the same as those unprimed (**Fig. 19** vs. **Fig. 20F-I**). Overall, this evidence suggests that the role of CNPY3 in regulating inflammasome is unlikely to be due to interference with TLR-misfolding or the resulting transcriptional induction. Instead, it may directly affect the regulation of inflammasome assembly and activation.

5.2.3 CNPY3 role in regulating functional inflammasome assembly

Dominant activity of caspase-1 relies on a proper, timely, and spatial assembly of organized supramolecular complexes. Mechanistically, upon inflammasome activation, NLPR3 associates with the ASC molecule via homotypic PYD domains and a supramolecular inflammasome structure forms around an ASC-oligomeric scaffold. This acts as a bridge between NLRP3 protein and inactive caspase-1, an event which drives caspase-1 proteolytic activation within the inflammasome complex (Man et al., 2014; Boucher et al., 2018; Chen and Chen, 2018; Magupalli et al., 2020; Seoane et al., 2020). In this study, the formation of cytoplasmic ASC large structures or “specks” in macrophages are challenged with nigericin and were visualized biochemically and microscopically (Fernandes-Alnemri et al., 2007; Stutz et al., 2013). We demonstrated that, despite significant impairment of proteolytic activation of caspase-1 in macrophages (**Fig. 17**, **Fig. 20**, **Fig. 25**), ASC-specks/oligomerization were formed independent of CNPY3 (**Fig. 21**), at least as determined by the nigericin-induced formation of ASC-specks. Similar result to live-cell imaging were obtained by staining with ASC specific antibody (**Fig. 22A, B**). However, confocal imaging revealed that ASC specks formed by

CNPY3$^{-/-}$ macrophages appear larger in size compared to those formed by wild type macrophages (**Fig. 22A**, **F**), indicating a dysregulated assembly of the inflammasome. Notably, the presence of NLRP3 reduces the size of ASC specks (Nagar et al., 2019), so that a threshold concentration must be reached to support the assembly of the inflammasome (Fitzgerald and Kagan, 2020).Although NLRP3 efficiently migrates to the MAM in CNYP3 deficient macrophages during the priming step (**Fig. 16B**), the level of NLRP3 migration to the ER was markedly lower compared to wild type macrophages. This reduction potentially might lead to the enlarged structure of ASC-specks formed by *CNPY3*$^{-/-}$ macrophages and thus may not be sufficient to induce robust and functional assembly of NLRP3 and subsequent activation of caspase-1. In addition, previous studies have established that size of ASC speck is reduced by the presence and duration of caspase-1 activity (Boucher et al., 2018; Nagar et al., 2019). This is in line with Stein et al., they have demonstrated that the enzymatically inactive caspase-1 variant (p.C284A) form larger ASC specks in size (Stein et al., 2016). Thus, our observations support these findings that CNPY3 drive a adequate recruitment of caspase-1 in ASC-containing inflammasome platforms. Which in turn associates with the multitude of downstream responses resulting after NLRP3-caspase-1 activation and ultimately the size/structure of ASC speck. Hence, ASC oligomerization is required to create a signal amplification mechanism for inflammasome activation (Dick et al., 2016). ASC speck formation per cell was unchanged for CNPY3, this does not associate with the CNPY3 phenotype, where inflammasome-mediated cytokine production and cell death were impaired. Thus, CNPY3 may elicit a functional formation of ASC-NLRP3 containing inflammasomes and without it the formed ASC oligomers are not efficient. Altogether, these results indicate that CNPY3 controls the dynamic of functional assembly and arming of NLRP3 inflammasome complex. Whether this role is directly or indirectly governed by CNPY3, needs further investigations to identify the interconnection of CNPY3 chaperoning role and function of inflammasome assembly. In this regard, over recent years there is a growing body of literature demonstrating that NLRP3 inflammasome assembly consists of different adaptor proteins, which are spatially and timely recruited into a single and prenuclear speck in most cell types(Man et al., 2014; Li et al., 2017; Chen and Chen, 2018; Magupalli et al., 2020). Recently, Magupalli et al., have shown that histone deacetylase 6 (HDAC6) is required for inflammasome assembly to migrate into the centrosome, where a single inflammasome speck per cell is formed (Magupalli et al., 2020). However, our results suggest that this perinuclear assembly in macrophages were not affected by CNPY3 deficiency (**Fig. 22A**). Since other inflammasome regulator can also be recruited into nigericin-mediated inflammasome assembly such as

caspase-8 (Man et al., 2014), NEK7 (Sharif et al., 2019), and GBP5 (Shenoy et al., 2012) to promote NLRP3 inflammasome activation and CNPY3 may serve as a co-factor for caspase-1 activity. Finally, a remaining question that needs to be addressed in future studies is whether or not activation of other inflammasomes is independent of ASC such as NLRP1, CARD8, and NLRC4 also require CNPY3 in macrophages.

5.2.4 CNPY3 role in regulation of inflammasome toward TLR-trafficking and EIEEs syndrome

To attain functionality in all cellular compartments, proteins must fold into their native state. Molecular chaperones are implicated in maintenance of proteostasis, gene regulatory networks, folding of immunologically important proteins and activation of the immune system (Randow and Seed, 2001; Nardai et al., 2006; Liu et al., 2010; Kim et al., 2013; Majer et al., 2019a; Schildknegt et al., 2019). Thus, mutations in genes encoding chaperones can have drastic effects on immune responses (Macario and Conway de Macario, 2005; Nardai et al., 2006; Casrouge et al., 2006; Yang et al., 2007). Although, the ER-resident chaperones UNC93B1, GP96 and CNPY3 govern the regulation and trafficking of multiple TLRs, they appear to differ in their *in vivo* functions. Whereas UNC93B1 deficiency is featured by increased susceptibility to developing herpes simplex encephalitis (Casrouge et al., 2006), while loss of *Hsp90b1* gene encoding Gp96 leads to embryonic lethality during mouse development (Yang et al., 2007). CNPY3 deficiency on the other hand is associated with neurological disorders known as EIEE along with growth impairment in human and mice (Mutoh et al., 2018). These differences suggest that UNC93B1, Gp96, and CNPY3 chaperones can substantially have more roles and functions *in vivo* than assisting in TLRs-trafficking. Here, we propose that the immune function of CNPY3 chaperone might be more widespread than previously thought and may not be only restricted to TLRs-trafficking. Here we studied the loss-of-function variant c.548delA in *CNPY3* in a pediatric patient born to an affected consanguineous family. The variant results in the loss of function of CNPY3 expression and associates with neurological disorders and impairment in growth and survival in an autosomal recessive manner. However, the clinical relevance between pathogenesis of CNPY3 deficiency and its chaperoning functions remains unclear. *Ex vivo* and consistent with results obtained from multiple clones of *CNPY3* deficient macrophages, we found this loss of function of CNPY3, impaired not only trafficking of TLRs but also NLRP3 inflammasome activation. This also caused failed trafficking of CNPY3-dependent TLRs in macrophages carrying c.548delA mutation as compared to unaffected controls (**Fig. 24, Fig. 25**). Thus, both the clinical phenotypes and the *in vitro* studies indicate that CNPY3 deficiency participates in the pathogenesis. However, it is yet premature to assign

the clinical neurological disorders to the immunological function of CNPY3 with the existing data defined in this study. These findings have gained potential to transform our understanding of the basic biology and clinical relevance of inflammasome and its activities to govern health and disease. Many factors could account for the clinical resulting phenotype of CNPY3 chaperone mutant in context of inflammasome activation. Also, one or more yet to be identified client proteins of the CNPY3 chaperoning activity beyond TLRs, could be regulators of the inflammasome activity and/or the patient phenotype reported herein. Canopy-1 (*CNPY1*), the zebrafish ortholog of human CNPY3 is needed for fibroblast growth factor (FGF) signaling in the brain (Hirate and Okamoto, 2006), illustrating that CNPY3 chaperone may control bona fide growth factor signaling by stabilizing important pathway constituents that could potentially interfere with inflammasome pathways. Notably, post-transcriptional modifications including ubiquitination, deubiquitination, phosphorylation, alkylation or S-nitrosylation (Shim and Lee, 2018; Seoane et al., 2020) control every aspect of inflammasome activities and could be coordinated with CNPY3. Thus, aberration of any one of these mechanisms can alter the transcriptional responses and cellular functions. Indeed, the inflammasomes are signaling complexes that are not only restricted to immune cells and also display cellular- and tissue-dependent activations (Schroder and Tschopp, 2010; Strowig et al., 2012; Latz et al., 2013; Heneka et al., 2018). In addition to promoting the secretion of cytokines like IL-1β and IL-18 during inflammation, caspase-1 is also involved in secretion of other mediators like FGF-2 and IL-1α through non-classical secretion pathway (Keller et al., 2008). FGF-2 is highly expressed in the brain (Ortega et al., 1998) and is required for promoting p21-activated kinase (PAK1) (Galisteo et al., 1996; Strochlic et al., 2010), which mediates phosphorylation and subsequent activation of caspase-1 (Basak et al., 2005). PAK1 is highly expressed in neuronal tissues and required as a main downstream effector of the Rho-GTPases Cdc42 and Rac, which mediates various extracellular signals into intracellular responses (Kelly and Chernoff, 2012; Geiger et al., 2013). Interestingly, loss of function of PAK1 associates with neurodevelopment (Kelly and Chernoff, 2012; Harms et al., 2018). Beyond its immune function, microglia, the resident macrophages in the brain, are involved at all stages of brain development. Thus, conventional cytokine production and release by microglia and other peripheral immune cells are critical for the development of nervous system and immune responses (Squarzoni et al., 2014; Mutoh et al., 2018). Given that the expression of CNPY3 in neurons and the gastrointestinal tract is high (Mutoh et al., 2018; Xiao et al., 2019; Schildknegt et al., 2019), it is very likely that it plays a role in the development of immune and nervous system. Emerging evidence supports that gut microbiota regulates the growth and development of the central and enteric nervous systems

after birth (Wang and Kasper, 2014; Vadder et al., 2018). Moreover, TLRs and inflammasome are progressively involved in the development of gut microbiota (Elinav et al., 2011; Man et al., 2016; Fulde et al., 2018; Xiao et al., 2019). In this regard, intestinal epithelial cells, which are uniquely positioned to interact and influence the luminal intestinal microbiota, exhibit distinct spatial and temporal uneven distribution of TLRs (Price et al., 2018; Fulde et al., 2018). In addition, the RNA-binding protein HuR coordinates function of intestinal epithelial cells by altering the localization of TLRs through post-transcriptional regulation of *Cnpy3* (Xiao et al., 2019). Thus, the contribution of gut microbiota cannot be ruled out in the phenotype of CNPY3 deficiency, and further studies are needed to elucidate the influence of CNPY3 in regulating gut microbiota. In humans, genetic studies indicate that activating mutations in genes encoding constituent and regulatory proteins of the inflammasomes are associated with an increased susceptibility to immune disorders and development of auto-inflammatory diseases such as CAPS and FMF (Kastner et al., 2010; Chae et al., 2011; Strowig et al., 2012; Zhou et al., 2012; Chae et al., 2015; Zhang et al., 2017). Moreover, the ability of CNPY3 as a chaperone to regulate the activation of NLRP3-inflammasome reported herein, highlights the dynamic and cooperative nature of innate immune sensors and chaperones, which are downstream of TLR signaling in macrophages. However, tiny variants in CNPY3 may occur and affect the course of infectious and auto-immune diseases. Collectively, this data suggest that CNPY3 serves not only to chaperone TLRs but also other client proteins that might be involved in regulating different biological and neurological processes.

6. Conclusion

This study provides a mechanistic insight into how the canonical and non-canonical inflammasome paths are inextricably linked. In this study we highlight, the importance of regulation and activation of core inflammasome components during innate immuno-suppression. Our results demonstrate striking differences in regulation and function of *CASP4* and *CASP5*, despite being highly related genes, during immunosuppression associated organ damage.. In contrast to other *CASP5* and *CAPS1* regulation, *CASP4* regulation appears to be transiently upregulated during sepsis (**Fig. 26**).

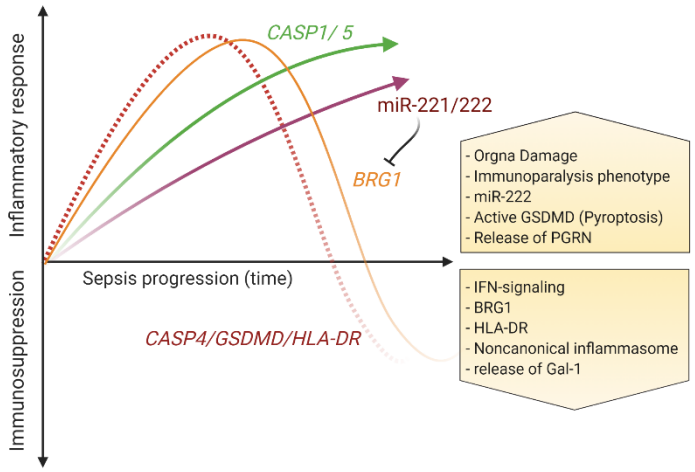

Fig. 26: A schematic summary of the sepsis progression explaining the regulation of genes and phenotypes observed in this study
Inflammatory caspases *CASP1*, *4*, and *5* and *GSDMD* and *HLA-DR* encoding genes were upregulated at early stage of sepsis. Elevated expression of miR-221/222 and their silencing effect on *BRG1* transcripts, indicating occurrence of immuno-suppression, which associates with high grades of organ failure, downregulation of *CASP4*, *GSDMD* and *HLA-DR*. Boxes summarize the outcome of the sepsis-induced innate immuno-suppression. (Created with BioRender.com).

The non-canonical inflammasome, which senses cytosolic LPS independently of TLR4 and drive lethal sepsis by causing pyroptosis and NLRP3 inflammasome activation, mediate release of DAMPs and alarmins, leaking from the cytosol and damaged intracellular organelles via active GSDMD during sepsis. Hence, GSDMD activation provides a mechanistical link between canonical and non-canonical inflammasome and presents an attractive target to block the unbridled inflammasome activation during sepsis. In this regard, this study emphasizes the importance for the stratification of patients according to their inflammatory states in order to provide the right treatment at the right time. This also demonstrates the potential of miR-222 expression as an indicator for sepsis-associated immunosuppression and organ failure. In addition, this thesis highlights the importance of IFN-signaling and its essential role to control the regulation and activation of non-canonical NLPR3 inflammasome pathway and suggests that treatment of sepsis-associated immunosuppression with IFN-γ might help patients with signs of impaired immunity.

Beyond its function in coordinating the subcellular distribution of TLRs, we revealed that CNPY3 is required for the proper assembly of caspase-1 to ASC-oligomers and thus associates with the magnitude of the signal resulting after NLRP3 activation, a mechanism that presumably dispensable for priming events (**Fig. 27**).

Another remarkable finding of the thesis is the discovery of a novel function of CNPY3 for inflammasome assembly, distinct from the TLR chaperoning function, that may be relevant to innate immunity and neuronal homeostasis.

Altogether, our findings may be a factor to understand the pathogenicity and links to possible therapeutical strategies of sepsis and EIEEs.

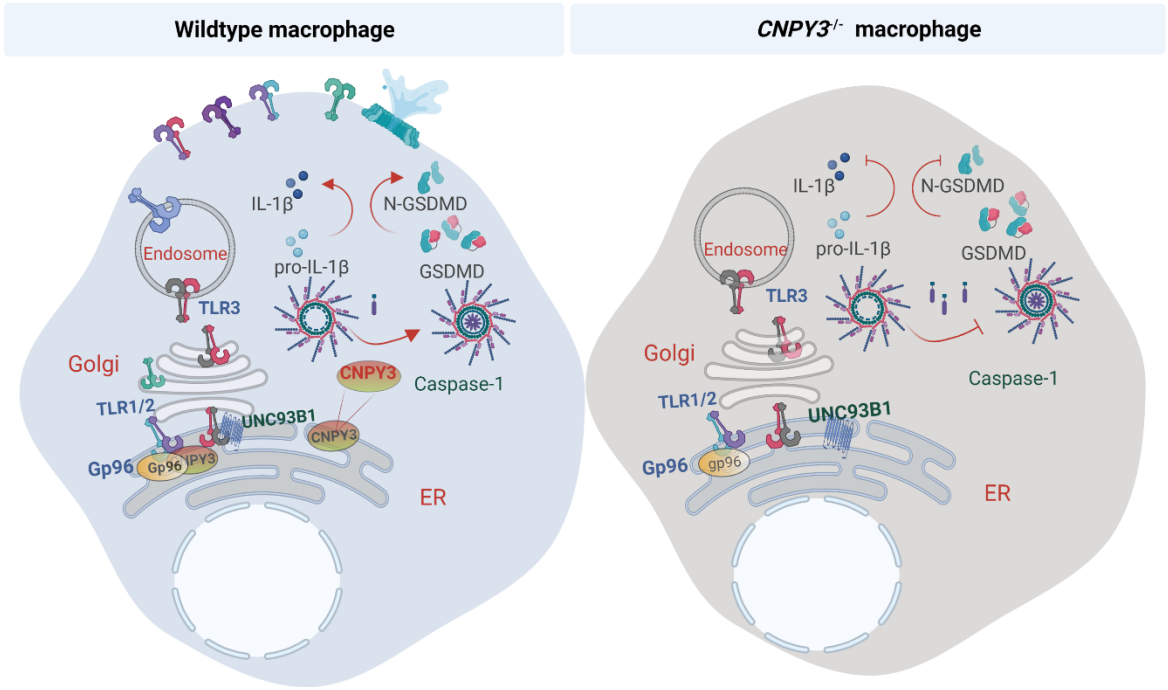

Fig. 27: Requirement of CNPY3 chaperone in TLR-trafficking and inflammasome assembly
Expression of functional multiple TLRs with exception of TLR3 requires CNPY3 chaperoning activity. Trafficking of CNPY3-dependent TLRs routs from ER to Golgi and ultimately into cell surface or endosomes. CNPY3 coordinates by yet unknown mechanism the dynamic of caspase-1 recruitment into NLRP3-ASC inflammasome. In the absence of CNPY3, TLRs are not functional and chiefly kept in the ER and fail to translocate into their destination. Impaired recruitment of caspase-1 into ASC-NLRP3-containing inflammasome in the absence of CNPY3. (Created with BioRender.com).

.

7. Perspectives

Sepsis is characterized by excessive activation of the innate immune system followed by concomitant anti-inflammatory responses that may results in immunosuppression in patients (Hotchkiss et al., 2013; Rubio et al., 2019). Hence multiple agents targeting the inflammatory response in sepsis have failed, new approaches in the preclinical evaluation of sepsis therapies need to be addressed. In this study, we highlight the importance of miR-222, as a surrogate to define patient with sings of immunosuppression and organ damage but not infection. This finding might help clinicians to distinguish between septic patients with and without sign of immunosuppression and organ damage to provide effective immunoinhibitory or immunostimulatory-based targeting therapy, respectively. LPS sensing in the cytosol by the non-canonical inflammasome leads to GSDMD-elicited pyroptosis and NLRP3 inflammasome activation in TLR4-independent manner (Baker et al., 2015; Kayagaki et al., 2015; Liu et al., 2016; Ding et al., 2016). In fact, different recent studies described that activation of canonical inflammasome requires a set of regulatory molecules to culminate its appropriate activation specially when pathogen invade the cell. In case e. g. the Gram-negative bacterium can invade the host cell successfully, LPS in the cytosol is recognized by caspase-4/5/11 to trigger pyroptosis and release of cytokines and alarmins (Kayagaki et al., 2011; Aachoui et al., 2013; Vanaja et al., 2016; Lorey et al., 2017; Lagrange et al., 2018; Russo et al., 2018; Russo et al., 2021). More recent studies reported, that LPS can bind to hGBP1 to disrupt bacterial cell envelope functions (Kutsch et al., 2020; Santos et al., 2020; Wandel et al., 2020) or binds to caspase-3 and caspase-7 resulting in blockade of apoptosis (Günther et al., 2020). Collectively, these receptors and their downstream signaling molecules such as GSDMD survey the cytosolic spaces for LPS sensing and operate in a complementary manner to induce specific functional responses (Kieser and Kagan, 2017). Therefore, this mechanism is more critical and complex than the LPS sensing via membrane-bound TLR4/CD14/LBP/MD-2 complex (Pfalzgraff and Weindl, 2019). Thus, cytosolic LPS sensing during sepsis provide a potential target as anti-sepsis drug. In addition, as GSDMD is the downstream of these caspases may blocking GSDMD resulting in protective effects (Rathkey et al., 2018). Caspase-4 and caspase-5 were thought to contribute to similar signaling pathways in inflammation due to the fact of their highly homologous sequence (Baker et al., 2015). We provide a mechanistic insight into the regulation of inflammatory caspases and its upstream (interferon) and downstream signaling (GSDMD activation and release of alarmins) in critically ill patients including sepsis and acute-on-chronic liver cirrhosis. We verify the shared features of sepsis and cirrhosis associated immunosuppression in context of NLRP3-inflammasome regulation and activation. However,

other inflammasome regulators which depend on IFN such GBPs require further investigation during sepsis-associated immunosuppression. In addition, other inflammasome pathways such as AIM2, NLRC4 and NLRP1 and its regulatory mechanisms need to be examined in conjugation with their specific pathogens. From pathogen perspective, the structure features of Lipid A moiety of LPS, is structurally variable, thus the structure features of LPS subtypes directly related to the virulence and their ability to evade our formidable immune detection. Given that several pathogens can alter their LPS structure during infections (Tan and Kagan, 2014; Pfalzgraff and Weindl, 2019), sepsis clinical *E. coli* strains may exploit this feature and selectively activate or even escape the recognition of LPS via caspase-4 and/or caspase-5, which can be in turn responsible for various pathological effects during sepsis. Thus, future studies aimed at understanding how different bacterial pathogens manipulate the nature of the interaction of LPS with caspase-4/5 or cytosolic LPS sensing will unravel novel regulatory molecules and highlight new selective pressure that may have promoted the evolution of bacterial immune evasion strategies to subvert host defense.

In a signaling network, not only the functions of PRRs are important but also precise spatial and temporal regulation of those functions to defend against pathogen infection. In addition to its known function in regulating multiple TLRs, we reported in this study that CNPY3 functions in regulating NLRP3-inflammasome activation. Although we could not identify deficiency of priming events via TLR3 activation in CNPY3 macrophages, NLRP3 activation via different NLRP3 stimuli and pathogens revealed the requirement of CNYP3 to efficiently activate caspase-1 and ultimately maturation of immature cytokines and induction of pyroptosis. CNPY3, as an ER-resident chaperone, ameliorates the nucleation of inactive caspase-1 into ASC oligomers. This mechanism provides a mechanistic insight into how the communication of different organelles are evolved. Clinically, CNPY3 deficiency associates with EIEEs in human, all these along with other unknown functional role of CNPY3, suggest that CNPY3 plays a fundamental role in regulating the microbiome and nervous systems, as all these processes are highly linked (Elinav et al., 2011; Man et al., 2016; Fulde et al., 2018; Xiao et al., 2019). In addition, CNPY3 protein as a chaperone regulates other proteins, which might directly or indirectly contribute to the activation of NLRP3 inflammasome or to the progression of EIEEs in human. However, it is very premature to judge that the impairment in the neurological function in the affected patients are due the impairment of caspase-1 activation. Thus, to address the involvement of inflammasome activation in infantile encephalopathies, other but similar diseases, could be examined for inflammasome activations. All these considerations strongly argue that unknown signaling proteins, not fully assigned to inflammatory PRR-triggered

pathways could modulated the critical role of CNPY3 in inflammasome activation documented in this study. Since caspase-1 inflammasome is a dynamic entity that is assembled from distinct adaptors in a stimulus-dependent response and in an ASC-dependent and independent manner. Thus, auto-activation of caspase-1 is for other inflammasome in ASC-dependent approach such as AIM2, NLRP1, Pyrin (ASC-dependent) and NLRC4 (through homotypic CARD-CARD binding) and CARD8 (ASC-independent) (Ball et al., 2019) warrant further studies for its CNPY3-dependency. In addition, enzymatically inactive caspase-1 appears to be functional (Boucher et al., 2018; Reinke et al., 2020), however, whether these kinetic and dynamic functions and additional facets of the overlapping of cell deaths involve CNPY3 chaperoning activity needs further investigations. This finding may highlight molecular determinants of chaperone protein client's specificity and challenge the idea that complexity is a prerequisite for innate immune pathway design.

8. References

Aachoui, Y., Y. Kajiwara, I. A. Leaf, D. Mao, J. P.-Y. Ting, J. Coers, A. Aderem, J. D. Buxbaum, and E. A. Miao. 2015. Canonical Inflammasomes Drive IFN-γ to Prime Caspase-11 in Defense against a Cytosol-Invasive Bacterium. *Cell host & microbe* 18(3):320–332. doi:10.1016/j.chom.2015.07.016.

Aachoui, Y., I. A. Leaf, J. A. Hagar, M. F. Fontana, C. G. Campos, D. E. Zak, M. H. Tan, P. A. Cotter, R. E. Vance, A. Aderem, and E. A. Miao. 2013. Caspase-11 protects against bacteria that escape the vacuole. *Science (New York, N.Y.)* 339(6122):975–978. doi:10.1126/science.1230751.

Aglietti, R. A., A. Estevez, A. Gupta, M. G. Ramirez, P. S. Liu, N. Kayagaki, C. Ciferri, V. M. Dixit, and E. C. Dueber. 2016. GsdmD p30 elicited by caspase-11 during pyroptosis forms pores in membranes. *Proceedings of the National Academy of Sciences of the United States of America* 113(28):7858–7863. doi:10.1073/pnas.1607769113.

Albillos, A., M. Lario, and M. Álvarez-Mon. 2014. Cirrhosis-associated immune dysfunction: distinctive features and clinical relevance. *Journal of hepatology* 61(6):1385–1396. doi:10.1016/j.jhep.2014.08.010.

Allam, R., M. N. Darisipudi, K. V. Rupanagudi, J. Lichtnekert, J. Tschopp, and H.-J. Anders. 2011. Cutting edge: cyclic polypeptide and aminoglycoside antibiotics trigger IL-1β secretion by activating the NLRP3 inflammasome. *Journal of immunology (Baltimore, Md. 1950)* 186(5):2714–2718. doi:10.4049/jimmunol.1002657.

Ampuero, J., M. Simón, C. Montoliú, R. Jover, M. Á. Serra, J. Córdoba, and M. Romero-Gómez. 2015. Minimal hepatic encephalopathy and critical flicker frequency are associated with survival of patients with cirrhosis. *Gastroenterology* 149(6):1483–1489. doi:10.1053/j.gastro.2015.07.067.

An, J., S. H. Kim, D. Hwang, K. E. Lee, M. J. Kim, E. G. Yang, S. Y. Kim, and H. S. Chung. 2019. Caspase-4 disaggregates lipopolysaccharide micelles via LPS-CARD interaction. *Scientific reports* 9(1):826. doi:10.1038/s41598-018-36811-4.

Angeli, P., M. Bernardi, C. Villanueva, C. Francoz, R. P. Mookerjee, J. Trebicka, and P. … Gines. 2018. EASL Clinical Practice Guidelines for the management of patients with decompensated cirrhosis. *Journal of hepatology* 69(2):406–460. doi:10.1016/j.jhep.2018.03.024.

Antonescu, C. N., and A. P. Liu. 2019. Editorial: Signaling Control by Compartmentalization Along the Endocytic Route. *Frontiers in cell and developmental biology* 7:237. doi:10.3389/fcell.2019.00237.

Aziz, M., A. Jacob, and P. Wang. 2014. Revisiting caspases in sepsis. *Cell death & disease* 5:e1526. doi:10.1038/cddis.2014.488.

Baillie, J. K., E. Arner, C. Daub, M. de Hoon, M. Itoh, H. Kawaji, T. Lassmann, P. Carninci, A. R. R. Forrest, Y. Hayashizaki, G. J. Faulkner, C. A. Wells, M. Rehli, P. Pavli, K. M. Summers, and D. A. Hume. 2017. Analysis of the human monocyte-derived macrophage transcriptome and response to lipopolysaccharide provides new insights into genetic aetiology of inflammatory bowel disease. *PLoS genetics* 13(3):e1006641. doi:10.1371/journal.pgen.1006641.

Baker, P. J., D. Boucher, D. Bierschenk, C. Tebartz, P. G. Whitney, D. B. D'Silva, M. C. Tanzer, M. Monteleone, A. A. B. Robertson, M. A. Cooper, S. Alvarez-Diaz, M. J. Herold, S. Bedoui, K. Schroder, and S. L. Masters. 2015. NLRP3 inflammasome activation downstream of cytoplasmic LPS recognition by both caspase-4 and caspase-5. *European journal of immunology* 45(10):2918–2926. doi:10.1002/eji.201545655.

Ball, D. P., C. Y. Taabazuing, A. R. Griswold, E. L. Orth, S. D. Rao, I. B. Kotliar, D. C. Johnson, and D. A. Bachovchin. 2019. Human caspase-1 autoproteolysis is required for ASC-dependent and -independent inflammasome activation.

Banerjee, I., B. Behl, M. Mendonca, G. Shrivastava, A. J. Russo, A. Menoret, A. Ghosh, A. T. Vella, S. K. Vanaja, S. N. Sarkar, K. A. Fitzgerald, and V. A. K. Rathinam. 2018. Gasdermin D Restrains Type I Interferon Response to Cytosolic DNA by Disrupting Ionic Homeostasis. *Immunity* 49(3):413-426.e5. doi:10.1016/j.immuni.2018.07.006.

Barrat, F. J., M. K. Crow, and L. B. Ivashkiv. 2019. Interferon target-gene expression and epigenomic signatures in health and disease. *Nature immunology* 20(12):1574–1583. doi:10.1038/s41590-019-0466-2.

Bartel, D. P. 2009. MicroRNAs: target recognition and regulatory functions. *Cell* 136(2):215–233. doi:10.1016/j.cell.2009.01.002.

Barton, G. M., and J. C. Kagan. 2009. A cell biological view of Toll-like receptor function: regulation through compartmentalization. *Nature reviews. Immunology* 9(8):535–542. doi:10.1038/nri2587.

Basak, C., S. K. Pathak, A. Bhattacharyya, D. Mandal, S. Pathak, and M. Kundu. 2005. NF-kappaB- and C/EBPbeta-driven interleukin-1beta gene expression and PAK1-mediated caspase-1 activation play essential roles in interleukin-1beta release from Helicobacter pylori lipopolysaccharide-stimulated macrophages. *The Journal of biological chemistry* 280(6):4279–4288. doi:10.1074/jbc.M412820200.

Bauernfeind, F. G., G. Horvath, A. Stutz, E. S. Alnemri, K. MacDonald, D. Speert, T. Fernandes-Alnemri, J. Wu, B. G. Monks, K. A. Fitzgerald, V. Hornung, and E. Latz. 2009. Cutting edge: NF-kappaB activating pattern recognition and cytokine receptors license NLRP3 inflammasome activation by regulating NLRP3 expression. *Journal of immunology (Baltimore, Md. 1950)* 183(2):787–791. doi:10.4049/jimmunol.0901363.

Bauernfried, S., M. J. Scherr, A. Pichlmair, K. E. Duderstadt, and V. Hornung. 2021. Human NLRP1 is a sensor for double-stranded RNA. *Science (New York, N.Y.)* 371(6528). doi:10.1126/science.abd0811.

Benaoudia, S., A. Martin, M. Puig Gamez, G. Gay, B. Lagrange, M. Cornut, K. Krasnykov, J.-B. Claude, C. F. Bourgeois, S. Hughes, B. Gillet, O. Allatif, A. Corbin, R. Ricci, and T. Henry. 2019. A genome-wide screen identifies IRF2 as a key regulator of caspase-4 in human cells. *EMBO reports* 20(9):e48235. doi:10.15252/embr.201948235.

Berres, M.-L., B. Schnyder, E. Yagmur, B. Inglis, S. Stanzel, J. J. W. Tischendorf, A. Koch, R. Winograd, C. Trautwein, and H. E. Wasmuth. 2009. Longitudinal monocyte human leukocyte antigen-DR expression is a prognostic marker in critically ill patients with decompensated liver cirrhosis. *Liver international official journal of the International Association for the Study of the Liver* 29(4):536–543. doi:10.1111/j.1478-3231.2008.01870.x.

Beutler, B. A. 2009. TLRs and innate immunity. *Blood* 113(7):1399–1407. doi:10.1182/blood-2008-07-019307.

Bone, R. C., W. J. Sibbald, and C. L. Sprung. 1992. The ACCP-SCCM consensus conference on sepsis and organ failure. *Chest* 101(6):1481–1483. doi:10.1378/chest.101.6.1481.

Boomer, J. S., J. M. Green, and R. S. Hotchkiss. 2014. The changing immune system in sepsis: is individualized immuno-modulatory therapy the answer? *Virulence* 5(1):45–56. doi:10.4161/viru.26516.

Boomer, J. S., K. To, K. C. Chang, O. Takasu, D. F. Osborne, A. H. Walton, T. L. Bricker, S. D. Jarman, D. Kreisel, A. S. Krupnick, A. Srivastava, P. E. Swanson, J. M. Green, and R. S. Hotchkiss. 2011. Immunosuppression in patients who die of sepsis and multiple organ failure. *JAMA* 306(23):2594–2605. doi:10.1001/jama.2011.1829.

Boucher, D., M. Monteleone, R. C. Coll, K. W. Chen, C. M. Ross, J. L. Teo, G. A. Gomez, C. L. Holley, D. Bierschenk, K. J. Stacey, A. S. Yap, J. S. Bezbradica, and K. Schroder. 2018. Caspase-1 self-cleavage is an intrinsic mechanism to terminate inflammasome activity. *The Journal of experimental medicine* 215(3):827–840. doi:10.1084/jem.20172222.

Brinkmann, M. M., E. Spooner, K. Hoebe, B. Beutler, H. L. Ploegh, and Y.-M. Kim. 2007. The interaction between the ER membrane protein UNC93B and TLR3, 7, and 9 is crucial for TLR signaling. *The Journal of cell biology* 177(2):265–275. doi:10.1083/jcb.200612056.

Broz, P., and V. M. Dixit. 2016. Inflammasomes: mechanism of assembly, regulation and signalling. *Nature reviews. Immunology* 16(7):407–420. doi:10.1038/nri.2016.58.

Broz, P., J. von Moltke, J. W. Jones, R. E. Vance, and D. M. Monack. 2010. Differential requirement for Caspase-1 autoproteolysis in pathogen-induced cell death and cytokine processing. *Cell host & microbe* 8(6):471–483. doi:10.1016/j.chom.2010.11.007.

Broz, P., T. Ruby, K. Belhocine, D. M. Bouley, N. Kayagaki, V. M. Dixit, and D. M. Monack. 2012. Caspase-11 increases susceptibility to Salmonella infection in the absence of caspase-1. *Nature* 490(7419):288–291. doi:10.1038/nature11419.

Brubaker, S. W., K. S. Bonham, I. Zanoni, and J. C. Kagan. 2015. Innate immune pattern recognition: a cell biological perspective. *Annual review of immunology* 33:257–290. doi:10.1146/annurev-immunol-032414-112240.

Brubaker, S. W., S. M. Brewer, L. M. Massis, B. A. Napier, and D. M. Monack. 2020. A Rapid Caspase-11 Response Induced by IFNγ Priming Is Independent of Guanylate Binding Proteins. *iScience* 23(10):101612. doi:10.1016/j.isci.2020.101612.

Bruns, T., H. W. Zimmermann, and A. Stallmach. 2014. Risk factors and outcome of bacterial infections in cirrhosis. *World journal of gastroenterology* 20(10):2542–2554. doi:10.3748/wjg.v20.i10.2542.

Burns, K., S. Janssens, B. Brissoni, N. Olivos, R. Beyaert, and J. Tschopp. 2003. Inhibition of interleukin 1 receptor/Toll-like receptor signaling through the alternatively spliced, short form of MyD88 is due to its failure to recruit IRAK-4. *The Journal of experimental medicine* 197(2):263–268. doi:10.1084/jem.20021790.

Carson, W. F., K. A. Cavassani, Y. Dou, and S. L. Kunkel. 2011. Epigenetic regulation of immune cell functions during post-septic immunosuppression. *Epigenetics* 6(3):273–283. doi:10.4161/epi.6.3.14017.

Casrouge, A., S.-Y. Zhang, C. Eidenschenk, E. Jouanguy, A. Puel, K. Yang, A. Alcais, C. Picard, N. Mahfoufi, N. Nicolas, L. Lorenzo, S. Plancoulaine, B. Sénéchal, F. Geissmann, K. Tabeta, K. Hoebe, X. Du, R. L. Miller, B. Héron, C. Mignot, T. B. de Villemeur, P. Lebon, O. Dulac, F. Rozenberg, B. Beutler, M. Tardieu, L. Abel, and J.-L. Casanova. 2006. Herpes simplex virus encephalitis in human UNC-93B deficiency. *Science (New York, N.Y.)* 314(5797):308–312. doi:10.1126/science.1128346.

Casson, C. N., J. Yu, V. M. Reyes, F. O. Taschuk, A. Yadav, A. M. Copenhaver, H. T. Nguyen, R. G. Collman, and S. Shin. 2015. Human caspase-4 mediates noncanonical inflammasome activation against gram-negative bacterial pathogens. *Proceedings of the National Academy of Sciences of the United States of America* 112(21):6688–6693. doi:10.1073/pnas.1421699112.

Chae, J. J., Y.-H. Cho, G.-S. Lee, J. Cheng, P. P. Liu, L. Feigenbaum, S. I. Katz, and D. L. Kastner. 2011. Gain-of-function Pyrin mutations induce NLRP3 protein-independent interleukin-1β activation and severe autoinflammation in mice. *Immunity* 34(5):755–768. doi:10.1016/j.immuni.2011.02.020.

Chae, J. J., Y. H. Park, C. Park, I.-Y. Hwang, P. Hoffmann, J. H. Kehrl, I. Aksentijevich, and D. L. Kastner. 2015. Connecting two pathways through Ca 2+ signaling: NLRP3 inflammasome activation induced by a hypermorphic PLCG2 mutation. *Arthritis & rheumatology (Hoboken, N.J.)* 67(2):563–567. doi:10.1002/art.38961.

Chang, C. H., J. Hammer, J. E. Loh, W. L. Fodor, and R. A. Flavell. 1992. The activation of major histocompatibility complex class I genes by interferon regulatory factor-1 (IRF-1). *Immunogenetics* 35(6):378–384. doi:10.1007/BF00179793.

Chaplin, D. D. 2010. Overview of the immune response. *The Journal of allergy and clinical immunology* 125(2 Suppl 2):S3-23. doi:10.1016/j.jaci.2009.12.980.

Chen, J., and Z. J. Chen. 2018. PtdIns4P on dispersed trans-Golgi network mediates NLRP3 inflammasome activation. *Nature* 564(7734):71–76. doi:10.1038/s41586-018-0761-3.

Chen, J., and L. B. Ivashkiv. 2010. IFN-γ abrogates endotoxin tolerance by facilitating Toll-like receptor-induced chromatin remodeling. *Proceedings of the National Academy of Sciences of the United States of America* 107(45):19438–19443. doi:10.1073/pnas.1007816107.

Chen, K. W., B. Demarco, and P. Broz. 2020. Beyond inflammasomes: emerging function of gasdermins during apoptosis and NETosis. *The EMBO journal* 39(2):e103397. doi:10.15252/embj.2019103397.

Christgen, S., D. E. Place, and T.-D. Kanneganti. 2020. Toward targeting inflammasomes: insights into their regulation and activation. *Cell research* 30(4):315–327. doi:10.1038/s41422-020-0295-8.

Chu, L. H., M. Indramohan, R. A. Ratsimandresey, A. Gangopadhyay, E. P. Morris, D. M. Monack, A. Dorfleutner, and C. Stehlik. 2018. The oxidized phospholipid oxPAPC protects from septic shock by targeting the non-canonical inflammasome in macrophages. *Nature communications* 9(1):996. doi:10.1038/s41467-018-03409-3.

Coll, R. C., A. A. B. Robertson, J. J. Chae, S. C. Higgins, R. Muñoz-Planillo, M. C. Inserra, I. Vetter, L. S. Dungan, B. G. Monks, A. Stutz, D. E. Croker, M. S. Butler, M. Haneklaus, C. E. Sutton, G. Núñez, E. Latz, D. L. Kastner, K. H. G. Mills, S. L. Masters, K. Schroder, M. A. Cooper, and L. A. J. O'Neill. 2015. A small-molecule inhibitor of the NLRP3 inflammasome for the treatment of inflammatory diseases. *Nature medicine* 21(3):248–255. doi:10.1038/nm.3806.

Cornut, M., E. Bourdonnay, and T. Henry. 2020. Transcriptional Regulation of Inflammasomes. *International journal of molecular sciences* 21(21). doi:10.3390/ijms21218087.

Cuesta, N., C. A. Salkowski, K. E. Thomas, and S. N. Vogel. 2003. Regulation of lipopolysaccharide sensitivity by IFN regulatory factor-2. *Journal of immunology (Baltimore, Md. 1950)* 170(11):5739–5747. doi:10.4049/jimmunol.170.11.5739.

Deaton, A. M., and A. Bird. 2011. CpG islands and the regulation of transcription. *Genes & development* 25(10):1010–1022. doi:10.1101/gad.2037511.

Deguine, J., and G. M. Barton. 2014. MyD88: a central player in innate immune signaling. *F1000prime reports* 6:97. doi:10.12703/P6-97.

Deng, M., Y. Tang, W. Li, X. Wang, R. Zhang, X. Zhang, X. Zhao, J. Liu, C. Tang, Z. Liu, Y. Huang, H. Peng, L. Xiao, D. Tang, M. J. Scott, Q. Wang, J. Liu, X. Xiao, S. Watkins, J. Li, H. Yang, H. Wang, F. Chen, K. J. Tracey, T. R. Billiar, and B. Lu. 2018. The Endotoxin Delivery Protein HMGB1 Mediates Caspase-11-Dependent Lethality in Sepsis. *Immunity* 49(4):740-753.e7. doi:10.1016/j.immuni.2018.08.016.

Deshmukh, S. D., B. Kremer, M. Freudenberg, S. Bauer, D. T. Golenbock, and P. Henneke. 2011. Macrophages recognize streptococci through bacterial single-stranded RNA. *EMBO reports* 12(1):71–76. doi:10.1038/embor.2010.189.

Deutsch, M., S. Manolakopoulos, I. Andreadis, M. Giannaris, G. Kontos, H. Kranidioti, M. Pirounaki, and J. Koskinas. 2018. Bacterial infections in patients with liver cirrhosis: clinical characteristics and the role of C-reactive protein. *Annals of gastroenterology* 31(1):77–83. doi:10.20524/aog.2017.0207.

Dick, M. S., L. Sborgi, S. Rühl, S. Hiller, and P. Broz. 2016. ASC filament formation serves as a signal amplification mechanism for inflammasomes. *Nature communications* 7:11929. doi:10.1038/ncomms11929.

Ding, J., K. Wang, W. Liu, Y. She, Q. Sun, J. Shi, H. Sun, D.-C. Wang, and F. Shao. 2016. Pore-forming activity and structural autoinhibition of the gasdermin family. *Nature* 535(7610):111–116. doi:10.1038/nature18590.

Döcke, W. D., F. Randow, U. Syrbe, D. Krausch, K. Asadullah, P. Reinke, H. D. Volk, and W. Kox. 1997. Monocyte deactivation in septic patients: restoration by IFN-gamma treatment. *Nature medicine* 3(6):678–681. doi:10.1038/nm0697-678.

Dubois, H., A. Wullaert, and M. Lamkanfi. 2016. General Strategies in Inflammasome Biology. *Current topics in microbiology and immunology* 397:1–22. doi:10.1007/978-3-319-41171-2_1.

Duduskar, S. N., M. Ghait, M. Zimmermann, A. Ramoji, B. Göhrig, M. Rooney, C. Sponholz, J. Popp, U. Neugebauer, Beemelmanns Christin, Guo H, B. Löffler, M. Singer, M. Bauer, and S. D. Deshmukh. 2019. Cytosolic innate immune pathway activation by Gram-positivebacteria during sepsis: "9th International Congress "Sepsis and Multiorgan Dysfunction". *Infection* 47(Suppl 1):1–67. doi:10.1007/s15010-019-01341-2.

Dutta, D., S. Dutta, M. V. Veettil, A. Roy, M. A. Ansari, J. Iqbal, L. Chikoti, B. Kumar, K. E. Johnson, and B. Chandran. 2015. BRCA1 Regulates IFI16 Mediated Nuclear Innate Sensing of Herpes Viral

DNA and Subsequent Induction of the Innate Inflammasome and Interferon-β Responses. *PLoS pathogens* 11(6):e1005030. doi:10.1371/journal.ppat.1005030.

Elinav, E., T. Strowig, A. L. Kau, J. Henao-Mejia, C. A. Thaiss, C. J. Booth, D. R. Peaper, J. Bertin, S. C. Eisenbarth, J. I. Gordon, and R. A. Flavell. 2011. NLRP6 inflammasome regulates colonic microbial ecology and risk for colitis. *Cell* 145(5):745–757. doi:10.1016/j.cell.2011.04.022.

Elliott, E. I., A. N. Miller, B. Banoth, S. S. Iyer, A. Stotland, J. P. Weiss, R. A. Gottlieb, F. S. Sutterwala, and S. L. Cassel. 2018. Cutting Edge: Mitochondrial Assembly of the NLRP3 Inflammasome Complex Is Initiated at Priming. *Journal of immunology (Baltimore, Md. 1950)* 200(9):3047–3052. doi:10.4049/jimmunol.1701723.

Endo, M., M. Mori, S. Akira, and T. Gotoh. 2006. C/EBP homologous protein (CHOP) is crucial for the induction of caspase-11 and the pathogenesis of lipopolysaccharide-induced inflammation. *Journal of immunology (Baltimore, Md. 1950)* 176(10):6245–6253. doi:10.4049/jimmunol.176.10.6245.

Esquerdo, K. F., N. K. Sharma, M. K. C. Brunialti, G. L. Baggio-Zappia, M. Assunção, L. C. P. Azevedo, A. T. Bafi, and R. Salomao. 2017. Inflammasome gene profile is modulated in septic patients, with a greater magnitude in non-survivors. *Clinical and Experimental Immunology* 189(2):232–240. doi:10.1111/cei.12971.

Feerick, C. L., and D. P. McKernan. 2017. Understanding the regulation of pattern recognition receptors in inflammatory diseases - a 'Nod' in the right direction. *Immunology* 150(3):237–247. doi:10.1111/imm.12677.

Fernandes-Alnemri, T., S. Kang, C. Anderson, J. Sagara, K. A. Fitzgerald, and E. S. Alnemri. 2013. Cutting edge: TLR signaling licenses IRAK1 for rapid activation of the NLRP3 inflammasome. *Journal of immunology (Baltimore, Md. 1950)* 191(8):3995–3999. doi:10.4049/jimmunol.1301681.

Fernandes-Alnemri, T., J. Wu, J.-W. Yu, P. Datta, B. Miller, W. Jankowski, S. Rosenberg, J. Zhang, and E. S. Alnemri. 2007. The pyroptosome: a supramolecular assembly of ASC dimers mediating inflammatory cell death via caspase-1 activation. *Cell death and differentiation* 14(9):1590–1604. doi:10.1038/sj.cdd.4402194.

Fernandes-Alnemri, T., J.-W. Yu, P. Datta, J. Wu, and E. S. Alnemri. 2009. AIM2 activates the inflammasome and cell death in response to cytoplasmic DNA. *Nature* 458(7237):509–513. doi:10.1038/nature07710.

Finethy, R., I. Jorgensen, A. K. Haldar, M. R. de Zoete, T. Strowig, R. A. Flavell, M. Yamamoto, U. M. Nagarajan, E. A. Miao, and J. Coers. 2015. Guanylate binding proteins enable rapid activation of canonical and noncanonical inflammasomes in Chlamydia-infected macrophages. *Infection and immunity* 83(12):4740–4749. doi:10.1128/IAI.00856-15.

Fisch, D., H. Bando, B. Clough, V. Hornung, M. Yamamoto, A. R. Shenoy, and E.-M. Frickel. 2019. Human GBP1 is a microbe-specific gatekeeper of macrophage apoptosis and pyroptosis. *The EMBO journal* 38(13):e100926. doi:10.15252/embj.2018100926.

Fisch, D., B. Clough, M.-C. Domart, V. Encheva, H. Bando, A. P. Snijders, L. M. Collinson, M. Yamamoto, A. R. Shenoy, and E.-M. Frickel. 2020. Human GBP1 Differentially Targets Salmonella and Toxoplasma to License Recognition of Microbial Ligands and Caspase-Mediated Death. *Cell reports* 32(6):108008. doi:10.1016/j.celrep.2020.108008.

Fitzgerald, K. A., and J. C. Kagan. 2020. Toll-like Receptors and the Control of Immunity. *Cell* 180(6):1044–1066. doi:10.1016/j.cell.2020.02.041.

Fitzgerald, K. A., E. M. Palsson-McDermott, A. G. Bowie, C. A. Jefferies, A. S. Mansell, G. Brady, E. Brint, A. Dunne, P. Gray, M. T. Harte, D. McMurray, D. E. Smith, J. E. Sims, T. A. Bird, and L. A. O'Neill. 2001. Mal (MyD88-adapter-like) is required for Toll-like receptor-4 signal transduction. *Nature* 413(6851):78–83. doi:10.1038/35092578.

Foster, S. L., D. C. Hargreaves, and R. Medzhitov. 2007. Gene-specific control of inflammation by TLR-induced chromatin modifications. *Nature* 447(7147):972–978. doi:10.1038/nature05836.

Franceschini, A., M. Capece, P. Chiozzi, S. Falzoni, J. M. Sanz, A. C. Sarti, M. Bonora, P. Pinton, and F. Di Virgilio. 2015. The P2X7 receptor directly interacts with the NLRP3 inflammasome scaffold

protein. *FASEB journal official publication of the Federation of American Societies for Experimental Biology* 29(6):2450–2461. doi:10.1096/fj.14-268714.

Franchi, L., A. Amer, M. Body-Malapel, T.-D. Kanneganti, N. Ozören, R. Jagirdar, N. Inohara, P. Vandenabeele, J. Bertin, A. Coyle, E. P. Grant, and G. Núñez. 2006. Cytosolic flagellin requires Ipaf for activation of caspase-1 and interleukin 1beta in salmonella-infected macrophages. *Nature immunology* 7(6):576–582. doi:10.1038/ni1346.

Franchi, L., T. Eigenbrod, R. Muñoz-Planillo, and G. Nuñez. 2009. The inflammasome: a caspase-1-activation platform that regulates immune responses and disease pathogenesis. *Nature immunology* 10(3):241–247. doi:10.1038/ni.1703.

Franchi, L., T.-D. Kanneganti, G. R. Dubyak, and G. Núñez. 2007. Differential requirement of P2X7 receptor and intracellular K+ for caspase-1 activation induced by intracellular and extracellular bacteria. *The Journal of biological chemistry* 282(26):18810–18818. doi:10.1074/jbc.M610762200.

Franchi, L., R. Muñoz-Planillo, and G. Núñez. 2012. Sensing and reacting to microbes through the inflammasomes. *Nature immunology* 13(4):325–332. doi:10.1038/ni.2231.

Franklin, B. S., L. Bossaller, D. de Nardo, J. M. Ratter, A. Stutz, G. Engels, C. Brenker, M. Nordhoff, S. R. Mirandola, A. Al-Amoudi, M. S. Mangan, S. Zimmer, B. G. Monks, M. Fricke, R. E. Schmidt, T. Espevik, B. Jones, A. G. Jarnicki, P. M. Hansbro, P. Busto, A. Marshak-Rothstein, S. Hornemann, A. Aguzzi, W. Kastenmüller, and E. Latz. 2014. The adaptor ASC has extracellular and 'prionoid' activities that propagate inflammation. *Nature immunology* 15(8):727–737. doi:10.1038/ni.2913.

Fukui, R., S. Saitoh, F. Matsumoto, H. Kozuka-Hata, M. Oyama, K. Tabeta, B. Beutler, and K. Miyake. 2009. Unc93B1 biases Toll-like receptor responses to nucleic acid in dendritic cells toward DNA- but against RNA-sensing. *The Journal of experimental medicine* 206(6):1339–1350. doi:10.1084/jem.20082316.

Fulde, M., F. Sommer, B. Chassaing, K. van Vorst, A. Dupont, M. Hensel, M. Basic, R. Klopfleisch, P. Rosenstiel, A. Bleich, F. Bäckhed, A. T. Gewirtz, and M. W. Hornef. 2018. Neonatal selection by Toll-like receptor 5 influences long-term gut microbiota composition. *Nature* 560(7719):489–493. doi:10.1038/s41586-018-0395-5.

Gaidt, M. M., T. S. Ebert, D. Chauhan, K. Ramshorn, F. Pinci, S. Zuber, F. O'Duill, J. L. Schmid-Burgk, F. Hoss, R. Buhmann, G. Wittmann, E. Latz, M. Subklewe, and V. Hornung. 2017. The DNA Inflammasome in Human Myeloid Cells Is Initiated by a STING-Cell Death Program Upstream of NLRP3. *Cell* 171(5):1110-1124.e18. doi:10.1016/j.cell.2017.09.039.

Gaidt, M. M., T. S. Ebert, D. Chauhan, T. Schmidt, J. L. Schmid-Burgk, F. Rapino, A. A. B. Robertson, M. A. Cooper, T. Graf, and V. Hornung. 2016. Human Monocytes Engage an Alternative Inflammasome Pathway. *Immunity* 44(4):833–846. doi:10.1016/j.immuni.2016.01.012.

Galisteo, M. L., J. Chernoff, Y. C. Su, E. Y. Skolnik, and J. Schlessinger. 1996. The adaptor protein Nck links receptor tyrosine kinases with the serine-threonine kinase Pak1. *The Journal of biological chemistry* 271(35):20997–21000. doi:10.1074/jbc.271.35.20997.

Garcia-Tsao, G. 2018. Acute-on-Chronic Liver Failure: An Old Entity in Search of Clarity. *Hepatology communications* 2(12):1421–1424. doi:10.1002/hep4.1287.

Gay, N. J., M. Gangloff, and L. A. J. O'Neill. 2011. What the Myddosome structure tells us about the initiation of innate immunity. *Trends in immunology* 32(3):104–109. doi:10.1016/j.it.2010.12.005.

Geiger, T., A. Velic, B. Macek, E. Lundberg, C. Kampf, N. Nagaraj, M. Uhlen, J. Cox, and M. Mann. 2013. Initial quantitative proteomic map of 28 mouse tissues using the SILAC mouse. *Molecular & cellular proteomics MCP* 12(6):1709–1722. doi:10.1074/mcp.M112.024919.

Göös, H., C. L. Fogarty, B. Sahu, V. Plagnol, K. Rajamäki, K. Nurmi, X. Liu, E. Einarsdottir, A. Jouppila, T. Pettersson, H. Vihinen, K. Krjutskov, P. Saavalainen, A. Järvinen, M. Muurinen, D. Greco, G. Scala, J. Curtis, D. Nordström, R. Flaumenhaft, O. Vaarala, P. E. Kovanen, S. Keskitalo, A. Ranki, J. Kere, M. Lehto, L. D. Notarangelo, S. Nejentsev, K. K. Eklund, M. Varjosalo, J. Taipale, and M. R. J. Seppänen. 2019. Gain-of-function CEBPE mutation causes noncanonical

autoinflammatory inflammasomopathy. *The Journal of allergy and clinical immunology* 144(5):1364–1376. doi:10.1016/j.jaci.2019.06.003.

Greten, F. R., M. C. Arkan, J. Bollrath, L.-C. Hsu, J. Goode, C. Miething, S. I. Göktuna, M. Neuenhahn, J. Fierer, S. Paxian, N. van Rooijen, Y. Xu, T. O'Cain, B. B. Jaffee, D. H. Busch, J. Duyster, R. M. Schmid, L. Eckmann, and M. Karin. 2007. NF-kappaB is a negative regulator of IL-1beta secretion as revealed by genetic and pharmacological inhibition of IKKbeta. *Cell* 130(5):918–931. doi:10.1016/j.cell.2007.07.009.

Greulich, W., M. Wagner, M. M. Gaidt, C. Stafford, Y. Cheng, A. Linder, T. Carell, and V. Hornung. 2019. TLR8 Is a Sensor of RNase T2 Degradation Products. *Cell* 179(6):1264-1275.e13. doi:10.1016/j.cell.2019.11.001.

Groslambert, M., and B. F. Py. 2018. Spotlight on the NLRP3 inflammasome pathway. *Journal of inflammation research* 11:359–374. doi:10.2147/JIR.S141220.

Guarda, G., M. Braun, F. Staehli, A. Tardivel, C. Mattmann, I. Förster, M. Farlik, T. Decker, R. A. Du Pasquier, P. Romero, and J. Tschopp. 2011. Type I interferon inhibits interleukin-1 production and inflammasome activation. *Immunity* 34(2):213–223. doi:10.1016/j.immuni.2011.02.006.

Günther, S. D., M. Fritsch, J. M. Seeger, L. M. Schiffmann, S. J. Snipas, M. Coutelle, T. A. Kufer, P. G. Higgins, V. Hornung, M. L. Bernardini, S. Höning, M. Krönke, G. S. Salvesen, and H. Kashkar. 2020. Cytosolic Gram-negative bacteria prevent apoptosis by inhibition of effector caspases through lipopolysaccharide. *Nature microbiology* 5(2):354–367. doi:10.1038/s41564-019-0620-5.

Guo, C., S. Xie, Z. Chi, J. Zhang, Y. Liu, L. Zhang, M. Zheng, X. Zhang, D. Xia, Y. Ke, L. Lu, and Di Wang. 2016. Bile Acids Control Inflammation and Metabolic Disorder through Inhibition of NLRP3 Inflammasome. *Immunity* 45(4):802–816. doi:10.1016/j.immuni.2016.09.008.

Gurung, P., B. Li, R. K. Subbarao Malireddi, M. Lamkanfi, T. L. Geiger, and T.-D. Kanneganti. 2015. Chronic TLR Stimulation Controls NLRP3 Inflammasome Activation through IL-10 Mediated Regulation of NLRP3 Expression and Caspase-8 Activation. *Scientific reports* 5:14488. doi:10.1038/srep14488.

Gurung, P., R. K. S. Malireddi, P. K. Anand, D. Demon, L. Vande Walle, Z. Liu, P. Vogel, M. Lamkanfi, and T.-D. Kanneganti. 2012. Toll or interleukin-1 receptor (TIR) domain-containing adaptor inducing interferon-β (TRIF)-mediated caspase-11 protease production integrates Toll-like receptor 4 (TLR4) protein- and Nlrp3 inflammasome-mediated host defense against enteropathogens. *The Journal of biological chemistry* 287(41):34474–34483. doi:10.1074/jbc.M112.401406.

Hagar, J. A., D. A. Powell, Y. Aachoui, R. K. Ernst, and E. A. Miao. 2013. Cytoplasmic LPS activates caspase-11: implications in TLR4-independent endotoxic shock. *Science (New York, N.Y.)* 341(6151):1250–1253. doi:10.1126/science.1240988.

Halff, E. F., C. A. Diebolder, M. Versteeg, A. Schouten, T. H. C. Brondijk, and E. G. Huizinga. 2012. Formation and structure of a NAIP5-NLRC4 inflammasome induced by direct interactions with conserved N- and C-terminal regions of flagellin. *The Journal of biological chemistry* 287(46):38460–38472. doi:10.1074/jbc.M112.393512.

Hara, H., S. S. Seregin, D. Yang, K. Fukase, M. Chamaillard, E. S. Alnemri, N. Inohara, G. Y. Chen, and G. Núñez. 2018. The NLRP6 Inflammasome Recognizes Lipoteichoic Acid and Regulates Gram-Positive Pathogen Infection. *Cell* 175(6):1651-1664.e14. doi:10.1016/j.cell.2018.09.047.

Hara, H., K. Tsuchiya, I. Kawamura, R. Fang, E. Hernandez-Cuellar, Y. Shen, J. Mizuguchi, E. Schweighoffer, V. Tybulewicz, and M. Mitsuyama. 2013. Phosphorylation of the adaptor ASC acts as a molecular switch that controls the formation of speck-like aggregates and inflammasome activity. *Nature immunology* 14(12):1247–1255. doi:10.1038/ni.2749.

Harms, F. L., K. Kloth, A. Bley, J. Denecke, R. Santer, D. Lessel, M. Hempel, and K. Kutsche. 2018. Activating Mutations in PAK1, Encoding p21-Activated Kinase 1, Cause a Neurodevelopmental Disorder. *American journal of human genetics* 103(4):579–591. doi:10.1016/j.ajhg.2018.09.005.

Harris, J., T. Lang, J. P. W. Thomas, M. B. Sukkar, N. R. Nabar, and J. H. Kehrl. 2017. Autophagy and inflammasomes. *Molecular immunology* 86:10–15. doi:10.1016/j.molimm.2017.02.013.

He, W., H. Wan, L. Hu, P. Chen, X. Wang, Z. Huang, Z.-H. Yang, C.-Q. Zhong, and J. Han. 2015. Gasdermin D is an executor of pyroptosis and required for interleukin-1β secretion. *Cell research* 25(12):1285–1298. doi:10.1038/cr.2015.139.

He, Y., M. Y. Zeng, D. Yang, B. Motro, and G. Núñez. 2016. NEK7 is an essential mediator of NLRP3 activation downstream of potassium efflux. *Nature* 530(7590):354–357. doi:10.1038/nature16959.

Heneka, M. T., R. M. McManus, and E. Latz. 2018. Inflammasome signalling in brain function and neurodegenerative disease. *Nature reviews. Neuroscience* 19(10):610–621. doi:10.1038/s41583-018-0055-7.

Hirate, Y., and H. Okamoto. 2006. Canopy1, a novel regulator of FGF signaling around the midbrain-hindbrain boundary in zebrafish. *Current biology CB* 16(4):421–427. doi:10.1016/j.cub.2006.01.055.

Hobart, M., V. Ramassar, N. Goes, J. Urmson, and P. F. Halloran. 1996. The induction of class I and II major histocompatibility complex by allogeneic stimulation is dependent on the transcription factor interferon regulatory factor 1 (IRF-1): observations in IRF-1 knockout mice. *Transplantation* 62(12):1895–1901. doi:10.1097/00007890-199612270-00037.

Horng, T., G. M. Barton, R. A. Flavell, and R. Medzhitov. 2002. The adaptor molecule TIRAP provides signalling specificity for Toll-like receptors. *Nature* 420(6913):329–333. doi:10.1038/nature01180.

Hornung, V., A. Ablasser, M. Charrel-Dennis, F. Bauernfeind, G. Horvath, D. R. Caffrey, E. Latz, and K. A. Fitzgerald. 2009. AIM2 recognizes cytosolic dsDNA and forms a caspase-1-activating inflammasome with ASC. *Nature* 458(7237):514–518. doi:10.1038/nature07725.

Hornung, V., F. Bauernfeind, A. Halle, E. O. Samstad, H. Kono, K. L. Rock, K. A. Fitzgerald, and E. Latz. 2008. Silica crystals and aluminum salts activate the NALP3 inflammasome through phagosomal destabilization. *Nature immunology* 9(8):847–856. doi:10.1038/ni.1631.

Hornung, V., R. Hartmann, A. Ablasser, and K.-P. Hopfner. 2014. OAS proteins and cGAS: unifying concepts in sensing and responding to cytosolic nucleic acids. *Nature reviews. Immunology* 14(8):521–528. doi:10.1038/nri3719.

Hoss, F., J. F. Rodriguez-Alcazar, and E. Latz. 2017. Assembly and regulation of ASC specks. *Cellular and molecular life sciences CMLS* 74(7):1211–1229. doi:10.1007/s00018-016-2396-6.

Hotchkiss, R. S., G. Monneret, and D. Payen. 2013. Immunosuppression in sepsis: a novel understanding of the disorder and a new therapeutic approach. *The Lancet infectious diseases* 13(3):260–268. doi:10.1016/S1473-3099(13)70001-X.

Hu, Z., Q. Zhou, C. Zhang, S. Fan, W. Cheng, Y. Zhao, F. Shao, H.-W. Wang, S.-F. Sui, and J. Chai. 2015. Structural and biochemical basis for induced self-propagation of NLRC4. *Science (New York, N.Y.)* 350(6259):399–404. doi:10.1126/science.aac5489.

Huh, J.-W., T. Shibata, M. Hwang, E.-H. Kwon, M. S. Jang, R. Fukui, A. Kanno, D.-J. Jung, M. H. Jang, K. Miyake, and Y.-M. Kim. 2014. UNC93B1 is essential for the plasma membrane localization and signaling of Toll-like receptor 5. *Proceedings of the National Academy of Sciences of the United States of America* 111(19):7072–7077. doi:10.1073/pnas.1322838111.

Humphries, F., L. Shmuel-Galia, N. Ketelut-Carneiro, S. Li, B. Wang, V. V. Nemmara, R. Wilson, Z. Jiang, F. Khalighinejad, K. Muneeruddin, S. A. Shaffer, R. Dutta, C. Ionete, S. Pesiridis, S. Yang, P. R. Thompson, and K. A. Fitzgerald. 2020. Succination inactivates gasdermin D and blocks pyroptosis. *Science (New York, N.Y.)* 369(6511):1633–1637. doi:10.1126/science.abb9818.

Iwasaki, A., and R. Medzhitov. 2010. Regulation of adaptive immunity by the innate immune system. *Science (New York, N.Y.)* 327(5963):291–295. doi:10.1126/science.1183021.

Iwasaki, A., and R. Medzhitov. 2015. Control of adaptive immunity by the innate immune system. *Nature immunology* 16(4):343–353. doi:10.1038/ni.3123.

Iyer, S. S., Q. He, J. R. Janczy, E. I. Elliott, Z. Zhong, A. K. Olivier, J. J. Sadler, V. Knepper-Adrian, R. Han, L. Qiao, S. C. Eisenbarth, W. M. Nauseef, S. L. Cassel, and F. S. Sutterwala. 2013.

Mitochondrial cardiolipin is required for Nlrp3 inflammasome activation. *Immunity* 39(2):311–323. doi:10.1016/j.immuni.2013.08.001.

Jaenisch, R., and A. Bird. 2003. Epigenetic regulation of gene expression: how the genome integrates intrinsic and environmental signals. *Nature genetics* 33 Suppl:245–254. doi:10.1038/ng1089.

Jin, M. S., and J.-O. Lee. 2008. Structures of the toll-like receptor family and its ligand complexes. *Immunity* 29(2):182–191. doi:10.1016/j.immuni.2008.07.007.

Jin, T., A. Perry, P. Smith, J. Jiang, and T. S. Xiao. 2013. Structure of the absent in melanoma 2 (AIM2) pyrin domain provides insights into the mechanisms of AIM2 autoinhibition and inflammasome assembly. *The Journal of biological chemistry* 288(19):13225–13235. doi:10.1074/jbc.M113.468033.

Jinek, M., K. Chylinski, I. Fonfara, M. Hauer, J. A. Doudna, and E. Charpentier. 2012. A programmable dual-RNA-guided DNA endonuclease in adaptive bacterial immunity. *Science (New York, N.Y.)* 337(6096):816–821. doi:10.1126/science.1225829.

Jonas, S., and E. Izaurralde. 2015. Towards a molecular understanding of microRNA-mediated gene silencing. *Nature reviews. Genetics* 16(7):421–433. doi:10.1038/nrg3965.

Jorgensen, I., M. Rayamajhi, and E. A. Miao. 2017. Programmed cell death as a defence against infection. *Nature reviews. Immunology* 17(3):151–164. doi:10.1038/nri.2016.147.

Juliana, C., T. Fernandes-Alnemri, S. Kang, A. Farias, F. Qin, and E. S. Alnemri. 2012. Non-transcriptional priming and deubiquitination regulate NLRP3 inflammasome activation. *The Journal of biological chemistry* 287(43):36617–36622. doi:10.1074/jbc.M112.407130.

Kagan, J. C., V. G. Magupalli, and H. Wu. 2014. SMOCs: supramolecular organizing centres that control innate immunity. *Nature reviews. Immunology* 14(12):821–826. doi:10.1038/nri3757.

Kagan, J. C., T. Su, T. Horng, A. Chow, S. Akira, and R. Medzhitov. 2008. TRAM couples endocytosis of Toll-like receptor 4 to the induction of interferon-beta. *Nature immunology* 9(4):361–368. doi:10.1038/ni1569.

Kajiwara, Y., T. Schiff, G. Voloudakis, M. A. Gama Sosa, G. Elder, O. Bozdagi, and J. D. Buxbaum. 2014. A critical role for human caspase-4 in endotoxin sensitivity. *Journal of immunology (Baltimore, Md. 1950)* 193(1):335–343. doi:10.4049/jimmunol.1303424.

Kang, K., M. Bachu, S. H. Park, K. Kang, S. Bae, K.-H. Park-Min, and L. B. Ivashkiv. 2019. IFN-γ selectively suppresses a subset of TLR4-activated genes and enhancers to potentiate macrophage activation. *Nature communications* 10(1):3320. doi:10.1038/s41467-019-11147-3.

Kanneganti, T.-D. 2019. Regulators of Inflammatory Responses. doi:10.1096/fasebj.2019.33.1_supplement.218.2.

Kanneganti, T.-D., and M. Lamkanfi. 2013. K^+ drops tilt the NLRP3 inflammasome. *Immunity* 38(6):1085–1088. doi:10.1016/j.immuni.2013.06.001.

Karaghiosoff, M., R. Steinborn, P. Kovarik, G. Kriegshäuser, M. Baccarini, B. Donabauer, U. Reichart, T. Kolbe, C. Bogdan, T. Leanderson, D. Levy, T. Decker, and M. Müller. 2003. Central role for type I interferons and Tyk2 in lipopolysaccharide-induced endotoxin shock. *Nature immunology* 4(5):471–477. doi:10.1038/ni910.

Karki, R., E. Lee, D. Place, P. Samir, J. Mavuluri, B. R. Sharma, A. Balakrishnan, R. K. S. Malireddi, R. Geiger, Q. Zhu, G. Neale, and T.-D. Kanneganti. 2018. IRF8 Regulates Transcription of Naips for NLRC4 Inflammasome Activation. *Cell* 173(4):920-933.e13. doi:10.1016/j.cell.2018.02.055.

Kastner, D. L., I. Aksentijevich, and R. Goldbach-Mansky. 2010. Autoinflammatory disease reloaded: a clinical perspective. *Cell* 140(6):784–790. doi:10.1016/j.cell.2010.03.002.

Kawai, T., and S. Akira. 2011. Toll-like receptors and their crosstalk with other innate receptors in infection and immunity. *Immunity* 34(5):637–650. doi:10.1016/j.immuni.2011.05.006.

Kawai, T., O. Takeuchi, T. Fujita, J. Inoue, P. F. Mühlradt, S. Sato, K. Hoshino, and S. Akira. 2001. Lipopolysaccharide stimulates the MyD88-independent pathway and results in activation of IFN-

regulatory factor 3 and the expression of a subset of lipopolysaccharide-inducible genes. *Journal of immunology (Baltimore, Md. 1950)* 167(10):5887–5894. doi:10.4049/jimmunol.167.10.5887.

Kawasaki, T., and T. Kawai. 2014. Toll-like receptor signaling pathways. *Frontiers in immunology* 5:461. doi:10.3389/fimmu.2014.00461.

Kayagaki, N., B. L. Lee, I. B. Stowe, O. S. Kornfeld, K. O'Rourke, K. M. Mirrashidi, B. Haley, C. Watanabe, M. Roose-Girma, Z. Modrusan, S. Kummerfeld, R. Reja, Y. Zhang, V. Cho, T. D. Andrews, L. X. Morris, C. C. Goodnow, E. M. Bertram, and V. M. Dixit. 2019. IRF2 transcriptionally induces GSDMD expression for pyroptosis. *Science signaling* 12(582). doi:10.1126/scisignal.aax4917.

Kayagaki, N., I. B. Stowe, B. L. Lee, K. O'Rourke, K. Anderson, S. Warming, T. Cuellar, B. Haley, M. Roose-Girma, Q. T. Phung, P. S. Liu, J. R. Lill, H. Li, J. Wu, S. Kummerfeld, J. Zhang, W. P. Lee, S. J. Snipas, G. S. Salvesen, L. X. Morris, L. Fitzgerald, Y. Zhang, E. M. Bertram, C. C. Goodnow, and V. M. Dixit. 2015. Caspase-11 cleaves gasdermin D for non-canonical inflammasome signalling. *Nature* 526(7575):666–671. doi:10.1038/nature15541.

Kayagaki, N., S. Warming, M. Lamkanfi, L. Vande Walle, S. Louie, J. Dong, K. Newton, Y. Qu, J. Liu, S. Heldens, J. Zhang, W. P. Lee, M. Roose-Girma, and V. M. Dixit. 2011. Non-canonical inflammasome activation targets caspase-11. *Nature* 479(7371):117–121. doi:10.1038/nature10558.

Kayagaki, N., M. T. Wong, I. B. Stowe, S. R. Ramani, L. C. Gonzalez, S. Akashi-Takamura, K. Miyake, J. Zhang, W. P. Lee, A. Muszyński, L. S. Forsberg, R. W. Carlson, and V. M. Dixit. 2013. Noncanonical inflammasome activation by intracellular LPS independent of TLR4. *Science (New York, N.Y.)* 341(6151):1246–1249. doi:10.1126/science.1240248.

Keller, M., A. Rüegg, S. Werner, and H.-D. Beer. 2008. Active caspase-1 is a regulator of unconventional protein secretion. *Cell* 132(5):818–831. doi:10.1016/j.cell.2007.12.040.

Kelly, M. L., and J. Chernoff. 2012. Mouse models of PAK function. *Cellular logistics* 2(2):84–88. doi:10.4161/cl.21381.

Kerur, N., M. V. Veettil, N. Sharma-Walia, V. Bottero, S. Sadagopan, P. Otageri, and B. Chandran. 2011. IFI16 acts as a nuclear pathogen sensor to induce the inflammasome in response to Kaposi Sarcoma-associated herpesvirus infection. *Cell host & microbe* 9(5):363–375. doi:10.1016/j.chom.2011.04.008.

Kesavardhana, S., R. S. Malireddi, and T.-D. Kanneganti. 2020. Caspases in Cell Death, Inflammation, and Gasdermin-Induced Pyroptosis. *Annual review of immunology* 38:567–595. doi:10.1146/annurev-immunol-073119-095439.

Kieser, K. J., and J. C. Kagan. 2017. Multi-receptor detection of individual bacterial products by the innate immune system. *Nature reviews. Immunology* 17(6):376–390. doi:10.1038/nri.2017.25.

Kim, Y. E., M. S. Hipp, A. Bracher, M. Hayer-Hartl, and F. U. Hartl. 2013. Molecular chaperone functions in protein folding and proteostasis. *Annual review of biochemistry* 82:323–355. doi:10.1146/annurev-biochem-060208-092442.

Kim, Y.-M., M. M. Brinkmann, M.-E. Paquet, and H. L. Ploegh. 2008. UNC93B1 delivers nucleotide-sensing toll-like receptors to endolysosomes. *Nature* 452(7184):234–238. doi:10.1038/nature06726.

Kiyokawa, T., S. Akashi-Takamura, T. Shibata, F. Matsumoto, C. Nishitani, Y. Kuroki, Y. Seto, and K. Miyake. 2008. A single base mutation in the PRAT4A gene reveals differential interaction of PRAT4A with Toll-like receptors. *International immunology* 20(11):1407–1415. doi:10.1093/intimm/dxn098.

Kobayashi, K., L. D. Hernandez, J. E. Galán, C. A. Janeway, R. Medzhitov, and R. A. Flavell. 2002. IRAK-M is a negative regulator of Toll-like receptor signaling. *Cell* 110(2):191–202. doi:10.1016/s0092-8674(02)00827-9.

Kofoed, E. M., and R. E. Vance. 2011. Innate immune recognition of bacterial ligands by NAIPs determines inflammasome specificity. *Nature* 477(7366):592–595. doi:10.1038/nature10394.

Köhn, L., K. Kadzhaev, M. S. I. Burstedt, S. Haraldsson, B. Hallberg, O. Sandgren, and I. Golovleva. 2007. Mutation in the PYK2-binding domain of PITPNM3 causes autosomal dominant cone dystrophy (CORD5) in two Swedish families. *European journal of human genetics EJHG* 15(6):664–671. doi:10.1038/sj.ejhg.5201817.

Kujirai, T., C. Zierhut, Y. Takizawa, R. Kim, L. Negishi, N. Uruma, S. Hirai, H. Funabiki, and H. Kurumizaka. 2020. Structural basis for the inhibition of cGAS by nucleosomes. *Science (New York, N.Y.)* 370(6515):455–458. doi:10.1126/science.abd0237.

Kumar, V. 2018. Inflammasomes: Pandora's box for sepsis. *Journal of inflammation research* 11:477–502. doi:10.2147/JIR.S178084.

Kutsch, M., L. Sistemich, C. F. Lesser, M. B. Goldberg, C. Herrmann, and J. Coers. 2020. Direct binding of polymeric GBP1 to LPS disrupts bacterial cell envelope functions. *The EMBO journal* 39(13):e104926. doi:10.15252/embj.2020104926.

Lagrange, B., S. Benaoudia, P. Wallet, F. Magnotti, A. Provost, F. Michal, A. Martin, F. Di Lorenzo, B. F. Py, A. Molinaro, and T. Henry. 2018. Human caspase-4 detects tetra-acylated LPS and cytosolic Francisella and functions differently from murine caspase-11. *Nature communications* 9(1):242. doi:10.1038/s41467-017-02682-y.

Latz, E., T. S. Xiao, and A. Stutz. 2013. Activation and regulation of the inflammasomes. *Nature reviews. Immunology* 13(6):397–411. doi:10.1038/nri3452.

Lee, B. L., and G. M. Barton. 2014. Trafficking of endosomal Toll-like receptors. *Trends in cell biology* 24(6):360–369. doi:10.1016/j.tcb.2013.12.002.

Lee, D.-J., F. Du, S.-W. Chen, M. Nakasaki, I. Rana, V. F. S. Shih, A. Hoffmann, and C. Jamora. 2015. Regulation and Function of the Caspase-1 in an Inflammatory Microenvironment. *The Journal of investigative dermatology* 135(8):2012–2020. doi:10.1038/jid.2015.119.

Leentjens, J., M. Kox, R. M. Koch, F. Preijers, L. A. B. Joosten, J. G. van der Hoeven, M. G. Netea, and P. Pickkers. 2012. Reversal of immunoparalysis in humans in vivo: a double-blind, placebo-controlled, randomized pilot study. *American journal of respiratory and critical care medicine* 186(9):838–845. doi:10.1164/rccm.201204-0645OC.

Li, D., R. Wu, W. Guo, L. Xie, Z. Qiao, S. Chen, J. Zhu, C. Huang, J. Huang, B. Chen, Y. Qin, F. Xu, and F. Ma. 2019. STING-Mediated IFI16 Degradation Negatively Controls Type I Interferon Production. *Cell reports* 29(5):1249-1260.e4. doi:10.1016/j.celrep.2019.09.069.

Li, W., T. Cao, C. Luo, J. Cai, X. Zhou, X. Xiao, and S. Liu. 2020. Crosstalk between ER stress, NLRP3 inflammasome, and inflammation. *Applied microbiology and biotechnology* 104(14):6129–6140. doi:10.1007/s00253-020-10614-y.

Li, W., W. Zhang, M. Deng, P. Loughran, Y. Tang, H. Liao, X. Zhang, J. Liu, T. R. Billiar, and B. Lu. 2018. Stearoyl Lysophosphatidylcholine Inhibits Endotoxin-Induced Caspase-11 Activation. *Shock (Augusta, Ga.)* 50(3):339–345. doi:10.1097/SHK.0000000000001012.

Li, X., S. Thome, X. Ma, M. Amrute-Nayak, A. Finigan, L. Kitt, L. Masters, J. R. James, Y. Shi, G. Meng, and Z. Mallat. 2017. MARK4 regulates NLRP3 positioning and inflammasome activation through a microtubule-dependent mechanism. *Nature communications* 8:15986. doi:10.1038/ncomms15986.

Liehl, P., V. Zuzarte-Luis, and M. M. Mota. 2015. Unveiling the pathogen behind the vacuole. *Nature reviews. Microbiology* 13(9):589–598. doi:10.1038/nrmicro3504.

Lin, K.-M., W. Hu, T. D. Troutman, M. Jennings, T. Brewer, X. Li, S. Nanda, P. Cohen, J. A. Thomas, and C. Pasare. 2014. IRAK-1 bypasses priming and directly links TLRs to rapid NLRP3 inflammasome activation. *Proceedings of the National Academy of Sciences of the United States of America* 111(2):775–780. doi:10.1073/pnas.1320294111.

Lin, X. Y., M. S. Choi, and A. G. Porter. 2000. Expression analysis of the human caspase-1 subfamily reveals specific regulation of the CASP5 gene by lipopolysaccharide and interferon-gamma. *The Journal of biological chemistry* 275(51):39920–39926. doi:10.1074/jbc.M007255200.

Liston, A., and S. L. Masters. 2017. Homeostasis-altering molecular processes as mechanisms of inflammasome activation. *Nature reviews. Immunology* 17(3):208–214. doi:10.1038/nri.2016.151.

Liu, B., Y. Yang, Z. Qiu, M. Staron, F. Hong, Y. Li, S. Wu, Y. Li, B. Hao, R. Bona, D. Han, and Z. Li. 2010. Folding of Toll-like receptors by the HSP90 paralogue gp96 requires a substrate-specific cochaperone. *Nature communications* 1:79. doi:10.1038/ncomms1070.

Liu, J., and X. Cao. 2016. Cellular and molecular regulation of innate inflammatory responses. *Cellular & molecular immunology* 13(6):711–721. doi:10.1038/cmi.2016.58.

Liu, X., Z. Zhang, J. Ruan, Y. Pan, V. G. Magupalli, H. Wu, and J. Lieberman. 2016. Inflammasome-activated gasdermin D causes pyroptosis by forming membrane pores. *Nature* 535(7610):153–158. doi:10.1038/nature18629.

Lorey, M. B., K. Rossi, K. K. Eklund, T. A. Nyman, and S. Matikainen. 2017. Global Characterization of Protein Secretion from Human Macrophages Following Non-canonical Caspase-4/5 Inflammasome Activation. *Molecular & cellular proteomics MCP* 16(4 suppl 1):S187-S199. doi:10.1074/mcp.M116.064840.

Lu, L.-F., M. P. Boldin, A. Chaudhry, L.-L. Lin, K. D. Taganov, T. Hanada, A. Yoshimura, D. Baltimore, and A. Y. Rudensky. 2010. Function of miR-146a in controlling Treg cell-mediated regulation of Th1 responses. *Cell* 142(6):914–929. doi:10.1016/j.cell.2010.08.012.

Lukaszewicz, A.-C., M. Grienay, M. Resche-Rigon, R. Pirracchio, V. Faivre, B. Boval, and D. Payen. 2009. Monocytic HLA-DR expression in intensive care patients: interest for prognosis and secondary infection prediction. *Critical care medicine* 37(10):2746–2752. doi:10.1097/CCM.0b013e3181ab858a.

Lv, D.-W., K. Zhang, and R. Li. 2018. Interferon regulatory factor 8 regulates caspase-1 expression to facilitate Epstein-Barr virus reactivation in response to B cell receptor stimulation and chemical induction. *PLoS pathogens* 14(1):e1006868. doi:10.1371/journal.ppat.1006868.

Macario, A. J. L., and E. Conway de Macario. 2005. Sick chaperones, cellular stress, and disease. *The New England journal of medicine* 353(14):1489–1501. doi:10.1056/NEJMra050111.

Magupalli, V. G., R. Negro, Y. Tian, A. V. Hauenstein, G. Di Caprio, W. Skillern, Q. Deng, P. Orning, H. B. Alam, Z. Maliga, H. Sharif, J. J. Hu, C. L. Evavold, J. C. Kagan, F. I. Schmidt, K. A. Fitzgerald, T. Kirchhausen, Y. Li, and H. Wu. 2020. HDAC6 mediates an aggresome-like mechanism for NLRP3 and pyrin inflammasome activation. *Science (New York, N.Y.)* 369(6510). doi:10.1126/science.aas8995.

Majer, O., B. Liu, L. S. M. Kreuk, N. Krogan, and G. M. Barton. 2019a. UNC93B1 recruits syntenin-1 to dampen TLR7 signalling and prevent autoimmunity. *Nature* 575(7782):366–370. doi:10.1038/s41586-019-1612-6.

Majer, O., B. Liu, B. J. Woo, L. S. M. Kreuk, E. van Dis, and G. M. Barton. 2019b. Release from UNC93B1 reinforces the compartmentalized activation of select TLRs. *Nature* 575(7782):371–374. doi:10.1038/s41586-019-1611-7.

Malik, A., and T.-D. Kanneganti. 2017. Inflammasome activation and assembly at a glance. *Journal of cell science* 130(23):3955–3963. doi:10.1242/jcs.207365.

Man, S. M., L. J. Hopkins, E. Nugent, S. Cox, I. M. Glück, P. Tourlomousis, J. A. Wright, P. Cicuta, T. P. Monie, and C. E. Bryant. 2014. Inflammasome activation causes dual recruitment of NLRC4 and NLRP3 to the same macromolecular complex. *Proceedings of the National Academy of Sciences of the United States of America* 111(20):7403–7408. doi:10.1073/pnas.1402911111.

Man, S. M., R. Karki, and T.-D. Kanneganti. 2016. DNA-sensing inflammasomes: regulation of bacterial host defense and the gut microbiota. *Pathogens and disease* 74(4):ftw028. doi:10.1093/femspd/ftw028.

Man, S. M., R. Karki, R. K. S. Malireddi, G. Neale, P. Vogel, M. Yamamoto, M. Lamkanfi, and T.-D. Kanneganti. 2015. The transcription factor IRF1 and guanylate-binding proteins target activation of the AIM2 inflammasome by Francisella infection. *Nature immunology* 16(5):467–475. doi:10.1038/ni.3118.

Mangan, M. S. J., E. J. Olhava, W. R. Roush, H. M. Seidel, G. D. Glick, and E. Latz. 2018. Targeting the NLRP3 inflammasome in inflammatory diseases. *Nature reviews. Drug discovery* 17(8):588–606. doi:10.1038/nrd.2018.97.

Mariathasan, S., K. Newton, D. M. Monack, D. Vucic, D. M. French, W. P. Lee, M. Roose-Girma, S. Erickson, and V. M. Dixit. 2004. Differential activation of the inflammasome by caspase-1 adaptors ASC and Ipaf. *Nature* 430(6996):213–218. doi:10.1038/nature02664.

Mariathasan, S., D. S. Weiss, K. Newton, J. McBride, K. O'Rourke, M. Roose-Girma, W. P. Lee, Y. Weinrauch, D. M. Monack, and V. M. Dixit. 2006. Cryopyrin activates the inflammasome in response to toxins and ATP. *Nature* 440(7081):228–232. doi:10.1038/nature04515.

Martínez-García, J. J., H. Martínez-Banaclocha, D. Angosto-Bazarra, C. de Torre-Minguela, A. Baroja-Mazo, C. Alarcón-Vila, L. Martínez-Alarcón, J. Amores-Iniesta, F. Martín-Sánchez, G. A. Ercole, C. M. Martínez, A. González-Lisorge, J. Fernández-Pacheco, P. Martínez-Gil, S. Adriouch, F. Koch-Nolte, J. Luján, F. Acosta-Villegas, P. Parrilla, C. García-Palenciano, and P. Pelegrin. 2019. P2X7 receptor induces mitochondrial failure in monocytes and compromises NLRP3 inflammasome activation during sepsis. *Nature communications* 10(1):2711. doi:10.1038/s41467-019-10626-x.

Martinon, F., K. Burns, and J. Tschopp. 2002. The Inflammasome. *Molecular Cell* 10(2):417–426. doi:10.1016/s1097-2765(02)00599-3.

Martinon, F., V. Pétrilli, A. Mayor, A. Tardivel, and J. Tschopp. 2006. Gout-associated uric acid crystals activate the NALP3 inflammasome. *Nature* 440(7081):237–241. doi:10.1038/nature04516.

Martinon, F., and J. Tschopp. 2004. Inflammatory caspases: linking an intracellular innate immune system to autoinflammatory diseases. *Cell* 117(5):561–574. doi:10.1016/j.cell.2004.05.004.

Mateos, R., and A. Albillos. 2019. Sepsis in Patients With Cirrhosis Awaiting Liver Transplantation: New Trends and Management. *Liver transplantation official publication of the American Association for the Study of Liver Diseases and the International Liver Transplantation Society* 25(11):1700–1709. doi:10.1002/lt.25621.

Mateos, R., M. Alvarez-Mon, and A. Albillos. 2019. Dysfunctional Immune Response in Acute-on-Chronic Liver Failure: It Takes Two to Tango. *Frontiers in immunology* 10:973. doi:10.3389/fimmu.2019.00973.

Matusiak, M., N. van Opdenbosch, and M. Lamkanfi. 2015. CARD- and pyrin-only proteins regulating inflammasome activation and immunity. *Immunological reviews* 265(1):217–230. doi:10.1111/imr.12282.

Mayor, A., F. Martinon, T. de Smedt, V. Pétrilli, and J. Tschopp. 2007. A crucial function of SGT1 and HSP90 in inflammasome activity links mammalian and plant innate immune responses. *Nature immunology* 8(5):497–503. doi:10.1038/ni1459.

McDaniel, M. M., L. C. Kottyan, H. Singh, and C. Pasare. 2020. Suppression of Inflammasome Activation by IRF8 and IRF4 in cDCs Is Critical for T Cell Priming. *Cell reports* 31(5):107604. doi:10.1016/j.celrep.2020.107604.

Medzhitov, R. 2008. Origin and physiological roles of inflammation. *Nature* 454(7203):428–435. doi:10.1038/nature07201.

Mehta, A., and D. Baltimore. 2016. MicroRNAs as regulatory elements in immune system logic. *Nature reviews. Immunology* 16(5):279–294. doi:10.1038/nri.2016.40.

Menu, P., A. Mayor, R. Zhou, A. Tardivel, H. Ichijo, K. Mori, and J. Tschopp. 2012. ER stress activates the NLRP3 inflammasome via an UPR-independent pathway. *Cell death & disease* 3:e261. doi:10.1038/cddis.2011.132.

Meunier, E., M. S. Dick, R. F. Dreier, N. Schürmann, D. Kenzelmann Broz, S. Warming, M. Roose-Girma, D. Bumann, N. Kayagaki, K. Takeda, M. Yamamoto, and P. Broz. 2014. Caspase-11 activation requires lysis of pathogen-containing vacuoles by IFN-induced GTPases. *Nature* 509(7500):366–370. doi:10.1038/nature13157.

Meyer, E., K. J. Carss, J. Rankin, J. M. E. Nichols, D. Grozeva, A. P. Joseph, N. E. Mencacci, A. Papandreou, J. Ng, S. Barral, A. Ngoh, H. Ben-Pazi, M. A. Willemsen, D. Arkadir, A. Barnicoat, H. Bergman, S. Bhate, A. Boys, N. Darin, N. Foulds, N. Gutowski, A. Hills, H. Houlden, J. A. Hurst, Z. Israel, M. Kaminska, P. Limousin, D. Lumsden, S. McKee, S. Misra, S. S. Mohammed, V. Nakou, J. Nicolai, M. Nilsson, H. Pall, K. J. Peall, G. B. Peters, P. Prabhakar, M. S. Reuter, P. Rump, R. Segel, M. Sinnema, M. Smith, P. Turnpenny, S. M. White, D. Wieczorek, S. Wiethoff, B. T. Wilson, G. Winter, C. Wragg, S. Pope, S. J. H. Heales, D. Morrogh, A. Pittman, L. J. Carr, B. Perez-Dueñas, J.-P. Lin, A. Reis, W. A. Gahl, C. Toro, K. P. Bhatia, N. W. Wood, E.-J. Kamsteeg, W. K. Chong, P. Gissen, M. Topf, R. C. Dale, J. R. Chubb, F. L. Raymond, and M. A. Kurian. 2017. Mutations in the histone methyltransferase gene KMT2B cause complex early-onset dystonia. *Nature genetics* 49(2):223–237. doi:10.1038/ng.3740.

Miao, E. A., C. M. Alpuche-Aranda, M. Dors, A. E. Clark, M. W. Bader, S. I. Miller, and A. Aderem. 2006. Cytoplasmic flagellin activates caspase-1 and secretion of interleukin 1beta via Ipaf. *Nature immunology* 7(6):569–575. doi:10.1038/ni1344.

Miao, E. A., I. A. Leaf, P. M. Treuting, D. P. Mao, M. Dors, A. Sarkar, S. E. Warren, M. D. Wewers, and A. Aderem. 2010. Caspase-1-induced pyroptosis is an innate immune effector mechanism against intracellular bacteria. *Nature immunology* 11(12):1136–1142. doi:10.1038/ni.1960.

Michalski, S., C. C. de Oliveira Mann, C. A. Stafford, G. Witte, J. Bartho, K. Lammens, V. Hornung, and K.-P. Hopfner. 2020. Structural basis for sequestration and autoinhibition of cGAS by chromatin. *Nature* 587(7835):678–682. doi:10.1038/s41586-020-2748-0.

Misawa, T., M. Takahama, T. Kozaki, H. Lee, J. Zou, T. Saitoh, and S. Akira. 2013. Microtubule-driven spatial arrangement of mitochondria promotes activation of the NLRP3 inflammasome. *Nature immunology* 14(5):454–460. doi:10.1038/ni.2550.

Moltke, J. von, N. J. Trinidad, M. Moayeri, A. F. Kintzer, S. B. Wang, N. van Rooijen, C. R. Brown, B. A. Krantz, S. H. Leppla, K. Gronert, and R. E. Vance. 2012. Rapid induction of inflammatory lipid mediators by the inflammasome in vivo. *Nature* 490(7418):107–111. doi:10.1038/nature11351.

Monneret, G., A. Lepape, N. Voirin, J. Bohé, F. Venet, A.-L. Debard, H. Thizy, J. Bienvenu, F. Gueyffier, and P. Vanhems. 2006. Persisting low monocyte human leukocyte antigen-DR expression predicts mortality in septic shock. *Intensive care medicine* 32(8):1175–1183. doi:10.1007/s00134-006-0204-8.

Monteiro, S., J. Grandt, F. E. Uschner, N. Kimer, J. L. Madsen, R. Schierwagen, S. Klein, C. Welsch, L. Schäfer, C. Jansen, J. Claria, J. Alcaraz-Quiles, V. Arroyo, R. Moreau, J. Fernandez, F. Bendtsen, G. Mehta, L. L. Gluud, S. Møller, M. Praktiknjo, and J. Trebicka. 2021. Differential inflammasome activation predisposes to acute-on-chronic liver failure in human and experimental cirrhosis with and without previous decompensation. *Gut* 70(2):379–387. doi:10.1136/gutjnl-2019-320170.

Morales, C., and Z. Li. 2017. Drosophila canopy b is a cochaperone of glycoprotein 93. *The Journal of biological chemistry* 292(16):6657–6666. doi:10.1074/jbc.M116.755538.

Moreau, R., R. Jalan, P. Gines, M. Pavesi, P. Angeli, J. Cordoba, F. Durand, T. Gustot, F. Saliba, M. Domenicali, A. Gerbes, J. Wendon, C. Alessandria, W. Laleman, S. Zeuzem, J. Trebicka, M. Bernardi, and V. Arroyo. 2013. Acute-on-chronic liver failure is a distinct syndrome that develops in patients with acute decompensation of cirrhosis. *Gastroenterology* 144(7):1426-37, 1437.e1-9. doi:10.1053/j.gastro.2013.02.042.

Mortimer, L., F. Moreau, J. A. MacDonald, and K. Chadee. 2016. NLRP3 inflammasome inhibition is disrupted in a group of auto-inflammatory disease CAPS mutations. *Nature immunology* 17(10):1176–1186. doi:10.1038/ni.3538.

Muñoz-Planillo, R., P. Kuffa, G. Martínez-Colón, B. L. Smith, T. M. Rajendiran, and G. Núñez. 2013. K^+ efflux is the common trigger of NLRP3 inflammasome activation by bacterial toxins and particulate matter. *Immunity* 38(6):1142–1153. doi:10.1016/j.immuni.2013.05.016.

Muruve, D. A., V. Pétrilli, A. K. Zaiss, L. R. White, S. A. Clark, P. J. Ross, R. J. Parks, and J. Tschopp. 2008. The inflammasome recognizes cytosolic microbial and host DNA and triggers an innate immune response. *Nature* 452(7183):103–107. doi:10.1038/nature06664.

Mutoh, H., M. Kato, T. Akita, T. Shibata, H. Wakamoto, H. Ikeda, H. Kitaura, K. Aoto, M. Nakashima, T. Wang, C. Ohba, S. Miyatake, N. Miyake, A. Kakita, K. Miyake, A. Fukuda, N. Matsumoto, and H. Saitsu. 2018. Biallelic Variants in CNPY3, Encoding an Endoplasmic Reticulum Chaperone, Cause Early-Onset Epileptic Encephalopathy. *American journal of human genetics* 102(2):321–329. doi:10.1016/j.ajhg.2018.01.004.

Nagar, A., R. A. DeMarco, and J. A. Harton. 2019. Inflammasome and Caspase-1 Activity Characterization and Evaluation: An Imaging Flow Cytometer-Based Detection and Assessment of Inflammasome Specks and Caspase-1 Activation. *Journal of immunology (Baltimore, Md. 1950)* 202(3):1003–1015. doi:10.4049/jimmunol.1800973.

Nakaya, Y., J. Lilue, S. Stavrou, E. A. Moran, and S. R. Ross. 2017. AIM2-Like Receptors Positively and Negatively Regulate the Interferon Response Induced by Cytosolic DNA. *mBio* 8(4). doi:10.1128/mBio.00944-17.

Napier, B. A., S. W. Brubaker, T. E. Sweeney, P. Monette, G. H. Rothmeier, N. A. Gertsvolf, A. Puschnik, J. E. Carette, P. Khatri, and D. M. Monack. 2016. Complement pathway amplifies caspase-11-dependent cell death and endotoxin-induced sepsis severity. *The Journal of experimental medicine* 213(11):2365–2382. doi:10.1084/jem.20160027.

Nardai, G., E. M. Végh, Z. Prohászka, and P. Csermely. 2006. Chaperone-related immune dysfunction: an emergent property of distorted chaperone networks. *Trends in immunology* 27(2):74–79. doi:10.1016/j.it.2005.11.009.

Netea, M. G., A. Schlitzer, K. Placek, L. A. B. Joosten, and J. L. Schultze. 2019. Innate and Adaptive Immune Memory: an Evolutionary Continuum in the Host's Response to Pathogens. *Cell host & microbe* 25(1):13–26. doi:10.1016/j.chom.2018.12.006.

Netea, M. G., C. Wijmenga, and L. A. J. O'Neill. 2012. Genetic variation in Toll-like receptors and disease susceptibility. *Nature immunology* 13(6):535–542. doi:10.1038/ni.2284.

Neudecker, V., M. Haneklaus, O. Jensen, L. Khailova, J. C. Masterson, H. Tye, K. Biette, P. Jedlicka, K. S. Brodsky, M. E. Gerich, M. Mack, A. A. B. Robertson, M. A. Cooper, G. T. Furuta, C. A. Dinarello, L. A. O'Neill, H. K. Eltzschig, S. L. Masters, and E. N. McNamee. 2017. Myeloid-derived miR-223 regulates intestinal inflammation via repression of the NLRP3 inflammasome. *The Journal of experimental medicine* 214(6):1737–1752. doi:10.1084/jem.20160462.

O'Connell, R. M., K. D. Taganov, M. P. Boldin, G. Cheng, and D. Baltimore. 2007. MicroRNA-155 is induced during the macrophage inflammatory response. *Proceedings of the National Academy of Sciences of the United States of America* 104(5):1604–1609. doi:10.1073/pnas.0610731104.

Ohmori, Y., and T. A. Hamilton. 2001. Requirement for STAT1 in LPS-induced gene expression in macrophages. *Journal of leukocyte biology* 69(4):598–604.

Groß, C. J., R. Mishra, K. S. Schneider, G. Médard, J. Wettmarshausen, D. C. Dittlein, H. Shi, O. Gorka, P.-A. Koenig, S. Fromm, G. Magnani, T. Ćiković, L. Hartjes, J. Smollich, A. A. B. Robertson, M. A. Cooper, M. Schmidt-Supprian, M. Schuster, K. Schroder, P. Broz, C. Traidl-Hoffmann, B. Beutler, B. Kuster, J. Ruland, S. Schneider, F. Perocchi, and O. Groß. 2016. K+ Efflux-Independent NLRP3 Inflammasome Activation by Small Molecules Targeting Mitochondria. *Immunity* 45(4):761–773. doi:10.1016/j.immuni.2016.08.010.

Opal, S. M., P.-F. Laterre, B. Francois, S. P. LaRosa, D. C. Angus, J.-P. Mira, X. Wittebole, T. Dugernier, D. Perrotin, M. Tidswell, L. Jauregui, K. Krell, J. Pachl, T. Takahashi, C. Peckelsen, E. Cordasco, C.-S. Chang, S. Oeyen, N. Aikawa, T. Maruyama, R. Schein, A. C. Kalil, M. van Nuffelen, M. Lynn, D. P. Rossignol, J. Gogate, M. B. Roberts, J. L. Wheeler, and J.-L. Vincent. 2013. Effect of eritoran, an antagonist of MD2-TLR4, on mortality in patients with severe sepsis: the ACCESS randomized trial. *JAMA* 309(11):1154–1162. doi:10.1001/jama.2013.2194.

Ortega, S., M. Ittmann, S. H. Tsang, M. Ehrlich, and C. Basilico. 1998. Neuronal defects and delayed wound healing in mice lacking fibroblast growth factor 2. *Proceedings of the National Academy of Sciences of the United States of America* 95(10):5672–5677. doi:10.1073/pnas.95.10.5672.

Osuchowski, M. F., F. Craciun, K. M. Weixelbaumer, E. R. Duffy, and D. G. Remick. 2012. Sepsis chronically in MARS: systemic cytokine responses are always mixed regardless of the outcome, magnitude, or phase of sepsis. *Journal of immunology (Baltimore, Md. 1950)* 189(9):4648–4656. doi:10.4049/jimmunol.1201806.

Pasare, C., and R. Medzhitov. 2004. Toll-like receptors: linking innate and adaptive immunity. *Microbes and infection* 6(15):1382–1387. doi:10.1016/j.micinf.2004.08.018.

Pathare, G. R., A. Decout, S. Glück, S. Cavadini, K. Makasheva, R. Hovius, G. Kempf, J. Weiss, Z. Kozicka, B. Guey, P. Melenec, B. Fierz, N. H. Thomä, and A. Ablasser. 2020. Structural mechanism of cGAS inhibition by the nucleosome. *Nature* 587(7835):668–672. doi:10.1038/s41586-020-2750-6.

Pelka, K., D. Bertheloot, E. Reimer, K. Phulphagar, S. V. Schmidt, A. Christ, R. Stahl, N. Watson, K. Miyake, N. Hacohen, A. Haas, M. M. Brinkmann, A. Marshak-Rothstein, F. Meissner, and E. Latz. 2018. The Chaperone UNC93B1 Regulates Toll-like Receptor Stability Independently of Endosomal TLR Transport. *Immunity* 48(5):911-922.e7. doi:10.1016/j.immuni.2018.04.011.

Peterson-Kaufman, K. J., C. D. Carlson, J. A. Rodríguez-Martínez, and A. Z. Ansari. 2010. Nucleating the assembly of macromolecular complexes. *Chembiochem a European journal of chemical biology* 11(14):1955–1962. doi:10.1002/cbic.201000255.

Pfalzgraff, A., and G. Weindl. 2019. Intracellular Lipopolysaccharide Sensing as a Potential Therapeutic Target for Sepsis. *Trends in pharmacological sciences* 40(3):187–197. doi:10.1016/j.tips.2019.01.001.

Phulphagar, K., L. I. Kühn, S. Ebner, A. Frauenstein, J. J. Swietlik, J. Rieckmann, and F. Meissner. 2021. Proteomics reveals distinct mechanisms regulating the release of cytokines and alarmins during pyroptosis. *Cell reports* 34(10):108826. doi:10.1016/j.celrep.2021.108826.

Piano, S., M. Bartoletti, M. Tonon, M. Baldassarre, G. Chies, A. Romano, P. Viale, E. Vettore, M. Domenicali, M. Stanco, C. Pilutti, A. C. Frigo, A. Brocca, M. Bernardi, P. Caraceni, and P. Angeli. 2018. Assessment of Sepsis-3 criteria and quick SOFA in patients with cirrhosis and bacterial infections. *Gut* 67(10):1892–1899. doi:10.1136/gutjnl-2017-314324.

Pilla, D. M., J. A. Hagar, A. K. Haldar, A. K. Mason, D. Degrandi, K. Pfeffer, R. K. Ernst, M. Yamamoto, E. A. Miao, and J. Coers. 2014. Guanylate binding proteins promote caspase-11-dependent pyroptosis in response to cytoplasmic LPS. *Proceedings of the National Academy of Sciences of the United States of America* 111(16):6046–6051. doi:10.1073/pnas.1321700111.

Piperno, G. M., A. Naseem, G. Silvestrelli, R. Amadio, N. Caronni, K. E. Cervantes-Luevano, N. Liv, J. Klumperman, A. Colliva, H. Ali, F. Graziano, P. Benaroch, H. Haecker, R. N. Hanna, and F. Benvenuti. 2020. Wiskott-Aldrich syndrome protein restricts cGAS/STING activation by dsDNA immune complexes. *JCI insight* 5(17). doi:10.1172/jci.insight.132857.

Poelzl, A., C. Lassnig, S. Tangermann, D. Hromadová, U. Reichart, R. Gawish, K. Mueller, R. Moriggl, A. Linkermann, M. Glösmann, L. Kenner, M. Mueller, and B. Strobl. 2021. TYK2 licenses non-canonical inflammasome activation during endotoxemia. *Cell death and differentiation* 28(2):748–763. doi:10.1038/s41418-020-00621-x.

Pohar, J., N. Pirher, M. Benčina, M. Manček-Keber, and R. Jerala. 2013. The role of UNC93B1 protein in surface localization of TLR3 receptor and in cell priming to nucleic acid agonists. *The Journal of biological chemistry* 288(1):442–454. doi:10.1074/jbc.M112.413922.

Poli, G., C. Fabi, M. M. Bellet, C. Costantini, L. Nunziangeli, L. Romani, and S. Brancorsini. 2020. Epigenetic Mechanisms of Inflammasome Regulation. *International journal of molecular sciences* 21(16). doi:10.3390/ijms21165758.

Praktiknjo, M., R. Schierwagen, S. Monteiro, C. Ortiz, F. E. Uschner, C. Jansen, J. Claria, and J. Trebicka. 2020. Hepatic inflammasome activation as origin of Interleukin-1α and Interleukin-1β in liver cirrhosis. *Gut*. doi:10.1136/gutjnl-2020-322621.

Price, A. E., K. Shamardani, K. A. Lugo, J. Deguine, A. W. Roberts, B. L. Lee, and G. M. Barton. 2018. A Map of Toll-like Receptor Expression in the Intestinal Epithelium Reveals Distinct Spatial, Cell

Type-Specific, and Temporal Patterns. *Immunity* 49(3):560-575.e6. doi:10.1016/j.immuni.2018.07.016.

Qiao, Y., E. G. Giannopoulou, C. H. Chan, S.-H. Park, S. Gong, J. Chen, X. Hu, O. Elemento, and L. B. Ivashkiv. 2013. Synergistic activation of inflammatory cytokine genes by interferon-γ-induced chromatin remodeling and toll-like receptor signaling. *Immunity* 39(3):454–469. doi:10.1016/j.immuni.2013.08.009.

Rajaiah, R., D. J. Perkins, D. D. C. Ireland, and S. N. Vogel. 2015. CD14 dependence of TLR4 endocytosis and TRIF signaling displays ligand specificity and is dissociable in endotoxin tolerance. *Proceedings of the National Academy of Sciences of the United States of America* 112(27):8391–8396. doi:10.1073/pnas.1424980112.

Ramachandran, G. 2014. Gram-positive and gram-negative bacterial toxins in sepsis: a brief review. *Virulence* 5(1):213–218. doi:10.4161/viru.27024.

Ramirez-Carrozzi, V. R., D. Braas, D. M. Bhatt, C. S. Cheng, C. Hong, K. R. Doty, J. C. Black, A. Hoffmann, M. Carey, and S. T. Smale. 2009. A unifying model for the selective regulation of inducible transcription by CpG islands and nucleosome remodeling. *Cell* 138(1):114–128. doi:10.1016/j.cell.2009.04.020.

Ramirez-Carrozzi, V. R., A. A. Nazarian, C. C. Li, S. L. Gore, R. Sridharan, A. N. Imbalzano, and S. T. Smale. 2006. Selective and antagonistic functions of SWI/SNF and Mi-2beta nucleosome remodeling complexes during an inflammatory response. *Genes & development* 20(3):282–296. doi:10.1101/gad.1383206.

Randow, F., and B. Seed. 2001. Endoplasmic reticulum chaperone gp96 is required for innate immunity but not cell viability. *Nature cell biology* 3(10):891–896. doi:10.1038/ncb1001-891.

Randow, F., U. Syrbe, C. Meisel, D. Krausch, H. Zuckermann, C. Platzer, and H. D. Volk. 1995. Mechanism of endotoxin desensitization: involvement of interleukin 10 and transforming growth factor beta. *The Journal of experimental medicine* 181(5):1887–1892. doi:10.1084/jem.181.5.1887.

Rathinam, V. A. K., S. K. Vanaja, L. Waggoner, A. Sokolovska, C. Becker, L. M. Stuart, J. M. Leong, and K. A. Fitzgerald. 2012. TRIF licenses caspase-11-dependent NLRP3 inflammasome activation by gram-negative bacteria. *Cell* 150(3):606–619. doi:10.1016/j.cell.2012.07.007.

Rathkey, J. K., J. Zhao, Z. Liu, Y. Chen, J. Yang, H. C. Kondolf, B. L. Benson, S. M. Chirieleison, A. Y. Huang, G. R. Dubyak, T. S. Xiao, X. Li, and D. W. Abbott. 2018. Chemical disruption of the pyroptotic pore-forming protein gasdermin D inhibits inflammatory cell death and sepsis. *Science immunology* 3(26). doi:10.1126/sciimmunol.aat2738.

Rauch, I., J. L. Tenthorey, R. D. Nichols, K. Al Moussawi, J. J. Kang, C. Kang, B. I. Kazmierczak, and R. E. Vance. 2016. NAIP proteins are required for cytosolic detection of specific bacterial ligands in vivo. *The Journal of experimental medicine* 213(5):657–665. doi:10.1084/jem.20151809.

Rayamajhi, M., Y. Zhang, and E. A. Miao. 2013. Detection of pyroptosis by measuring released lactate dehydrogenase activity. *Methods in molecular biology (Clifton, N.J.)* 1040:85–90. doi:10.1007/978-1-62703-523-1_7.

Reinke, S., M. Linge, H. H. Diebner, H. Luksch, S. Glage, A. Gocht, A. A. B. Robertson, M. A. Cooper, S. R. Hofmann, R. Naumann, M. Sarov, R. Behrendt, A. Roers, F. Pessler, J. Roesler, A. Rösen-Wolff, and S. Winkler. 2020. Non-canonical Caspase-1 Signaling Drives RIP2-Dependent and TNF-α-Mediated Inflammation In Vivo. *Cell reports* 30(8):2501-2511.e5. doi:10.1016/j.celrep.2020.01.090.

Rice, T. W., A. P. Wheeler, G. R. Bernard, J.-L. Vincent, D. C. Angus, N. Aikawa, I. Demeyer, S. Sainati, N. Amlot, C. Cao, M. Ii, H. Matsuda, K. Mouri, and J. Cohen. 2010. A randomized, double-blind, placebo-controlled trial of TAK-242 for the treatment of severe sepsis. *Critical care medicine* 38(8):1685–1694. doi:10.1097/CCM.0b013e3181e7c5c9.

Roers, A., B. Hiller, and V. Hornung. 2016. Recognition of Endogenous Nucleic Acids by the Innate Immune System. *Immunity* 44(4):739–754. doi:10.1016/j.immuni.2016.04.002.

Rubio, I., M. F. Osuchowski, M. Shankar-Hari, T. Skirecki, M. S. Winkler, G. Lachmann, P. La Rosée, G. Monneret, F. Venet, M. Bauer, F. M. Brunkhorst, M. Kox, J.-M. Cavaillon, F. Uhle, M. A. Weigand, S. B. Flohé, W. J. Wiersinga, M. Martin-Fernandez, R. Almansa, I. Martin-Loeches, A. Torres, E. J. Giamarellos-Bourboulis, M. Girardis, A. Cossarizza, M. G. Netea, T. van der Poll, A. Scherag, C. Meisel, J. C. Schefold, and J. F. Bermejo-Martín. 2019. Current gaps in sepsis immunology: new opportunities for translational research. *The Lancet infectious diseases* 19(12):e422-e436. doi:10.1016/S1473-3099(19)30567-5.

Rudd, K. E., S. C. Johnson, K. M. Agesa, K. A. Shackelford, D. Tsoi, D. R. Kievlan, D. V. Colombara, K. S. Ikuta, N. Kissoon, S. Finfer, C. Fleischmann-Struzek, F. R. Machado, K. K. Reinhart, K. Rowan, C. W. Seymour, R. S. Watson, T. E. West, F. Marinho, S. I. Hay, R. Lozano, A. D. Lopez, D. C. Angus, C. J. L. Murray, and M. Naghavi. 2020. Global, regional, and national sepsis incidence and mortality, 1990–2017: analysis for the Global Burden of Disease Study. *The Lancet* 395(10219):200–211. doi:10.1016/S0140-6736(19)32989-7.

Russo, A. J., B. Behl, I. Banerjee, and V. A. K. Rathinam. 2018. Emerging Insights into Noncanonical Inflammasome Recognition of Microbes. *Journal of molecular biology* 430(2):207–216. doi:10.1016/j.jmb.2017.10.003.

Russo, A. J., S. O. Vasudevan, S. P. Méndez-Huergo, P. Kumari, A. Menoret, S. Duduskar, C. Wang, J. M. Pérez Sáez, M. M. Fettis, C. Li, R. Liu, A. Wanchoo, K. Chandiran, J. Ruan, S. K. Vanaja, M. Bauer, C. Sponholz, G. A. Hudalla, A. T. Vella, B. Zhou, S. D. Deshmukh, G. A. Rabinovich, and V. A. Rathinam. 2021. Intracellular immune sensing promotes inflammation via gasdermin D-driven release of a lectin alarmin. *Nature immunology* 22(2):154–165. doi:10.1038/s41590-020-00844-7.

Saito, K., K. Kukita, G. Kutomi, K. Okuya, H. Asanuma, T. Tabeya, Y. Naishiro, M. Yamamoto, H. Takahashi, T. Torigoe, A. Nakai, Y. Shinomura, K. Hirata, N. Sato, and Y. Tamura. 2015. Heat shock protein 90 associates with Toll-like receptors 7/9 and mediates self-nucleic acid recognition in SLE. *European journal of immunology* 45(7):2028–2041. doi:10.1002/eji.201445293.

Santos, J. C., D. Boucher, L. K. Schneider, B. Demarco, M. Dilucca, K. Shkarina, R. Heilig, K. W. Chen, R. Y. H. Lim, and P. Broz. 2020. Human GBP1 binds LPS to initiate assembly of a caspase-4 activating platform on cytosolic bacteria. *Nature communications* 11(1):3276. doi:10.1038/s41467-020-16889-z.

Santos, J. C., M. S. Dick, B. Lagrange, D. Degrandi, K. Pfeffer, M. Yamamoto, E. Meunier, P. Pelczar, T. Henry, and P. Broz. 2018. LPS targets host guanylate-binding proteins to the bacterial outer membrane for non-canonical inflammasome activation. *The EMBO journal* 37(6). doi:10.15252/embj.201798089.

Sato, M., T. Taniguchi, and N. Tanaka. 2001. The interferon system and interferon regulatory factor transcription factors -- studies from gene knockout mice. *Cytokine & growth factor reviews* 12(2-3):133–142. doi:10.1016/s1359-6101(00)00032-0.

Saxena, M., and G. Yeretssian. 2014. NOD-Like Receptors: Master Regulators of Inflammation and Cancer. *Frontiers in immunology* 5:327. doi:10.3389/fimmu.2014.00327.

Saxonov, S., P. Berg, and D. L. Brutlag. 2006. A genome-wide analysis of CpG dinucleotides in the human genome distinguishes two distinct classes of promoters. *Proceedings of the National Academy of Sciences of the United States of America* 103(5):1412–1417. doi:10.1073/pnas.0510310103.

Schauvliege, R., J. Vanrobaeys, P. Schotte, and R. Beyaert. 2002. Caspase-11 gene expression in response to lipopolysaccharide and interferon-gamma requires nuclear factor-kappa B and signal transducer and activator of transcription (STAT) 1. *The Journal of biological chemistry* 277(44):41624–41630. doi:10.1074/jbc.M207852200.

Schildknegt, D., N. Lodder, A. Pandey, A. Satchisvili, M. Egmond, F. Pena, I. Braakman, and P. van der Sluijs. 2019. Characterization of CNPY5 and its family members. *Protein science a publication of the Protein Society* 28(7):1276–1289. doi:10.1002/pro.3635.

Schmid-Burgk, J. L., D. Chauhan, T. Schmidt, T. S. Ebert, J. Reinhardt, E. Endl, and V. Hornung. 2016. A Genome-wide CRISPR (Clustered Regularly Interspaced Short Palindromic Repeats) Screen

Identifies NEK7 as an Essential Component of NLRP3 Inflammasome Activation. *The Journal of biological chemistry* 291(1):103–109. doi:10.1074/jbc.C115.700492.

Schmid-Burgk, J. L., M. M. Gaidt, T. Schmidt, T. S. Ebert, E. Bartok, and V. Hornung. 2015. Caspase-4 mediates non-canonical activation of the NLRP3 inflammasome in human myeloid cells. *European journal of immunology* 45(10):2911–2917. doi:10.1002/eji.201545523.

Schmittgen, T. D., and K. J. Livak. 2008. Analyzing real-time PCR data by the comparative C(T) method. *Nature protocols* 3(6):1101–1108. doi:10.1038/nprot.2008.73.

Schroder, K., and J. Tschopp. 2010. The inflammasomes. *Cell* 140(6):821–832. doi:10.1016/j.cell.2010.01.040.

Seeley, J. J., R. G. Baker, G. Mohamed, T. Bruns, M. S. Hayden, S. D. Deshmukh, D. E. Freedberg, and S. Ghosh. 2018. Induction of innate immune memory via microRNA targeting of chromatin remodelling factors. *Nature* 559(7712):114–119. doi:10.1038/s41586-018-0253-5.

Seeley, J. J., and S. Ghosh. 2016. Molecular mechanisms of innate memory and tolerance to LPS. *Journal of leukocyte biology* 101(1):107–119. doi:10.1189/jlb.3MR0316-118RR.

Seoane, P. I., B. Lee, C. Hoyle, S. Yu, G. Lopez-Castejon, M. Lowe, and D. Brough. 2020. The NLRP3-inflammasome as a sensor of organelle dysfunction. *The Journal of cell biology* 219(12). doi:10.1083/jcb.202006194.

Sester, D. P., S. J. Thygesen, V. Sagulenko, P. R. Vajjhala, J. A. Cridland, N. Vitak, K. W. Chen, G. W. Osborne, K. Schroder, and K. J. Stacey. 2015. A novel flow cytometric method to assess inflammasome formation. *Journal of immunology (Baltimore, Md. 1950)* 194(1):455–462. doi:10.4049/jimmunol.1401110.

Sha, W., H. Mitoma, S. Hanabuchi, M. Bao, L. Weng, N. Sugimoto, Y. Liu, Z. Zhang, J. Zhong, B. Sun, and Y.-J. Liu. 2014. Human NLRP3 inflammasome senses multiple types of bacterial RNAs. *Proceedings of the National Academy of Sciences of the United States of America* 111(45):16059–16064. doi:10.1073/pnas.1412487111.

Shalova, I. N., J. Y. Lim, M. Chittezhath, A. S. Zinkernagel, F. Beasley, E. Hernández-Jiménez, V. Toledano, C. Cubillos-Zapata, A. Rapisarda, J. Chen, K. Duan, H. Yang, M. Poidinger, G. Melillo, V. Nizet, F. Arnalich, E. López-Collazo, and S. K. Biswas. 2015. Human monocytes undergo functional re-programming during sepsis mediated by hypoxia-inducible factor-1α. *Immunity* 42(3):484–498. doi:10.1016/j.immuni.2015.02.001.

Shankar-Hari, M., D. Datta, J. Wilson, V. Assi, J. Stephen, C. J. Weir, J. Rennie, J. Antonelli, A. Bateman, J. M. Felton, N. Warner, K. Judge, J. Keenan, A. Wang, T. Burpee, A. K. Brown, S. M. Lewis, T. Mare, A. I. Roy, J. Wright, G. Hulme, I. Dimmick, A. Gray, A. G. Rossi, A. J. Simpson, A. Conway Morris, and T. S. Walsh. 2018. Early PREdiction of sepsis using leukocyte surface biomarkers: the ExPRES-sepsis cohort study. *Intensive care medicine* 44(11):1836–1848. doi:10.1007/s00134-018-5389-0.

Sharif, H., L. Wang, W. L. Wang, V. G. Magupalli, L. Andreeva, Q. Qiao, A. V. Hauenstein, Z. Wu, G. Núñez, Y. Mao, and H. Wu. 2019. Structural mechanism for NEK7-licensed activation of NLRP3 inflammasome. *Nature* 570(7761):338–343. doi:10.1038/s41586-019-1295-z.

Sharma, D., and T.-D. Kanneganti. 2016. The cell biology of inflammasomes: Mechanisms of inflammasome activation and regulation. *The Journal of cell biology* 213(6):617–629. doi:10.1083/jcb.201602089.

Shenoy, A. R., D. A. Wellington, P. Kumar, H. Kassa, C. J. Booth, P. Cresswell, and J. D. MacMicking. 2012. GBP5 promotes NLRP3 inflammasome assembly and immunity in mammals. *Science (New York, N.Y.)* 336(6080):481–485. doi:10.1126/science.1217141.

Shi, H., Y. Wang, X. Li, X. Zhan, M. Tang, M. Fina, L. Su, D. Pratt, C. H. Bu, S. Hildebrand, S. Lyon, L. Scott, J. Quan, Q. Sun, J. Russell, S. Arnett, P. Jurek, D. Chen, V. V. Kravchenko, J. C. Mathison, E. M. Y. Moresco, N. L. Monson, R. J. Ulevitch, and B. Beutler. 2016. NLRP3 activation and mitosis are mutually exclusive events coordinated by NEK7, a new inflammasome component. *Nature immunology* 17(3):250–258. doi:10.1038/ni.3333.

Shi, J., Y. Zhao, K. Wang, X. Shi, Y. Wang, H. Huang, Y. Zhuang, T. Cai, F. Wang, and F. Shao. 2015. Cleavage of GSDMD by inflammatory caspases determines pyroptotic cell death. *Nature* 526(7575):660–665. doi:10.1038/nature15514.

Shi, J., Y. Zhao, Y. Wang, W. Gao, J. Ding, P. Li, L. Hu, and F. Shao. 2014. Inflammatory caspases are innate immune receptors for intracellular LPS. *Nature* 514(7521):187–192. doi:10.1038/nature13683.

Shibata, T., N. Takemura, Y. Motoi, Y. Goto, T. Karuppuchamy, K. Izawa, X. Li, S. Akashi-Takamura, N. Tanimura, J. Kunisawa, H. Kiyono, S. Akira, T. Kitamura, J. Kitaura, S. Uematsu, and K. Miyake. 2012. PRAT4A-dependent expression of cell surface TLR5 on neutrophils, classical monocytes and dendritic cells. *International immunology* 24(10):613–623. doi:10.1093/intimm/dxs068.

Shim, D.-W., and K.-H. Lee. 2018. Posttranslational Regulation of the NLR Family Pyrin Domain-Containing 3 Inflammasome. *Frontiers in immunology* 9:1054. doi:10.3389/fimmu.2018.01054.

Singer, M., C. S. Deutschman, C. W. Seymour, M. Shankar-Hari, D. Annane, M. Bauer, R. Bellomo, G. R. Bernard, J.-D. Chiche, C. M. Coopersmith, R. S. Hotchkiss, M. M. Levy, J. C. Marshall, G. S. Martin, S. M. Opal, G. D. Rubenfeld, T. van der Poll, J.-L. Vincent, and D. C. Angus. 2016. The Third International Consensus Definitions for Sepsis and Septic Shock (Sepsis-3). *JAMA* 315(8):801–810. doi:10.1001/jama.2016.0287.

Smale, S. T. 2014. Transcriptional regulation in the immune system: a status report. *Trends in immunology* 35(5):190–194. doi:10.1016/j.it.2014.03.003.

Solé, C., E. Solà, M. Morales-Ruiz, G. Fernàndez, P. Huelin, I. Graupera, R. Moreira, G. de Prada, X. Ariza, E. Pose, N. Fabrellas, S. G. Kalko, W. Jiménez, and P. Ginès. 2016. Characterization of Inflammatory Response in Acute-on-Chronic Liver Failure and Relationship with Prognosis. *Scientific reports* 6:32341. doi:10.1038/srep32341.

Song, N., Z.-S. Liu, W. Xue, Z.-F. Bai, Q.-Y. Wang, J. Dai, X. Liu, Y.-J. Huang, H. Cai, X.-Y. Zhan, Q.-Y. Han, H. Wang, Y. Chen, H.-Y. Li, A.-L. Li, X.-M. Zhang, T. Zhou, and T. Li. 2017. NLRP3 Phosphorylation Is an Essential Priming Event for Inflammasome Activation. *Molecular Cell* 68(1):185-197.e6. doi:10.1016/j.molcel.2017.08.017.

Song, Z., X. Zhang, L. Zhang, F. Xu, X. Tao, H. Zhang, X. Lin, L. Kang, Y. Xiang, X. Lai, Q. Zhang, K. Huang, Y. Dai, Y. Yin, and J. Cao. 2016. Progranulin Plays a Central Role in Host Defense during Sepsis by Promoting Macrophage Recruitment. *American journal of respiratory and critical care medicine* 194(10):1219–1232. doi:10.1164/rccm.201601-0056OC.

Sponholz, C., M. Kramer, F. Schöneweck, U. Menzel, K. Inanloo Rahatloo, E. J. Giamarellos-Bourboulis, V. Papavassileiou, K. Lymberopoulou, M. Pavlaki, I. Koutelidakis, I. Perdios, A. Scherag, M. Bauer, M. Platzer, and K. Huse. 2016. Polymorphisms of cystathionine beta-synthase gene are associated with susceptibility to sepsis. *European journal of human genetics EJHG* 24(7):1041–1048. doi:10.1038/ejhg.2015.231.

Squarzoni, P., G. Oller, G. Hoeffel, L. Pont-Lezica, P. Rostaing, D. Low, A. Bessis, F. Ginhoux, and S. Garel. 2014. Microglia modulate wiring of the embryonic forebrain. *Cell reports* 8(5):1271–1279. doi:10.1016/j.celrep.2014.07.042.

Stack, J., S. L. Doyle, D. J. Connolly, L. S. Reinert, K. M. O'Keeffe, R. M. McLoughlin, S. R. Paludan, and A. G. Bowie. 2014. TRAM is required for TLR2 endosomal signaling to type I IFN induction. *Journal of immunology (Baltimore, Md. 1950)* 193(12):6090–6102. doi:10.4049/jimmunol.1401605.

Stein, R., F. Kapplusch, M. C. Heymann, S. Russ, W. Staroske, C. M. Hedrich, A. Rösen-Wolff, and S. R. Hofmann. 2016. Enzymatically Inactive Procaspase 1 stabilizes the ASC Pyroptosome and Supports Pyroptosome Spreading during Cell Division. *The Journal of biological chemistry* 291(35):18419–18429. doi:10.1074/jbc.M116.718668.

Stengel, S., A. Steube, N. Köse-Vogel, T. Kirchberger-Tolstik, S. Deshmukh, and T. Bruns. 2020. Primed circulating monocytes are a source of IL-1β in patients with cirrhosis and ascites. *Gut* 70(3):622–623. doi:10.1136/gutjnl-2020-321597.

Storek, K. M., and D. M. Monack. 2015. Bacterial recognition pathways that lead to inflammasome activation. *Immunological reviews* 265(1):112–129. doi:10.1111/imr.12289.

Strochlic, T. I., J. Viaud, U. E. E. Rennefahrt, T. Anastassiadis, and J. R. Peterson. 2010. Phosphoinositides are essential coactivators for p21-activated kinase 1. *Molecular Cell* 40(3):493–500. doi:10.1016/j.molcel.2010.10.015.

Strowig, T., J. Henao-Mejia, E. Elinav, and R. Flavell. 2012. Inflammasomes in health and disease. *Nature* 481(7381):278–286. doi:10.1038/nature10759.

Stutz, A., G. L. Horvath, B. G. Monks, and E. Latz. 2013. ASC speck formation as a readout for inflammasome activation. *Methods in molecular biology (Clifton, N.J.)* 1040:91–101. doi:10.1007/978-1-62703-523-1_8.

Subramanian, N., K. Natarajan, M. R. Clatworthy, Z. Wang, and R. N. Germain. 2013. The adaptor MAVS promotes NLRP3 mitochondrial localization and inflammasome activation. *Cell* 153(2):348–361. doi:10.1016/j.cell.2013.02.054.

Tabeta, K., K. Hoebe, E. M. Janssen, X. Du, P. Georgel, K. Crozat, S. Mudd, N. Mann, S. Sovath, J. Goode, L. Shamel, A. A. Herskovits, D. A. Portnoy, M. Cooke, L. M. Tarantino, T. Wiltshire, B. E. Steinberg, S. Grinstein, and B. Beutler. 2006. The Unc93b1 mutation 3d disrupts exogenous antigen presentation and signaling via Toll-like receptors 3, 7 and 9. *Nature immunology* 7(2):156–164. doi:10.1038/ni1297.

Taganov, K. D., M. P. Boldin, K.-J. Chang, and D. Baltimore. 2006. NF-kappaB-dependent induction of microRNA miR-146, an inhibitor targeted to signaling proteins of innate immune responses. *Proceedings of the National Academy of Sciences of the United States of America* 103(33):12481–12486. doi:10.1073/pnas.0605298103.

Takahashi, K., T. Shibata, S. Akashi-Takamura, T. Kiyokawa, Y. Wakabayashi, N. Tanimura, T. Kobayashi, F. Matsumoto, R. Fukui, T. Kouro, Y. Nagai, K. Takatsu, S. Saitoh, and K. Miyake. 2007. A protein associated with Toll-like receptor (TLR) 4 (PRAT4A) is required for TLR-dependent immune responses. *The Journal of experimental medicine* 204(12):2963–2976. doi:10.1084/jem.20071132.

Takeda, K., and S. Akira. 2004. TLR signaling pathways. *Seminars in immunology* 16(1):3–9. doi:10.1016/j.smim.2003.10.003.

Takeuchi, O., and S. Akira. 2010. Pattern recognition receptors and inflammation. *Cell* 140(6):805–820. doi:10.1016/j.cell.2010.01.022.

Tan, Y., and J. C. Kagan. 2014. A cross-disciplinary perspective on the innate immune responses to bacterial lipopolysaccharide. *Molecular Cell* 54(2):212–223. doi:10.1016/j.molcel.2014.03.012.

Tanaka, N., T. Kawakami, and T. Taniguchi. 1993. Recognition DNA sequences of interferon regulatory factor 1 (IRF-1) and IRF-2, regulators of cell growth and the interferon system. *Molecular and cellular biology* 13(8):4531–4538. doi:10.1128/mcb.13.8.4531.

Tang, Y., R. Zhang, Q. Xue, R. Meng, X. Wang, Y. Yang, L. Xie, X. Xiao, T. R. Billiar, and B. Lu. 2018. TRIF signaling is required for caspase-11-dependent immune responses and lethality in sepsis. *Molecular medicine (Cambridge, Mass.)* 24(1):66. doi:10.1186/s10020-018-0065-y.

Tripathy, R., I. Leca, T. van Dijk, J. Weiss, B. W. van Bon, M. C. Sergaki, T. Gstrein, M. Breuss, G. Tian, N. Bahi-Buisson, A. R. Paciorkowski, A. T. Pagnamenta, A. Wenninger-Weinzierl, M. F. Martinez-Reza, L. Landler, S. Lise, J. C. Taylor, G. Terrone, G. Vitiello, E. Del Giudice, N. Brunetti-Pierri, A. D'Amico, A. Reymond, N. Voisin, J. A. Bernstein, E. Farrelly, U. Kini, T. A. Leonard, S. Valence, L. Burglen, L. Armstrong, S. M. Hiatt, G. M. Cooper, K. A. Aldinger, W. B. Dobyns, G. Mirzaa, T. M. Pierson, F. Baas, J. Chelly, N. J. Cowan, and D. A. Keays. 2018. Mutations in MAST1 Cause Mega-Corpus-Callosum Syndrome with Cerebellar Hypoplasia and Cortical Malformations. *Neuron* 100(6):1354-1368.e5. doi:10.1016/j.neuron.2018.10.044.

Unterholzner, L., S. E. Keating, M. Baran, K. A. Horan, S. B. Jensen, S. Sharma, C. M. Sirois, T. Jin, E. Latz, T. S. Xiao, K. A. Fitzgerald, S. R. Paludan, and A. G. Bowie. 2010. IFI16 is an innate immune sensor for intracellular DNA. *Nature immunology* 11(11):997–1004. doi:10.1038/ni.1932.

Vadder, F. de, E. Grasset, L. Mannerås Holm, G. Karsenty, A. J. Macpherson, L. E. Olofsson, and F. Bäckhed. 2018. Gut microbiota regulates maturation of the adult enteric nervous system via enteric serotonin networks. *Proceedings of the National Academy of Sciences of the United States of America* 115(25):6458–6463. doi:10.1073/pnas.1720017115.

van der Poll, T., and S. M. Opal. 2008. Host–pathogen interactions in sepsis. *The Lancet infectious diseases* 8(1):32–43. doi:10.1016/S1473-3099(07)70265-7.

van Gorp, H., P. H. V. Saavedra, N. M. de Vasconcelos, N. van Opdenbosch, L. Vande Walle, M. Matusiak, G. Prencipe, A. Insalaco, F. van Hauwermeiren, D. Demon, D. J. Bogaert, M. Dullaers, E. de Baere, T. Hochepied, J. Dehoorne, K. Y. Vermaelen, F. Haerynck, F. de Benedetti, and M. Lamkanfi. 2016. Familial Mediterranean fever mutations lift the obligatory requirement for microtubules in Pyrin inflammasome activation. *Proceedings of the National Academy of Sciences of the United States of America* 113(50):14384–14389. doi:10.1073/pnas.1613156113.

Vanaja, S., V. K. Rathinam, and K. A. Fitzgerald. 2015. Mechanisms of inflammasome activation: recent advances and novel insights. *Trends in cell biology* 25(5):308–315. doi:10.1016/j.tcb.2014.12.009.

Vanaja, S. K., A. J. Russo, B. Behl, I. Banerjee, M. Yankova, S. D. Deshmukh, and V. A. K. Rathinam. 2016. Bacterial Outer Membrane Vesicles Mediate Cytosolic Localization of LPS and Caspase-11 Activation. *Cell* 165(5):1106–1119. doi:10.1016/j.cell.2016.04.015.

Viganò, E., C. E. Diamond, R. Spreafico, A. Balachander, R. M. Sobota, and A. Mortellaro. 2015. Human caspase-4 and caspase-5 regulate the one-step non-canonical inflammasome activation in monocytes. *Nature communications* 6:8761. doi:10.1038/ncomms9761.

Voet, S., S. Srinivasan, M. Lamkanfi, and G. van Loo. 2019. Inflammasomes in neuroinflammatory and neurodegenerative diseases. *EMBO molecular medicine* 11(6). doi:10.15252/emmm.201810248.

Wacker, M. A., A. Teghanemt, J. P. Weiss, and J. H. Barker. 2017. High-affinity caspase-4 binding to LPS presented as high molecular mass aggregates or in outer membrane vesicles. *Innate immunity* 23(4):336–344. doi:10.1177/1753425917695446.

Wakabayashi, Y., M. Kobayashi, S. Akashi-Takamura, N. Tanimura, K. Konno, K. Takahashi, T. Ishii, T. Mizutani, H. Iba, T. Kouro, S. Takaki, K. Takatsu, Y. Oda, Y. Ishihama, S. Saitoh, and K. Miyake. 2006. A protein associated with toll-like receptor 4 (PRAT4A) regulates cell surface expression of TLR4. *Journal of immunology (Baltimore, Md. 1950)* 177(3):1772–1779. doi:10.4049/jimmunol.177.3.1772.

Walev, I., J. Klein, M. Husmann, A. Valeva, S. Strauch, H. Wirtz, O. Weichel, and S. Bhakdi. 2000. Potassium regulates IL-1 beta processing via calcium-independent phospholipase A2. *Journal of immunology (Baltimore, Md. 1950)* 164(10):5120–5124. doi:10.4049/jimmunol.164.10.5120.

Wandel, M. P., B.-H. Kim, E.-S. Park, K. B. Boyle, K. Nayak, B. Lagrange, A. Herod, T. Henry, M. Zilbauer, J. Rohde, J. D. MacMicking, and F. Randow. 2020. Guanylate-binding proteins convert cytosolic bacteria into caspase-4 signaling platforms. *Nature immunology* 21(8):880–891. doi:10.1038/s41590-020-0697-2.

Wang, I. M., J. C. Blanco, S. Y. Tsai, M. J. Tsai, and K. Ozato. 1996. Interferon regulatory factors and TFIIB cooperatively regulate interferon-responsive promoter activity in vivo and in vitro. *Molecular and cellular biology* 16(11):6313–6324. doi:10.1128/mcb.16.11.6313.

Wang, S., M. Miura, Y. Jung, H. Zhu, E. Li, and J. Yuan. 1998. Murine Caspase-11, an ICE-Interacting Protease, Is Essential for the Activation of ICE. *Cell* 92(4):501–509. doi:10.1016/s0092-8674(00)80943-5.

Wang, W., D. Hu, C. Wu, Y. Feng, A. Li, W. Liu, Y. Wang, K. Chen, M. Tian, F. Xiao, Q. Zhang, M. A. Shereen, W. Chen, P. Pan, P. Wan, K. Wu, and J. Wu. 2020. STING promotes NLRP3 localization in ER and facilitates NLRP3 deubiquitination to activate the inflammasome upon HSV-1 infection. *PLoS pathogens* 16(3). doi:10.1371/journal.ppat.1008335.

Wang, Y., and L. H. Kasper. 2014. The role of microbiome in central nervous system disorders. *Brain, behavior, and immunity* 38:1–12. doi:10.1016/j.bbi.2013.12.015.

Wasmuth, H. E., D. Kunz, E. Yagmur, A. Timmer-Stranghöner, D. Vidacek, E. Siewert, J. Bach, A. Geier, E. A. Purucker, A. M. Gressner, S. Matern, and F. Lammert. 2005. Patients with acute on chronic liver failure display "sepsis-like" immune paralysis. *Journal of hepatology* 42(2):195–201. doi:10.1016/j.jhep.2004.10.019.

Widdrington, J. D., A. Gomez-Duran, A. Pyle, M.-H. Ruchaud-Sparagano, J. Scott, S. V. Baudouin, A. J. Rostron, P. E. Lovat, P. F. Chinnery, and A. J. Simpson. 2018. Exposure of Monocytic Cells to Lipopolysaccharide Induces Coordinated Endotoxin Tolerance, Mitochondrial Biogenesis, Mitophagy, and Antioxidant Defenses. *Frontiers in immunology* 9. doi:10.3389/fimmu.2018.02217.

Wiegand, J., and T. Berg. 2013. The etiology, diagnosis and prevention of liver cirrhosis: part 1 of a series on liver cirrhosis. *Deutsches Arzteblatt international* 110(6):85–91. doi:10.3238/arztebl.2013.0085.

Wiggins, K. A., A. J. Parry, L. D. Cassidy, M. Humphry, S. J. Webster, J. C. Goodall, M. Narita, and M. C. H. Clarke. 2019. IL-1α cleavage by inflammatory caspases of the noncanonical inflammasome controls the senescence-associated secretory phenotype. *Aging cell* 18(3):e12946. doi:10.1111/acel.12946.

Winkler, M. S., A. Rissiek, M. Priefler, E. Schwedhelm, L. Robbe, A. Bauer, C. Zahrte, C. Zoellner, S. Kluge, and A. Nierhaus. 2017. Human leucocyte antigen (HLA-DR) gene expression is reduced in sepsis and correlates with impaired TNFα response: A diagnostic tool for immunosuppression? *PloS one* 12(8):e0182427. doi:10.1371/journal.pone.0182427.

Wolk, K., W. D. Döcke, V. von Baehr, H. D. Volk, and R. Sabat. 2000. Impaired antigen presentation by human monocytes during endotoxin tolerance. *Blood* 96(1):218–223.

World Medical Association. 2013. World Medical Association Declaration of Helsinki: ethical principles for medical research involving human subjects. *JAMA* 310(20):2191–2194. doi:10.1001/jama.2013.281053.

Wu, H. 2013. Higher-order assemblies in a new paradigm of signal transduction. *Cell* 153(2):287–292. doi:10.1016/j.cell.2013.03.013.

Wu, J., and Z. J. Chen. 2014. Innate immune sensing and signaling of cytosolic nucleic acids. *Annual review of immunology* 32:461–488. doi:10.1146/annurev-immunol-032713-120156.

Wu, S., F. Hong, D. Gewirth, B. Guo, B. Liu, and Z. Li. 2012. The molecular chaperone gp96/GRP94 interacts with Toll-like receptors and integrins via its C-terminal hydrophobic domain. *The Journal of biological chemistry* 287(9):6735–6742. doi:10.1074/jbc.M111.309526.

Wu, Y.-H., W.-C. Kuo, Y.-J. Wu, K.-T. Yang, S.-T. Chen, S.-T. Jiang, C. Gordy, Y.-W. He, and M.-Z. Lai. 2014. Participation of c-FLIP in NLRP3 and AIM2 inflammasome activation. *Cell death and differentiation* 21(3):451–461. doi:10.1038/cdd.2013.165.

Xiao, L., X.-X. Li, H. K. Chung, S. Kalakonda, J.-Z. Cai, S. Cao, N. Chen, Y. Liu, J. N. Rao, H.-Y. Wang, M. Gorospe, and J.-Y. Wang. 2019. RNA-Binding Protein HuR Regulates Paneth Cell Function by Altering Membrane Localization of TLR2 via Post-transcriptional Control of CNPY3. *Gastroenterology* 157(3):731–743. doi:10.1053/j.gastro.2019.05.010.

Xu, H., J. Yang, W. Gao, L. Li, P. Li, L. Zhang, Y.-N. Gong, X. Peng, J. J. Xi, S. Chen, F. Wang, and F. Shao. 2014. Innate immune sensing of bacterial modifications of Rho GTPases by the Pyrin inflammasome. *Nature* 513(7517):237–241. doi:10.1038/nature13449.

Yamamoto, M., S. Sato, H. Hemmi, K. Hoshino, T. Kaisho, H. Sanjo, O. Takeuchi, M. Sugiyama, M. Okabe, K. Takeda, and S. Akira. 2003a. Role of adaptor TRIF in the MyD88-independent toll-like receptor signaling pathway. *Science (New York, N.Y.)* 301(5633):640–643. doi:10.1126/science.1087262.

Yamamoto, M., S. Sato, H. Hemmi, S. Uematsu, K. Hoshino, T. Kaisho, O. Takeuchi, K. Takeda, and S. Akira. 2003b. TRAM is specifically involved in the Toll-like receptor 4-mediated MyD88-independent signaling pathway. *Nature immunology* 4(11):1144–1150. doi:10.1038/ni986.

Yan, W., A. Ding, H.-J. Kim, H. Zheng, F. Wei, and X. Ma. 2016. Progranulin Controls Sepsis via C/EBPα-Regulated Il10 Transcription and Ubiquitin Ligase/Proteasome-Mediated Protein

Degradation. *Journal of immunology (Baltimore, Md. 1950)* 197(8):3393–3405. doi:10.4049/jimmunol.1600862.

Yang, J., Y. Zhao, J. Shi, and F. Shao. 2013. Human NAIP and mouse NAIP1 recognize bacterial type III secretion needle protein for inflammasome activation. *Proceedings of the National Academy of Sciences of the United States of America* 110(35):14408–14413. doi:10.1073/pnas.1306376110.

Yang, X., X. Cheng, Y. Tang, X. Qiu, Y. Wang, H. Kang, J. Wu, Z. Wang, Y. Liu, F. Chen, X. Xiao, N. Mackman, T. R. Billiar, J. Han, and B. Lu. 2019. Bacterial Endotoxin Activates the Coagulation Cascade through Gasdermin D-Dependent Phosphatidylserine Exposure. *Immunity* 51(6):983-996.e6. doi:10.1016/j.immuni.2019.11.005.

Yang, Y., B. Liu, J. Dai, P. K. Srivastava, D. J. Zammit, L. Lefrançois, and Z. Li. 2007. Heat shock protein gp96 is a master chaperone for toll-like receptors and is important in the innate function of macrophages. *Immunity* 26(2):215–226. doi:10.1016/j.immuni.2006.12.005.

Yi, Y.-S. 2017. Caspase-11 non-canonical inflammasome: a critical sensor of intracellular lipopolysaccharide in macrophage-mediated inflammatory responses. *Immunology* 152(2):207–217. doi:10.1111/imm.12787.

Zambelli, F., G. Pesole, and G. Pavesi. 2009. Pscan: finding over-represented transcription factor binding site motifs in sequences from co-regulated or co-expressed genes. *Nucleic Acids Research* 37(Web Server issue):W247-52. doi:10.1093/nar/gkp464.

Zanoni, I., R. Ostuni, L. R. Marek, S. Barresi, R. Barbalat, G. M. Barton, F. Granucci, and J. C. Kagan. 2011. CD14 controls the LPS-induced endocytosis of Toll-like receptor 4. *Cell* 147(4):868–880. doi:10.1016/j.cell.2011.09.051.

Zaret, K. S., and J. S. Carroll. 2011. Pioneer transcription factors: establishing competence for gene expression. *Genes & development* 25(21):2227–2241. doi:10.1101/gad.176826.111.

Zhang, H., L. Zeng, M. Xie, J. Liu, B. Zhou, R. Wu, L. Cao, G. Kroemer, H. Wang, T. R. Billiar, H. J. Zeh, R. Kang, J. Jiang, Y. Yu, and D. Tang. 2020. TMEM173 Drives Lethal Coagulation in Sepsis. *Cell host & microbe* 27(4):556-570.e6. doi:10.1016/j.chom.2020.02.004.

Zhang, L., S. Chen, J. Ruan, J. Wu, A. B. Tong, Q. Yin, Y. Li, L. David, A. Lu, W. L. Wang, C. Marks, Q. Ouyang, X. Zhang, Y. Mao, and H. Wu. 2015. Cryo-EM structure of the activated NAIP2-NLRC4 inflammasome reveals nucleated polymerization. *Science (New York, N.Y.)* 350(6259):404–409. doi:10.1126/science.aac5789.

Zhang, P., M. Zhang, R. Han, K. Zhang, H. Ding, C. Liang, and L. Zhang. 2018. The correlation between microRNA-221/222 cluster overexpression and malignancy: an updated meta-analysis including 2693 patients. *Cancer management and research* 10:3371–3381. doi:10.2147/CMAR.S171303.

Zhang, Q., and X. Cao. 2019. Epigenetic regulation of the innate immune response to infection. *Nature reviews. Immunology* 19(7):417–432. doi:10.1038/s41577-019-0151-6.

Zhang, Q., M. Raoof, Y. Chen, Y. Sumi, T. Sursal, W. Junger, K. Brohi, K. Itagaki, and C. J. Hauser. 2010. Circulating mitochondrial DAMPs cause inflammatory responses to injury. *Nature* 464(7285):104–107. doi:10.1038/nature08780.

Zhang, Z., G. Meszaros, W. He, Y. Xu, H. de Fatima Magliarelli, L. Mailly, M. Mihlan, Y. Liu, M. Puig Gámez, A. Goginashvili, A. Pasquier, O. Bielska, B. Neven, P. Quartier, R. Aebersold, T. F. Baumert, P. Georgel, J. Han, and R. Ricci. 2017. Protein kinase D at the Golgi controls NLRP3 inflammasome activation. *The Journal of experimental medicine* 214(9):2671–2693. doi:10.1084/jem.20162040.

Zhao, J. L., D. S. Rao, M. P. Boldin, K. D. Taganov, R. M. O'Connell, and D. Baltimore. 2011a. NF-kappaB dysregulation in microRNA-146a-deficient mice drives the development of myeloid malignancies. *Proceedings of the National Academy of Sciences of the United States of America* 108(22):9184–9189. doi:10.1073/pnas.1105398108.

Zhao, Y., J. Yang, J. Shi, Y.-N. Gong, Q. Lu, H. Xu, L. Liu, and F. Shao. 2011b. The NLRC4 inflammasome receptors for bacterial flagellin and type III secretion apparatus. *Nature* 477(7366):596–600. doi:10.1038/nature10510.

Zheng, D., T. Liwinski, and E. Elinav. 2020. Inflammasome activation and regulation: toward a better understanding of complex mechanisms. *Cell discovery* 6:36. doi:10.1038/s41421-020-0167-x.

Zhong, Z., A. Umemura, E. Sanchez-Lopez, S. Liang, S. Shalapour, J. Wong, F. He, D. Boassa, G. Perkins, S. R. Ali, M. D. McGeough, M. H. Ellisman, E. Seki, A. B. Gustafsson, H. M. Hoffman, M. T. Diaz-Meco, J. Moscat, and M. Karin. 2016. NF-κB Restricts Inflammasome Activation via Elimination of Damaged Mitochondria. *Cell* 164(5):896–910. doi:10.1016/j.cell.2015.12.057.

Zhou, Q., G.-S. Lee, J. Brady, S. Datta, M. Katan, A. Sheikh, M. S. Martins, T. D. Bunney, B. H. Santich, S. Moir, D. B. Kuhns, D. A. Long Priel, A. Ombrello, D. Stone, M. J. Ombrello, J. Khan, J. D. Milner, D. L. Kastner, and I. Aksentijevich. 2012. A hypermorphic missense mutation in PLCG2, encoding phospholipase Cγ2, causes a dominantly inherited autoinflammatory disease with immunodeficiency. *American journal of human genetics* 91(4):713–720. doi:10.1016/j.ajhg.2012.08.006.

Zhou, R., A. S. Yazdi, P. Menu, and J. Tschopp. 2011. A role for mitochondria in NLRP3 inflammasome activation. *Nature* 469(7329):221–225. doi:10.1038/nature09663.

Zhu, Q., S. M. Man, R. Karki, R. K. S. Malireddi, and T.-D. Kanneganti. 2018. Detrimental Type I Interferon Signaling Dominates Protective AIM2 Inflammasome Responses during Francisella novicida Infection. *Cell reports* 22(12):3168–3174. doi:10.1016/j.celrep.2018.02.096.

9. Appendix

Figures:

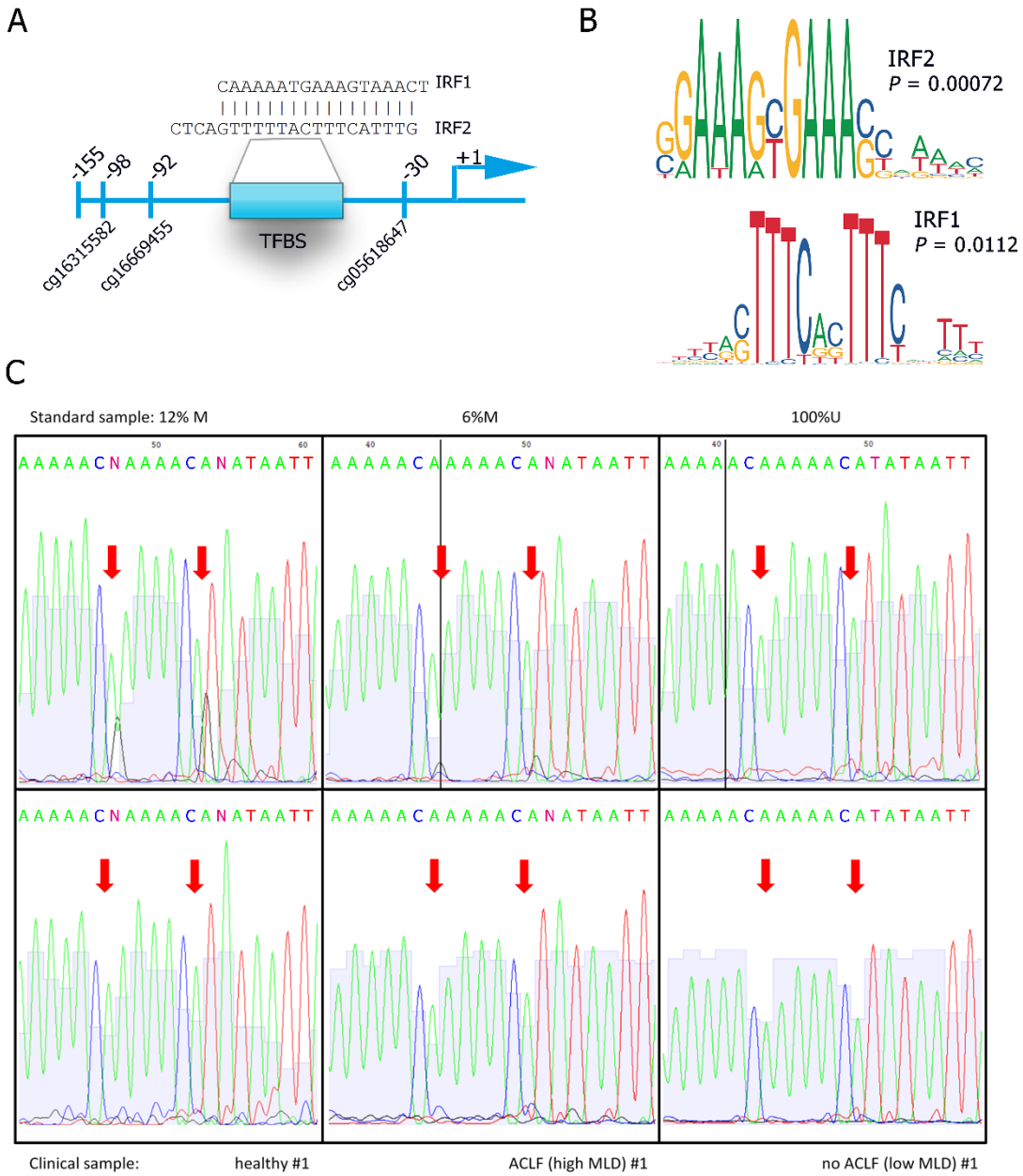

Fig. 28: CpG Islands located in the close proximity of IRF1 and IRF2 TFBS and TSS of *CASP4* gene.
Transcription factor binding motifs of IRF2 and IRF1 found by the Pscan algorithm on the promoter region of Caspase-4 gene. **(C)** Sanger sequencing profiles of the reverse strand from BS-PCR products. Shown are standards (upper panel: 12% methylation, 6% methylation, unmethylated DN) and exemplarily samples from a healthy donor and patients without ACLF or with ACLF (lower panel). Importantly, all clinical samples did not show a methylation above the detection limit of 10% methylation. Red arrows mark the positions of CpGs. A methylated cytosine would result in a guanine on the reverse strand as seen in the standard samples (underrepresented guanine signal, black curve).

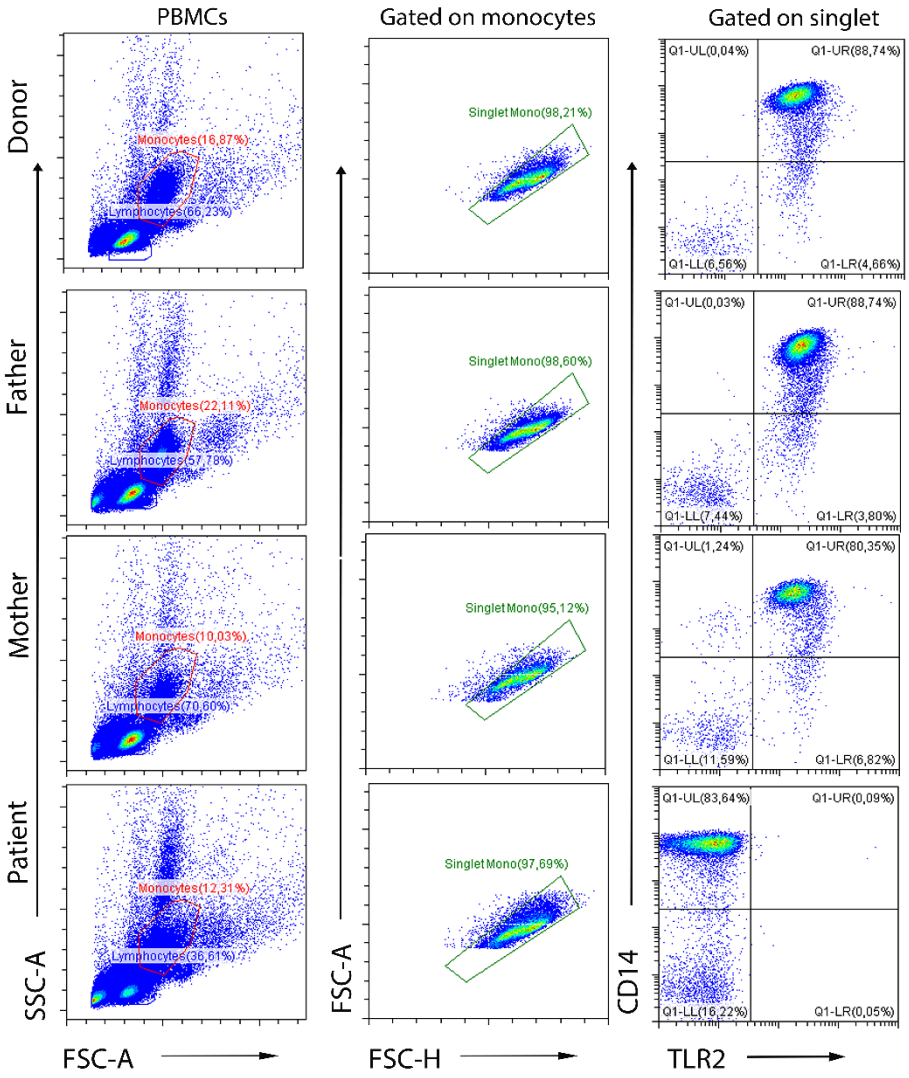

Fig. 29: Gating strategy for CD14+ monocytes and TLR2 expression
PBMCs derived from loss-of-function CNPY3 variant family and healthy donor were subjected to FACS analysis. Monocytes were selected (red) in the forward sidescatter plot (**left**). Initial gating was done on FSC-H and FSC-A to discriminate singlet (**middle**). Monocytes $CD14^+$ cells (high FSC-A) were copied to a $TLR2^+$ cells (high FSC-H) plot (**right**). Using isotype control samples, gates were set in the TLR2 plot so that at least 99% of the isotype control were negative for TLR2 expression. This gate was then used to identify the percentage of TLR2 positive shown in **Fig. 23D**.

Patient characteristics.

Table 16: Clinical characteristics correspond to analysis of PBMCs and plasma of patients with decompensated liver disease

	Acute Decompensation without organ failure N=20	Acute Decompensation with organ failure (ACLF) N=19	Comparison of case groups (*P* value)
Age (years)	59 (52-66)	55 (51-68)	0.74
Male sex	14 (70%)	16 (84%)	0.45
Alcoholic liver disease	18 (90%)	15 (79%)	0.41
Ascites	20 (100%)	19 (100%)	1.00
ACLF grade (1 / 2 / 3)	0 / 0 / 0	9 (47%) /5 (26%) /5 (26%)	N/A
Infection			
None	17 (85%)	9 (47%)	0.02* infection vs. no infection
Peritonitis	2 (10%)	6 (32%)	
Urinary tract	1 (5%)	2 (11%)	
Pneumonia	0	1 (5%)	
Other	0	1 (5%)	
Creatinine (µmol/l)	87 (74-108)	236 (188-297)	<0.001
Total bilirubin (µmol/l)	16 (11-25)	174 (44-423)	<0.001
MELD score	10 (9-10)	31 (24-34)	<0.001
WBC counts ($x10^3$/µl)	6.4 (5.6-8.2)	10.2 (8.0-19.4)	0.02
CRP (mg/l)	18 (9-25)	46 (24-118)	0.002
Liver transplant or death within 30 days	1 (5%)	10 (53%)	0.001

Patients are classified according to the absence or presence of multiple organ failure syndrome (according to the EASL CLIF-C criteria for acute-on-chronic liver failure). Data are given as frequencies or medians with interquartile. N/A: not applicable. *P* values from Fisher's exact test for discrete data or Mann-Whitney U for continuous data.

Table 17: Clinical characteristics correspond to analysis of $CD14^+$ monocytes of patients with decompensated liver disease

	Acute Decompensation without organ failure N=5	Acute Decompensation with organ failure (ACLF) N=5	Comparison of case groups (*P* value)
Age (years)	59 (53-70)	54 (46-59)	0.20
Male sex	5 (100%)	4 (80%)	1.00
Alcoholic liver disease	4 (80%)	5 (100%)	1.00
ACLF grade (I/II/III)	0	4 (80%) / 0 (0%) / 1 (20%)	N/A
Bacterial infection			
None	5 (100%)	0	0.008* infection vs. no infection
Peritonitis	0	5 (100%)	
Urinary tract	0	0	
Pneumonia	0	0	
Creatinine (µmol/l)	92 (52-110)	193 (123-367)	0.008
Total bilirubin (µmol/l)	16 (11-23)	57 (43-146)	0.008
MELD score	10 (9-11)	28 (21-36)	0.008
WBC counts ($x10^3/µl$)	7.2 (5.3-9.6)	13.6 (6.0-19.7)	0.22
CRP (mg/l)	33 (28-84)	76 (27-146)	0.75
Liver transplant or death within 30 days**	0	4 (80%)	0.048

Patients are classified according to the absence or presence of multiple organ failure syndrome (according to the EASL CLIF-C criteria for acute-on-chronic liver failure). Data are given as frequencies or medians with interquartile. N/A: not applicable. P values from Fisher's exact test for discrete data or Mann-Whitney U for continuous data.

Table 18: Basic characteristic of the septic patient cohort

Age [years]	68	[51.0 - 74.0]
Gender, male	16	(64 %)
APACHE-II on admission	23	[16.0 - 27.0]
SAPS-II on admission	49	[35.0 - 63.0]
28-day mortality	5	(20 %)
Site of infection		
Abdominal	10	(40 %)
Pneumonia	5	(20 %)
Primary bacteremia	5	(20 %)
Soft tissue	3	(12 %)
Urogenital	1	(4 %)
Endocarditis	1	(4 %)

Table 19: Characteristics of patients with sepsis for ex vivo endotoxin tolerance.

	Patient 1	**Patient2**	**Patient 3**	**Patient 4**
Age [years]	53	75	60	43
Gender, male	male	Female	male	male
clinical diagnosis	Septic shock	Sigma diverticulitis	Infected pacemaker	Impaired postsurgical wound healing
Sepsis	Yes	Yes	Yes	Yes
Organ damage	Yes	Yes	Yes	Yes
Infection	pneumonia	peritonitis	pneumonia	Wound infection

List of figures

List of tables

Acknowledgement

First and foremost, I would like to thank Allah, Whose many blessings have made me who I am today and for the accomplishment of the thesis. The course of my PhD has been tough and challenging, but I am extremely fortunate to be surrounded by amazing people that made this journey so rewarding. I would like to express my sincere appreciation and gratitude to my PhD advisor Dr. Sachin D. Deshmukh, for his guidance, patience, critique, valuable advices, continuous supports and enthusiasm. He has given me motivation throughout my doctoral studies, and he also gave me freedom to pursue independent work. I have truly learnt a lot during this time, and I am extremely honored to be his PhD student!

A special thanks goes out to Prof. Michael Bauer for his intellectual stimulation and immense knowledge. I am fortunate to work with Prof. Tony Bruns and Dr. Ralf Hussain. Thank you people for kindly providing patients' samples and data and also for useful discussions. I would like to thank all members of NeoSep Group for creating such a pleasant working environment. I have learnt a lot from all of you and I am glad we had the opportunity to spend some fun time outside the lab. A special thanks to Bianca Göhrig for instilling good laboratory practice and organization skills, these skill sets have helped me a lot during the course of my PhD and for keeping the lab well stocked at all times.

I have to thank Prof. Reinhard Wetzker in particular for reviewing my thesis. I am also fortunate to work with the members of Gastroenterology group. Thank you for providing essential reagents. Thank you, Katja Lehmann-Pohl and her colleagues for ensuring a smooth PhD. It´s also my privilege to thank the collaborators and everyone who provided me with all the facilities at the division throughout my doctoral studies.

Last but not least, a big thanks to my family at overseas, for supporting my decision to pursue PhD. Thank you, my friends, for being awesome and always available when I needed help. A big and special thanks to my wife for her unlimited and continuous support and making sure that my children (Hamza and Arwa) are always in good hands while I was pursuing my lab work. You all have my love and appreciation.

Ehrenwörtliche Erklärung

Hiermit erkläre ich, dass mir die Promotionsordnung der Medizinischen Fakultät der Friedrich-Schiller-Universität bekannt ist,

ich die Dissertation selbst angefertigt habe und alle von mir benutzten Hilfsmittel, persönlichen Mitteilungen und Quellen in meiner Arbeit angegeben sind,

mich folgende Personen bei der Auswahl und Auswertung des Materials sowie bei der Herstellung des Manuskripts unterstützt haben:

Dr. Sachin Deshmukh beim Studiendesign, der Auswahl der Methoden sowie bei der Ergebnissinterpretation und -darstellung, Prof. Michael Bauer und Prof. Reinhardt Wetzker bei Durchsicht des Manuskripts, Dr. Sachin Deshmukh, Prof. Dr. Tony Bruns, und Dr. med Ralf Husain bei der Übermittlung von Patientendaten, Dr. Norman Häfner bei der Auswertung der DNA Methylierungsexperimente, und apl. Prof. Dr. Ralf Claus und Prof. Rubio Igancio bei Durchsicht der von mir auf Deutsch verfassten Zusammenfassung.

die Hilfe eines Promotionsberaters nicht in Anspruch genommen wurde und dass Dritte weder unmittelbar noch mittelbar geldwerte Leistungen von mir für Arbeiten erhalten haben, die im Zusammenhang mit dem Inhalt der vorgelegten Dissertation stehen,

dass ich die Dissertation noch nicht als Prüfungsarbeit für eine staatliche oder andere wissenschaftliche Prüfung eingereicht habe und

dass ich die gleiche, eine in wesentlichen Teilen ähnliche oder eine andere Abhandlung nicht bei einer anderen Hochschule als Dissertation eingereicht habe.

Ort, Datum Unterschrift des Verfassers

Jena, den 27.04.2021